KARST INVENTORY OF GUAM, MARIANA ISLANDS

Danko Taborosi

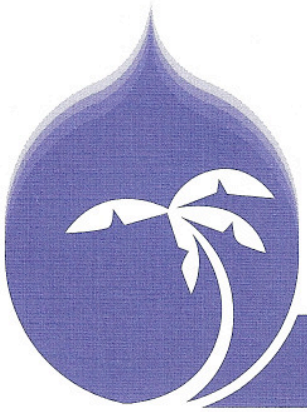

WERI
WATER AND ENVIRONMENTAL RESEARCH INSTITUTE
OF THE WESTERN PACIFIC
UNIVERSITY OF GUAM

Technical Report No. 112
August 2006

Karst Inventory of Guam, Mariana Islands

by

Danko Taborosi

Water and Environmental Research Institute
of the Western Pacific

University of Guam

Technical Report No. 112

August, 2006

The work reported herein was funded, in part, by the Department of Interior via the Water Resources Research Institute Program of the U. S. Geological Survey (Award No. 1434-HQ-96-GR-02665), administered through the Water and Environmental Research Institute of the Western Pacific at the University of Guam, and by the Guam Hydrologic Survey Program, institute by the 24th Guam Legislature. The content of this report does not necessarily reflect the views and policies of the Department of Interior, not does the mention of trade names or commercial products constitute their endorsement by the United States Government.

ABSTRACT

Guam is a rapidly developing island with over 70% of its water supply coming from the carbonate Northern Guam Lens Aquifer (NGLA). Identifying, mapping and interpreting karst features of the NGLA is crucial to its successful development and protection. This project is a detailed inventory, interpretation, and discussion of karst features of the NGLA and other limestone areas of Guam.

Guam exhibits characteristic island karst features resulting from interaction of marine and fresh ground water as well as numerous classic continental karst features. The categories of Guam's karst features are: karren and phytokarst, epikarst, surface flow landforms, closed contour depressions, caves, and springs. Karren and phytokarst are diverse. The epikarst appears identical to the epikarst of other carbonate islands. Closed depressions on Guam are dissolutional, constructional, and human-modified. Dissolutional closed depressions include large cockpit karst sinkholes, point recharge sinkholes, collapse sinkholes, and blind valleys. The largest closed depressions are probably constructional. Many depressions have been modified to act as ponding basins. The main categories of caves on Guam are pit caves, stream caves and flank margin caves. Numerous pit caves vary widely in size and reach depths up to 50 meters. Stream caves are associated with allogenic rainwater catchment by volcanic rocks. Flank margin caves, formed along margin of the fresh-water lens, are exposed on the cliffs in Northern Guam and indicate previous sea-level still stands. Additional types of caves found include fracture caves and voids created on the top, bottom and within the freshwater lens. Springs discharge freshwater at the coastline.

ACKNOWLEDGEMENTS

I would like to thank Dr. John Jenson for giving me the opportunity to study and enjoy the karst of Guam. Thanks for the friendship, guidance, insight and support, for the long talks in the field, and meetings and schedules that kept me organized. To Dr. H. G. Siegrist I am grateful for the introduction to geology of Pacific islands and coral reefs, and for the constant support masked by wit, humor and sarcasm. To Dr. Gustav Paulay—for his patient reading of the thesis draft and for all the helpful comments and information on the invertebrates of Guam's caves.

To USGS for funding the project that made my research possible. To Dragomir Nikolitch Charitable Trust, Studenica Foundation and the Open Society Institute for their altruism and financial support.

To David Vann—for being a driving force over the years as both a friend and a colleague, for all the hikes in the karrenfelds, Wendy's burgers, and for EVERYTHING—see you in Peru. To Mauryn Quenga, John Jocson and Karel Smit—for the adventures at WERI, the friendship, the help, the fieldwork, and the lunches—I will miss you. To Dolores Santos and Norma Blas for the help and support... the staplers and the paychecks. To Dr. Denton and other WERI employees—thanks for making WERI such a fun place to work. To Dr. John Mylroie, Dr. Jim Carew, and the collaborating teams from Mississippi, South Carolina, and Puerto Rico for their insight, answers and theories. To Dr. Ivan Gill for friendship and skateboarding.

To my friends Brent Tibbatts, Lisa Kirkendale, and Jenn Coleson-Dolph for time, thoughts, and travel. To Todd Pitlik (DAWR) for flights of fancy. To Braxton Plunkett for surveying skills and underwater photography. To Mike Ward—gracias por viviendo de bajo de tierra; nos vemos en Oklahoma. To Matt Howes for showing me the submarine caves, cave diving expertise, and the fun days on the boat. To Brett & Kathryn Wallace, and Tosca, for friendship, caving, and rappelling. To Curt Wexel and Micronesian Cavers for sharing their wealth of knowledge, and for showing me the ropes (rappelling) and caves. To Aubri and Linda Jenson for company in the field and help with surveying. To Dishu Parmar for leading me to Ritidian Cave. To Greg Castro for access to Castro's Cave. To the US Navy, US Air Force, US Fish and Wildlife Service, Perez Bros. Co., Hawaiian Rock Products, and private landowners for graciously allowing me to roam their property in pursuit of caves. To those who did not grant me permission—thanks for not shooting when I trespassed. To Joan Swaddell for being my liaison on the upper campus and a friend—see you in Lomar.

To my parents, Branka and Slavko, and my sister Ivana—hvala vam sto ste me pustili da odem ovako daleko, sto ste me pazili i mazili preko sedam mora, za posete i puteve koji su me odrzali, za ljubav. To ISP and Vigor Majic—za prvu pecinu, inspiraciju i uvod u nauku. To Nicole Scheman and Heather Tinsman for being great friends, flying the distance and for visits during which I could briefly forget about karst. To Justin Udovch, a.k.a. G-money, and Amanda G. Sanchez, the Queen of All That is Good—I can't put it into words, but feel free to recognize I saved the best for last.

TABLE OF CONTENTS

LIST OF FIGURES

LIST OF TABLES

LIST OF PLATES

APPENDICES

MAPS

ABSTRACT

Guam is a rapidly developing island with over 70% of its water supply coming from the carbonate Northern Guam Lens Aquifer (NGLA). Identifying, mapping and interpreting karst features of the NGLA is crucial to its successful development and protection. This project is a detailed inventory, interpretation, and discussion of karst features of the NGLA and other limestone areas of Guam.

Guam exhibits characteristic island karst features resulting from interaction of marine and fresh ground water as well as numerous classic continental karst features. The categories of Guam's karst features are: karren and phytokarst, epikarst, surface flow landforms, closed contour depressions, caves, and springs. Karren and phytokarst are diverse. The epikarst appears identical to the epikarst of other carbonate islands. Closed depressions on Guam are dissolutional, constructional, and human-modified. Dissolutional closed depressions include large cockpit karst sinkholes, point recharge sinkholes, collapse sinkholes, and blind valleys. The largest closed depressions are probably constructional. Many depressions have been modified to act as ponding basins. The main categories of caves on Guam are pit caves, stream caves and flank margin caves. Numerous pit caves vary widely in size and reach depths up to 50 meters. Stream caves are associated with allogenic rainwater catchment by volcanic rocks. Flank margin caves, formed along margin of the fresh-water lens, are exposed on the cliffs in Northern Guam and indicate previous sea-level still stands. Additional types of caves found include fracture caves and voids created on the top, bottom and within the freshwater lens. Springs discharge freshwater at the coastline.

ACKNOWLEDGEMENTS

I would like to thank Dr. John Jenson for giving me the opportunity to study and enjoy the karst of Guam. Thanks for the friendship, guidance, insight and support, for the long talks in the field, and meetings and schedules that kept me organized. To Dr. H. G. Siegrist I am grateful for the introduction to geology of Pacific islands and coral reefs, and for the constant support masked by wit, humor and sarcasm. To Dr. Gustav Paulay—for his patient reading of the thesis draft and for all the helpful comments and information on the invertebrates of Guam's caves.

To USGS for funding the project that made my research possible. To Dragomir Nikolitch Charitable Trust, Studenica Foundation and the Open Society Institute for their altruism and financial support.

To David Vann—for being a driving force over the years as both a friend and a colleague, for all the hikes in the karrenfelds, Wendy's burgers, and for EVERYTHING—see you in Peru. To Mauryn Quenga, John Jocson and Karel Smit—for the adventures at WERI, the friendship, the help, the fieldwork, and the lunches—I will miss you. To Dolores Santos and Norma Blas for the help and support... the staplers and the paychecks. To Dr. Denton and other WERI employees—thanks for making WERI such a fun place to work. To Dr. John Mylroie, Dr. Jim Carew, and the collaborating teams from Mississippi, South Carolina, and Puerto Rico for their insight, answers and theories. To Dr. Ivan Gill for friendship and skateboarding.

To my friends Brent Tibbatts, Lisa Kirkendale, and Jenn Coleson-Dolph for time, thoughts, and travel. To Todd Pitlik (DAWR) for flights of fancy. To Braxton Plunkett for surveying skills and underwater photography. To Mike Ward—gracias por viviendo de bajo de tierra; nos vemos en Oklahoma. To Matt Howes for showing me the submarine caves, cave diving expertise, and the fun days on the boat. To Brett & Kathryn Wallace, and Tosca, for friendship, caving, and rappelling. To Curt Wexel and Micronesian Cavers for sharing their wealth of knowledge, and for showing me the ropes (rappelling) and caves. To Aubri and Linda Jenson for company in the field and help with surveying. To Dishu Parmar for leading me to Ritidian Cave. To Greg Castro for access to Castro's Cave. To the US Navy, US Air Force, US Fish and Wildlife Service, Perez Bros. Co., Hawaiian Rock Products, and private landowners for graciously allowing me to roam their property in pursuit of caves. To those who did not grant me permission—thanks for not shooting when I trespassed. To Joan Swaddell for being my liaison on the upper campus and a friend—see you in Lomar.

To my parents, Branka and Slavko, and my sister Ivana—hvala vam sto ste me pustili da odem ovako daleko, sto ste me pazili i mazili preko sedam mora, za posete i puteve koji su me odrzali, za ljubav. To ISP and Vigor Majic—za prvu pecinu, inspiraciju i uvod u nauku. To Nicole Scheman and Heather Tinsman for being great friends, flying the distance and for visits during which I could briefly forget about karst. To Justin Udovch, a.k.a. G-money, and Amanda G. Sanchez, the Queen of All That is Good—I can't put it into words, but feel free to recognize I saved the best for last.

TABLE OF CONTENTS

LIST OF FIGURES

LIST OF TABLES

LIST OF PLATES

APPENDICES

MAPS

— Chapter 1 —
INTRODUCTION

The study of carbonate aquifers is an important topic in hydrogeology. Because carbonate aquifers are characterized by a high degree of spatial heterogeneity of porosity and permeability, which vary across many orders of magnitude, they are not adequately described by conventional groundwater flow models. Reliable modeling of such an aquifer, therefore, requires developing of a comprehensive general model of the overall "plumbing" of the aquifer. The necessary step towards such a comprehensive conceptual model is a systematic inventory and characterization of karst features of a carbonate aquifer. Our capacity to understand and successfully manage carbonate aquifers is therefore fundamentally determined by the accuracy of our knowledge regarding the specific karst features of an aquifer.

Critical Water Problems on Guam

Carbonate islands worldwide are experiencing ever-increasing demands on their limited water resources as populations and demand for utilities and water-based services grow (UNU, 1995). Guam has seen spectacular growth in the last two decades. Annual tourist attendance on Guam has grown from a few tens of thousands in the early 1980s to over one million in 1994, to over one-and-a-half million in 1996 and 1997. Guam extracts over 40 mgd of the current estimated sustainable yield of 57 mgd from the limestone aquifer (Northern Guam Lens Aquifer—NGLA) occupying the northern half of the island to provide 80% of the water consumed by its 150,000 permanent residents and 15,000 to 20,000 tourists per day.

On Guam and other carbonate islands, water occurrence, storage, movement, accessibility, and quality are fundamentally controlled by the karst features of the carbonate aquifers. Furthermore, carbonate island aquifers are vulnerable to overuse and contamination due to limited recharge (especially at times of drought), potential of seawater intrusion in case of overpumping, and the ease with which contaminants move through porous limestone. Considering the limited supply of water and vulnerability to overuse and contamination, accurate understanding of the hydrologic properties of the basic karst features of Guam is crucial to successful aquifer development and protection. It is, therefore, imperative that we learn more about the nature of the NGLA and other potential carbonate aquifers if we are to properly develop, manage and protect our island's freshwater resources.

Nature of Research

In addition to porous-media flow, karst aquifers exhibit fracture and conduit flow. The relative contributions of each of these flow types are largely unknown and variable, both spatially and temporally (Sasowsky, 1997). This situation can be further complicated by occasional overflow from one subsurface basin to others as a result of high recharge events. Because of this complexity, interpreting the behavior of karst aquifers is extremely difficult and can best be approached by acquiring as much field information as possible and developing detailed conceptual models, incorporating observed features and behavior. Until this project, the field knowledge of Guam's karst features was extremely limited, which posed a major deficiency for developing of a reliable model of the Northern Guam Lens Aquifer.

Research Objectives

The aim of this study is to inventory, investigate, and characterize karst features of the Northern Guam Lens Aquifer and other carbonate areas on Guam. The necessary steps involved were to 1) locate karst landforms and features in Guam, 2) categorize them based on their inferred origin and hydrologic significance, 3) compile an inventory and set up an appropriate database of karst features, 4) generate maps showing the distribution of inventoried features, 5) survey selected sites in detail (those deemed to be representative) and 6) provide discussion and descriptions of the characteristic karst features found on Guam.

Research Benefits

The inventory of Guam's karst features will benefit scientists, planners, managers, regulators, and other water resource researchers. A clearer picture of the "plumbing" and history of the aquifer will increase the reliability of predictions made on the bases of

drilling and geophysical exploration. Information gained from this project contributes to our understanding of groundwater storage and flow, supports better storm water and sewer overflow management practices, allows more accurate predictions of the effects of sinkhole modifications (such as filling in or paving), and supports better decisions in choosing sites for solid waste disposal and monitoring wells. In summary, the report presented here is a valuable tool for water resource researchers and managers for more efficient assessments and predictions dealing with groundwater exploration, monitoring, and protection practices.

Structure of the Thesis

Chapter 1 provides a brief introduction to the scope of this thesis. Rationale for conducting the investigations is provided.

The thesis begins with a review of geology, hydrology and climate of Guam and a summary of concepts necessary for the understanding and interpretation of the research undertaken (Chapter 2). This is followed by a literature review, description of field methods, software used, and methodology of creating the karst inventory of Guam (Chapter 3). This is followed by eight chapters presenting the karst features of Guam, grouped according to their hydrologic properties.

Chapter 4. *Karren and Phytokarst:* This chapter describes the small-scale karst features on limestone surfaces exposed to impact of meteoric water and biota. Types of karren and phytokarst from Guam are presented.

Chapter 5. *Karst features in the subcutaneous zone:* Epikarst on Guam and karst features in the epikarst are described. Discussion of vadose features allowing meteoric water to by-pass part of the epikarst is also included here. Finally, an inventory of storm water disposal wells on Guam, acting as man-made vadose by-passes, is presented.

Chapter 6. *Karst features related to surface drainage*: This chapter presents an inventory, classification and descriptions of karst features related to past or present surface drainage, such as sinking streams, dry valleys, etc. An inventory and a tentative classification of high level springs in Guam are also provided.

Chapter 7. *Closed contour depressions:* An inventory, classification, and descriptions of closed contour depressions is provided in this chapter. Various types of sinkholes, as well as constructional and man-made or modified depressions are discussed. Morphometric characteristics of depressions on Guam are analyzed in this chapter.

Chapter 8. *Vadose caves and conduits:* This chapter presents and inventory, classification and descriptions of vadose caves on Guam. Vadose conduits are briefly discussed.

Chapter 9. *Phreatic caves and conduits:* Caves and other voids made by phreatic dissolution are discussed in this chapter. An inventory, classification, and descriptions of individual features are provided.

Chapter 10. *Coastal discharge features:* Coastal springs, seeps and related features are presented in this chapter. An inventory, classification, and description of selected features is provided.

Chapter 11. *Submarine karst features:* This chapter presents a brief discussion of submarine karst features of Guam. Unlike in the previous chapters, features included here do not share common genetic or hydrologic properties. They are grouped together based on their present location below the sea level. Coastal pseudo-karst (sea caves, primary caves in reefs) is also discussed here.

— Chapter 2 —
GEOLOGICAL CONDITIONS ON GUAM

This chapter briefly reviews the geography, climate, and geology of Guam.

2. 1. Geography and Physiography of Guam

Guam is a small island located in Micronesia, in the western Pacific, at 13°30' N and 144°45' W (Fig. 2. 1). It is the southernmost island in the Mariana Islands chain. Although only 549 km^2 in area, it is the largest of the Mariana Islands and the largest island in Micronesia. It is elongate in shape, its NE-SW axis being approximately 48 km long. The width of the island ranges from 6.4 to 17.7 kilometers. Guam is a part of the Mariana island arc lying west of the Mariana Trench into which the Pacific plate is being subducted underneath the Philippine plate. Located about 110 km northwest of the Mariana Trench, it is in an active seismic zone. Guam is a territory of the United States.

The island is sharply divided along its narrow waist into nearly equal halves by the Pago-Adelupe geologic fault. Northern Guam (north of the fault) is an undulating limestone plateau, sloping to the southwest. The limestone is about 30 meters thick at its southern end and reaches 180 meters in the north. The plateau is bordered by cliffs that precipitously abut against the ocean or a narrow coastal plain. The plateau's generally flat surface is interrupted by a limestone hill, Barrigada Hill (203 m), and two volcanic inliers, Mt. Santa Rosa (261.5 m) and Mataguac Hill (192 m). No perennial streams exist on the northern plateau (except for Agana and Chaot rivers in its southern end) because of the limestone's high permeability. Meteoric water quickly disappears in the permeable limestone or forms ephemeral flows in short channels leading to closed contour depressions. Coastal plains are dominated by limestone forests. Uncleared portions of the plateau are dominated by thick shrub jungle.

Southern Guam is a rugged volcanic highland, deeply incised by numerous streams and eroded into peaks, ridges and basins. It is divided by

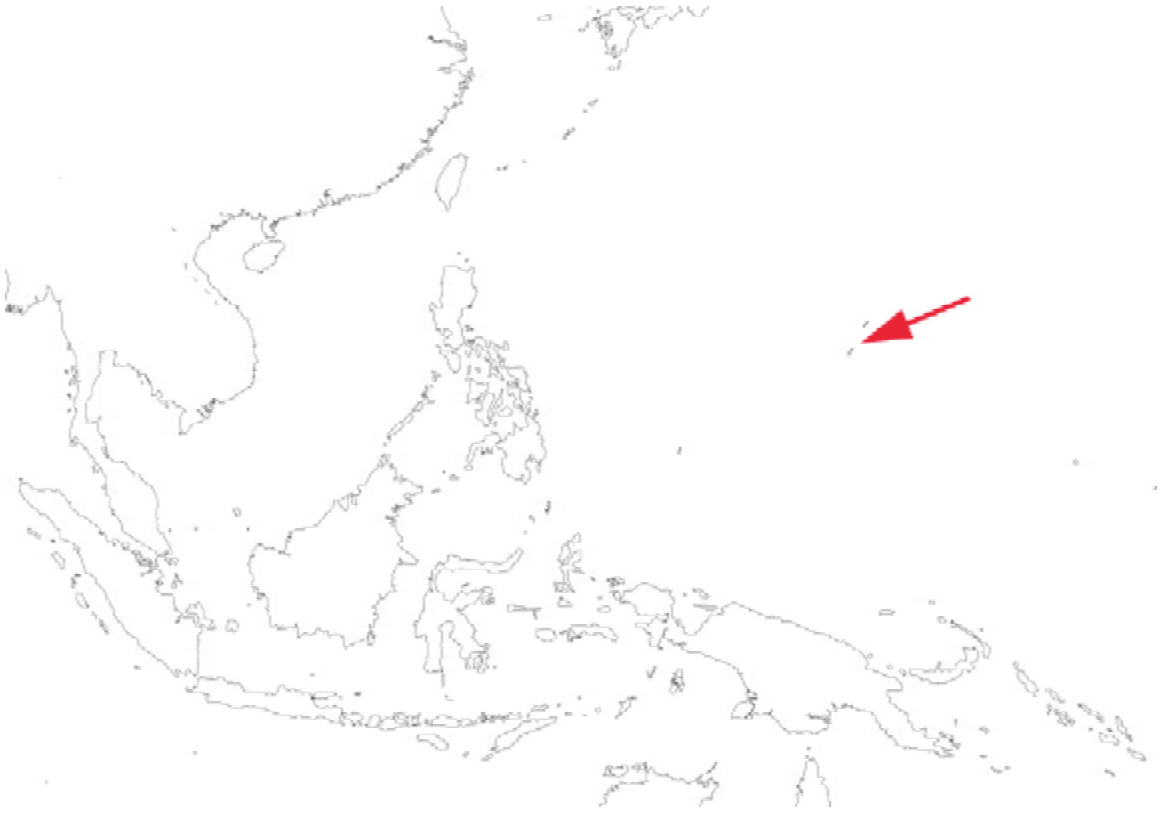

Figure 2. 1: Location of Guam in western Pacific (red arrow marks the island).

a nearly continuous north-south mountain ridge running from Piti on the west coast of southern Guam to Merizo, on the southern tip. The highest peak on Guam is Mt. Lamlam (407 m) and is one of several 300+ m peaks in the southern ridge. Part of the southern ridge is capped by limestone. Drainage pattern on the western half of southern Guam is characterized by steeply-sloping, parallel streams. Eastern half of southern Guam has generally dendritic drainage, partially influenced by geologic faults. Eastern slopes of the mountains merge with a narrow coastal emerged limestone band, standing up to 100 meters above sea level. Volcanic terranes are usually covered by savanna-like grasslands or are unvegetated badlands. Limestone caps and coastal areas are densely vegetated by shrub forests, thus clearly indicating the contact between limestone and volcanic rocks.

2. 2. Climate of Guam

The following information is summarized from Blumenstock (1959) and Mink (1976). Guam's climate is warm and humid, with distinct wet and dry seasons. January through May is the dry season, broken by occasional showers. Wet season lasts from July to November, often with heavy rains and tropical storms. About 2/3 of the annual precipitation falls in the wet season. Droughts are common. Mean annual temperature is 27.2°C, with daily maximum and minimum variations of no more than 5°C. The relative humidity ranges from an average of 65 to 80% in the afternoon to 85 to 100% at night.

Mean annual rainfall over the island ranges from 216 cm on the west coast near Apra Harbour to about 292 cm on the limestone peaks of southern Guam. The northern plateau receives an average of 215-250 cm. Variations from year to year are high (Mink, 1976). Meteorological data collection agencies, archives and points of contact are listed in Dumaliang et al. (1998).

2. 3. Geology of Guam

Most of the information below is summarized and slightly modified from the comprehensive report on the geology of Guam completed by Tracey et al. (1964).

Facpi Formation (Reagan and Meijer, 1984), Eocene and Oligocene in age, is the oldest rock unit on Guam. This formation is characterized by mafic lava flows and pillow basalts, deposited in a submarine environment. Facpi units are often cut by dikes.

The Alutom Formation, originally thought to be the oldest (Tracey et al., 1964) is also Eocene and Oligocene in age, characterized by well-bedded, fine-grained tuffs and sandstones. This formation was made by explosive submarine volcanism.

Umatac Formation, Miocene in age, is next in the geologic succession and is made up of three members: Maemong Limestone (Tum), Bolanos Pyroclastic Member (Tub), and the Dandan Flow Member (Tud).

Maemong Limestone (Tum) is exposed in two principal areas. In southwest Guam, Memong Limestone is exposed on the steep mountain slopes, as a fine-grained, compact limestone, containing reef detritus and foraminifera. It is interbedded with layers of white foraminiferal limestone and weathered volcanic detritus. It was deposited in the Oligocene, in a fore-reef environment. In Talofofo area in central Guam, Maemong Limestone is a compact, white, recrystallized limestone, containing corals in position of growth, benthic foraminifera, mollusks and algae. It was probably deposited in the Miocene, as shallow water patch reefs.

The Bolanos Pyroclastic Member (Tub) was deposited in the Miocene, underwater as well as subaerially. It is made up of tuffaceous breccia and sandstones, often with lenses of volcanic conglomerate. This unit frequently contains fragments of Maemong Limestone.

Dandan Flow Member (Tud) occurs as the scattered boulders throughout southern Guam, believed to be residuals of weathered basaltic lava flows, Miocene in age.

Bonya Limestone (Tb), Miocene in age, is a coarse-grained, well-bedded limestone. It was deposited off-reef in a moderately deep water. Its lithology is variable, ranging from coraliferous limestone and foraminiferal limestone to conglomerates containing volcanic and xenolith limestone fragments.

Janum Formation (Tj), deposited in the Miocene and Pliocene, is well-bedded foraminiferal limestone, deposited in deep water in the vicinity of volcanic highlands. It contains abundant planktonic foraminiferal fossils as well as sand and silt-sized volcanic debris.

Barrigada Limestone (Tbl), also of Miocene and Pliocene age, is a well-lithified to friable white limestone, deposited in deep water. It contains predominantly benthic foraminiferal fossils, and some later shallow water deposits, such as corals, mollusks and algae. Barrigada Limestone is the principal aquifer unit and the main water source for Guam.

Alifan Limestone (Tal) was deposited as a Miocene reef, containing lagoonal, back reef and reef margin facies. The lithology of outcrops varies widely, from heavily burrowed mudstones to recrystallized coraliferous rocks. Common fossils include casts of bivalves, algae, foraminifera and corals. Talisay Member (Tt) is the basal unit of the Alifan Limestone and consists of volcanic conglomerate, bedded clay, marl and clayey limestone as well as carbonaceous inclusions of peat and lignite.

Mariana Limestone, Pliocene and Pleistocene in age, forms about 80% of the exposed limestone of Guam. It is a complex of reef and lagoonal limestones, mapped as five units by Tracey et al. (1964). The reef facies (Qtmr) forms a discontinuous peripheral belt at or near the present cliffline. It is a massive, generally compact limestone, often highly porous and cavernous. It contains corals in position of growth in a matrix of encrusting calcareous algae. This facies encloses the detrital facies (Qtmd) and the molluscan facies (Qtmm), both of lagoonal origin. Detrital facies is friable to well-cemented white detrital limestone, ranging in lithology from coquina to coarse rubble to coral congomerate. Molluscan facies is fine-grained detrital limestone, containing casts and molds of mollusks in a medium to fine-grained matrix. The fore-reef facies of the Mariana Limestone (Qtmf) was deposited seaward of the reef margin and ranges in lithology from foraminiferal sands to rubbly-reef detritus. The Agana Argillaceous Member of the Mariana Limestone (Qtma) fringes most of the volcanic mass of southern Guam. It is a clayey limestone, with clay disseminated throughout (2-5%) and contained in pockets and cavities (20%). The facies is lagoonal in nature and has developed as patch reefs adjacent to volcanic highlands (which were the source of clays). Lithology ranges from coral conglomerates to fossiliferous limymudstones.

Merizo Limestone (Qrm) is a Holocene reef limestone locally capping Mariana reef rocks and basaltic rocks at sea level.

Modern Reefs grow around the coastline of Guam and were built by coral and algae during the past 3,500 years, and even longer in places. Most reefs on Guam are fringing reefs, and the largest are in Agana, Tumon and Pago bays. Small patch reefs are also common, the most notable example being at Double Reef. Reef surrounding the Cocos Lagoon on the southern tip of Guam and Luminao Reef in Apra Harbor are barrier reefs.

— *Chapter 3* —
INVENTORY OF KARST FEATURES ON GUAM

This chapter explains the process and methodology involved in the inventory of karst features on Guam. The inventory presented here is the first such attempt on Guam. It was performed as a part of a research project on island karst, a collaborative effort between the University of Guam, Mississippi State University, University of Charleston, South Carolina, and University of Puerto Rico. The purpose of this inventory was to obtain current information on the number, types and significance of karst features on Guam. It will provide the departure point for future studies of karst on Guam.

The inventory was performed in three phases. Phase I included collection and analysis of existing data. Phase II consisted of performing detailed field study of karst areas and mapping of selected features. Phase III included compilation of field and other data into a comprehensive database and creation of supporting maps and photo-documentation of the karst features on Guam.

3. 1. Review of Literature, Maps, Photographs and Anecdotal Information

3. 1. 1. General geology of Guam

"Historical Review of the Geology of Guam with References" (Pacific Islands Engineers, Noy-13626 [year unknown]) mentions that the earliest published records on the geology of Guam was by Dana and Agassiz (1903). However, the first island-wide geologic study was a generalized report concerned primarily with water supply, written in 1937 by H. T. Stearns. After Guam was regained from the Japanese in 1944, the first geological surveys were performed by A. Piper in 1946, who wrote a report on the water resources of Micronesian islands, and by J. Bridge who did mineralogical survey work on Guam in 1948. In 1950, Pacific Islands Engineers prepared a two-volume "Geology of Middle Guam" for the Department of Navy. The first comprehensive geologic studies of the entire island were done by the United States Geologic Survey (USGS) during the two decades following World War II. A preliminary report by Cloud (1951) was followed by a series of USGS Professional Papers published in the early 1960s, most notably the report by Tracey, Schlanger, Stark, Doan, and May, (1964) on the general geology of Guam, which included a 1:50,000-scale map of the surface geology of the island. (Other reports in the series were Emery, 1963; Stark and Tracey, 1963; Schlanger, 1964; Cole, 1963; Carroll and Hathaway 1963; Stensland, 1963; Johnson, 1964; Ward, Hofford and Davis, 1965; and Todd, 1966). Ward and Brookhart (1962) published an earlier report on the Military Geology of Guam which included a water resources supplement. An exhaustive bibliography of 20th century geoscience literature of Guam and other Mariana Islands was compiled by Siegrist (1992).

3. 1. 2. Hydrology of Guam

The first comprehensive hydrologic study was published by Ward et al. in 1965. The next was in 1976 by Mink. In 1980, the Guam EPA commissioned the most exhaustive study of the aquifer to date, directed by Mink. The study is locally known as the Northern Guam Lens Study (NGLS). The chief contractor for the study was Barrett, Harris, and Assoc., who published the study report in 1982. Local contributions to the NGLS by WERI included a hydrogeologic analysis by Ayers (1981) and a preliminary study of aquifer discharge by Zolan (1982). In 1992, Barrett Consulting Group prepared a revision of the 1982 study for Guam EPA, but the report was not published nor widely circulated. A report on the modeling effort was published by Contractor (1981) and Contractor et al. (1981). Contractor and Srivastava (1990) conducted calibration studies of the groundwater model on the NGLA using a microcomputer. Matson (1993) conducted studies on the nutrient flux through the aquifer and made estimates on the groundwater discharge along the coast. The most recent papers on the hydrogeology of Guam are the "Hydrogeology of Northern Guam" by Mink and Vacher (1997) and a groundwater modeling study completed by Jocson (1998) and Jocson et al. (1999).

3. 1. 3. Karst geology and hydrology of Guam

Stearns (1937) and Piper (1946) list freshwater (inland) springs of Guam. In their "Geology of Middle Guam" report, Pacific Islands Engineers (1950) briefly discuss the basics of karst

erosion and the modifying factors operating on Guam, and give a classification outline of solution phenomena on Guam. Tracey et al. (1964) provide a limited discussion of surface dissolution features of the limestone plateau. They suggest that sinkhole alignment in some places may be fault controlled.

Since 1994, WERI has been compiling an unpublished map of sinkhole distribution and fractures in northern Guam. WERI field data have continuously been entered into a GIS database, into an as yet unpublished hydrogeologic map of Northern Guam. Existing karst-related coverages, prior to this study, included the major fractures and faults and closed-contour depressions (found on USGS topographic maps), and a partial coverage of coastal springs and seep fields. Coastal springs and seeps (including underwater vents) in the northwestern part of Guam have been mapped in detail during the last two years by WERI (Jenson et al., 1997; Jocson, 1998, 1999). Recent dye tracing projects were conducted as part of Air Force environmental remediation project (Andersen Air Force Base, 1995) and US Navy's activities at Finagayan (Ogden Environmental and Energy Services Co., Inc., 1995).

As for the specific karst features, published data are limited. A report by Rogers and Legge, submitted to the Guam Department of Parks and Recreation in 1992, lists some of the main caves on Guam - predominantly those of cultural significance, known to have been used by ancient Chamorus. This report includes information from Vandegrift's (1958) memo to US Marine Corps regarding potential fallout shelters list. An exhaustive search revealed no other published report listing specific karst features of Guam.

The most recent published works on karst of Guam are the preliminary reports on karst geology and hydrology of Guam (Mylroie et al., 1999, and Mylroie et al., submitted).

3. 1. 4. Karst geology of other carbonate islands

The scientific literature on karst rarely addresses peculiarities of island karst. Development of karst on carbonate islands is a unique process, distinctly different from classic karst development in Europe, North America, and Asia. The most comprehensive model of island karst so far is that developed during the past two decades by Mylroie and Carew (Mylroie et al, 1995, Mylroie and Carew, 1995, 1997). This model is based exclusively on Caribbean Islands and it has successfully predicted the development of karst and consequent effects on island hydrology. Guam, being a Pacific island, possesses important differences from the Caribbean islands, islands that have been the basis for conceptual models of island karst up to date. Efforts are under way to incorporate complexities of karst on Guam into a general Carbonate Island Karst Model (Mylroie at al., 1999).

Very little work has been done on the karst of Pacific Islands (exclusive of continental islands of Indonesia and New Guinea), limited to brief speleogenetic studies on Tonga, Cook Islands and probably other islands. This project is a necessary step towards a greater awareness of complexities of Guam's karst system as well as a step towards a general carbonate island karst model.

3. 1. 5. Maps and aerial photographs of Guam

A geologic map of Guam, at a 1:50,000 scale was included in the USGS Professional Paper 403-A, General Geology of Guam by Tracey et al. (1964). Another report in this series, 403-H, Hydrology of Guam by Ward et al. (1965) included a water resource map of Guam at 1:50,000. USGS topographic maps that cover Guam include 1:50,000 Topographic Map of Guam, Mariana Islands and nine 1:24,000 topographic quadrangle maps (Agana, Agat, Apra, Dededo, Inarajan, Merizo, Pati Point, Ritidian, and Talofofo).

WERI's collection of ortho-corrected aerial photographs was extremely helpful in pinpointing areas of interest and locating specific karst features in the field.

3. 1. 6. Anecdotal information on karst of Guam

Activities in Phase I of the karst inventory included the acquiring as much anecdotal information as possible, so that it could be tested by field study. Representatives of federal and Government of Guam agencies were contacted for available information. WERI's points of contact with the US Air Force and US Navy were also interviewed. Village officials were particularly helpful and knowledgeable about karst features in their areas. During field trips, interviews with local residents often revealed significant new information. Local cavers, divers and hikers provided valuable specific information and often led various karst features' location and exploration efforts.

3. 2. Fieldwork

The most extensive and intensive part of the karst inventory was Phase II — fieldwork. I have been systematically exploring caves, sinkholes,

fractures and other karst features since January 1998. Most of my field work so far has been done together with my thesis advisor Dr. John Jenson, fellow graduate students David Vann, Mauryn Quenga and Karel Smit, WERI hydrologist John Jocson, and Curt Wexel and members of the Micronesian Cavers club.

In July 1998, Dr. John Mylroie from Mississippi State University joined us to conduct two weeks of preliminary fieldwork to lay the groundwork for anticipated comprehensive study. Dr. John Mylroie is one of the eminent world authorities on karst, and has given us some enlightening assistance in beginning to decipher the complexities of Guam karst. In July 1998, after funding for a two-year project was awarded by the USGS National Institute for Water Resources Research National Competitive Grants Program, we began systematic field study of Guam. In June 1999, our collaborating scientists Dr. Mylroie (Mississippi State University) and Dr. Carew (University of Charleston, South Carolina) visited Guam, to carry out additional fieldwork and sampling.

3. 2. 1. Hiking

The basis of most fieldwork included traversing karst areas on foot, looking for new karst features. Areas known to be rich in karst features, coastal areas, cliff lines and areas adjacent to volcanic terrain were examined most closely. Since many important karst features are exposed on cliff faces, rappelling and climbing was often necessary for direct investigation. Informal fieldwork schedules were usually prepared for a week or two in advance. The major time constraints were difficulties in finding partners on weekdays and being limited to low tides for coastal hikes. Fieldwork was carried out on weekdays and weekends and included camping overnight in some of the more remote locations, such as the northeast coast.

Access to privately or military owned areas was requested in advance. Private property owners were generally helpful. US Air Force and the US Navy provided valuable assistance and allowed access to even some of the more restricted areas such as the Navy Magazine. Locations in the field were determined using USGS topographic maps, aerial photos, compass and a hand-held GPS unit.

3. 2. 2. Aerial surveys and boat surveys

Surveys using small aircraft were extremely beneficial. On several occasions, small plane was chartered from Micronesian Aviation System, Inc. and flown at low altitude over areas of interest. I was also given the opportunity to fly with the Government of Guam's Department of Aquatic and Wildlife Resources biologist Todd Pitlik during his aerial surveys of fishing effort. Aerial observations were particularly helpful in locating cliff-face cave entrances, coastal depressions and fractures and examining overall coastal geomorphology.

UOG Marine Lab and private boats were used to access field sites and to carry out general reconnaissance of coastal areas. Boat surveys were particularly useful in identifying locations of sea caves and cave entrances in sea cliffs, especially in high surf areas where hiking at sea level is nearly impossible.

3. 2. 3. Cave mapping

Selected karst features deemed representative of a certain genetic or hydrologic type were surveyed and mapped in detail. Surveying and mapping were done using standard National Speleological Society techniques described in detail by Dasher (1994). In addition to typical caving equipment, devices used for surveying included an open reel tape, Suunto clinometer, Autohelm digital compass, and a Brunton standard compass. Whenever possible, caves and sinkholes were surveyed as a team effort, but time constraints made frequent solo surveying trips necessary (only carried out in small caves and sinkholes). In several instances, particularly to make a detailed map of Double Reef coastline, outside surveys were carried out using cave surveying techniques.

3. 2. 4. SCUBA exploration

Many of Guam's karst features lie permanently below the groundwater table. Being flooded, very little direct observational evidence was collected prior to this study. This lack of direct information on submerged karst is not unique to Guam— even Florida's flooded karst, despite its large and accessible caverns and Florida's sizable cave diving community, has been described as terra incognita (Lane, 1993).

Although members of Guam's recreational diving community have probably tried diving in some freshwater caves, no such dives were described or documented (with the exception of a memo describing a dive in Tarague Well #4 (Hogan, 1959) and a part of Micronesian Divers Association's "Aquaquest Micronesia" videotape). Freshwater cave diving and snorkeling are dangerous and potentially life-threatening activities and should be properly planned

and carried out.

Exploration of caves using SCUBA were limited due to inherent dangers involved in freshwater/ confined environment diving and were carried out in company of experienced cave divers. No surveying took place during SCUBA trips. Only sketches and general observations were made. Snorkeling observations were made in every karst features containing freshwater.

Several submarine features (see Chapter 11) were explored using SCUBA as well. Such features are much safer to dive in and were investigated both by snorkeling and using SCUBA.

3. 2. 5. Photography

Photo documentation of karst features was an important part of inventory efforts. Most inventoried features were photographed and a collection of several hundred slides and photographs was deposited at WERI. The best and most illustrative photographs are included in the Plates section of this report. For outside photography, a Canon Rebel X camera was used, with 28-80 and a 70-300 mm lenses. Film of choice was Fujichrome Velvia 100 ASA slide film, but a variety of other films were used as well. In caves, photography was assisted by a Canon flash and by slave strobes. Underwater photographs were taken using a Nikonos V camera with one or two strobes and a 35 mm lens. Slides and photographs were scanned for presentation and publication purposes using an Olympus ES-1 slide scanner and an HP ScanJet 3C flatbed scanner respectively.

3. 3. Database Compilation, Mapping Methods and Software

Phase III of the karst inventory included careful analysis and summarization of field notes and other data and compiling a karst inventory database. Locations of inventoried karst features were plotted on corresponding maps. This phase of the inventory process required extensive use of various software.

3. 3. 1. Karst inventory database

Phase I and Phase II of the inventory resulted in obtaining data on over 800 individual karst features. These karst features were inventoried and grouped based on their genetic and hydrologic properties. They were listed in a series of Microsoft Excel spreadsheets, grouped into following categories:

+ surface flow related features from northern Guam (SW)
+ surface flow related features from southern Guam (SWs)
+ high level springs from northern Guam (HSP)
+ high level springs from southern Guam (HSPs)
+ closed contour depressions from northern Guam (CCD)
+ closed contour depressions from southern Guam (sCCD)
+ caves from northern Guam (CAVE)
+ caves from southern Guam (sCAVE)
+ natural bridges, arches and cliff collapse scars (COL)
+ voids intercepted by drilling
+ coastal discharge features from Guam (CDF)
+ submarine karst features from Guam (SBM) and sea caves (SEA)
+ permitted storm water disposal wells (GEPA ID numbers)

Each of the categories above is represented by a unique spreadsheet containing all inventoried features of that category. Each feature was assigned a unique number (to ease map representation). Assigned ID numbers begin with a letter code indicating the type of a feature. Letter codes are listed in parentheses in the previous bulleted list. Inventory and maps of permitted storm water disposal wells use GEPA assigned ID numbers. All the karst inventory spreadsheets are included in this report as appendices.

Maps that correspond to the Appendices were generated using GIS software, as explained in one of the following sections. The maps illustrate the distribution of inventoried karst features and are included throughout this report, in appropriate chapters, with discussion of particular categories of karst features.

3. 3. 2. Specific data included

Because karst features inventoried during this project belong to vastly different types, it was necessary to collect different data for different types of features.

In Appendix 1 (inventory of permitted storm water disposal wells), the only data presented are GEPA ID number of wells and their owners. All 171 permitted wells are included in this Appendix. Corresponding locations of wells are shown on a map in Fig. 5. 3.

Appendices 2 and 3 present the inventory of surface water related karst features from northern and southern Guam respectively and include, in addition to name and ID number of a feature, landform type, an estimate of permanence of associated surface flow, source of water (allogenic vs. autogenic) and the geologic formation in which the feature has developed. A total of 21 such features was inventoried in northern Guam, and 16 in the south.

Appendices 4 and 5 (high level springs in northern and southern Guam) include name and ID number of a spring, type of spring, elevation, latitude and longitude, an estimate of minimum and maximum flow and water quality data, as well as the geologic units involved. A total of 7 high level springs were identified in northern Guam, and 15 in southern Guam.

Appendices 6 and 7 contain the inventory of closed contour depressions in northern and southern Guam. Although a total of 1252 depressions were identified in northern Guam and another 197 in southern Guam, only those deeper than 3.3 m (10 feet) were inventoried. At the conclusion of the project, a total of 208 such depressions were inventoried in northern Guam and a total of 72 in southern Guam.

Each closed contour depression listed in the inventory was separately evaluated for a number of characteristics and each inventory entry consists of the following:

1) Identifiers:
   a) KARST ID number
   b) Name; (if unknown, assigned based on USGS topographic maps)
2) Type or origin of the depression; (dominant mechanism, if known)
3) Geometry of individual features:
   a) length in meters (as defined by (Williams, 1971)
   b) width in meters (as defined by (Williams, 1971)
   c) orientation of the long axis (in degrees from 270° to 90°)
   d) depth in ft (listed in feet since it is based on maps with a contour interval in feet)
   e) area in square meters
4) Information regarding the location and general setting of the depression:
   a) distance to nearest neighbor in meters (distance to nearest known closed contour depression deeper than 10 ft)
   b) orientation of line to nearest neighbor (in degrees from 270° to 90°)
   c) geologic formation in which the depression has developed (according to Geologic Map of Guam by Tracey et al., 1964)
   d) description of general location of the depression (i. e., plateau, plateau edge, terrace, valley, etc.)
   e) past or current use of the depression, if any and if known
   f) location of the depression, in latitude and longitude (referring to the deepest point in the depression of geometric center if deepest point is unknown)

Information listed in the inventory is based on orthophotos and derived digital topographic lines as well as fieldwork. Type or origin of the features was determined by observations in the field, if possible. Geologic formation in which the depression has formed was determined based on the Geologic Map of Guam (Tracey et al., 1964). Past or current use of the depressions was determined based on USGS topographic maps (which indicate whether any quarrying has taken place), aerial photos and observations in the field. Locations of inventoried depressions are shown on a map in Fig. 7.2.

Appendices 8 and 9 present the inventory of caves in northern and southern Guam. Inventory of caves in northern Guam was carried out as a part of the inventory of karst features of Guam and a necessary step for further investigation of the Northern Guam Lens Aquifer. Caves on Guam appear to be belong in five major categories, with numerous sub-types: 1) pit caves, 2) stream caves, 3) fracture caves, 4) flank margin caves, and 5) lens voids. The word "cave" is not a genetic definition but a descriptive one, being defined as anything from "solutional cavities >5-16 mm in diameter" (Ford, 1978) to "natural opening in the earth, large enough to admit a human being" (White, 1988). Because this thesis is organized into chapters based on hydrologic and genetic qualities of karst features, "caves" cannot be discussed in their entirety in any given section. Nevertheless, an integrated inventory of all known caves in northern Guam is presented in Appendix 8, and in southern Guam in Appendix 9. A total of 79 caves was inventoried in northern Guam and 60 caves in southern Guam.

Specific information associated with inventoried caves include the following:

1) Identifiers:
   a) KARST ID number
   b) Name
2) Type or origin of the cave
3) Description of the entrance
   a) Setting or type of entrance

b) width in meters
c) height in meters

4) Information on the size of rooms and passages
5) Cave setting
   a) cave floor
   b) presence of water in the cave
   c) geologic formation
6) Location of cave entrance
7) Any additional data

Appendix 10 lists the inventoried natural bridges, arches and large collapse areas in northern Guam (suspected of being collapsed karst features).

Appendix 11 contains information on about 300 voids intercepted by drilling of wells in northern Guam. Location of well, depth to void and size of void (if known) are given.

Appendix 12 is an inventory of coastal discharge features. All documented discharge sites along Guam's coastline are listed here, along with discharge volume estimates if any were made.

Appendix 13 is a brief inventory of known submarine karst features. No extensive work was done on the submarine karst and this list is biased towards better known features, particularly popular dive sites.

3. 3. 3. Karst inventory GIS maps

Geographic Information System (GIS) software is the standard software used for representation of spatial data and generation of maps. Software used to make maps presented in this report is ESRI ArcView GIS 3.1. The main data sources used by GIS software are GIS coverages — digital maps representing distribution of a particular group of features. Coverages may be point, arc or polygon coverages and are used to represent point, linear and area features, respectively. For example, a map showing distribution of cave entrances would be a point coverage file, a map of sinking streams would be an arc coverage, and a map of sinkholes could be a polygon coverage. Coverages are used to generate GIS maps and are regarded as "layers" of a map. Specific GIS coverages are combined to build customized maps. It is necessary that all coverages are in the same coordinate system. Coordinate system used to generate GIS maps presented in this report is the Guam Grid (feet) coordinate system.

Existing published data, such as on topographic maps, was digitized using a digitizer board and ESRI ArcInfo software. The vast majority of data presented in the maps of this report, however, were collected in the field. Because GPS locations acquired in the field proved to be inaccurate, locations of specific features were entered into GIS maps based on ortho-corrected aerial photos. These aerial photos are formatted as GIS coverages so that other maps may be overlain on top of them. This enabled me to zoom into particular areas of interest, compare field notes with aerial photos and pinpoint exact locations of karst features. The result of this effort is a series of over thirty GIS coverages illustrating the distribution of various types of karst features. All coverages are included in maps throughout this report. The exact locations of particular features may not be obvious on large scale maps included in this report, but more precise locations can be viewed directly from GIS coverages on a CD deposited at WERI.

3. 3. 4. Other software used

In addition to GIS software, a number of other programs was used to analyze and present the data. Cave survey data was entered into Compass Survey Editor 2.0 and were viewed and printed in Cave Viewer 2.99 (both available as shareware programs at www.karst.net). Maps were then sketched by hand, scanned and finalized using Adobe PhotoShop 5.0. The same program was used for processing photographs. All figures and photographs included in this report were made or scanned at 300 dpi resolution.

To analyze lineament orientation and prepare rose diagrams, RockWare's RockWorks 98 was used. Blue Marble Geographics was used to convert locations of karst features between Guam Grid coordinate system and latitude and longitude. The karst inventory database was compiled in Microsoft Excel 98. The same program was used to make tables and graphs. Word processing was done in Microsoft Word 98, and final layout of text and graphics was prepared using Adobe Page Maker 6.5.

— Chapter 4 —
KARREN AND PHYTOKARST

This chapter investigates the minor dissolutional and accretional features found on subaerially exposed surfaces of soluble rocks. If made by water dissolution, such features are known as karren. If living organisms contribute to their development, such features are termed phytokarst. This chapter presents overall diversity of karren and phytokarst on Guam.

4. 1. Karren

Subaerially exposed surfaces of soluble rocks are the first to come in contact with meteoric water. Precipitation attacks free rock surfaces and modifies them by solution. Raindrop impact, sheet flow, channeled flow, and stagnant water create a plethora of small solution sculpturings on the bedrock surface of soluble rocks. These sculpturings are known as karren or lapiéz (Bögli, 1960). Karren have been described as the most widespread karst features (Ginés, 1995). They are extremely diverse, affected by very specific environmental conditions and are often transitional into one another (White, 1988).

Karren forms develop best in massive, thick-bedded, fine grained and homogeneous limestones (Ford and Williams, 1989). Limestones exposed in northern Guam are not like that. They are young, have not fully undergone diagenesis and are mostly coarse-grained heterogeneous reef limestones retaining high primary porosity. These qualities prevent even small-scale flow of water over rock surfaces. Consequently, there are very few types of hydraulically controlled karren in northern Guam. Nevertheless, karren in general are well developed and common in all limestones. One exception is Barrigada limestone, which is a friable foraminiferal limestone and as such shows no solutional sculpturing (the only small-scale groves seen on Barrigada Limestone rocks were slickensides). Porous and mechanically weak rocks could be unfavorable to karren development (Jennings, 1985).

Dissolutional topography can be recognized at extremely small scales, even micrometers (Ford and Williams, 1989). Such small-scale features are known as microkarren, which is not a genetic term. Karren can also develop below the soil mantle, in which case it is different from "free" karren. Microkarren and subsoil karren were not investigated during this project.

Karren forms can be seen in northern Guam anywhere limestone rocks are exposed. Karren is ubiquitous around the perimeter of northern Guam, between the coastline and the cliffline, as well as limestone outcrops elsewhere. Karren are rare in the interior of the northern plateau because few limestone outcrops are found there.

4. 2. Karren Types in Northern Guam

No comprehensive text has been written about karren, so definitions vary and multiple terms for same features are still used in scientific literature. Bögli (1960) classified karren based on soil and vegetation coverage. White (1988) attempted to create a genetic classification and divided karren into etched forms and hydraulic forms. Etched forms were subdivided into those in massive bedrock (with no control by structural weaknesses) and those controlled by structural weaknesses. Hydraulic forms were subdivided into those made by channel flow and those made by sheet flow. Ford and Williams (1989) argue that karren genesis is not sufficiently understood and present a classification scheme based on morphology. Discussion of karst features in this thesis is organized based on their genetic and hydrologic properties instead of morphology, and the same approach was attempted in this chapter as well. Because of that, I have followed the genetic classification by White (1988) but individual karren names, descriptions and interpretations come from a variety of sources.

The following is an inventory and description of karren forms identified in northern Guam. A summary is given in Table 4. 1. Karren from northern Guam are mostly etched, with few hydraulic forms and no channel flow forms. This is because limestones in northern Guam have not undergone sufficient diagenesis and do not support any surface water flow, even at very small scales or under heavy rainfall. Surprisingly, even the argillaceous facies of Mariana Limestone, whose high clay content makes it less permeable, shows no channel flow controlled forms. A summary of field observations, showing types of karren documented in different lithologies is shown in Table 4. 2.

Mylroie et al. (1999) suggest that karren development is almost entirely independent of the

setting (island vs. continental), except in coastal areas. However, because the strongest controlling factors in development of karren are lithological and environmental (Ginés, 1996), karren forms differ significantly in various settings. Main differences between karren on Guam and karren in continental settings are the rarity of hydraulically controlled forms on Guam and absence of channel flow forms in northern Guam. Such forms are the most common forms in continental karst. Also, algae and other biota probably play a greater role in shaping karren on Guam and other tropical locales than they do in non-tropical continental settings. Karren on Guam is rarely devoid of at least some algae. Influence of algae may be the reason karren on Guam, unlike karren of continental karst, is so chaotic, with little gravitational control or linearity. Visually, relief of karren forms in Guam and probably other similar islands appears greater than that in classical karst areas. Finally, in some respects karren differs even within tropical carbonate islands: solutional basins (kamenitzas), which were observed on Isla de Mona, Puerto Rico, are absent in northern Guam.

Table 4. 1: Karren (except microkarren and subsoil karren), phytokarst and karrenfeld types in northern Guam.

ETCHED FORMS			
Massive bedrock		Structural weaknesses	
Solution pits[1]	+	Kluftkarren (cleft karren, splitkarren)	+
Rain pits	+	Groovekarren (splitkarren)	*!
Kamenitzas (Tinajitas, solution pans)[2]	*	Trenchkarren (splitkarren)	-
Spitzakarren	+	"Giant grikes"	!
HYDRAULIC FORMS			
Chanel flow		Sheet flow	
Rinnenkarren	!	Rillenkarren	+
Wandkarren (decantation runnels)	-	Trittkarren (heelprints, stepped karren)	-
Meanderkarren	-	Ausgleichflache (planar solution surfaces)[4]	+
Fluted scallops (solution ripples)[3]	-	Decantation flutings[5]	+
MIXED CONTROL FORMS			
Pit-and-tunnel karren	+	Solution wells (karren shafts, wells)	+
PHYTOKARST[6]			
Destructive (erosional)		Constructive + Root Action	
Amorphous (speleothem decay, moonmilk)	+	Tuffaceous stalactites	+
Directed phytokarst	*	Directed speleothems	+
Littoral phytokarst, lacework morphology	+	Tufa deposits in waterfalls	!
Black coated pits[7]	+	Root accretions, Root grooves[8]	+
KARRENFELDS			
Littoral karst	+	Stony grounds[9]	+
Littoral phytokarst	+	Pinnacle karst	+
Rainfall solution karrenfeld	+	Karst pavement	*

+ present in northern Guam, - absent, * similar features present, ! absent in northern Guam but found in southern Guam. Classification of karren modified from White (1988). Changes: 1- from Ford and Williams (1989), 2- originally listed as sheet flow feature, 3-5- added from Ford and Williams (1989), 6- from Bull and Laverty (1982), 7- from field observations on Guam, 8- from Wall and Willford (1966), 9- from Gines (1996)

Table 4. 2: Types of karren observed in different limestones in northern Guam.

	Karren type \ Geol. Formation	Qtmr	Qtmd	Qtmm	Qtmf	Qtma	Tal	Tbl	Tj	Tb
Etched forms	Solution pits	+	+			+	+			
	Kamenitzas (solution pans)	+	-	-	-	+	-	-	-	
	Spitzakarren	+	+	+	+	+	+	-	-	
	Rain pits	+	+	+	+	+	+	-	+?	
	Kluftkarren	+				+	+		-	
	Groovekarren	+				+	+		-	
Hydraulic	Karren from channel flow	-	-	-	-	-	-	-	-	
	Rillenkarren	+	+			+	+	-	-	
	Ausgleichflache	+	+					-	-	
	Decantation flutings	+	+	-	-			-	-	
Mix	Pit-and-tunnel karren	+	+	+			+	-	-	
	Solution wells, pipes, shafts	+	+	+		+	+	+		

+ feature present, - feature absent, (blank) feature not observed. Bonya Limestone was not observed. Explanations of geologic formation abreviations are found in section 2. 3.

4. 2. 1. Etched forms in massive bedrock

Solution pits

Solution pits (Plate 2, photo 1) are the most widespread karren forms. They are circular, elliptical or irregular pits, occur singly or grouped, and rarely exceed 1 meter in diameter. They are predominant where rocks are very heterogeneous, as in reef limestones (Ford and Williams, 1989). These features, as can be expected, are extremely common in northern Guam. They seem to develop from primary pores, places where a fossil had been removed or random places. Solution pits should not be confused with solution wells and shafts which drain into the epikarst. Solution pits drain by evaporation, overspill and/or seepage through pores or microfissures (Ford and Williams, 1989).

Rain pits

The smallest solution pits have been attributed to rain impact. Rain pits are small pits in bedrock, no more than 3 cm across and 2 cm deep (Jennings, 1985). Although small pits with sharp points and ridges (spitzkarren) are the most common karren type on Guam, it is not known whether pits in karren are made by rain. White (1988) regards spitzkarren one of the least understood karren types. Rainpits probably occur in all limestones in Guam but are difficult to notice because they become part of chaotic spitzkarren.

Janum Limestone, which is exposed in northern Guam in few sites near Catalina point, is the single limestone in northern Guam lacking spitzkarren development. Because Janum Limestone rock surface is unaffected by other karren types, potential rain pits are easily discernible. Small pits found in Janum limestone are up to 3 centimeters in diameter, circular or elliptical with no obvious directionality (Plate 2, photo 2). These features might be rain pits. They are not present everywhere in Janum rocks' surfaces but only at a single location few m^2 in area where they occur in a cluster.

Spitzkarren

This is one of the most variable and least understood karren types (White, 1988). Limestones surfaces are etched in such a way, as to leave a chaotic network of sharp points, solution pits and irregular holes (Plate 2, photo 3). Sharp points develop in the nodal points between the pits.

Small pinnacles and pits in spitzkarren reach a height of a few centimeters. There is a continuum in scale between this type of karren sculpturing, few centimeters tall, and entire karrenfeld landscapes, with pinnacles over a meter in height (White, 1988).

In northern Guam, spitzkarren is a very common karren type and occurs in all limestones (except Janum Formation). Development of spitzkarren probably takes place in absence of soil cover and may be heavily influenced by plants and algae (White, 1988). This is certainly true in coastal areas of Guam where spitzkarren grades into sharper and more complex "phytokarst" (Folk et al., 1971).

Kamenitzas (solution pans)

Water that ponds in flat limestone areas creates a solution basin (White, 1988). These features are known by the Serbo-Croatian term kamenitza or the Spanish term tinajita. Stagnant water in the basin accumulates carbon dioxide from algae and plant debris and becomes very corrosive (White, 1988). They are found on most rock pavements (White, 1988) and bare or lightly vegetated rock areas (Ford and Williams, 1989). During the course of this project, kamenitzas have been identified on karst pavements on Isla de Mona, a carbonate island near Puerto Rico. In northern Guam however, no true kamenitzas have been found.

Nonetheless, kamenitza-like forms are common, but only in the spray zone of Guam's coastal areas (Plate 2, photo 4). Flat-bottomed, shallow basins (pans) have developed nestled among coastal karst pinnacles. These "littoral kamenitzas" frequently show structural control and develop at intersections of joints (Plate 2, photo 5). When joints become solutionally widened enough to quickly drain water, the pans stop to function (Plate 2, photo 6). These features may also develop along a single joint in which case they are elongate (Plate 2, photo 7).

The basins do not show overflow or inlet or outlet channels and may be active or dry. Water salinity and temperature varies extremely, both temporally and spatially. Waters of various chemistries, from freshwater (accumulated rainfall) to hypersaline water (evaporating seawater) and even salt crystals (Plate 2, photo 8) can be seen in these basins. Nothing like kamenitzas has been found in northern Guam away from the coastal sea-spray zone.

4. 2. 2. Etched forms controlled by structural weaknesses

Kluftkarren (solutionally-widened joints)

Ford and Williams (1989) state that vertical fissure-controlled linear karren, known as kluftkarren (or grikes) are the main features in most karren assemblages and act as principal drains into the epikarst. They also note that kluftkarren is often the only type of linear karren developing in young reef rocks. In northern Guam, kluftkarren is the only common linear karren type (Plate 3, photo 1). Other forms (except rare groovekarren) are restricted by textural complexity and lack of bedding planes in reef limestones.

Since kluftkarren develop along sets of joints, they tend to intersect at 60°, 90° and 120° angles. At the points where kluftkarren intersect, cylindrical pits develop (Jennings, 1985). In their early stages of development, pits at joint intersections may be star-shaped (Plate 3, photo 2).

Joints may get extremely enlarged and become large enough to be traversed by people. Joints that large are not common in northern Guam, but notable examples exist. Tweed's Cave inland from Double Reef is one such feature. Not really a cave, this enlarged joint is about 2.5 meters wide and 16 meters long. The joint is northwest-southeast trending and is found in the reef facies of Mariana Limestone.

Groovekarren (solutionally-widened bedding planes)

Groovekarren are a horizontal equivalent to kluftkarren. They develop as horizontal grooves along bedding planes (White, 1988). Limestones in northern Guam are generally not horizontally bedded and groovekarren development is not favored. Nevertheless, some examples of groovekarren have been found (Plate 3, photo 1). They probably develop by widening horizontal joints rather than bedding planes. Accordingly, similar karren occur in all orientations, not just vertical and horizontal (Plate 3, photo 3). Such features are known as splitkarren, an umbrella term introduced by Pluhar and Ford (1970) to encompass all karren developing along joints and small fractures.

4. 2. 3. Hydraulic forms resulting from channel flow

No such karren forms have been identified in northern Guam. The limestone rocks are too porous and too irregularly etched to allow focused water flow at the surface.

4. 2. 4. Hydraulic forms resulting from sheet flow

Rillenkarren

Rillenkarren are a type of channel karren, probably a result of sheet flow. An excellent example of rillenkarren can be seen along the vertical walls of a pit cave developed in detrital Mariana Limestone at Amantes point (Plate 3, photo 4). Evenly-spaced, parallel troughs, with rounded cross-sections and sharp cusps between adjacent rills extend vertically along more than 5 meters. These rillenkarren are of exceptional length and dominate the walls of the cave. The length of rillenkarren increases with an increase in slope (White, 1988) and their depth diminishes down slope (Ford and Williams, 1989).

Rillenkarren at Amantes point pit cave are a textbook example and all other rillenkarren found in northern Guam are less ideal. This may be because

most limestones in northern Guam are coarse-grained and very heterogeneous. Ford and Williams (1989) write that rilling is partial or absent in such rocks.

Nevertheless, rillenkarren exist in many places in northern Guam, but never in such good condition as in Amantes pit cave. They may have been well developed but are now less ordered and mixed with other karren types. They are always on vertical or nearly vertical rock surfaces (pit caves, cliffs and walls of boulders). For example, a pit cave near Taga'chang Beach has rillenkarren along its walls, but the rills are difficult to notice in the rough and irregularly etched Mariana reef limestone. The same can be said for rillenkarren found on coastal cliffs (Plate 3, photo 5).

Closely spaced solution rills can be formed on steep-slopes of boulders (White, 1988). Some have been observed near the tops of large coastal boulders in northern Guam. However, the limestone surfaces in northern Guam are extremely irregularly etched and linear karren features are difficult to notice due to overprinting by irregular karren. Linear patterns are best seen from a distance.

Ausgleichflache (planar solution surfaces)

Rillenkarren diminish in depth down slope (Ford and Williams, 1989) and are eventually replaced by a planar solution surface (Ausgleichflache) (Bögli, 1960). The water moves over these surfaces as a thin sheet (Jennings, 1985). Ausgleichflache can only be identified in northern Guam in a few areas where sheet flow happens on vertical rocks that are protected from meteoric environment, thus preventing overprinting by other karren. A good example of a planar solution surface are smooth rock walls of lower parts of Amantes pit cave, below areas where rillenkarren have developed.

Decantation flutings

Decantation flutings are adjoining, shallow linear channels. They form on steep or overhanging slopes, by water released from a linear source, such as a soil mat at the top of the cliff (Ford and Williams, 1989). A thin film of water retained on the slope by surface tension is necessary for fluting to develop. Such films cause "lineations" oriented in the direction of flow (Allen, 1977). Decantation flutings are common on the Mariana limestone cliffs along northern coast of Guam. They appear as vertical lineations visible on the cliff-faces from a distance (Plate 3, photo 6). The difference between decantation flutings and rillenkarren is that decantation flutings are made by water released from up-slope storage, whereas rillenkarren are a product of direct rainfall (Ford and Williams, 1989).

4. 2. 5. Mixed hydraulic and structural control forms

Pit-and-tunnel karren

This karren type was described by Pluhar and Ford (1970). It is a form of cavernous weathering where a series of pipe-like blind circular passages criss-cross a rock. The small tunnels do not lead water into the epikarst; they are just a superficial phenomenon (Ford and Williams, 1989). On Guam, this type of karren is common and is most easily observed in separated limestone boulders (Plate 3, photo 7). It appears to be present only in boulders that have been unearthed. White (1988) suggests a soil cover may be useful in developing of this karren form.

Solution wells, soil pipes, solution chimneys and shafts

Solution along joint and fracture intersections may allow localized water input to generate vertical solution features (White, 1988). The scale of these features is highly variable and continuous from holes a fraction of a meter deep to large vertical shafts and pit caves. Although many authors discuss these features alongside other karren types (White, 1988; Ford and Williams, 1989), in this paper they are included in Chapter 5, with the discussion of the subcutaneous zone. This is because unlike other karren forms, which are merely solutional sculpturing of the rock surface, solution wells, pipes and shafts play an important role in the transport of vadose water. They provide by-passes to descending meteoric waters and are highly significant hydrologically. If such features are traversable, they are considered vadose caves and are discussed in Chapter 8.

4. 3. Calcrete, Case-hardening and Beachrock

Calcrete occurs in areas where evaporation exceeds precipitation. It involves chemical precipitation of soil, alluvium or weathered rock by carbonate-rich waters (Goudie, 1983). A good example occurs at Tarague, in a few closed depressions, that commonly act as sediment traps. Tarague Well #3 is a shallow, flat-floored sinkhole containing calcrete. Flat floors of sinkholes may be indicative of a thick layer of sediment infilling (White,

1988). Mariana limestone calcified paleosol rocks from the sinkhole floor are calcrete floatstones containing coral and mollusk fragments cemented in a soil matrix (Plate 4, photo 1).

Case-hardening was first recognized in the Caribbean region. It is a phenomenon of strengthening rocks via vadose diagenesis, thus allowing karst development in mechanically weak rocks such as aeolianites (Ford and Williams, 1989). Case-hardening is important in stronger rocks as well, such as emergent coral reefs. Primary pores within coral-algal framework can get infilled by flowstone, thus making the rock in the vadose zone less permeable. Flowstone-infilling of primary voids is common on Guam and can be observed in quarries and road cuts. Infilling of primary porosity occurs at the small scale as well, as can be seen in thin sections from drilling cores (Jenson and Siegrist, 1994).

Beachrock is consolidated deposits made by lithification of calcium carbonate sediment in the intertidal zone, mostly along tropical coasts (Scoffin and Stoddart, 1983). On Guam, beachrock occurs locally in all beaches along the west and north coast of northern Guam (Plate 4, photo 2). It usually dips seawards, like the unlithified beach surface, and its composition appears identical to the composition of surrounding calcareous sand (Plate 4, photo 3).

4. 4. Phytokarst

In addition to solution by meteoric waters, living organisms may also influence the development of karren and related karst features. These forms have been described as phytokarst (Folk et al., 1971) and biokarst (Viles, 1984). The original name phytokarst, coined by Folk et al. (1971) to refer to algae-made jagged tropical littoral karrenfelds was later expanded by Bull and Laverty (1982) to include many more rock-biota interactions, grouped as biolithogenic, destructional, physical (root-action) and constructional. In this paper, the term "phytokarst" will be used *sensu lato*, as re-defined by Bull and Laverty (1982) who called Folk's (1971) original "phytokarst," lacework morphology.

4. 4. 1. Destructive (erosional) phytokarst

Bull and Laverty (1982) list several types of destructive phytokarst, grouping them into amorphous, directed and subaerial types. All three types have been documented on Guam.

Amorphous phytokarst is caused by erosional activity of algae and microorganisms and results in speleothem decay. It appears as loose powder or wet pasty mass (Plate 4, photo 4). On Guam, it is visible at cave entrances and especially along the cliffs, in bio-erosional notches and breached flank margin caves.

Directed phytokarst consists of an assemblage of light-oriented karren-like forms on rocks, made by algal action. It was first recognized from tropical cave entrances in Malaysia (Brook and Waltham, 1978). Not much work has been done on these features, but they appear common and diverse in Sarawak. In Guam, small-scale features similar to directed phytokarst but covered by green algae (Plate 4, photo 5) were documented in caves at Ritidian, whose large entrances and wide twilight zone provide a suitable environment. These features are rare.

The third type of erosional phytokarst is the lacework morphology originally described by Folk, et al. (1971) and named "phytokarst." In this paper, such lacework morphology is referred to as littoral phytokarst.

Lacework morphology (phytokarst — Folk et al., 1971, coastal karren)

Lacework morphology phytokarst dominates the coastline of northern Guam. It is a common type of biologically mediated karrenfeld, found in the tropics, predominantly along the coastlines. It is characterized by pits with extremely jagged edges and sharp pinnacles (Plate 4, photo 6). This grotesque sculpturing is thought to be caused by endolithic filamentous blue-green algae. The dark color of the algae is apparently an adaptation to strong sunlight and a way to preserve chlorophyll (Folk et al., 1973). Pits, pinnacles, sharp edges, and completely penetrating holes are characteristic morphology, repeated on a continuum of scales. The tallest pinnacles on Guam, found north of Haputo Beach, are four to five meters tall, but typically, the relief is about .5 to 1.5 meters. There is no gravitational orientation to this type of karst. Its development seems to be under no structural or lithologic control. Paleosols, often found incorporated in coastal limestones are readily identifiable by their brown color, but not by texture, which frequently gets sculpted the same way as the bedrock.

The presence of paleosol in lacework morphology phytokarst on Guam is interesting, not only as an indicator of a past lower sea level but as a potential clue to the origin of lacework morphology. Folk et al., 1973, do not discuss development of

phytokarst in different lithologies and list dark, almost black, rock color as the primary characteristic of phytokarst. In Guam, pockets of paleosol, orange to brown to bronze in color, are sculpted in nearly the same way as the bedrock. Lighter color of paleosol surfaces may indicate presence of fewer endolithic algae than in the surrounding limestone, yet the dissolutional morphology is the same (Plate 4, photo 7). This raises the question of whether algae are really fundamental in the process. Mylroie and Carew (1995) refer to this type of dissolutional morphology as coastal karren and regard phytokarst as an inappropriate term. Viles (1984) argues that biological activity in the development of coastal karren has been overstated. Sculpted pockets of paleosol in Mariana Limestone on Guam support this idea. Paleosol pockets in coastal phytokarst can be found throughout Guam's coastline, but some of the best examples are in Mangilao (Thousand Steps) and in southern Guam (south side of Orote Peninsula, Asanite area in Ipan, Anae Island, etc.)

Black coated pits

Another type of phytokarst, not mentioned in Bull and Laverty's (1982) review, was documented in coastal caves in northern Guam. It can best be described as shallow pits in a vertical wall, coated by a layer of black colored algae or cyanobacteria (Plate 4, photo 8-left). They occur in coastal cave entrances with enough light. It is unclear if the pits are made by algae or the algae colonized the pitted wall. Identical pits without black coating exist in areas with no direct sunlight (Plate 4, photo 8-right).

4. 4. 2. Root-action phytokarst

Roots may have both erosional and binding effect on calcareous rocks (Wilford and Wall, 1964, Wall and Wilford, 1966). It has been argued that roots may influence the development of important karst features, such as calcrete (Klappa, 1978) and pinnacle and shaft development (Tricart and DaSilva, 1960).

During this project, fieldwork has revealed curious small solution or accretion features not previously described in literature. They are up to 7 cm tall tufaceous stalks found in the centers of small solution pits within limestone bedrock. The base of the stalks, at the bottom of solution pits, is weak enough to be broken by hand. There appears to be a partially-infilled hole running the length of the stalks. These features are shown on Plate 5, photo 1. The roots may have grown in the soil that accumulated in solution pits and then had a binding effect on the soil and caused the creation of the tufaceous stalks.

Another root-made feature on limestone is called root grooves. They were named and described by Wall and Wilford (1966) as irregular ramifying series of hemispherical groves, up to 12 mm in diameter, based on examples from Sarawak. Excellent examples of root grooves were found on the walls of a cave-collapse boulder at Taragüe (Plate 5, photo 2).

4. 4. 3. Constructive (depositional) phytokarst

Tufa deposits and travertine are commonly associated with karst springs, outflowing rivers and waterfalls. They are made by waters supersaturated with respect to calcium carbonate, after evaporation causes simultaneous formation of clusters, crystallites and small crystals. The newly made solid, known as tufa, is of high porosity, poorly ordered, lacks the luster of crystalline surfaces and feels crumbly and "earthy" (Ford and Williams, 1989). Organic processes are very important, and it has been shown that mineralization occurs around algal filaments (Casanova, 1981) and that bacterially precipitated calcite can form a large portion of tufa deposits (Chafetz and Folk, 1984).

In northern Guam, tufa deposits are found in two environments: on the cliff faces as tufaceous stalactites, and in cave entrances as directed speleothems.

Tufaceous stalactites

Bioerosional notches and breached flank margin caves along the cliffs in northern Guam often have significant speleothem deposits in them. These speleothems, however, are tufaceous, feeling crumbly, slimy and powdery. It is presently not known if tufaceous speleothems are a result of cave speleothem degradation when exposed to outside atmosphere or if they are currently growing tufa deposits.

Tufa stalactites and tufa "flowstones" have been found in the Double Reef area inside low elevation notches that are bioerosional in nature and have never been inside cave atmosphere. Entrances of large caves in Ritidian and Taragüe that have been broadly open to outside atmosphere by cliff retreat also have significant tufaceous speleothems in them, including large and thick columns. A thick white stalagmite from a Ritidian cave was collected and examined. The sample is white in color, powdery and very lightweight, yet 20 cm in diameter. Its texture was uniform throughout, from the outer surface to its core (Plate 5, photo 3).

Directed speleothems

Tufaceous stalactites leaning towards the light source are found in cave entrances at Ritidian. In low cave entrances with limited light penetration they look like they are made of mud (Plate 5, photos 4 and 5), while in large, cliff-side entrances of caves they look like they are made of white powder. These "stalactites" are entirely made of tufa deposits and are often not vertical (Plate 5, photo 6). It is thought that bacteria and/or algae cause preferential deposition on the "speleothem" side that faces the light, thus causing the leaning (Bull and Laverty, 1982).

4. 5. Karren Assemblages in Northern Guam (Karrenfelds)

Multitudes of karren forms are rarely simple or monogenetic. Most karren forms are composite, widely varied and polygenetic (Ford and Williams, 1989). Extensive areas of karren develop in most soluble rock terranes; they often contain many different karren types and are known as karrenfeld (karren fields). In northern Guam, four common karrenfeld types have been identified. Areas immediately adjacent to the coast are dominated by littoral karst and littoral phytokarst (lacework morphology). From the peritidal zone, littoral karst grades inland into littoral phytokarst, which dominates the sea-spray zone, and grades landward into normal rainfall-solution karrenfeld. Further inland, usually adjacent to the cliffs, land surface is covered by scattered boulders, blocks, and rubble. Two additional karrenfeld types are less common. Inland pinnacle karst, similar to phytokarst but found away from the coastline exists in the limestone forests around the perimeter of the island and in the Alifan Limestone near Mt. Santa Rosa. A few limited bare areas near the coast have low smooth topography reminiscent of karst pavements. Most of the northern plateau shows no karrenfelds because the surface karst features are covered by soil or destroyed by development.

4. 5. 1. Littoral karst

Coastal limestones, in addition to being attacked by chemical dissolution and bio-erosion by marine organisms, are also sculpted by wave erosion, wetting and drying, hydration and salt weathering (Ford and Williams, 1989). According to the same authors, the factors influencing littoral karst development are wave energy, tidal range, lithological variations and climate. Relative contribution of these factors in a given environment shapes the overall appearance of littoral karrenfeld.

The most characteristic features of littoral karrenfelds in northern Guam are the bioerosional notches and a high density of pits, pans, and pinnacles (Plate 6, photo 1). Also common are leftover portions of eroded Pleistocene reef bedrock remaining on the modern reef as small phytokarst platforms (Plate 6, photo 2). These "islands" are continually attacked by grazing mollusks, boring algae and sponges, also responsible for the bioerosional notches. When larger individual limestone blocks discontinuous with the coast get bioeroded, the circumferential notch gives it a mushroom form (Plate 6, photo 3).

4. 5. 2. Littoral phytokarst

Immediately inland from the wave-affected littoral karst, endolithic algae become the dominant force shaping littoral tropical karrenfelds. They erode limestone in an extremely irregular manner, giving it a distinguishing dark color and grotesque lacework morphology. Karrenfelds dominated by lacework morphology are full of pits and pinnacles and are extensive along the northern Guam coastline (Plate 6, photo 4). They form truly the most fascinating karrenfeld landscapes on Guam. The overall topography decreases inland, with pits being infilled with soil and supporting some vegetation (Plate 6, photo 5).

Different littoral karst and littoral phytokarst development in various locations in northern Guam are shown in Fig. 4. 1.

4. 5. 3. Rainfall-solution karrenfeld

This is the dominant landscape wherever bedrock limestone is exposed in northern Guam away from the coast. It is typically found in limestone forests and slopes between the coast and the cliffs. It is usually continuous with littoral phytokarst and quite similar to it, often retaining dark color and algal cover. However, endolithic algae play a lesser role in dissolution of inland rocks. Because of this, several important differences exist between littoral and rainfall-solution karrenfelds. The latter are not as irregular and jagged and not as dark as the littoral phytokarst (Plate 6, photo 6). They occasionally show limited linear features, such as fluting.

Folk et al. (1973) described "black phytokarst" and ordinary rainfall solution karst as two end members of small scale dissolution features on a carbonate island (Cayman Islands). On Guam, both coastal phytokarst and inland rainfall solution karst

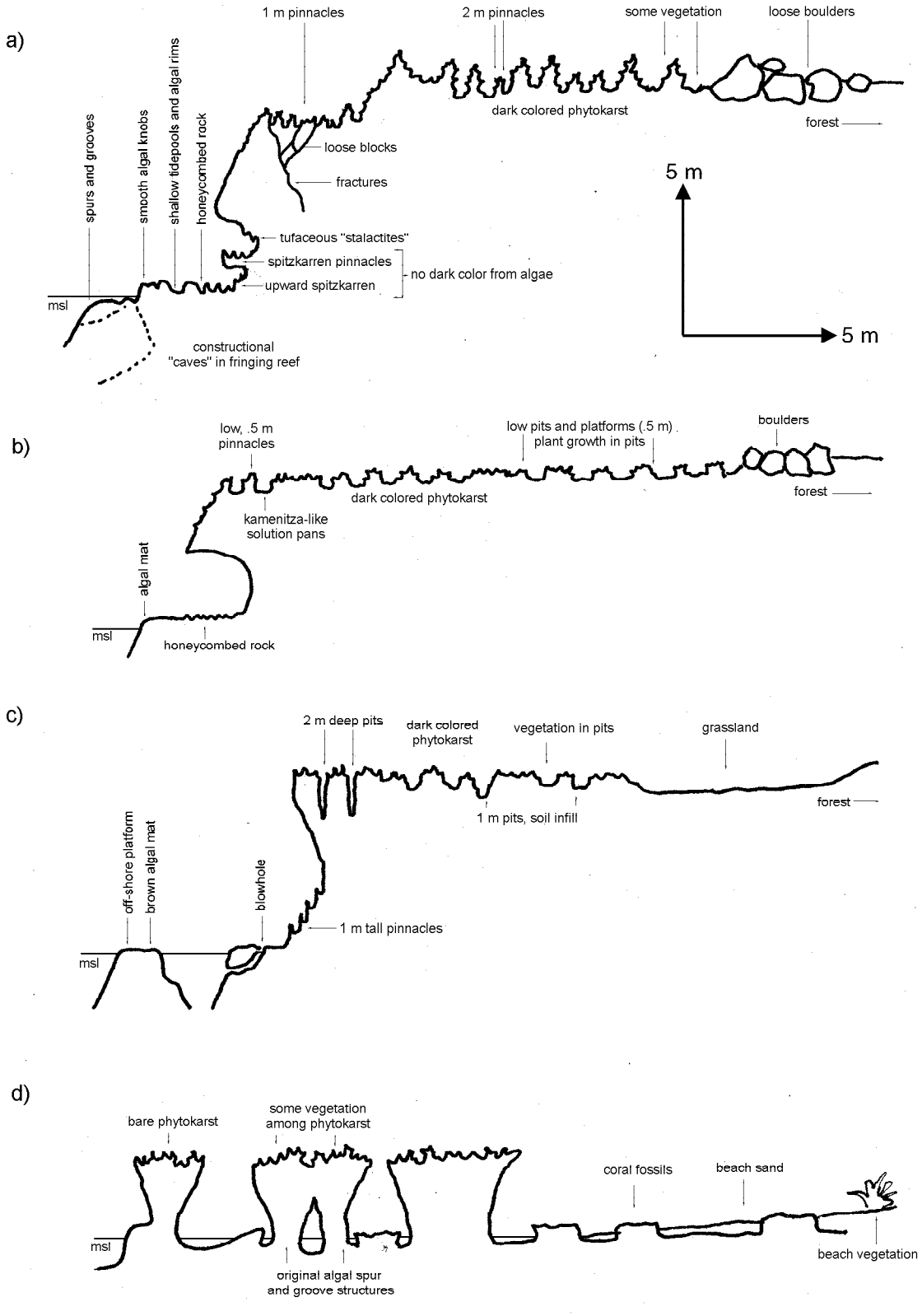

Fig 4. 1: Littoral karst and karrenfeld coast-normal profiles from northern Guam. (a) Double Reef; (b) Tarague; (c) Marbo; (d) Fadian

appear less "extreme" than Folk's examples.

Table 4. 3 compares Folk's end members with the equivalents on Guam.

4. 5. 4. Stony grounds

This type of karrenfeld is typical in some limestone areas around the world (Macaluso and Sauro, 1996). It is dominated by blocks, slabs, chips and rubble made by past or very recent processes of rock fragmentation (Ginés, 1996). In northern Guam, stony grounds are locally common, especially at the bases of cliffs. In such instances, stony grounds are clearly made by colluvium from erosion of cliffs. Stony grounds can also be found on gentle slopes away from cliffs, such as in parts of the limestone forest inland from Double Reef (Plate 6, photo 7). Since rock breakdown creates new surfaces available to dissolution, relative age of stony grounds may be estimated based on the stage of karren development on the breakdown blocks.

Table 4. 3: Comparison between phytokarst and "normal karst" from Caiman islands (Folk et al. 1973), and coastal and inland karrenfelds on Guam

	Folk et al. 1973 Black phytokarst	Northern Guam littoral phytokarst	Northern Guam rainfall-solution karrenfeld	Folk et al. 1973 "Normal karst"
surface color	very dark to black	grey (+ light paleosol)	white to grey	light
dissection	intricate, spongy	intricate, spongy rare fluting	less intricate, with some linear patterns	simple, fluted
orientation	absent	mostly absent	mostly absent with some gravitational/ structural	gravitational
algal coat	very heavy	heavy	light	very light
erosive agent	boring algae	boring algae, some rain	rainfall and boring algae	rainfall solution

4. 5. 5. Karst pavement

There are no true karst pavements in northern Guam. However, in a few coastal areas, such as Fadian, littoral karst grades locally into a smooth, low-topography bare limestone pavement-like surface, intersected by numerous widened-joints (Plate 6, photo 8).

4. 5. 6. Pinnacle karst

Pinnacle karst is made by solution along joints and fractures which lowers the rock mass and leaves limestone blocks standing as pinnacles above the surrounding surface (White, 1988). Pinnacle karst on Guam is found in limestone forests on the flanks of the northern Guam plateau. It is best developed east of Mt. Santa Rosa where extensive areas of the Alifan and Mariana Limestones between the eastern flank of the mountain and coastal cliffs are covered by pinnacle karst with pinnacles being up to 5 meters tall. This is also an area of extensive pit cave development. In most areas, however, pinnacles are not extensive and are usually isolated, up to 3 meters tall and are surrounded by regular inland solution karrenfeld.

The pinnacles are generally similar to coastal phytokarst but there is a more pronounced gravity-shaped component to them. Small linear flutes and smooth surfaces can be seen on pinnacles, in addition to chaotic algae-covered surfaces. Color of inland pinnacles is not as dark as in the coastal ones. In addition to excellent pinnacle karst east of Mt. Santa Rosa, isolated examples can be seen in the forests along hiking trails to Double Reef and to Thousand Steps in Mangilao.

4. 6. Karren and Phytokarst in Southern Guam

Maemong Limestone Member of the Umatac Formation is found in two parts of southern Guam as two distinct facies. Reef facies in Talofofo area shows excellent cavernous weathering, complex pit-and-tunnel developments, but not much surface karren. The foraminiferal facies of Maemong Limestone, in the southwestern Guam is very interesting and shows dissolutional structures not found anywhere else in Guam. The surface of the rocks has small scale etching, probably from impact of rain drops. Because this limestone has distinct bedding planes, water can move through horizontal planes of weakness and preferentially dissolve parts of the rock. These features are the only true groovekarren on Guam and are shown on Plate 7, photo 1. The outcrops of foraminiferal Maemong Limestone were probably deposited as a forereef facies and they sit on top of the Facpi Formation, like modern barriers on very steep slopes. Water running down the volcanic slopes cuts through Maemong walls and forms vertical dissolutionally-enlarged splitkaren, or grikes. There appears to be a continuum of scale from a few centimeter wide grikes to large canyon-like structures (two were found). This

"grike-canyon" is probably related to bogaz of Adriatic karst and zanjones of Puerto Rico (Monroe, 1964), or "solution corridors" (White, 1988). Its origin is obvious: an ephemeral stream flowing from the volcanic terrane above cuts through the entire limestone outcrop, reaching the underlying volcanic units and splitting the outcrop into two. An example of this type is illustrated by Plate 7, photo 2. This feature is about 2 meters wide at its maximum width and is about 10 meters tall.

Bonya limestone is the only limestone on Guam showing channel flow karren. This is a dense, diagenetically-altered, recrystallized limestone, obviously capable of supporting limited surface water flow. In the Fena lake area, Bonya limestone forms ridges separating the many sinkholes in a cockpit karst terrain (Plate 7, photo 3). Steep slopes of the ridges have numerous rinnenkarren channels meandering downhill. The size of rinnenkarren is quite uniform, with channels being about 20 cm deep and 20 cm wide and no overhanging walls. One of these runnels is shown on Plate 7, photo 4.

A depositional phytokarst feature found in southern Guam but not in the north are tufa deposits in the small waterfalls. Fena Lake area has several small streams flowing into ephemeral swamps in some sinkholes. These streams are supersaturated with respect to $CaCO_3$ and form tufa deposits as they flow down small waterfalls. These deposits are shaped as tapered domes reflecting the trajectory of cascading water (Plate 7, photo 5).

The Alifan Limestone outcrops exhibit a combination of rainfall solution karren and phytokarst. The Alifan Limestone capping Mt. Lamlam and Mt. Almagosa shows excellent karrenfeld development, with spitzkarren and solution pits being the characteristic karren forms. Also common are very interesting large dissolutionally enlarged joints, found throughout the outcrop but most frequent in the peripheral parts, along the contact with volcanic units. The Alifan Limestone area nearest to volcanic Mt. Jumullong Manglo contains a large number of enlarged joints, often wide enough to be traversed. Unvegetated portions of the Alifan Limestone ridge show development of karst pavement-like surfaces (Plate 7, photo 6).

The Agana Argillaceous Member of Mariana Limestone on the east coast of southern Guam and Mariana reef in Orote peninsula show no karren features different from those in the north. Littoral karst and littoral phytokarst are the dominant karrenfelds and are very well developed. Orote peninsula also shows excellent examples of pinnacle karst terrain and dissolutionally enlarged joints. An interesting example of this type is a cave developed by joint enlargement (Orote Channel Cave), about 20 meters inland from the beach at the tip of Orote peninsula, facing Orote Island. This enlarged joint is wide enough to be traversable and contains a shallow brackish pool at its bottom. Two specimens of an unidentified 1-cm-long red shrimp species were collected here.

— Chapter 5 —
KARST FEATURES IN THE SUBCUTANEOUS ZONE

The subcutaneous zone is the heavily weathered layer of rocks that lies beneath the soil cover, but above the main mass of largely unweathered rock. Subcutaneous zone and karren together comprise the epikarst. This chapter investigates the karst features found in the subcutaneous zone and their function in the movement of water via the subcutaneous zone. Features that start in the subcutaneous zone but extend deeper into the vadose zone below the epikarst are also addressed. This chapter focuses almost exclusively on northern Guam.

5. 1. Epikarst

Epikarst is the top layer in a karst terrain, and is made of karren and the heavily weathered layer of rocks immediately below the surface. It is the uppermost part of the vadose zone. This zone is of extreme importance to water circulation in karst areas. Williams (1983) explains the role of the subcutaneous zone as threefold: 1) it often acts as a storage reservoir for vadose water, 2) water flow in it shows a significant lateral component, especially after heavy rainfall and 3) it frequently provides baseflow water for streams.

Significant chemical solution occurs in this zone, giving it a high secondary permeability.
An amazing example of the magnitude of dissolution in the epikarst is given by Kogovsek and Habic (1980). They showed that a vertical trickle of 43 m^3 of water dissolved 7 kg of limestone and transported 6 kg of suspended matter into an underlying cave, over a 17 hour period.

Most dissolution occurs in the epikarst. As the water moves downward through the remainder of the vadose zone, it gets closer to calcite saturation (Ford and Williams, 1989). Because the solution potential of water decreases with depth, so does the permeability of the epikarst. Upper portions of the epikarst contain numerous dissolutionally enlarged joints and shafts allowing rapid water movement. The diameter and frequency of these pathways diminishes with depth. On Guam, this phenomenon is easily observed in limestone quarries.

As a consequence of the vertical decrease in permeability, the epikarst can act as a storage reservoir for percolating vadose water. The stored water locally forms a perched water table, sloping towards areas of rapid vertical percolation (Williams, 1983). This causes lateral movement of the water, towards the most permeable areas, such as underneath dolines.

5. 2. Flow and Storage in the Epikarst and the Vadose Zone

Flow in the epikarst typically has both lateral and vertical components. In very young limestones, lateral flow near the surface is very important because vertical secondary porosity has not yet developed. As karstification progresses and distinct vertical pathways develop, the lateral component of flow may diminish in relative importance. On Guam, vertical preferential pathways certainly exist, but could be widely scattered. Guam is a young island, with not many obvious natural dolines, and karstification processes may not have had time to create sufficient and efficient vertical pathways. This probably favors extensive lateral transport. In a dye trace study conducted by Andersen Air Force Base, dye injected in the vadose zone moved 90-240 m/day along linear paths consistent with fracture orientations (Barner, 1997).

As karstification progresses downward in the vadose zone, new and relatively unweathered rocks are encountered at depth (Williams, 1983). Vertical permeability is likely to develop well throughout the vadose zone only if there was a long still-stand in the base level of erosion. Because northern Guam is still undergoing uplift, it is possible that extensive vertical permeability pathways have not yet developed in portions of the bedrock. Therefore, significant lateral flow in the vadose zone is to be expected. The numerous closed contour depressions on the surface in northern Guam are of unclear origin and may not be true dolines. Many of them are probably depositional depressions and not real karst depressions, which means they lack efficient vertical conduits. Many closed contour depressions on Guam often fill up with water following heavy rainfall (this is not necessarily a result of the lack of vertical conduits and could be caused by sedimentation). Some depressions, however, never show any water accumulation. All this could indicate that vertical preferential pathways are not associated with every depression and efficient vertical conduits may be far

apart, thus increasing the need for lateral transport in the vadose zone. The horizontal distances covered by vadose waters are probably greater following heavy rainfall, when inefficient pathways get overburdened.

Because the top layers of the epikarst are full of enlarged joints and shafts, they allow rapid percolation of meteoric water. However, joints become narrower with depth and the permeability diminishes. A study by Julian and Young (1995) in Tennessee has revealed a transmisivity of 46 m^2/day in the upper two meters of epikarst. Underlying rocks had highly variable local transmisivities, with values up to 100 times smaller than in the top two meters of the epikarst. Because of this diminishing permeability, percolating water is not rapidly transported to the phreatic zone and is stored in the epikarst and the vadose zone.

In Guam, the storage ability of the epikarst and the vadose zone seems to depend on the previous meteorological conditions. During the rainy season, hydrographs from observation wells on Guam have shown that water level can rise in a matter of hours in response to heavy rainfall (Jocson et al., 1999). In the dry season, however, a heavy rainfall episode failed to produce a sharp rise of the water level in the lens. It is possible that the entire rainfall was stored in the epikarst and the vadose zone and then slowly released to the phreatic zone (Jocson et al., 1999).

The storage ability of the epikarst and the vadose zone is probably highly variable and highly localized. McLean (1977) has shown that percolation times and storage capacity vary with the complexity of joint network leading to a percolation point. Experiments in Carlsbad Caverns, New Mexico (McLean, 1977) and Waitomo, New Zealand (Gunn, 1978) revealed storage times of up to 14 weeks. Those data are consistent with predictions made for Guam by Contractor and Jenson (in press) who hypothesize that water can be stored in the vadose zone for at least a few months.

Percolation times (and thus storage times) for northern Guam should be determined experimentally in order to improve the accuracy of modeling of the Northern Guam Lens Aquifer. No such experiments were attempted during this project due to time constraints but suitable experimental strategy and locations have been identified. Vessels could be placed inside caves, in places where percolating vadose waters can be captured. Vessels with blocked input should be used as controls for evaporation. Oscillation of water levels in the vessels can be related to rainfall in the area, thus providing information about percolation times and changes in storage. Caves suitable for such experiments are located in the Mt. Santa Rosa area.

5. 3. Karst Features of the Subcutaneous Zone in Northern Guam

Features of the subcutaneous zone show no expression on the surface and are difficult to investigate directly. During this project, the observations on the epikarst were made almost exclusively in quarries, road cuts, cave ceilings, and loose blocks of limestone. Features that start in the subcutaneous zone but extend below into the remainder of the vadose zone are also discussed in this section. Gunn (1983) named three input mechanisms by which water moves vertically through the vadose zone: 1) seepage through the smallest joints and fissures, 2) flow through enlarged joints and fractures and 3) flow through shafts. Additionally, as observed in Guam in areas at the bases of cliffs and inside rubble-filled caves and sinkholes, vadose water can move by flow through rock rubble. Each of these mechanisms has been documented on Guam and is characterized by specific karst (epikarst) features.

Geologic faults also play a role in the percolation and movement of water through the subcutaneous zone. They may provide preferential pathways for flow of water, but may also impede flow of water. In Mt. Santa Rosa area, extensive geologic faults are probably involved in controlling the movement of rainwater through the limestone (Plate 8, photo 1). Places where geologic faults intersect the coastal cliffline show evidence of dissolutional enlargement (Plate 8, photo 1-inset). This is probably because they provide the easiest spots for rain water to spill over the cliffs.

Like with the karren features discussed in the previous chapter, no systematic inventory of epikarst features is possible (pit caves excepted and their inventory is included in Appendices 8 and 9). However, individual types of epikarst features occurring on Guam were identified, interpreted, sketched, and photographed. Additionally, an inventory of storm water disposal wells in Guam was carried out, as described in Chapter 3 and shown in Appendix 1. These artificial vadose by-passes are the most efficient way of vertically transporting vadose water and, as such, are hydrologically very significant in a karst aquifer.

5. 3. 1. Seepage

Water may slowly move through the rock via tight joints and fissures and. this process is known as vadose seepage (Gunn, 1981). According to Jennings (1985), vadose seepage is the smallest component of vertically transmitted waters.

On Guam, in addition to joints and fissures, seepage probably also occurs via primary pores in reef rocks. The process of vadose seepage can be directly observed on cave ceilings and the overhangs of coastal bioerosional grooves. This mechanism is responsible for building of stalactites and stalagmites.

Preferential seepage pathways may be observed in the walls of quarries on Guam. Quarry walls of Perez Brothers Quarry and Hawaiian Rock Quarry show several faults that seem to release groundwater and cause preferential growth of vegetation.

5. 3. 2. Soil-infilled enlarged joints and fractures

Geologic organs (soil pipes)

Geologic organs are cylindrical pits in the epikarst, fully infilled by soil or sediment (Cvijic, 1960). The term geologic organ encompasses a plethora of other terms mentioned in karst literature, such as filled sinks, structural sinks, solution synclines, some vertical shafts, solution pockets, solution wells, sand pipes and soil pipes. All these features, although morphologically different, develop by dissolution in structurally determined zones of higher permeability. Joints and fractures become solutionally enlarged and infilled by sediment or soil. They are large vertical features, permitting localized input of groundwater. They are not dolines and are too equidimensional to be cutters or cluftkarren (White, 1988).

Geologic organs on Guam are mostly soil pipes. Typical examples are up to about 0.5 meters wide and a few meters deep (Plate 8, photos 2 and 3). They can be quite numerous and a large number of them may be seen in quarry walls (Plate 8, photo 4). Usually, the walls of soil pipes on Guam are smoothly etched and lack fluting, indicating the presence of a soil plug during the solution process (Plate 8, photo 5). However, many examples of soil pipes on Guam exhibit fluted walls, which suggests that they were originally generated as empty shafts, with no soil plug to retard the velocity of descending water. After the shafts were made, soil infilling took place and buried the fluted walls (Plate 8, photo 6).

Soil pipes can develop along joints in compact and crystalline limestones (Jennings, 1985). This type of soil pipe developments has been documented in the Mariana Limestone on Guam, where soil pipes and similar features often occur at intersections of joints. However, many examples of soil pipes in the Mariana Limestone fail to exhibit joint-controlled origin. It is possible that because Mariana is a reef limestone of high primary porosity and quite heterogeneous in appearance, primary holes in the rock provided initial focusing of water flow to make soil pipes and related features (shafts, etc.).

In structurally weaker limestones, development of soil pipes and cylindrical holes is not controlled by joints (Kirkaldy, 1950). This is the case with the Barrigada Limestone where development of soil pipes and similar solution holes is a positive feedback mechanism; their development may be initiated by the smallest irregularities in rock surface or composition. Anything that promotes dissolution in one location over the other may be a controlling factor of soil pipe development. In raised reef limestones even deposits of guano have been documented to promote solution pipe development (Jennings, 1985).

Small soil-infilled solution-basins were also noticed in quarry walls. They look like small dolines, filled with soil. They show no surface expression (no topographic low) and may be a genetic equivalents of soil pipes.

If the soil pipe infilling lithifies, fossil soil pipes containing paleosol are made (Plate 8, photo 8). The limestone can subsequently get eroded and casts of soil pipes may remain. Such casts have been identified in Harmon sink (Plate 8, photo 9).

Other features allowing vadose flow

Unusual solution features have been identified in the reef rampart of cliffs overlooking Tarague embayment (Plate 8, photo 10). They are shallow, shaft-like features, not infilled by soil. They appear to reach depths of a few meters but do not exhibit typical vertical orientation and contain horizontal voids as well. They occur in a cluster of about 10 individual features and their origin is unknown.

5. 3. 3. Shafts (vadose by-passes)

Vadose by-passes identified in Guam include vertical shafts and solution chimneys. For discussion purposes, those vertical shafts large enough to be traversed by people are termed pit caves.

Vertical shafts

Vertical shafts are cylindrical voids in carbonate rocks, ranging in diameter from few centimeters to tens of meters, and reaching depths of hundreds of meters. They are produced by vertically descending vadose ground water, from perched reservoirs or the surface. The water flows as

supercritical sheet flow along the walls of the shaft (Brucker et al., 1972). Most initial research on shafts tried to characterize them as parts of underlying cave systems. Pohl (1955) was the first to point out that shafts are much younger than associated cave systems and are a part of contemporaneous landscape. Shafts can develop under no structural control.

Vertical shafts are common on Guam, in all limestones. Their main characteristics are circular or nearly circular cross-sections and absolutely vertical walls. Typical vertical shafts reach depths of about 7 meters, and have a diameter of about .6 meters. Larger shafts are also common, and are termed pit caves (discussed in the next section) for the purposes of this study. All shafts documented on Guam receive water from the surface or the epikarst. Vertical shafts probably also drain perched water tables in Guam but no such features could be identified.

In shafts found on Guam, the top of the shaft is often covered by a soil plug (which must be removed to investigate the shaft). Collapse of roof soil plug may leave some shafts open to the surface. The bottoms of shafts are filled in by soil. Although typical vertical shafts often have abandoned drain passages above the current floor, indicating previous base levels, no such side passages have been found in any shafts in Guam. This could mean that shafts located in Guam so far are relatively young features and have not experienced any changes in the base level. The walls of shafts on Guam frequently exhibit vertical fluting. Although most shafts appear young, there is evidence of older features. Plate 9, photo 1 shows a shaft in the Agana Argillaceous Member which shows prior infilling by soil, now paleosol, during a past relative sea level low.

Brucker et al. (1972) write that shafts usually occur in groups known as shaft complexes. The most notable shaft complex in Guam occurs in and adjacent to the autogenic ephemeral sinking stream leading into the Harmon Sink. At least ten shafts were identified in this area, but the number is probably much larger. They are difficult to notice most of the time because of the soil plug at the top. Shafts here often occur very close to each other and even overlap in a horizontal plane to produce voids with figure-8 shaped cross-sections. Plate 9, photos 2, 3 and 4 show active shafts from Harmon Sink. Plate 9, photo 5 shows a displaced limestone boulder full of holes left by old vadose shafts.

The number of shafts in a given area may seem high for the size of drainage basin. However, not all vertical shafts are active at the same time, and development of one shaft ceases when another shaft pirates its recharge. This process makes possible the development of more shafts than seem justified based on available catchment (Pace et al., 1993).

Vertical shafts provide the most effective natural route through the vadose zone. They can thus be thought of as vadose-by-passes, which can provide direct connections to the ground water. No such direct connections to the ground water were observed on Guam where rapid uplift of the thick limestone section has produced a vadose zone of 60 to 180 meters. Nevertheless, shafts are extremely sensitive to pollution by solid and liquid pollutants. They are much more sensitive to pollution than sinkholes (Brucker et al., 1972).

It has been hypothesized that the water flowing into Harmon sink gets discharged in Tumon Bay, where pollution or high nutrient content of the groundwater causes algal blooms. The fact that Harmon sink contains the largest known shaft complex on Guam may prove significant.

Pit caves

Pit caves are defined here as vertical shafts traversable by people. Just like the previously discussed smaller shafts, their genetic equivalent, pit caves are vertically extensive voids made by descending vadose water (Pace et al., 1993).

Although they penetrate deep into the limestone, no pit cave on Guam has been found to deliver water straight to the water lens. Water from pit caves moves to the lens via diffuse flow (Mylroie and Carew, 1995) or possibly via small fractures. Pit caves occur in complexes (Pace et al., 1993). During this project, a pit cave complex in Isla de Mona, Puerto Rico, was observed, where a large number of pits occur in one location on the limestone plateau. On Guam, pit caves occur singly and in complexes. They are almost never found far from the edge of the plateau. Because northern Guam plateau is a highly developed area, it is possible that pit caves in the interior have been filled in or destroyed.

The most spectacular and well known pit cave on Guam is the Two Lovers Point Pit Cave. It is easily observed thanks to the bridge built over it as part of the development of Two Lovers' Point as a tourist attraction. It is roughly elliptical in diameter and reaches a depth of 50 meters. It is entirely within Mariana Limestone detrital facies (Qtmd) and has well-developed vertical fluting on the walls. The entrance to this pit cave is shown on Plate 9, photo 6.

Other locations of isolated pit caves in northern Guam are Taga'chang Beach (Plate 9, photo 7) and the Tarague embayment. The largest pit cave complex in northern Guam is located east of Mt. Santa

Rosa, between volcanic terrain and coastal cliff. Hundreds of small pit caves, usually a meter or two in diameter and three to ten meters deep can be found in the limestone forest in this area. In southern Guam, pit caves have been found in the Fena Lake area.

Pit caves may also develop with no opening to the surface, created by vadose water from the epikarst rather than the surface, in which case they represent significant geologic hazards (Mylroie and Carew, 1997). Triple Shaft Cave (Mylroie and Carew, 1997) in the Bahamas is one example. It is unknown whether such caves exist in the interior of northern Guam plateau. However, remnants of pit caves with no surface opening can be seen along some coastal cliffs in northern Guam, particularly the cliff parallel to the beach at Ritidian. They have been exposed by cliff retreat and appear to have been parts of larger caves. In southern Guam, one of the Talofofo caves is a 33 meter deep pit cave, completely roofed over by limestone bedrock. Another (collapsed) cave in the Talofofo cave complex has an 11-meter vertical shaft in its walls, also not open to the surface.

Inventoried pit caves from northern Guam are included in Appendix 8, and pit caves from southern Guam are included in Appendix 9.

Solution chimneys

Disolutionally enlarged fractures (solution chimneys) are common wherever rock outcrops exist. Solution chimneys develop along structurally controlled pathways and may contain sloping and horizontal components in addition to vertical portions (White, 1988). In northern Guam, particularly striking examples can be found on the east side of Mt. Santa Rosa and include large fractures such as Earl's Bottomless Pit which is only about 60 cm wide but can be rappelled into to a depth of 27 meters (C. Wexel, pers. comm). In southern Guam, the best examples can be encountered in Orote peninsula and the Alifan Limestone ridge immediately north of Mt. Jumullong Manglo.

5. 3. 4. Storm water disposal wells

Storm water disposal wells are an artificial equivalent of vadose shafts and pit caves. They are designed to quickly eliminate storm water from surface and they provide the most direct infiltration pathway for the meteoric water.

They are more efficient than any natural vadose by-pass on Guam and can deliver water straight into the lens. Since 1981, however, Government of Guam regulations state that no storm water disposal well can extend below 200 feet from the top of the lens.

There are 171 permitted storm water disposal wells on Guam, operated by 7 entities. Table 5. 1 shows permitted well owners on Guam and the number of wells they operate.

Most wells, 103, are owned by the United States Air Force and all are located on Andersen Air Force Base. The entire area of AAFB is divided into 77 drainage basins, drained exclusively by the storm water disposal wells, singly or in clusters (Plate 9, photo 8).

Although storm water disposal wells are not natural karst features, they are nevertheless extremely important in recharging the freshwater lens. An inventory of storm water disposal wells was carried out as part of this project and the first GIS map showing all such wells on Guam was made. Data regarding the storm water disposal wells was provided by the U. S. Air Force and Guam Environmental Protection Agency. Appendix 1 lists the existing storm water disposal wells, their GEPA numbers and owners, and Fig. 5. 1 shows the locations of storm water disposal wells on Guam.

Table 5. 1: Owners of storm water disposal wells on Guam.

owner	# wells	owner	# wells
USAF	103	GPA	2
DPW	28	PIC	1
PACDIV CSO	27	Island Equipment	1
GIAA	9	Total	171

Abbreviations: USAF- United States Air Force; DPW- Government of Guam Department of Public Works; PACDIV CSO- Pacific Division Caretaker Site Office; GIAA- Guam International Airport Authority; GPA- Guam Power Authority; PIC- Pacific Islands Club.

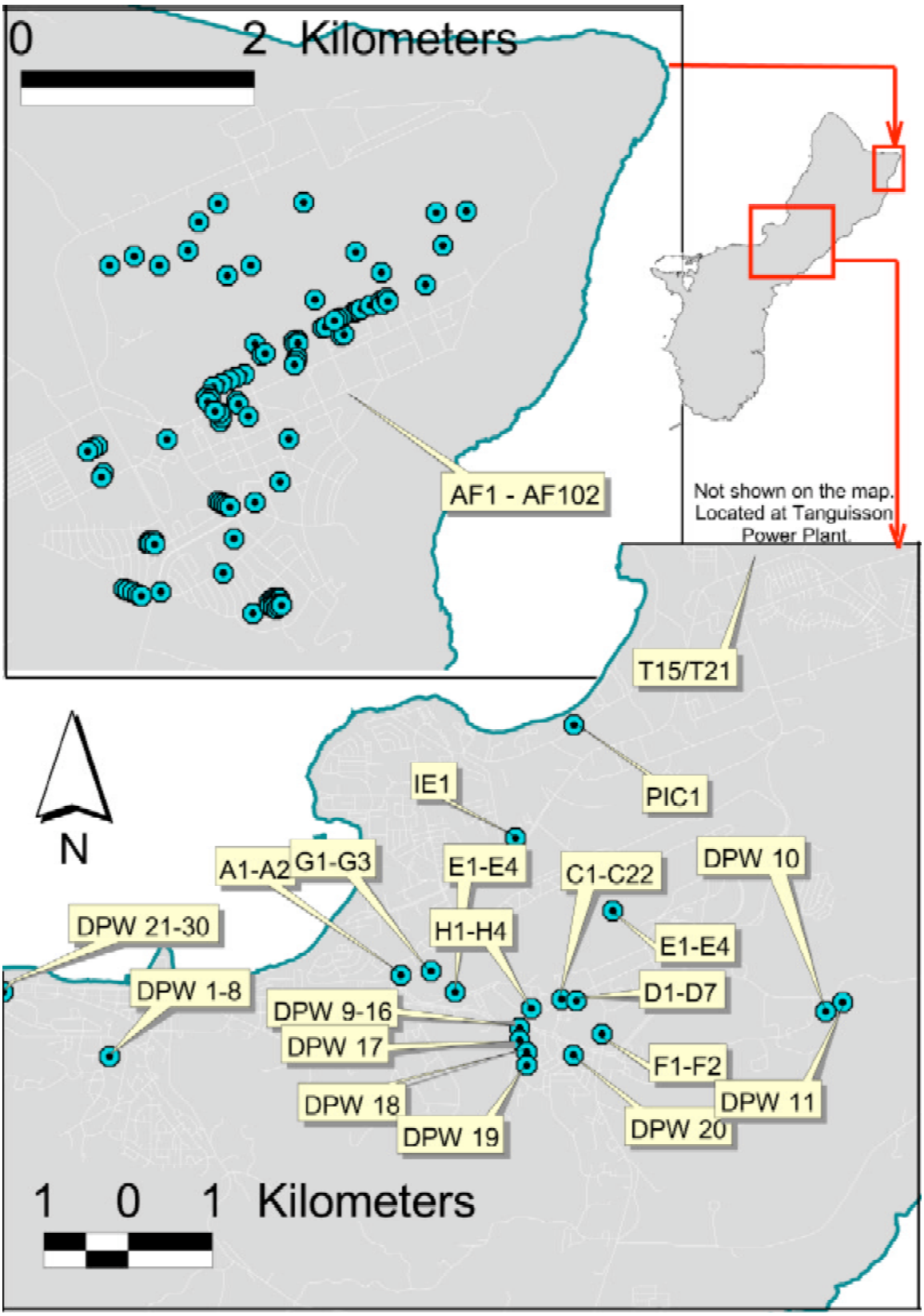

Fig 5. 1: Permitted storm water disposal wells on Guam.

— Chapter 6 —
KARST FEATURES RELATED TO SURFACE DRAINAGE

Some of the typical tropical and continental karst landforms, such as sinking streams, springs, blind valleys and tower karst are not found in carbonate island environments, their absence caused by lack of allogenic recharge. However, the complex geology of Guam makes it an exception. Guam's karst features include sinking streams, springs, blind valleys, cockpit karst and other allogenic surface water related features. This chapter investigates those features. They are organized into units based on hydrologic significance and morphology. Northern Guam and southern Guam are discussed separately.

6. 1. Surface Drainage in Karst

Disrupted surface drainage, having been diverted underground, is one of the defining characteristics of karst terranes. Because of high permeability of limestones, surface drainage in karst areas can be rare, intermittent or completely absent (Jennings, 1985). Generally, karst terranes can have two drainage components: fluvial (surface) and karst (underground) (White, 1988). A few regions, such as parts of the Adriatic karst and many oceanic carbonate islands, have entirely karstic drainage. Cvijic (1960) named such areas holokarst. Those karst regions that have a surface drainage component in addition to karstic drainage are known as fluviokarst (originally named merokarst by Cvijic, 1960).

On Guam, both fluvial (surface) drainage and karstic drainage are extremely well developed. Most of southern Guam, being made of relatively impervious volcanic rocks at the surface, has a fully developed surface drainage network. Most of northern Guam, being made of emerging reef limestones, has a fully karstic (underground) drainage. Nevertheless, many mixed drainage systems and corresponding karst landforms exist in various parts of Guam, namely limestone areas found adjacent to the volcanic terrane.

In Guam's karst areas, the extent of surface drainage varies from none to well developed rivers and is controlled by the following geologic factors:

1) Type of limestone
   a) pure limestone facies — favors holokarst development
   b) argillaceous or clay-rich facies — associated with fluviokarst development
2) Presence of insoluble rocks at the surface
   a) volcanic terrane in the vicinity — allows formation of streams
   b) no water input from volcanic terrane — difficult to form streams
3) Base level of erosion/dissolution by streams
   a) determined by the current sea level
   b) determined by local water table, unrelated to the sea level

The type of limestone involved appears to be an important factor. According to Cvijic (1960), holokarsts tend to develop in very pure limestones. Impure limestones, contaminated by volcanoclastics such as clay, may allow "perching" of water and limited surface drainage. Karst developing in such limestones is generally fluviokarst/ merokarst (Cvijic, 1960).

The presence of non-soluble rocks in the area allows development of normal surface drainage. Rivers from such areas flow into karstlands where they may sink into limestone if the limestone is relatively pure, or flow over it if the limestone is clay-rich or alluviated. Such waters, collected in non-karst areas and then transported to karst areas, are known as allogenic. Conversely, water that rains straight onto karst terranes is called autogenic.

Finally, the base level of dissolution and erosion plays a role in determining whether there will be any surface waters in a karst area. In most of Guam, the base level is the current sea level. The closer a valley is to the sea level, the more likely it is to have a river flowing in it. Base level can be locally set and unrelated to the sea level if an area is isolated from the ocean by mountains. Under such conditions, surface flow on karst is possible even at higher elevations.

6. 2. Surface Drainage Karst Features in Northern Guam

Northern Guam is a limestone plateau, rising about 200 meters above sea level in its northern end. The southern end of the plateau has a lower elevation and is located adjacent to the volcanic highlands of southern Guam. This southern end of northern Guam was mapped by Tracey et al. (1964) as Agana Argillaceous member of the Mariana Limestone, a clay-rich facies, with clay materials derived from

adjacent volcanic rocks. Such impure limestones are less favorable to karst development, because impurities may lead to accumulation of impervious residual covers (Cvijic, 1925). Features associated with surface flow (current or past) are numerous in the Agana Argillaceous member. The remaining area of northern Guam is covered by purer facies of Mariana Limestone and Barrigada Limestone. In those areas, karst features related to surface flow are virtually absent. Distribution of clay-rich Agana Member facies and the pure limestones in northern Guam is shown in Fig. 6. 1. It is presently not known how much terrigenous sediment in this facies was incorporated during deposition and how much was deposited into interstices of pre-existing rock by groundwater (Mylroie et al., 1999).

In addition to acting as a source of insoluble contaminants to neighboring limestones, exposed volcanic terrane also provides catchment area for allogenic streams. Allogenic streams may be fully developed before they enter karstlands, in which case they often deposit enough alluvium to extend their own surface flow. More commonly, especially in case of smaller streams, allogenic waters tend to sink into pure limestone immediately after they enter karstlands. Both of these situations exist in northern Guam. Northern Guam has three areas of allogenic catchment: the southern mountains adjacent to the Agana Argillaceous Member; and two volcanic outcrops protruding through the northern plateau, Mt. Santa Rosa and Mataguac Hill. Locations of allogenic catchment areas for northern Guam are shown in Fig. 6. 2.

In the Agana Argillaceous Member area, two allogenic rivers (Fonte and Pago) and two autogenic rivers (Chaot and Agana) flow over limestone covered by extensive alluvium. Their low hydraulic gradients and near-sea-level elevations allow surface flow. Most river valleys in this area, lacking substantial alluvial cover and being slightly elevated, are completely dry. Their flow has been pirated by underground drainage and they now exhibit ephemeral flow only after high rainfall events.

On the slopes of Mt. Santa Rosa and Mataguac Hill, the fate of allogenic waters reaching karstlands is completely different. Allogenic streams here are ephemeral, and limestones involved are purer. Therefore, the streams sink into the limestone via ponors (swallow holes), at or near the volcanic-limestone contact. Such streams are known as sinking streams.

Fig. 6. 1: Distribution of Agana Argillaceous Member of Mariana Limestone, and other, purer limestones in Northern Guam (from Tracey et al., 1964)

Fig. 6. 2: Areas that capture allogenic recharge for northern Guam and areas of autogenic recharge areas in Northern Guam

The following types of surface flow related features have been identified in northern Guam:

1) sinking streams (ephemeral allogenic streams from volcanic inliers)
2) losing streams (allogenic rivers flowing over limestone terrane)
3) dry valleys (past autogenic streams with flow diverted underground)
4) swamp and autogenic rivers (past valleys flooded by sea level rise)
5) sinking streams (ephemeral autogenic streams)
6) perched waters on karst terranes (stagnant, in closed contour depressions)
7) high-level springs (discharging rainwater or perched groundwater)

6. 2. 1. Allogenic sinking streams

Volcanic rock, inferred by Tracey et al. (1964) to be of the Alutom Formation underlies the entire northern Guam. Two peaks (Mataguac Hill and Mt. Santa Rosa) of the Alutom Formation protrude through the limestone and comprise volcanic inliers in the Northern Guam limestone plateau (Plate 10, photo 1).

Volcanic terrane supports the development of normal Hortonian type surface drainage. The catchment areas of Mt. Santa Rosa and Mataguac Hill are 1.29 km2 and 0.36 km2 respectively and all surface drainage comes solely from the rain events. Therefore, only ephemeral streams exist. As these ephemeral (sinking) streams enter the surrounding Mariana, Alifan or Barrigada Limestone karst, they lose their entire volumes underground.

Sinking streams commonly lose their volumes gradually, into alluvium or in a series of sinking points (Jennings, 1985). The allogenic sinking streams in northern Guam, however, lose all volume at once in a single ponor generally found at the surface contact of volcanic units and limestone. Virtually no surface flow penetration into karst areas occurs, demonstrating high permeability of northern Guam limestones. Only in the Gayinero Sink area on the southwest side of Mt. Santa Rosa, extensive alluvial deposits allow several sinking streams to travel a short distance away from the volcanic terrane, to the far end of a flat-bottomed depression where the ponors are located. Ponors may be either traversable cave entrances (Plate 10, photo 2) or sediment-clogged pits (Plate 10, photo 3) with or without associated traversable cave entrances.

At least six ephemeral streams flow down the slopes of Mt. Santa Rosa and two down the slopes of Mataguac Hill. Fig. 6. 3. shows a map of Mt. Santa Rosa and Mataguac Hill, created from orthophotos and showing the locations of sinking streams. Existing topographic maps have insufficient resolution to show relief associated with ephemeral stream valleys. These ephemeral streams are included in the inventory of surface flow karst phenomena in Appendix 2.

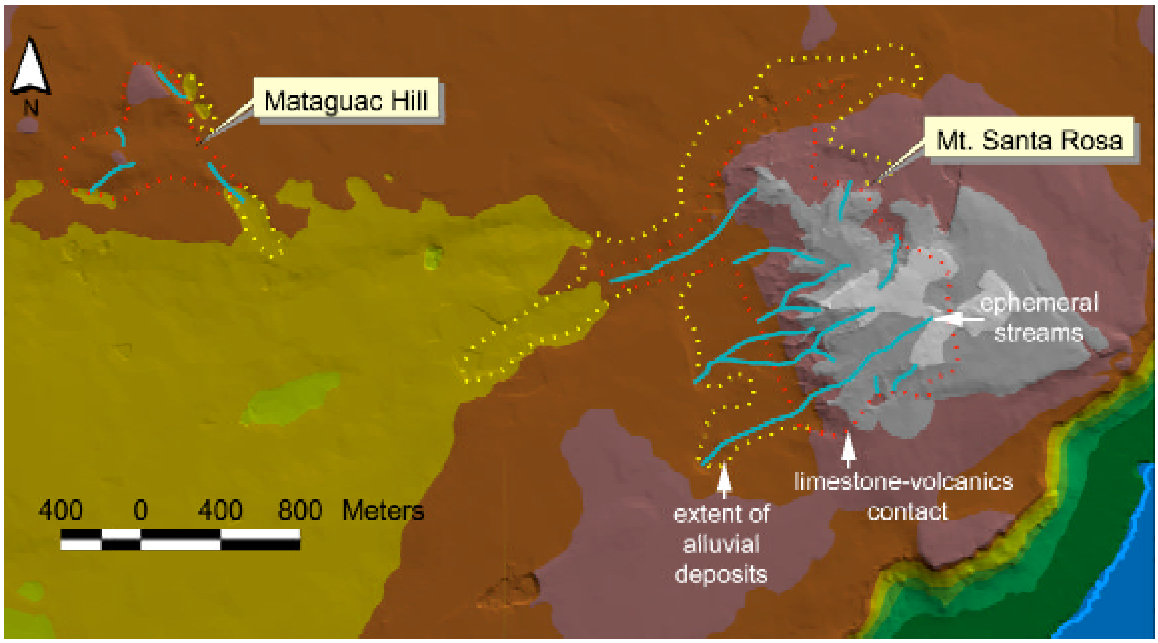

Fig. 6. 3: A map of Mt. Santa Rosa and Mataguac Hill showing locations of sinking streams

6. 2. 2. Allogenic losing streams

In karst areas with surface water flow, rivers almost certainly lose water. The water losses along river channels are usually not via discernible ponor zones, but via barely perceptible small fissures at the bottoms of the channels (Bonacci, 1987). In northern Guam, two developed rivers (Fonte and Pago) enter the northern karstlands from the southern volcanic highlands (Fig. 6. 4). They fail to sink into the limestone because impure clay-rich facies of Mariana limestone allows limited surface flow and accumulation of alluvium and their hydraulic gradients are very low. Fonte and Pago rivers (Plate 10, photo 4), flow to the Philippine Sea and Pacific Ocean, respectively. Neither receives permanent tributaries while they travel across limestone areas, but dry valleys indicate that this was not always the case.

Although Fonte and Pago valleys have been eroded close to the modern sea level and their hydraulic gradients are low, they may still be losing some of their water underground. Water loses may occur despite the extensive alluvial deposits that line the valleys of these two rivers. Both rivers flow along

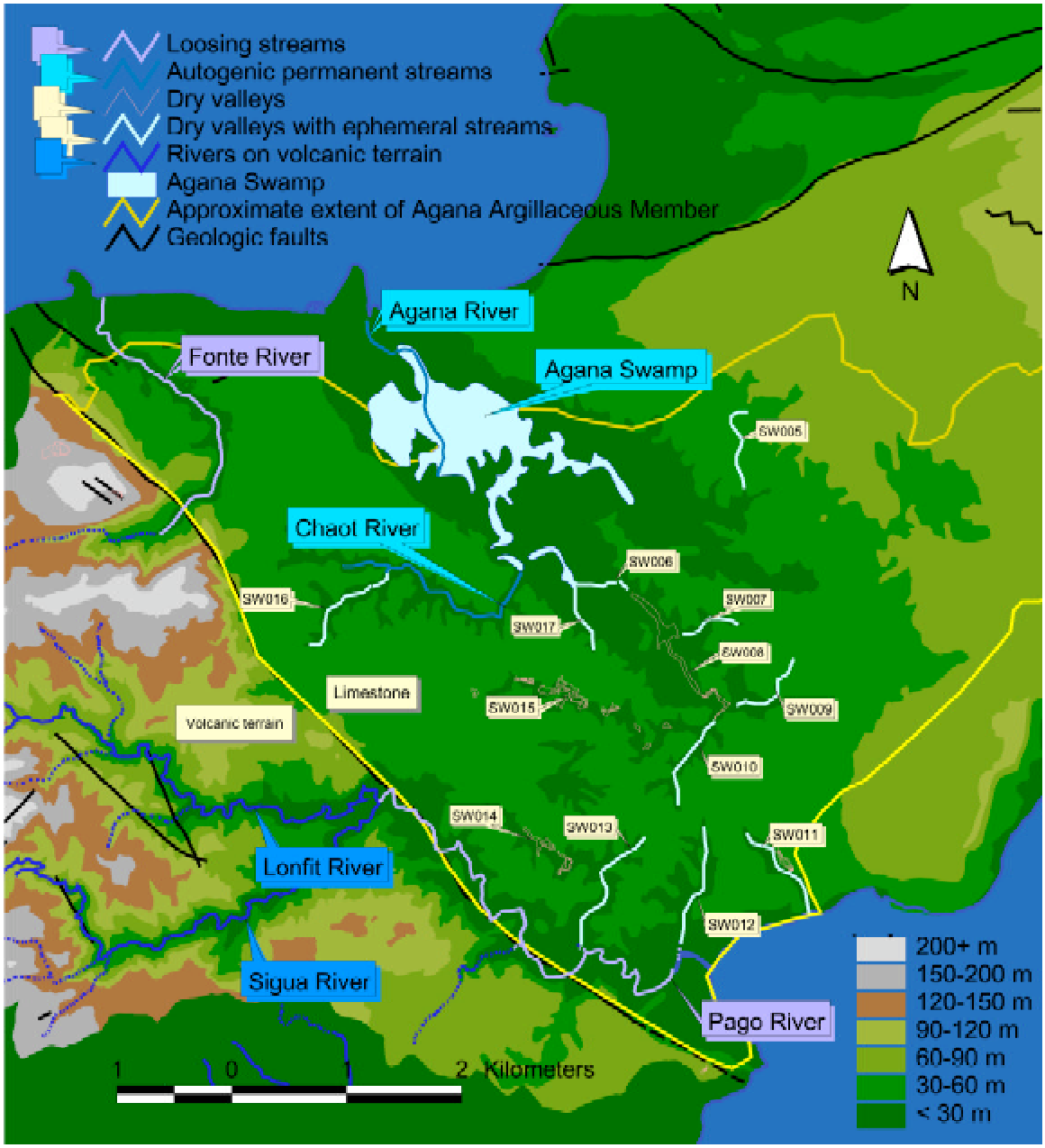

Fig. 6. 4: Map of Agana Argillaceous Member in northern Guam, showing locations of losing streams, autogenic rivers, dry valleys and ephemeral autogenic streams

major fracture zones which may increase the permeability of the underlying rock or destabilize the alluvium. If, in some parts of the riverbed, alluvial deposits are thin or missing, and water comes in contact with the limestone, sinking of water certainly occurs. No experiments checking this hypothesis have been attempted during this project.

To determine potential water loses from Fonte and Pago rivers, a process of "simultaneous discharge measurements" would need to be carried out. This process involves the measurement of as many flow discharge values as possible, carried out under identical hydrologic conditions (Bonacci, 1987).

In case of Pago River, such an experiment is recommended. Pago River receives flow from its tributary, Lonfit River, which in turn receives leachate from the Ordot landfill. The Ordot landfill was used as an uncontrolled solid waste disposal site in the years following World War II and may be the source of potentially hazardous substances. The leachate from the landfill may be finding its way into the Northern Guam Lens Aquifer if Pago River indeed loses some of its flow underground.

6. 2. 3. Dry valleys

Dry valleys are elongate depressions and valleys, with no permanent watercourses in them. Ephemeral streams may flow short distances through these valleys, but only during major floods. Dry valleys do not have a continuous gradient, as their bottom is dominated by dolines—dissolutional closed contour depressions, often arranged in a linear series (Cvijic, 1960). They destroy the profile of a valley. If soluble rocks are thick and cover a large area, all traces of valley morphology may be lost as dissolution progresses, leaving only a line of sinkholes (White, 1988).

In northern Guam, dry valleys exist only in the Agana Argillaceous Member, whose high clay content and lower matrix porosity as well as the proximity to volcanic terrane once allowed the flow of permanent watercourses, before karstification processes diverted flow underground. The remnants of these rivers exist today and are particularly striking in Chalan Pago area where deeply incised valleys stay permanently dry (Plate 10, photos 5 and 6). Small dry valleys may develop unintegrated into a larger drainage system and a good example of this type is the small dry valley leading to Pago Bay (Plate 10, photo 7). Remnants of previous drainage may exist both as true dry valleys with existing valley walls, as well as strings of sinkholes with no valley morphology remaining (Fig. 6. 4). An inventory of dry valleys is included in Appendix 2.

Dry valleys and lines of sinkholes are remnants of previous surface drainage. Surface drainage in limestone areas tends to get diverted underground as soon as the karstification process becomes stronger and faster than the valley formation process (Bonacci, 1987). This is what occurred in the Agana Argillaceous Member of the Mariana Formation, where dissolution processes eventually eliminated the conditions necessary for surface flow. The old surface drainage system can be reconstructed based on a number of geologic clues, such as removal of "noise" produced by numerous depressions and looking for patterns of dissected river valleys (Miller, 1987). Such an analysis was performed for the area covered by Agana Argillaceous Member, in northern Guam (Fig 6. 5 (a)). In addition to clues recommended by Miller (1987), locations of alluvial deposits, locations of volcanic basement exposures by erosion of limestone and locations of springs and seeps were considered. This analysis resulted in the reconstruction of an approximate network of surface paleo-drainage in southern part of north Guam (Fig 6. 5 (b)). There is no evidence that any kind of surface paleo-drainage existed elsewhere in northern Guam.

Rectilinear orientation is clearly visible in the drainage pattern. Orientation of permanent and ephemeral water courses in the Agana Argillaceous Member area and Pago and Fonte rivers allogenic drainage basins was analyzed and illustrated using rose diagrams. The results of these analyses are included in section 7. 3. 9., on morphometric analyses of the distribution of closed contour depressions.

6. 2. 4. Swamp

Dry valleys develop as surface streams whose flow has been diverted underground. A sea level rise can flood dry valleys, turning them into swamps. Dry valleys coalescing into Agana River appear to have been flooded to create the Agana Swamp (Plate 10, photo 8). The Agana River, which flows out of the swamp, and the Chaot River, which flows into the swamp (Fig. 6. 4), are the remnants of the only autogenic river system in northern Guam. Their flow follows a low gradient very close to the modern sea level.

6. 2. 5. Sinking streams (autogenic)

Only one autogenic sinking stream has been identified in northern Guam. It is a blind valley with ephemeral flow, fed by runoff from the Guam

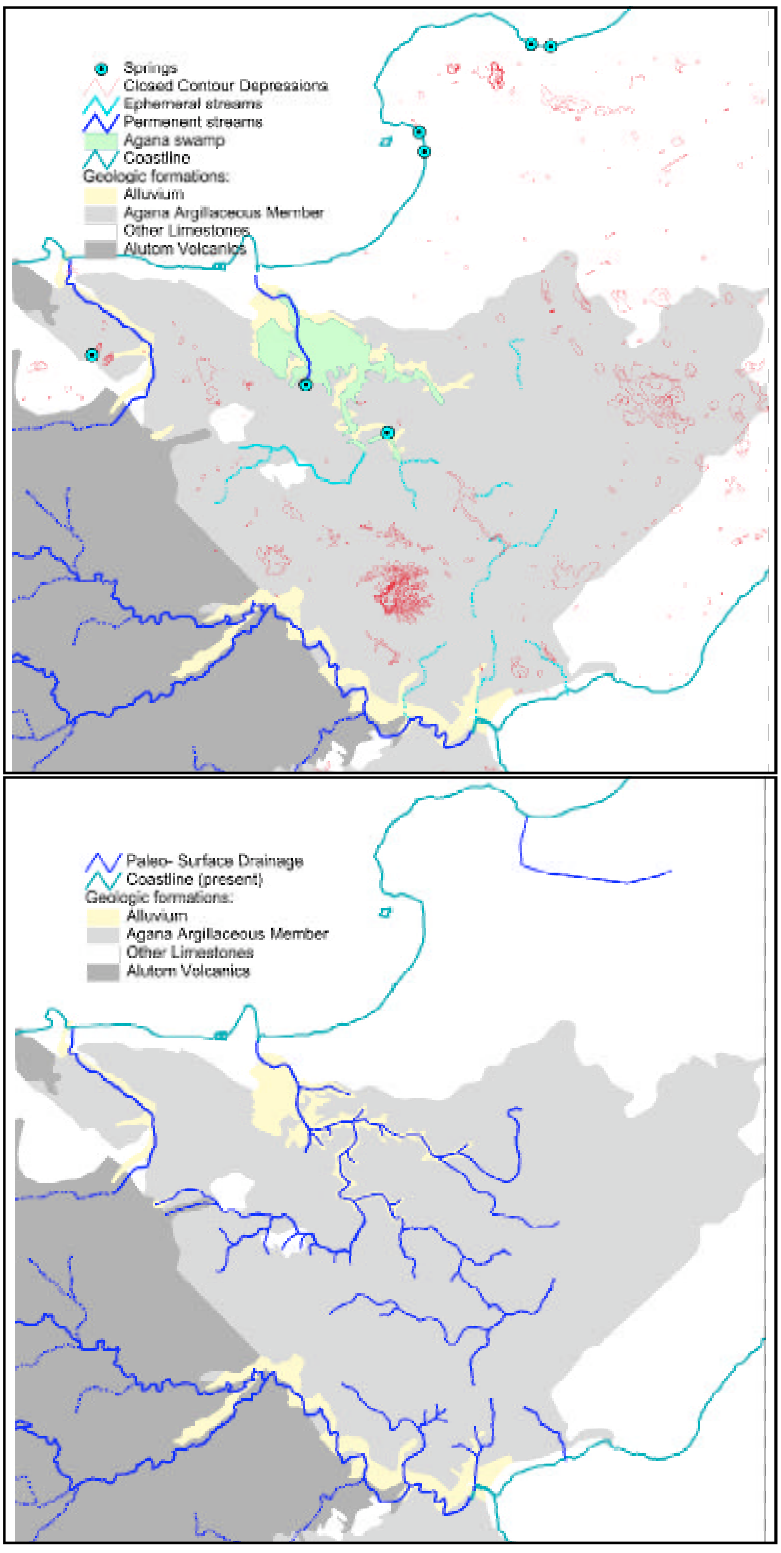

Fig. 6. 5: Reconstruction of a surface drainage system in the Agana Argillaceous Member area in northern Guam. a) Present day topography characterized by closed contour depressions, dry valleys, underground drainage and springs; b) Reconstructed paleo-drainage, prior to karstification and diversion of flow underground.

International Airport and its vicinity. It terminates in the Harmon Sink.

This valley has a series of inefficient ponors, receiving successive portions of the storm flow volume. There are four ponors in a sequence and all are shallow, cauldron-like depressions (Plate 10, photo 9). They are progressively activated as flow increases. Under low rainfall conditions, the most upstream ponor probably receives all inflow. As the volume of storm water increases, the first ponor gets overwhelmed and successive ponors downstream become limits of flow. If rainfall exceeds the capacity of all ponors, the water ponds at the bottom of Harmon sink. The lowest part of the Harmon Sink is filled with alluvium and debris, and allows frequent pooling of water, as evidenced by permanent wetland vegetation. Geometry of this sinkhole has been altered by development and the bottom of the sinkhole has been interrupted by Marine Drive.

The blind valley feeding Harmon Sink has been surveyed in detail. A map and profile of the valley are included in Chapter 7, on closed contour depressions.

6. 2. 6. Perched water on karst terranes

In the developed areas of the northern Guam plateau, infilling of depressions, waste disposal in depressions, and paving of large land areas, percolation of rainwater into the ground has been greatly impaired. Numerous natural depressions and ponding basins have accumulated enough debris to allow perching of water (Plate 10, photo 10). Perching of rainwater indicates a diminished ability of depressions to conduct water into the aquifer, thus causing flood hazards, particularly in paved low-lying areas.

6. 2. 7. High level springs

Carbonate island aquifers discharge along the coast where the groundwater lens is the thinnest. This is also the case with northern Guam, where freshwater from the Northern Guam Lens Aquifer discharges via numerous coastal springs. Aquifer discharge via coastal springs will be discussed in detail in Chapter 7. However, there are other types of springs in northern Guam, located above the modern sea level. Such high level springs are found inland and they represent discharge from allogenic stream caves, perched groundwater, or remnants of a fluvial drainage system. They do not represent discharge from the aquifer. In fact, they may contribute water to aquifer recharge. Agana Spring may be an exception to this.

High level springs were not investigated in detail during this study. However, existing data were reviewed, analyzed and supplemented by limited fieldwork to produce an inventory of high level springs (Appendix 4).

Springs were classified according to a (modified) scheme provided by Ford and Williams (1989). Clues used to classify inland springs were acquired from geological observations in the field, geologic map of Guam (Tracey et al., 1964) and documented or estimated spring discharge behavior (Ward and Brookhart, 1962, Rogers and Legge, 1992). Locations of high level springs in northern Guam are shown on Fig. 6. 6.

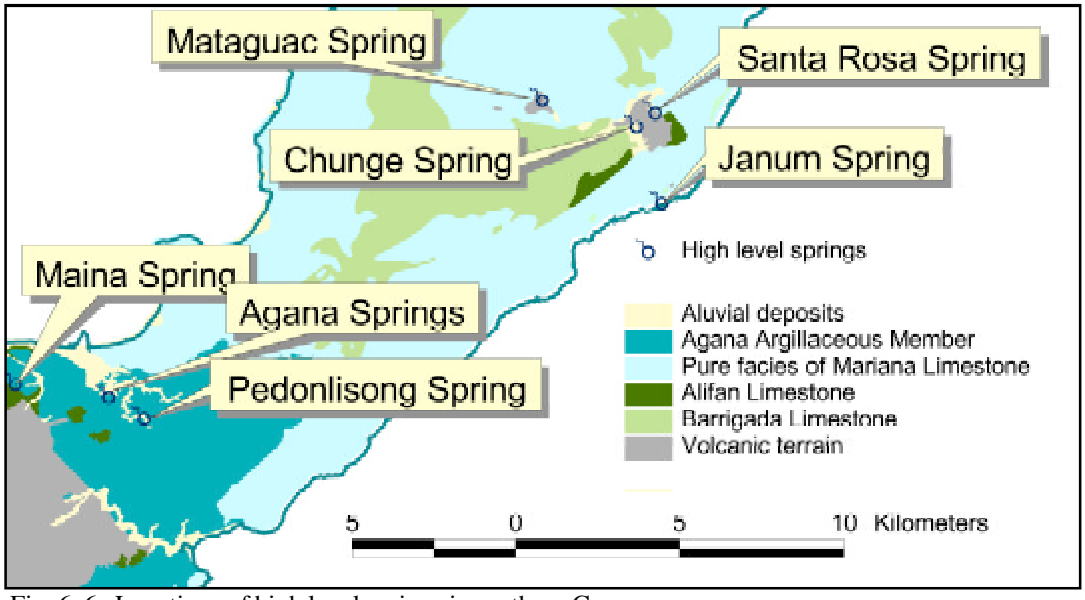

Fig. 6. 6: Locations of high level springs in northern Guam

The following types of high level springs occur in northern Guam. They have been interpreted based on existing data and limited field observations. Because of that, the following classification and diagrams (Fig. 6. 7) of northern Guam high-level springs should be thought of as hypotheses only.

Free draining, contact springs, with allogenic water

Mataguac Spring (Plate 12, photo 1)—Water feeding this spring is rainwater collected by the exposed volcanic Alutom Formation. Water emerges from a 30-meter long cave, about a meter wide and 2-3 meters high. The cave is essentially a vadose-cut passage in the detrital facies of Mariana Limestone (Fig. 6. 7 (a)). Alluvium deposits exist outside the cave.

Free draining springs, with allogenic water

Janum Spring—Water feeding this spring is probably allogenic water collected by the volcanic terrane at Mt. Santa Rosa. Basement conduits allow gravity-driven flow toward the coast, where the spring discharges from a cave, about 0.6 meters above mean sea level (Fig. 6. 7 (b)). The cave is a single passage more than 20 meters long, but its entrance was buried in the 1993 earthquake. Although shallow volcanic units probably provide basement for the conduits feeding this spring, no evidence of volcanic rock exists at the spring itself. A plume of sediment-laden water in the ocean adjacent to Janum Spring has been observed after a heavy rainfall episode (J. Jenson, pers. comm.).

Dammed spring, impounded by a faulted contact with another lithology

Maina Spring is fed by the groundwater from an Alifan Limestone inlier. This water is perched on Alutom Formation basement and discharges at the faulted contact with the Agana Argillaceous member of Mariana Limestone (Fig. 6.7 (c)).

Stream resurgence spring

This type of spring occurs where water from sinking streams emerges after flowing underground. Pedonlisong spring is a remnant of such a system, but has completely lost its upstream surface portion, which was replaced by dry valleys and ephemeral streams. It is fed by water that originally flowed in upstream valleys but was diverted underground.

Agana Spring

Agana Spring (Plate 12, photo 2) is located at the edge of Agana Swamp, approximately a 1.5 km inland from the coast. It used to discharge about 2.5 mgd (Ward et al., 1965) but is no longer flowing. It is currently a stagnant pond and the local residents report that the flow ceased after installation of GWA wells about 400 meters away. This spring may be the only classic karst spring in northern Guam but the exact mechanism responsible for the spring is unknown.

Non-karst springs

Santa Rosa Spring and Chunge Spring are associated with faults and fractures in volcanic rock, draining water captured by volcanic rocks exposed at Mt. Santa Rosa. They are entirely within Alutom volcanic units and are not karst springs.

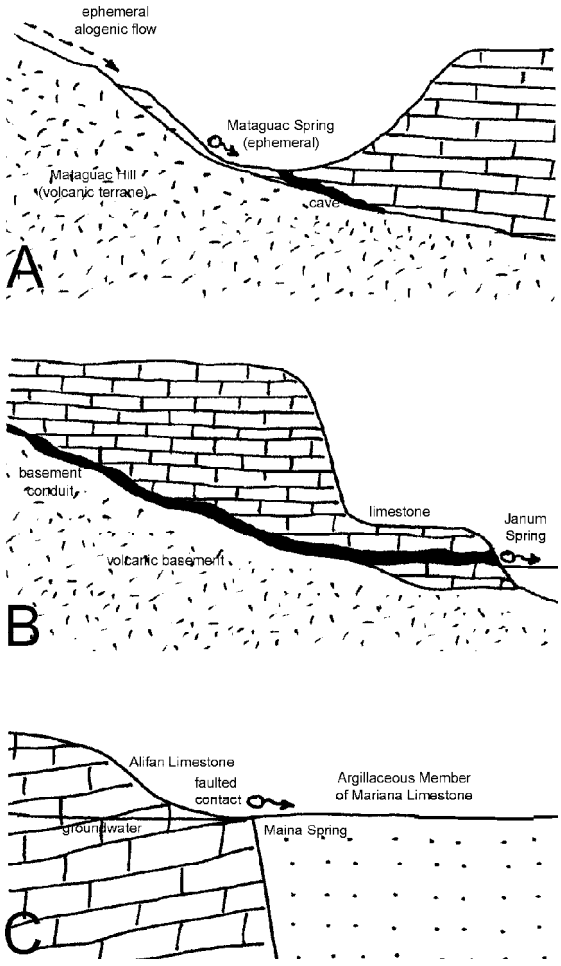

Fig. 6.7: High-level springs in northern Guam. a) Mataguac Spring; b) Janum Spring; c) Maina Spring

6. 3. Surface Drainage Karst Features in Southern Guam

There are four important karst areas in southern Guam. The east coast of southern Guam is flanked by the Agana Argillaceous member of the Mariana limestone (Tracey et al., 1964). Orote Peninsula is made of the reef facies of the same unit. Mountains from Mt. Alifan to Mt. Lamlam are capped by Alifan limestone, and the area northeast of Fena Reservoir is occupied by Bonya Limestone.

The Alifan Limestone and reef facies of Mariana Limestone are pure limestones, isolated from any input from volcanic highlands and as such do not support any surface flow. There are no indications that surface flow ever existed in Orote peninsula and Alifan-capped mountains. Certain closed contour depressions in the Alifan Limestone cap may be a result of undercutting by allogenic water from adjacent mountains (Mylroie et al., 1999)

The east coast of southern Guam is located adjacent to the volcanic highlands that give rise to several allogenic rivers. These rivers flow into limestone areas, and through them, to their mouths on the Pacific coast. This flow over karst is possible because of the low hydraulic gradients, large discharge volumes, extensive alluvial deposits and high clay content of limestone.

The most interesting karst features related to surface water flow and its diversion underground are found in central Guam, northeast of the Fena Reservoir. This area contains a mature karst terrane formed in the Bonya Limestone, which is a remnant unit surrounded by volcanic terrane. This area shows a high concentration of sinkholes (cockpit karst discussed in section 7. 4. 1.), some well-developed sinking and emerging karst streams and a large number of active and abandoned stream caves.

The following types of surface-flow-related features have been identified and inventoried (Appendix 3) in south Guam (first four are found in Agana Argillaceous member in the southeast, the final four occur in limestone inliers in central Guam):

1) through valleys (permanent allogenic streams crossing karst terranes)
2) gorge (allogenic river carving a gorge in limestone)
3) gently sinking stream (water disappearing into a river bed, no ponor)
4) abandoned valley (valley with no surface nor underground drainage)
5) underground rivers (sinking streams that resurface later)
6) natural bridges (remnants of river caves, bridging over surface flow)
7) sinkhole ponds (semi-permanent water accumulations in depressions)
8) high-level springs (discharging perched groundwater and rainwater)

6. 3. 1. Through valleys

Several allogenic rivers flow across the Agana Argillaceous limestone to reach the Pacific coast of southern Guam. These rivers are Ylig, Togcha, Talofofo, Asalonso and Pauliluc (Fig. 6. 8). Such flow over karst is possible because limestone involved is clay-rich Argillaceous facies of the Mariana formation and because the extensive alluvial deposits in the valleys isolate the underlying limestone. Also, these rivers enter karst areas as fully developed allogenic streams whose input exceeds the capacity of local limestone to absorb them over the short reach to the sea. Finally, with the exception of Togcha and Asalonso rivers, these streams have a very low hydraulic gradient that further facilitates surface flow. Although water losses underground probably occur, these rivers mostly reach their mouths on the Pacific coast, having traversed the southeastern Guam karst belt (Plate 11, photo 1). River mouths are associated with disruptions in fringing reef growth and the most spectacular such example is the Togcha River channel, which may be a result of geologic faults as well as freshwater discharge (Plate 11, photo 2).

6. 3. 2. Gorges

If a through river exhibits sufficient hydraulic gradient and a discharge large enough to maintain competent flow, a through gorge will form (Ford and Williams, 1989). The best example of a gorge on Guam is located in the upper Togcha River (Fig. 6. 8). What makes Togcha River different from other through valleys on the southeast coast of Guam is that it flows under a greater hydraulic gradient and flows through an isolated outcrop of Bonya Limestone. In its upper part, Togcha has incised a sheer-walled canyon in the Bonya Limestone and has partially eroded the Bonya Limestone and exposed underlying Bolanos volcanic rocks. Further downstream, Togcha flows through Bonya limestone, carving a several hundred meter long gorge with nearly vertical 50-m tall walls (Plate 11, photo 3). Talofofo and Ylig valleys may also have gorge-like sections.

6. 3. 3. Gently sinking streams

The Togcha River does not always maintain a discharge large enough to reach the ocean. On July 17, 1999, I have observed the lower portion of Togcha River bed completely dry. At the same time, river maintained significant flow in its upstream portion (Plate 11, photo 4). No single sink point can be detected along the river. The water appears to be lost by gently sinking into the gravel bed (Plate 11, photo 5).

6. 3. 4. Abandoned valleys

It appears that the final ephemeral tributary of Pauliluc river in the southeast of Guam used to flow over the Agana Argillaceous Member into the ocean, at Nomna Bay. This is evidenced by valley topography, coastal geomorphology and alluvial deposits. This valley was abandoned when the flow of its ephemeral stream was captured by the Pauliluc River (Fig. 6. 8).

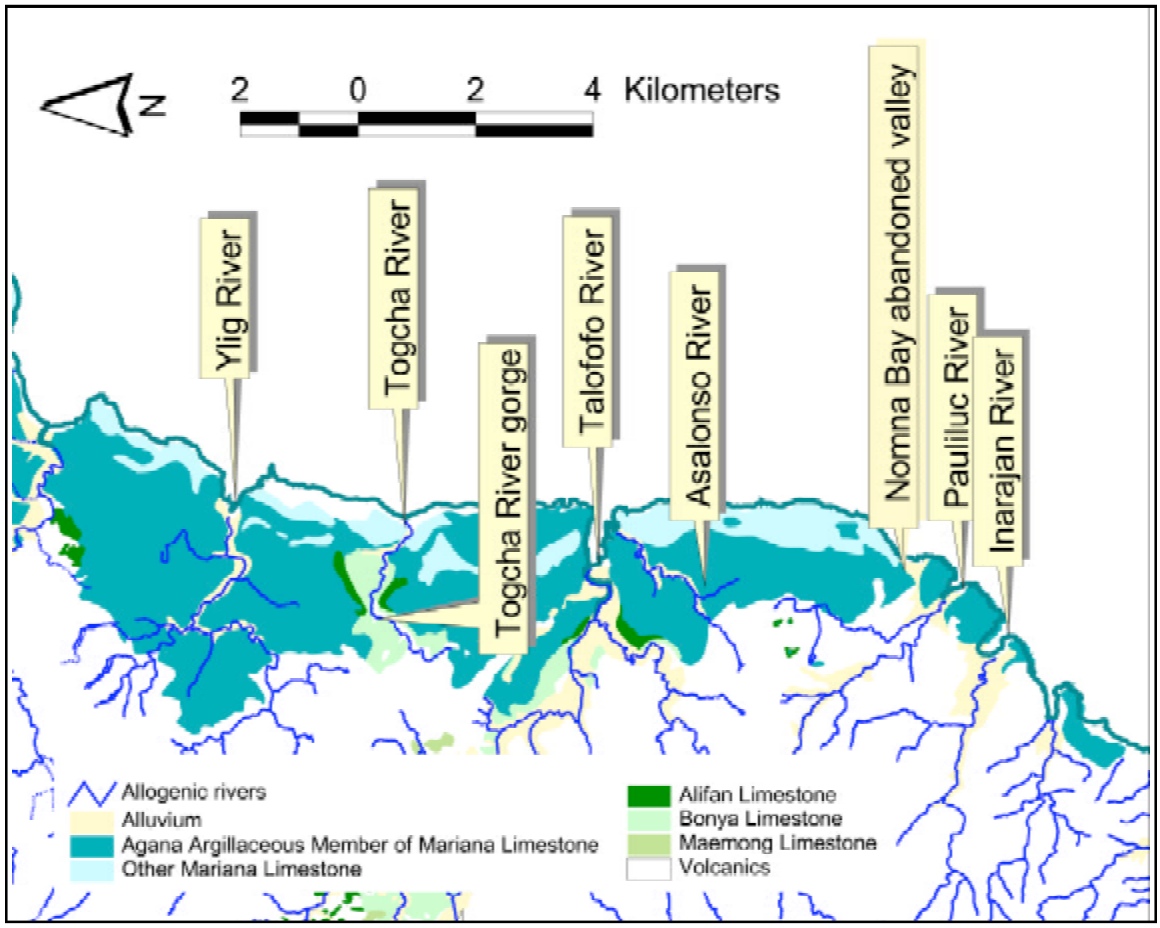

Fig 6. 8: Allogenic through valleys and related features in southeastern Guam

6. 3. 5. Underground rivers

True sinking and re-emerging rivers exist only in the karst of central Guam. Outcrops of Bonya limestone northeast of the Fena Reservoir are entirely surrounded by volcanic terrane. This gives rise to several allogenic rivers that flow through the Bonya outcrop. Bonya and Maemong rivers enter Bonya outcrops as well developed surface streams. Within the Bonya karst area, they join to form Tolae Yu'us river, which eventually flows into the Talofofo River. Both the Maemong and Tolae Yu'us rivers travel part of their course via subsurface conduits (Fig 6. 9).

The Maemong river flows into the area from the north, over a well alluviated valley cut through Bonya limestone. It used to flow into the Bonya River at the surface, as indicated by alluvial deposits and topography. However, the flow of the Maemong River was diverted into a sinkhole from where it now continues underground via a conduit at least 100

meters long. The conduit undercuts a low ridge of Bonya Limestone. The Maemong River then rises to the surface on the opposite side of the ridge, at its base, where it joins the Bonya River to form the Tolae Yu'us River.

The Tolae Yu'us River continues as a surface stream, until it disappears in a ponor at the end of a classical blind valley. It flows via a stream cave, at least 420 meters long, undercutting Bonya Limestone. The river emerges at a resurgence point underneath a limestone ledge (Plate 11, photo 6). About 4 meters above the current resurgence is an abandoned stream cave that may have been a resurgence cave before the local base level was lowered. Alluvial deposits and sinkhole arrangement indicate that, in the past, the Tolae Yu'us River may have followed another, now abandoned, underground conduit (Fig. 6. 9).

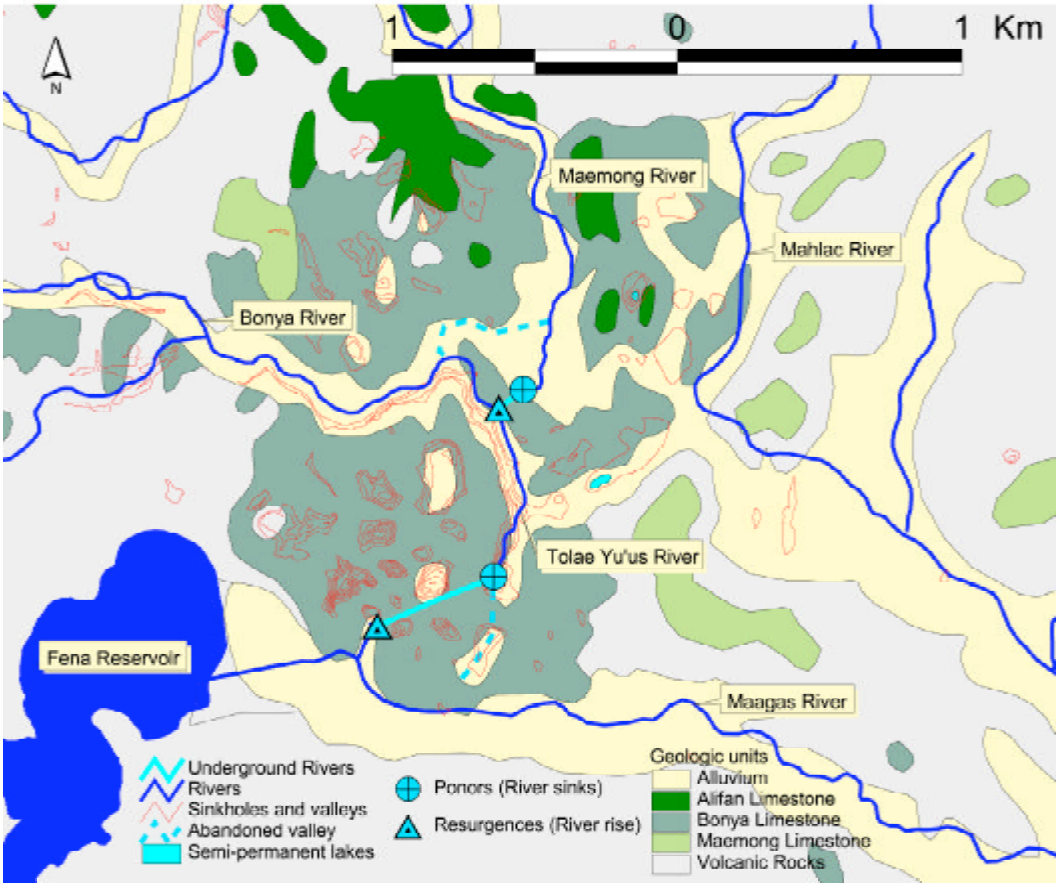

Fig. 6. 9: Allogenic streams flowing through Bonya Limestone karst. Also shown are their ponors, river caves, resurgences, abandoned valleys and semi-permanent water accumulations in depressions.

6. 3. 6. Natural bridges

Natural bridges are karst features through which a river runs or has run (Cleland, 1910) and through which light penetrates (Jennings, 1985). Because they are remnants of vadose caves, natural bridges are discussed in section 8. 4. 4. in the chapter on vadose caves.

6. 3. 7. Sinkhole ponds

Aligned sinkholes (Fig. 6. 9) with significant alluvial deposits in the Bonya limestone outcrops in central Guam indicate past surface streams whose flow was diverted underground or abandoned in favor of other passages. One such depression, about 450 meters northeast of Tolae Yu'us River ponor, is the

site of a semi-permanent stagnant body of water. The depression is heavily lined by alluvium and appears as a small lake on USGS topographic maps. When I visited this site on August 1, 1999, it was a shallow wetland, receiving flow from one small, unmapped stream.

Another depression, some 590 meters away, north-northeast, also harbors a small semi-permanent body of water. This lake was not visited during fieldwork, but analysis of aerial photographs indicates that water is present at the bottom of this sinkhole, nestled between two hills of Alifan limestone.

6. 3. 8. High Level Springs

High level springs are much more common in southern Guam than in the north. The most common type of springs in the south are those draining high level perched groundwater tables of limestone remnants supported by volcanic rock. There are sixteen such springs known in southern Guam, ten of which drain the Alifan Limestone cap in the mountains at the headwaters of Talofofo River basin. Another group of springs is associated with small Maemong Limestone inliers on the Facpi Formation. In addition to those, there are several other isolated springs in southern Guam.

An inventory of inland springs in presented in Appendix 5 and their distribution is shown on the GIS map in Fig. 6. 10. Data included in the table (on minimum and maximum flow and quality of water) is from Ward and Brookhart (1962) and Rogers and Legge (1992). Locations, geologic formations and spring types are based on USGS topographic maps and the Tracey et al. (1964) geologic map of Guam, as well as my own observations in the field. The following are the types of high level springs found in southern Guam.

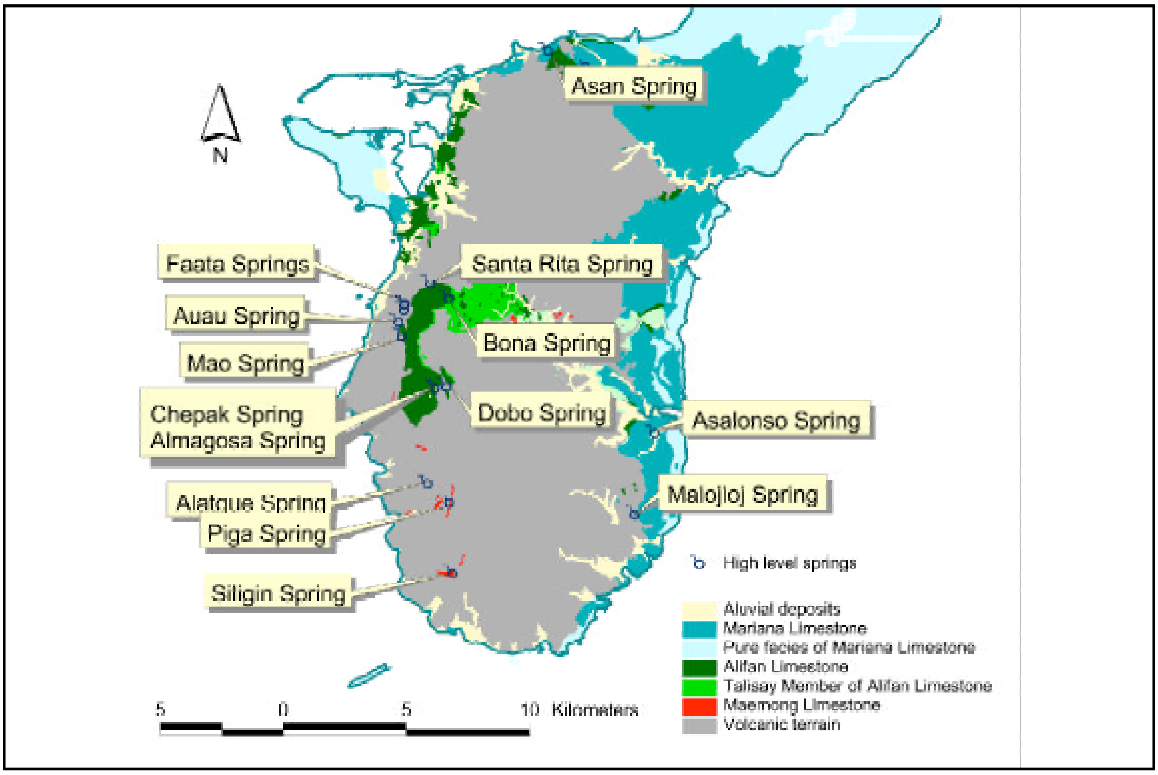

Fig. 6. 10: Locations of high level springs in southern Guam

Free draining, contact springs, with autogenic water

Most high level springs in southern Guam drain the large Alifan limestone remnant capping the ridge from Mt. Alifan to Mt. Lamlam. The Alifan Limestone is comfortably underlain by the volcanic Alutom and Bolanos formations. Springs scattered around the Alifan inlier, along the contact with the volcanic units, all show a reliable flow indicating significant storage. Groundwater accumulated by the Alifan limestone is perched on the volcanic basement and discharges at the contact (Fig. 6 11 (a)). All springs in this area are flashy, indicating the presence of vadose passages as well, feeding rainwater more or less straight into the spring. The following springs probably belong to this type: Dobo, Chepak and

Almagosa springs (Plate 12, photo 3) which drain to Talofofo river basin area, and Auau, Mao, Santa Rita and three Faata springs which drain to Guam's west coast.

Two additional springs probably operate by the same mechanism: Asan Spring (Plate 12, photo 4) in the northern part of southern Guam, draining a small Alifan limestone outcrop at the contact with the volcanic Alutom Formation, and Malojloj Spring in the southeast which drains local groundwater table in Agana Argillaceous member at the contact with underlying Bolanos formation.

Free draining, contact springs, with allogenic water

The three springs associated with small Maemong Limestone outcrops embedded in the Facpi Formation probably belong to this type. Maemong lenses are too small to accumulate any significant amounts of perched rainwater. It is possible that adjacent volcanic units are jointed enough to allow passage of rainwater into limestone lenses. From Maemong inliers, water probably flows along their contact with underlying volcanic units to the springs (Fig. 6. 11(b)). Some groundwater, whether from the Maemong or the Facpi units, must be involved in feeding the springs, as they have small but fairly stable minimum discharge. The three springs in this category are Alatgue, Piga and Siligin springs. Siligin spring is associated with a Maemong outcrop much larger than the other springs and probably receives some autogenic water as well, from a perched groundwater source (Fig. 6. 11(c)).

Dammed spring, impounded by comfortable contact with another lithology

The large Alifan Limestone remnant in southern Guam locally grades into its clayey basal facies, the Talisay Member. Whereas the Alifan Limestone is generally a pure unit, its Talisay member is much less permeable and even supports development of several autogenic streams on its surface. It is possible that contact between Alifan limestone and Talisay member acts as a boundary to Alifan's perched groundwater table. Such a barrier in the path of underground drainage would cause a spring discharge at the contact (Fig. 6. 11(d)). This is probably the mechanism that made Bona Spring, which is located at the surface contact between Alifan Limestone and Talisay member and drains into Talofofo river basin.

Spring draining into a karst stream

A single spring, Asalonso spring, exists in Argillaceous member of Mariana Limestone in the southeast of Guam and drains straight into a tributary of Asalonso river. This spring gets water from a local groundwater table and drains at the local base level set by a surface stream.

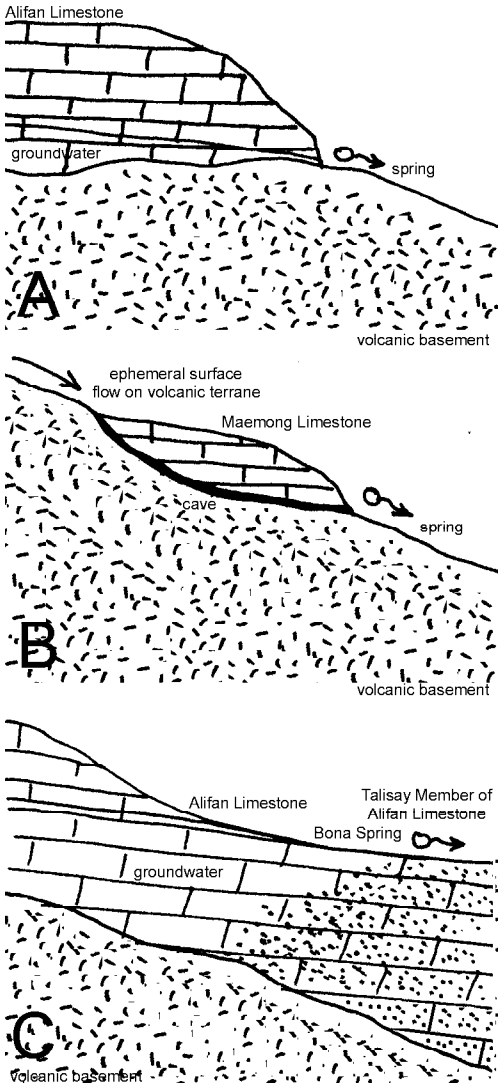

Fig. 6. 11: High-level springs in southern Guam. a) springs draining groundwater and rainwater from the large Alifan limestone inlier; b) Alatgue and Piga springs; c) Bona Spring

— Chapter 7 —
CLOSED CONTOUR DEPRESSIONS

This chapter describes the numerous closed contour depressions scattered throughout northern Guam and parts of southern Guam. Depressions in northern and southern Guam were examined separately. The first step in my investigation of depressions was to compile an inventory of closed contour depressions and develop GIS maps showing their distribution. The next step was to select individual features deemed representative of a certain type of depression and map them in detail. Finally, an attempt was made to classify depressions based on probable origin.

Additionally, for northern Guam, I conducted morphometric analyses of depression geometry, arrangement and distribution. This was deemed necessary after field observations proved insufficient to determine the nature of most depressions.

7. 1. Closed Contour Depressions in Karst

Depressions known as sinkholes or dolines are characteristic features of karst terranes. They are internally-drained, topographically closed depressions, widely ranging in size (few meters to about a kilometer) and shape (pit to funnel to saucer) (Ford and Williams, 1989). They play a very important role in the recharge of karst aquifers, as they usually provide the easiest pathways for meteoric water to percolate to the groundwater table.

The terms sinkhole and doline are interchangeable and refer to depressions resulting from a variety of mechanisms. However, the dominant process or an essential trigger for the formation of all dolines is aqueous dissolution of bedrock (Zambo and Ford, 1997). If a depression was not made by dissolution or caused by dissolution, it is not considered a doline. Such depressions are either depositional or constructional, or man-made.

7. 2. Types of Closed Contour Depressions in Northern Guam

After identifying and compiling an inventory of closed contour depressions in northern Guam (Figs. 7.1. and 7.2, and Appendix 6) the next step was to evaluate the nature of inventoried depressions and classify them into different genetic categories.

Cvijic (1893) recognized that most depressions in karst are made by dissolution or collapse. Genetic distinction between the two is often unclear and most dolines are thought to be polygenetic in origin (Ford and Williams, 1989). Closed contour depressions on carbonate islands appear to be a result of any combination of three processes: dissolution (and collapse), original construction, and human modification (Mylroie et al., 1999). In Guam, often all three processes have probably operated at various times to produce depressions observed today. One of the goals of this project was to estimate the relative contribution of various processes to individual features and classify them based on the dominant genetic mechanism.

Fieldwork on the closed contour depressions in northern Guam has revealed that most of closed contour depressions cannot be easily classified. They lack features that may provide clues to their origin and may be of non-dissolutional origin. Since the dominant genetic mechanism was rarely obvious, it was necessary to inventory all closed contour depressions, whether of dissolutional origin or not. Consequently, the inventory of closed contour depressions of Guam is the only portion of the overall karst inventory presented in this thesis that contains some non-dissolutional features. Nevertheless, even depositional depressions are hydrologically significant and play an important role in the recharge of the Northern Guam Lens Aquifer because they have become internally-drained, despite their non-karst origin.

Every attempt was made to recognize dominant forces involved and genetically classify closed contour depressions. In case of northern Guam, the specific mechanisms involved in creation of dolines include point recharge (autogenic and allogenic), drawdown of the epikarstic perched water table, collapse and valley degradation processes.

Autogenic recharge areas, as is most of the northern Guam plateau, are unlikely to develop large depressions because dissolution tends to be widespread instead of focused (Mylroie et al., 1999). According to Mylroie and Carew (1995), depressions developing on carbonate islands lacking allogenic recharge are often depositional. That means that the majority of the volume of a depression was never deposited, instead of having been removed by

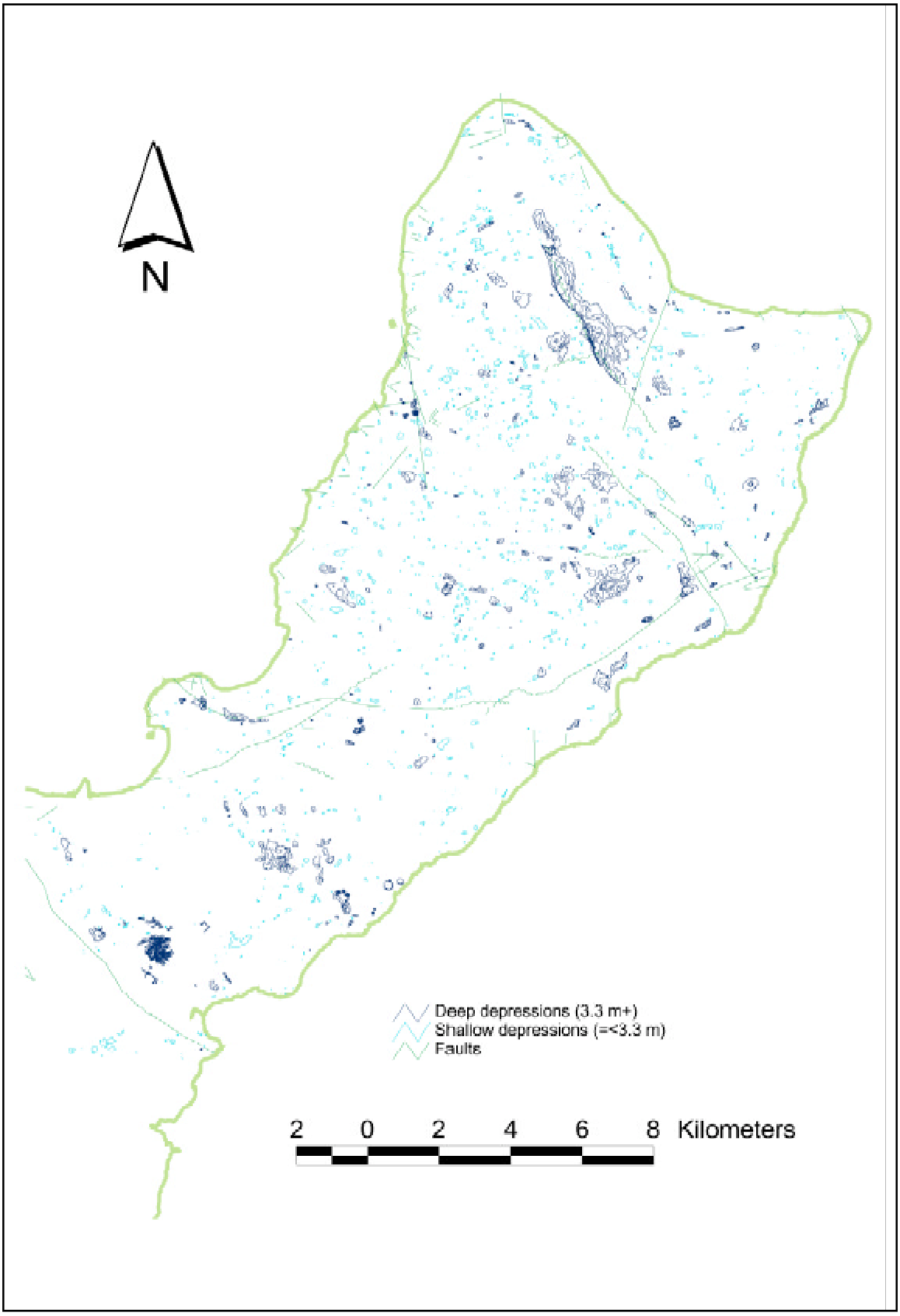

Fig. 7.1: Map of closed contour depressions in northern Guam.

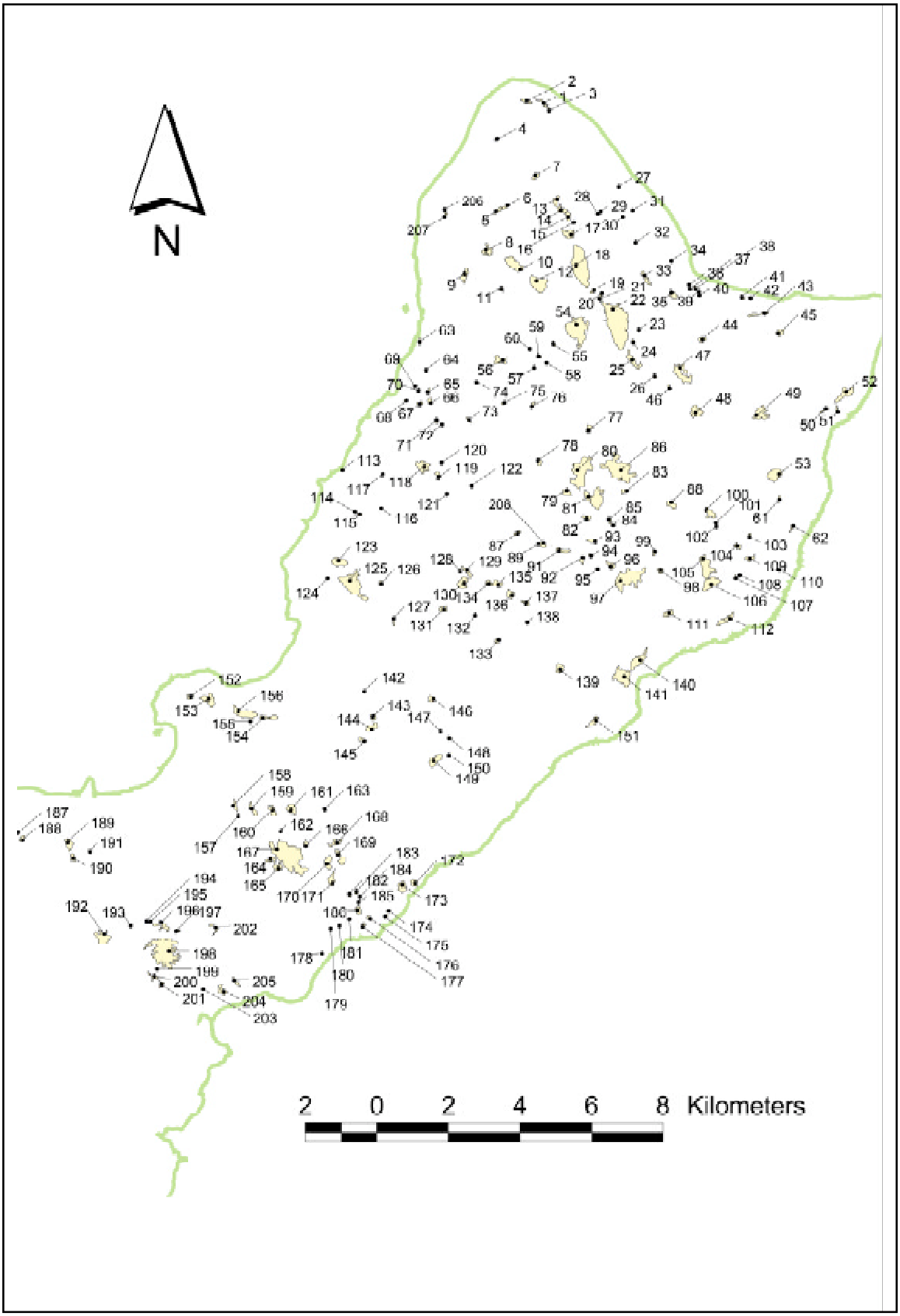

Fig. 7.2: Inventoried closed contour depressions in northern Guam (depressions deeper than 3.3+ m).

dissolution. Such depressions are not true karst features although they have developed internal drainage as a result of dissolutional processes. This may be the case with many closed contour depressions in northern Guam.

All known types of closed contour depressions in northern Guam are discussed under the following headings. They include morphologic terms (uvalas, poljes), descriptive terms (cenotes), modified karst (ponding basins) and non-karst (depositional) depressions. It is not a genetic classification scheme, but simply a descriptive list of types of depressions. This departure from genetic scheme was necessary in order to best present the diversity of closed contour depressions in northern Guam.

7. 2. 1. Point-recharge dolines (autogenic input)

For a doline to form there has to exist a mechanism which focuses corrosion (Ford and Williams, 1989). Surface drainage commonly provides this mechanism by flowing into closed contour depressions and furthering dissolution. Such depressions are known as point-recharge depressions (Ford and Williams, 1989). This type is very common in continental karst where dolines receive surface flow from autogenic or allogenic streams, which disappears into ponors (swallow holes at the bottom of dolines).

No significant surface flow is supported by young, highly permeable limestones in northern Guam. Therefore, point-recharge dolines made by autogenic flow are almost absent. A single exception to this may be Harmon Sink (Fig. 7. 3., Plate 13, photo 1). It is a deep elongate depression situated in a valley terminating at Chalan Mamajanao, some 600 meters inland from Tumon Bay. The sinkhole is fed by an ephemeral autogenic stream flowing in a classical blind valley, receiving runoff from the Guam International Airport (Fig. 7.3-a). The valley has four inefficient ponors arranged in a series (Fig. 7.3-c), so that as storm water volume increases, each successive ponor receives input after the preceding ponors become overwhelmed. The blind valley terminates in the lowest point of the depression, in a swampy area often containing a perched pond (Fig. 7.3-b).

Previous studies have suggested that the Harmon Sink may not be a true dissolutional feature, but a modified depositional depression. In a remedial investigation for ground water restoration, Ogden Environmental and Energy Services Co. (1995) stated that no evidence exists for whether Harmon Sink is a true sinkhole or a depositional depression. They observe that the deepest area of the basin, where drainage must sink, has no discrete sinking point or shaft. However, lack of a visible sinking point should not be taken as evidence against dissolutional origin of Harmon sink. Sinkholes can be covered by soil or waste mantle (Jennings, 1985) and in case of Harmon Sink the accumulations of alluvium and debris in its deepest portion are obvious. The accumulated debris causes frequent perching of water in a pond and probably hides the sinking point in the deepest portion of the depression, which has been blocked off by construction of the Marine Drive.

In conclusion, Harmon Sink appears to be different from other internally-drained depressions in northern Guam. It contains the only identified true non-allogenic blind valley in Guam. The valley is well developed and reminiscent of continental karst. It seems to be an old landform, antedating human-modification of drainage and urbanization of northern Guam.

7. 2. 2. Point-recharge dolines (allogenic input)

The primary reason for near absence of point-recharge dolines from northern Guam is the inability of very porous young reef limestone to support surface flow and allow focusing of water. However, the existence of two volcanic inliers in northern Guam allows catchment of allogenic water. Temporary streams flow down volcanic slopes of Mt. Santa Rosa and Mataguac Hill, focused in deeply incised valleys. The valleys usually terminate at the very point of contact with the limestone, in small dolines. Typical examples of this type of dolines are Mataguac Spring Sink, Awesome Sink and Interesting Sink.

Mataguac Spring Sink (Plate 13, photo 2) is a small, deep sink situated at the base of Mataguac Hill, on the contact between Alutom Formation outcrop and the surrounding Mariana Limestone. It has a maximum diameter of 100 meters, and a depth of about 15 meters. The floor of the sink is covered by alluvium derived from the volcanic material, with scattered limestone outcrops and partially exposed volcanic saprolite. Dense hydrophilic vegetation lines the bottom of the sinkhole and a small stream meanders along its bottom. This stream is fed not only by direct allogenic runoff, but also by Mataguac spring, a small ephemeral spring fed by limited water storage in the limestone immediately adjacent to and overlaying the volcanic basement. At the southeastern end of the sink is a distinct ponor, leading to a cave traversable to some 30 meters. Location of Mataguac Spring Sink with respect to neighboring volcanic terrane and a schematic diagram representing its

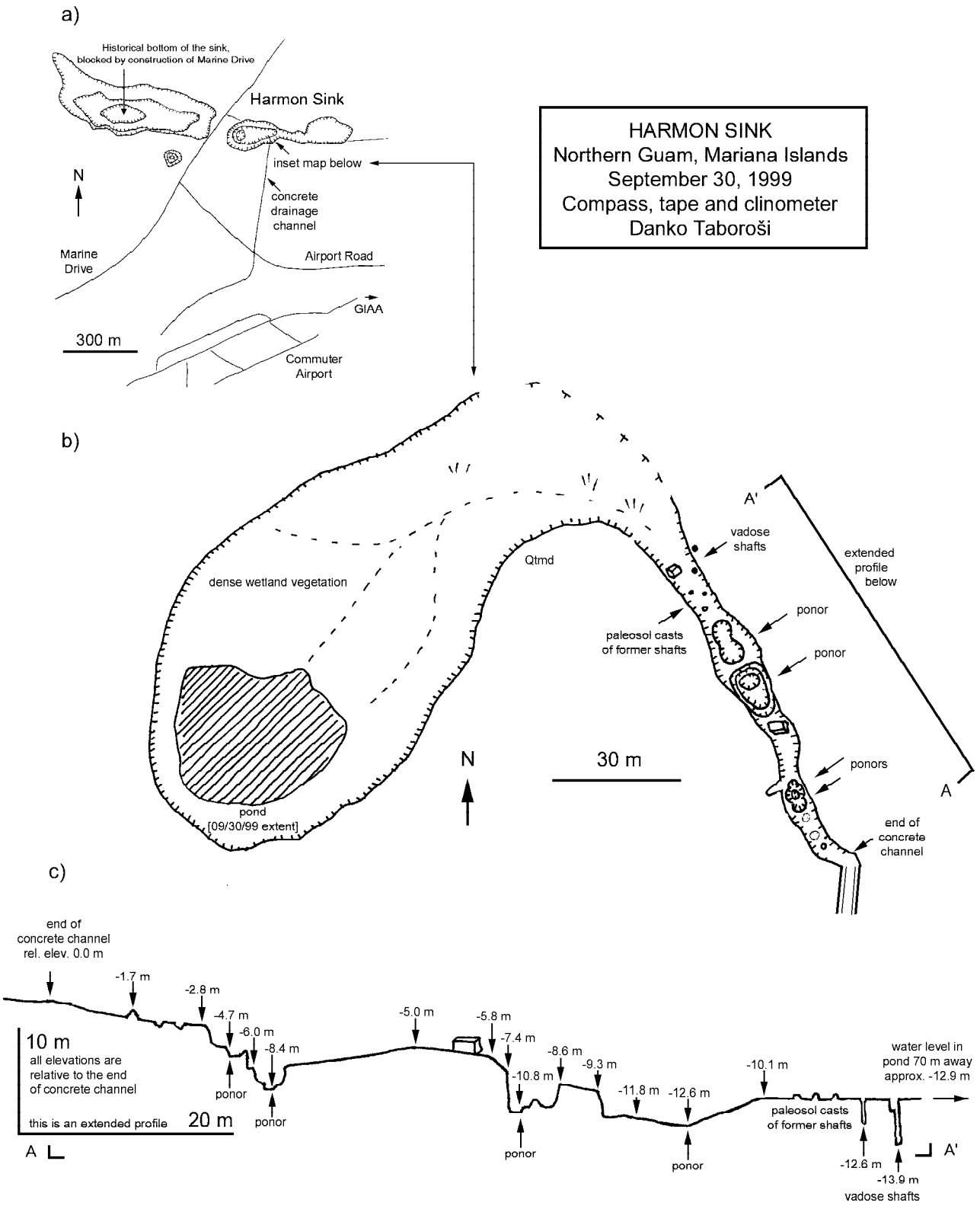

Fig. 7. 3: Harmon Sink. (a) general location; (b) map of sinking stream and main depression; (c) profile of sinking stream.

profile are shown in Fig. 7.4-b. There are several other sinkholes surrounding the Mataguac Hill, which are particularly well developed along its northern and southwestern flanks. They contain several contact stream caves and are sites of ephemeral ponds (Plate 13, photo 3).

Similar features exist associated with Mt. Santa Rosa, the larger of the two volcanic inliers in northern Guam (Fig. 7.4-a). Like Mataguac Spring Sink, Awesome and Interesting sinks (Plate 13, photo 4) are located right on the contact between volcanic units and limestone, they are small in area, about 100 and 50 m in diameter and 10 m and 7 meters deep, respectively. They are each fed by a temporary allogenic stream that sinks into mud-filled ponors. There are traversable stream caves associated with the sinkholes, and will be discussed in the next chapter. The caves are not entered via ponors but through nearby collapse entrances.

Allogenic point recharge sinks are not always located right on the contact. In one instance, there is evidence of water flowing over the limestone surface partially coated with alluvium, for up to 2 kilometers. This is the case of Yigo Sink, which does not appear to receive such allogenic input anymore, probably due to land development. However, its geometry and a trail of alluvium (mapped by Tracey et al., 1964) leading to the flanks of Mt. Santa Rosa make this a typical allogenic point-recharge sink, although apparently inactive.

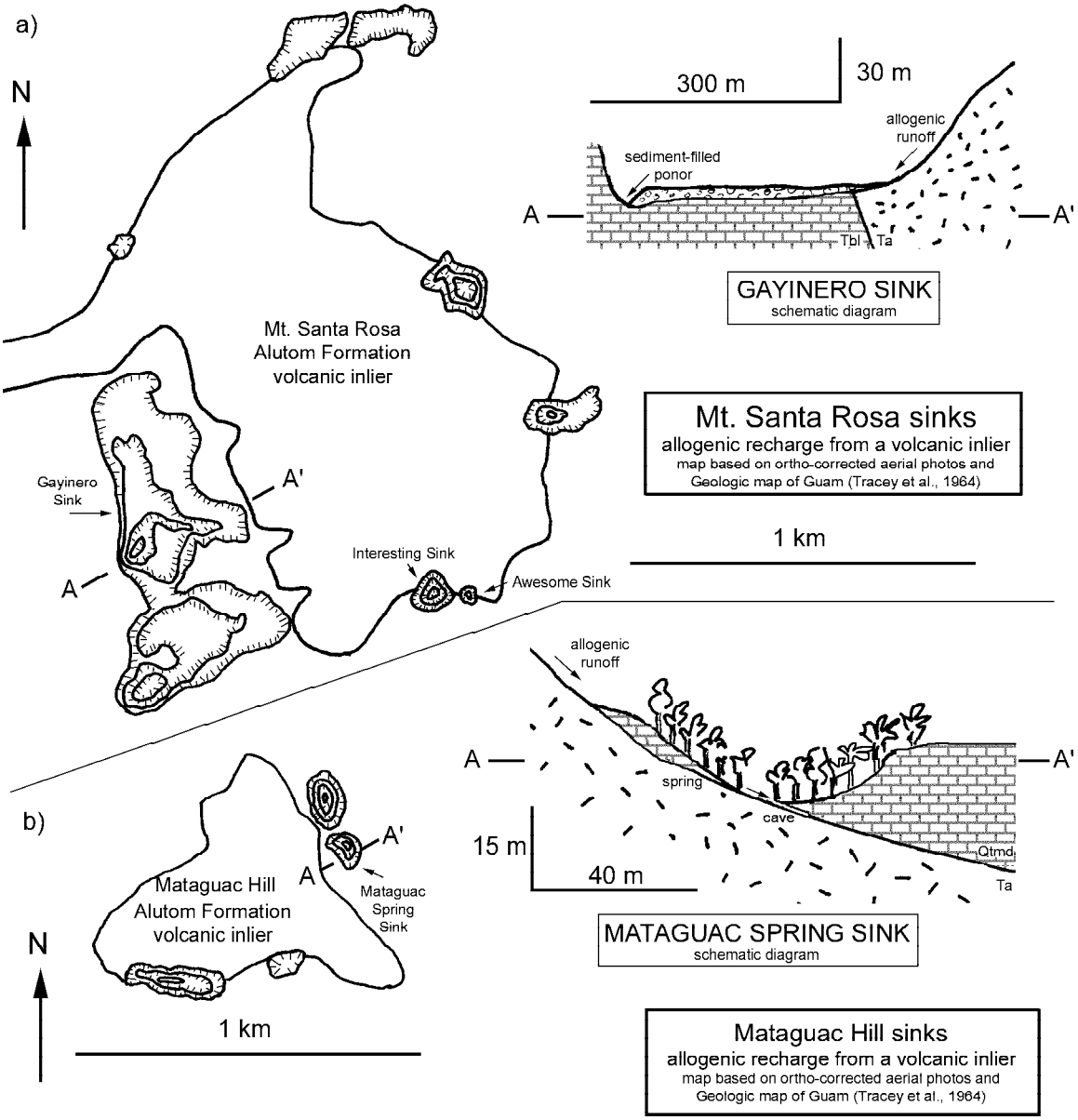

Fig. 7. 4: Allogenic point recharge dolines. (a) map of Mt. Santa Rosa inlier with associated dolines and a schematic diagram of Gayinero Sink profile; (b) map of Mataguac Hill inlier with associated dolines and a schematic diagram of Mataguac Spring Sink profile.

Another special case is the Gayinero Sink, which has a sinking stream flowing over its alluviated floor for about 500 meters. This feature is reminiscent of large, flat-bottomed depressions from the Dinaric karst known as poljes, and will be discussed in section 7.2.8.

Surprisingly, there are no depressions along the faulted contact between northern Guam limestones and southern volcanic highlands. Contrary to expectations, fieldwork has revealed no sinking streams and no blind valleys. All allogenic water is captured by the Fonte and Pago Rivers and flows to the Philippine Sea and Pacific Ocean, respectively. The only large depressions associated with the mid-island fault are in Maina along the contact of Alifan Limestone on the upthrown south side of the fault and the Agana Argillaceous Member of the Mariana Limestone on the downthrown north side. They seem to be a result of freshwater discharge from perched water in the Alifan outcrop. The depression to the south contains Maina Spring.

7. 2. 3. Drawdown dolines

As previously suggested, the corrosion necessary for the formation of depressions in the young and permeable limestones of northern Guam plateau could not have been focused by point recharge. With the exception of Harmon sink and the areas mapped as Agana Argillaceous Member (Tracey et al., 1964), no evidence of autogenic flow exists elsewhere in northern Guam.

However, surface flow and point recharge are not necessary for the formation of dolines. Solution dolines may develop by subcutaneous processes, as a result of the spatial variations in hydraulic conductivity. This mechanism was described by Williams (1983). He stated that diffuse recharge will cause significant dissolution in the top several meters of the surface, resulting in dissolutionally widened fissures rapidly closing with depth. This phenomenon has been observed in quarries and roadcuts on Guam, as described in Chapter 5. Thus, infiltration into the epikarst becomes easier than drainage out of it. Wherever efficient vertical drainage paths exist in the epikarst, the epikarstic water table will tend to get drawn down. This bottle-neck effect focuses corrosion and a true dissolutional depression is made in the cone of depression. Such a draw-down doline is distinct from point-recharge dolines (Williams, 1985).

This process is made easier if there exists a "vestigial conduit network" developed in an earlier karst phase (Ford and Williams, 1989). In case of northern Guam, it is certainly possible that frequent relative sea level changes have created a vertically dispersed distribution of phreatic dissolution voids which, after having been placed into the vadose zone by island uplift, may have provided elements for a growing network of vertical conduits (by being connected by vadose dissolution). This would have positively influenced the development of sinkholes on the surface of emerging northern Guam plateau.

Drawdown dolines will not develop if vertical hydraulic conductivity is great throughout the vadose zone or if vertical permeability is spatially uniform (Williams, 1985). This is a situation applicable to some raised coral atolls (Ford and Williams, 1989). However, previous studies in northern Guam have documented storage of water in the epikarst over extended periods of time (Jocson et al., 1999) as well as significant lateral movement in the vadose zone (Barner, 1995). Together these observations suggest the existence of the epikarstic water table and distinct permeable vertical leakage pathways, the two requirements for the development of drawdown dolines.

The influence of this mechanism on development of depressions in northern Guam is yet to be examined. There are several clusters of depressions on the northern Guam plateau found near its edge (above Haputo Beach, above Tarague Embayment, and in Pinate area and near the Hawaiian Rock Quarry in Mangilao) that I believe are most likely drawdown dolines. The sinkholes in Pinate are particularly impressive thanks to their close clustering and nearly identical shape and size (Plate 13, photo 5). This conclusion is based on the following observations: the aforementioned dolines are funnel-shaped, deep depressions (up to 30 meters), small in area and circular in plan, with no point recharge. Some evidence of collapse was observed, but this should not be taken as evidence against draw-down origin as most draw-down dolines have an element of rock subsistence or settling in their development (Williams, 1985).

Nevertheless, collapse also should be considered as a potential origin of these depressions. They may be a result of collapse with subsequent breakdown of the sides and filling of the bottom, coming to mimic other non-collapse dolines. It is quite possible that a collapse feature is so completely mantled by soil and debris that it cannot be distinguished from dolines of other origins (White, 1988).

In any case, the dolines described here are true karst features. It is difficult to imagine depressions of such geometry being depositional in nature. Contour maps of these dolines are shown in Fig. 7.5-a and 7.5-b, along with profiles of two selected dolines (Fig. 7.5-c and 7.5-d).

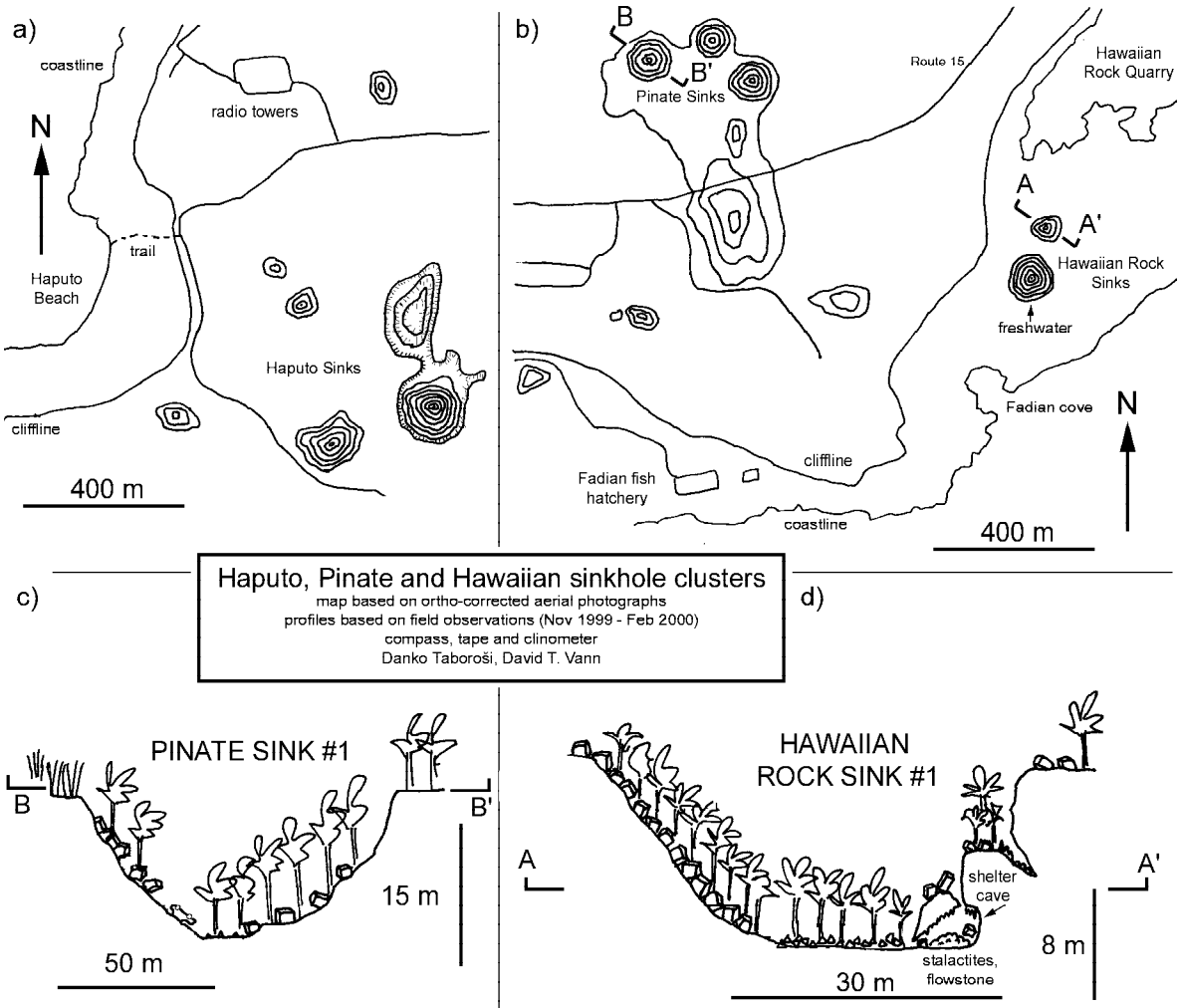

Fig. 7. 5: Probable drawdown dolines. (a) map of Haputo Sinks cluster; (b) map of Pinate and Hawaiian Rock sinks clusters; (c) profile of Pinate Sink #1; (d) profile of Hawaiian Rock Sink #1.

7. 2. 4. Collapse dolines

Closed contour depressions can form by collapse within the bedrock (White, 1988). In northern Guam several types of collapse dolines have been identified, including collapse of former and active conduits and collapse of phreatic voids. Some of these intersect the freshwater lens, in which case they are termed cenotes.

Collapse of former conduit caves

Dolines can form by roof collapse of a cave. They tend to be vertical walled but with further collapse may come to closely resemble solution dolines. Collapse dolines are not common on Guam, but do occur in both the coastal lowlands as well as the plateau. In the northern Guam plateau only one vertical-walled collapse doline (Carino Sink, Plate 13, photo 6) has been identified, but probably many more exist. Carino Sink is located in Chalan Pago, on a slope of a ridge dividing the large Chalan Pago uvala and Guacluluyao dry valley. It is about 20 meters deep, and has vertical walls and two traversable cave passages leading from its base. The passages could not be explored due to low oxygen conditions from organic decay of large amounts of trash in the sink. A similar feature exists in Barrigada (Barrigada Sink).

The scarcity of collapse sinks in northern Guam may be a result of infilling by land owners who are not too keen on having such environmental hazards on their property.

In case of collapse of active, water-filled conduits, sinkholes provide access to freshwater, in which event they are termed cenotes. Such features occur on Guam and are discussed in the following section.

Cenotes

Originally described from Yucatán, classic cenotes appear as water-filled shafts but are in fact collapsed portions of extensive conduit systems (Beddows, 1999). Cenotes may also be solution dolines, vertical shafts and stoping chambers with bell-shaped and small surface openings (White, 1988) but those described in this section follow the former definition.

All vertical-walled collapse cenotes on Guam are found within Tarague Embayment, on the north coast of Guam. The most similar to the classic model is Tarague Well #4 (Fig. 7. 6). It is a vertical-walled, 10-meters-deep collapse feature, filled with water in its southern end (Plate 14, photo 1). The water-filled portion of the cenote was partially explored on SCUBA and contains a large collapse chamber reaching a depth of 15 meters. From this chamber, a narrow fracture (Plate 14, photo 2) allows access to the second chamber, reaching 21 meters in depth. The entire subaqueous portion of the cenote is characterized by collapse, with no depositional features in the ceiling and the entire floor being covered by collapse rubble (Plate 14, photo 3). Collapse rubble shows extensive phreatic mixing zone dissolution, characterized by extremely jagged dissolution features. The ceiling is quite unstable and even disturbances from air bubbles hitting the ceiling during SCUBA diving cause a rain of limestone particles to fall through the water column. The underwater portion of the cenote was not explored in its entirety and there may be additional penetrable fractures. Navy divers who dove in this cave reported seeing a large cavern beyond the depth of 21 meters but did not explore it (Hogan, 1959).

A similar cenote is the nearby Tarague Well #1, which is about 5 meters deep to the top of the collapse rubble but provides access to a 10 meter deep water-filled cave. This cave contains submerged stalactites. Water is several meters deep but collapse rubble is extensive and blocks access to any potential passages (Fig. 7. 7).

Collapse in Tarague Well #2 (Plate 14, photo 4) was even more extensive, and access to freshwater in this vertical-walled cenote is limited to a very small pool in its southern end. This cenote contains several rusty 55 gallon drums. It appears to be fracture controlled, with a dissolutionaly enlarged fracture leading from the cenote's southern end. The fracture is filled with stalactites and flowstone (Fig. 7. 8).

Fourth in this series is Tarague Well #3, which undoubtedly looked like the other Tarague wells before, but extensive collapse has eliminated most of vertical walls and almost all access to freshwater. There is a shelter cave in its southwestern end (Plate 14, photo 5) with a very small pool. Most of the perimeter of this sinkhole is gently sloping, the floor is flat and filled with sediment (Plate 14, photo 6) and the cenote is difficult to recognize as a collapse feature (Fig. 7. 9).

Three additional features known as Tarague Wells #6, #7 and #8 are reported to be collapse sinkholes with caves containing freshwater but could not be examined due to restricted access. Tarague Well #5 is different from the rest and is a small cave not associated with a sinkhole.

In addition to cenotes in Tarague, two more water-filled sinkholes exist in northern Guam. One is in Hilaan on the Philippine Sea coast and is known as Lost Pond (a. k. a. Hilaan Pool), and the other is in Huchunao, near the Hawaiian Rock Quarry on the Pacific coast. Neither of the two is vertical-walled. They could be drawdown or collapse dolines.

The more famous of the two is Lost Pond at Hilaan, a popular hiking destination (Plate 14, photo 7). This doline intersecting the freshwater lens is located about 200 meters inland from a beach about 1 kilometer north of Tanguisson Point. The bottom of the doline is covered by very fine sediment, nearly suspended at the bottom of the freshwater pool. Robert and Company (1948) tested the water for chlorides as part of their "Reconnaissance Survey for New Fresh Water Sources on the Northern Section of Guam, M. I.," carried out for the Corps of Engineers, Department of Navy. They found water in the pool to have about 500 ppm chlorides at the surface and 1532 ppm at a depth of 2 meters (on 14th and 16th of August, 1948, respectively). Freshwater fish (*Eleotris fusca* and eel *Anguilla marmorata*) and shrimp (*Macrobrachium lar*) were observed in the pool on several occasions. Interestingly, a marine fish species, the garden eel (*Moringua* sp.) was also recorded in this pond (B. Tibbatts, pers. comm.) Garden eels are a benthic species and water on the bottom of the pool is apparently saline enough for them to survive.

The cenote at Hawaiian Rock (Hawaiian Rock Sinkhole #2) (Plate 14, photo 8) quarry is about 90 meters in diameter, reaching a depth of 20 meters. It intersects the freshwater lens, with the freshwater pool being about 30 meters in diameter, and 2-3 meters deep. Water in the sinkhole was tested by Robert and Company (1948) who found the chloride concentration to be 1050 parts per million. Obligate freshwater plant *Barringtonia racemosa* grows around the perimeter of the cenote. Freshwater sponges of the Spongilidae family were recorded in

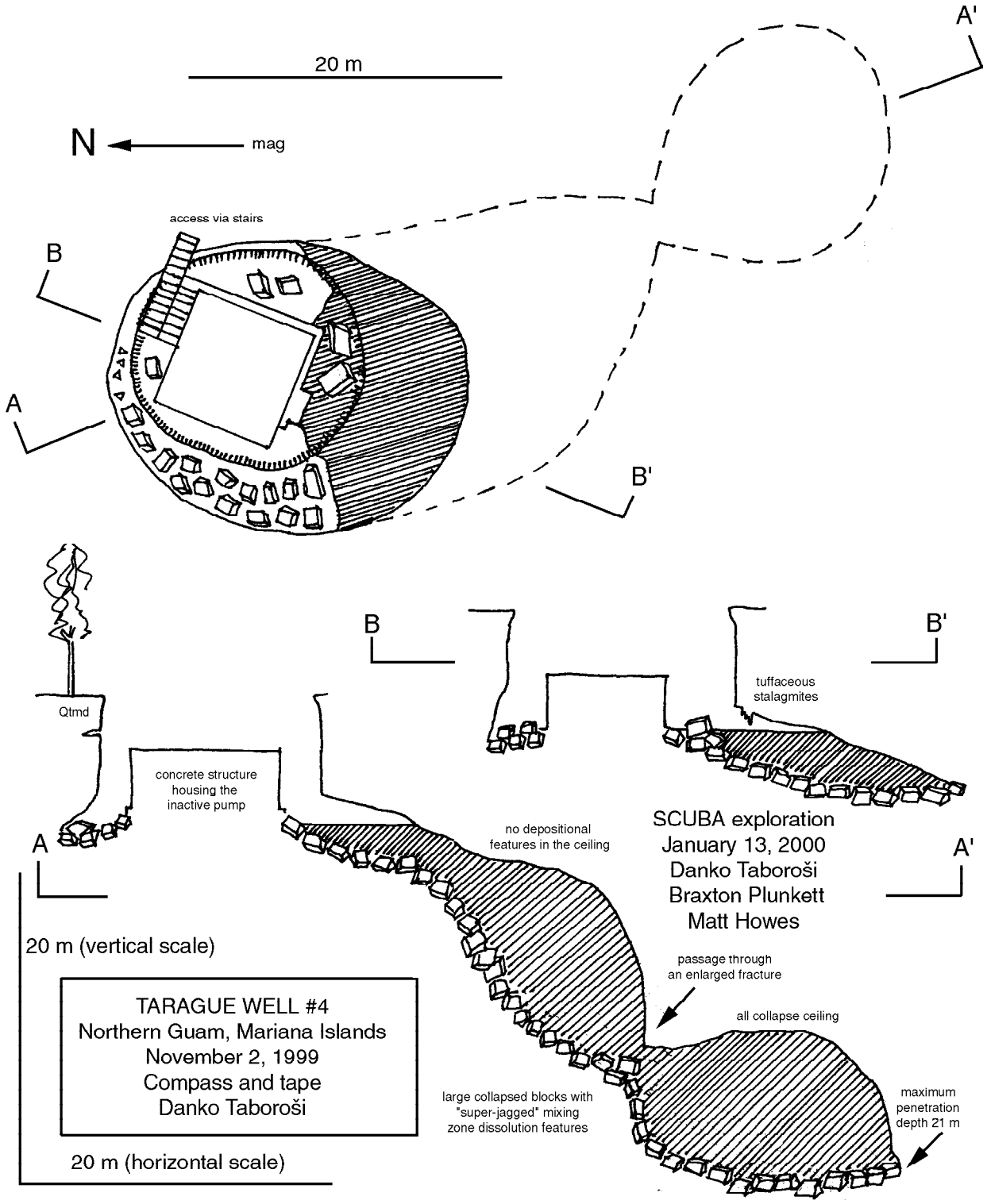

Fig. 7. 6: Map and profiles of Tarague Well #4.

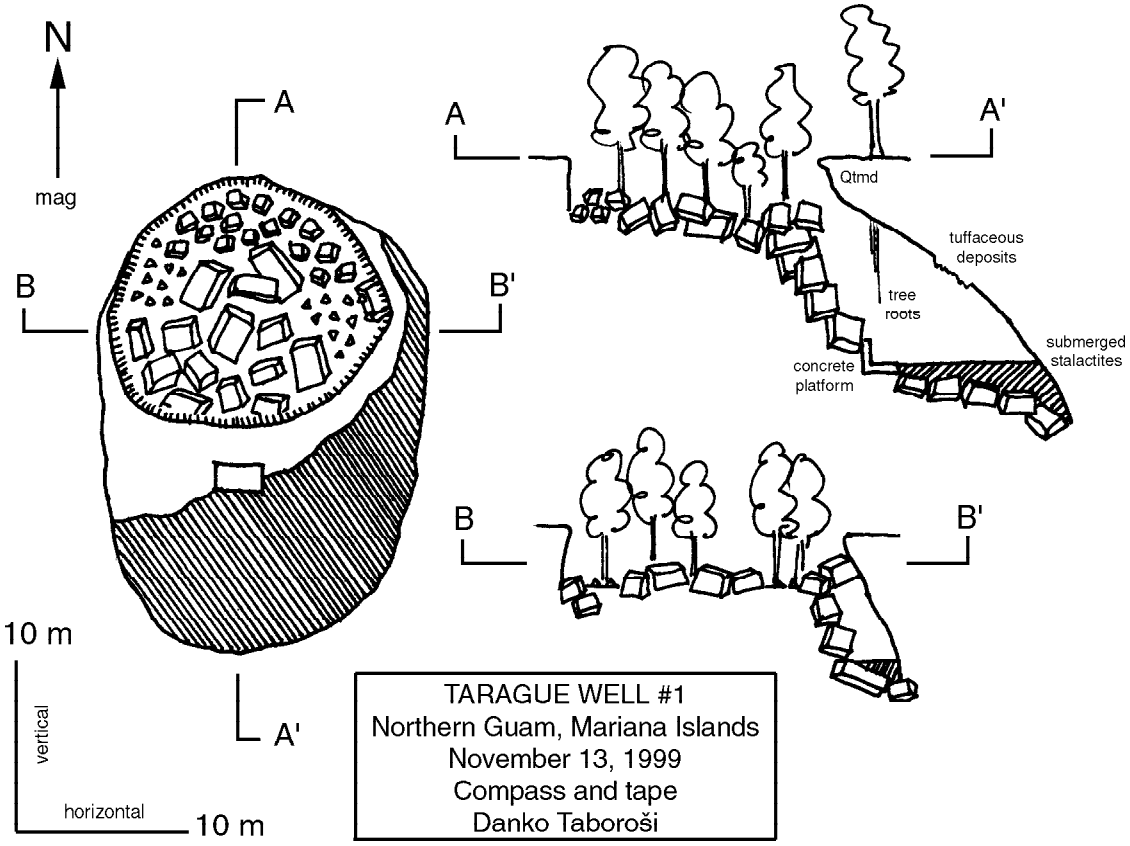

Fig. 7. 7: Map and profiles of Taragüe Well #1.

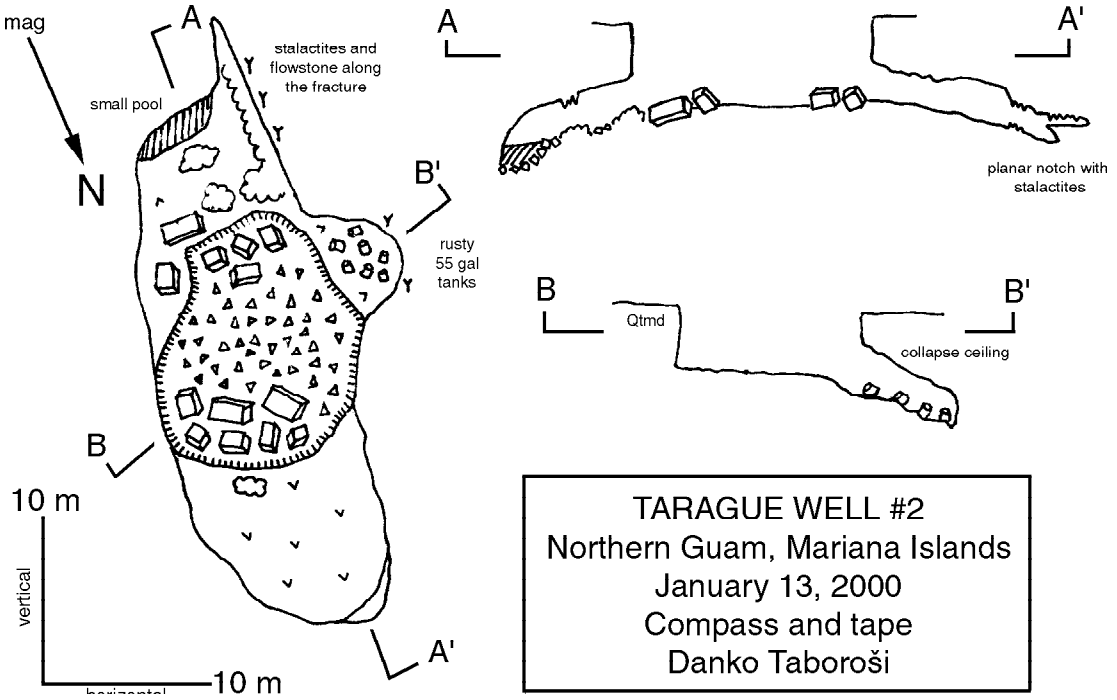

Fig. 7. 8: Map and profiles of Taragüe Well #2.

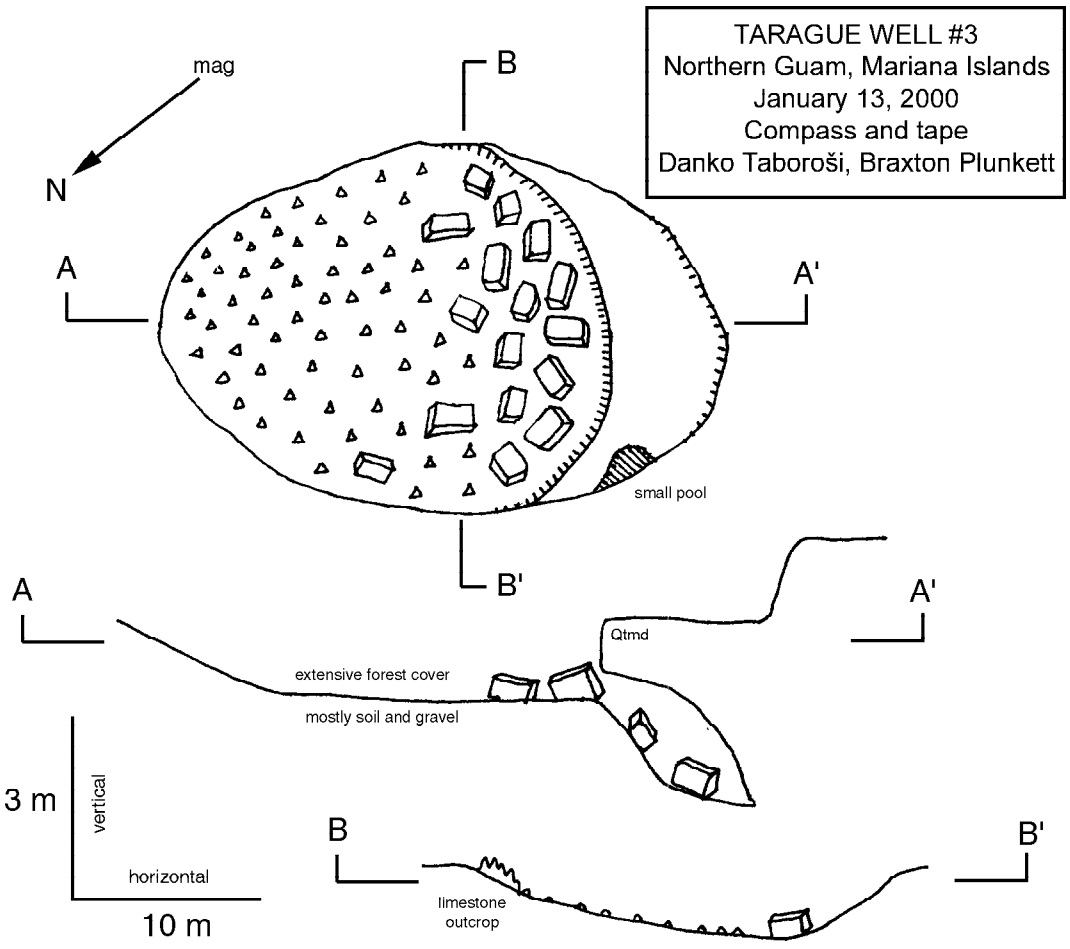

Fig. 7. 9: Map and profiles of Taragueue Well #3.

the pond. Fish *Eleotris fusca* and *Anguilla marmorata* (eel) and shrimp *Macrobrachium lar* are known to inhabit the pond (B. Tibbatts, pers. comm.) All of these are amphidromous species (having a marine larval stage).

In addition to these two dolines, only one other similar feature is known to have existed in northern Guam. Robert and Company (1948) reported that they had been informed by local residents that a depression near Ritidian Point used to contain freshwater, but it turned out to be filled with debris and had to be excavated about 1 meter to reach the water level.

Collapse of lens voids

Phreatic dissolution features, particularly voids that have preferentially developed on the top of the freshwater lens, may collapse and form collapse dolines. One such feature was discovered near the Navy housing area in Finagayan. It resembles banana holes described from the Bahamas (Harris et al., 1995). Such features were originally classified as "depression karst" by Mylroie (1988) but were later reclassified as horizontal dissolution features (Pace, 1992) to reflect their genetic history.

The Finagayan Banana Hole (Fig. 7. 10, Plate 15, photo 1) is 3 meters deep and circular in plan. Collapse portion of the ceiling is 3 meters in diameter, with the subsurface void reaching about 6 meters in diameter. Central part of the banana hole is filled by collapse rubble, but the periphery contains fine sediment. Walls of the banana hole show pronounced horizontal dissolution planes, and contain stalactites. In a dye trace test in July 1999, dye injected into this banana hole was chased with large amounts of water and was detected at the coast only 4 hours after injection (P. Casey, pers. comm., cited in Mylroie et al., 1999). The sinkhole now receives stormwater drainage from the capped Navy's Finagayan landfill.

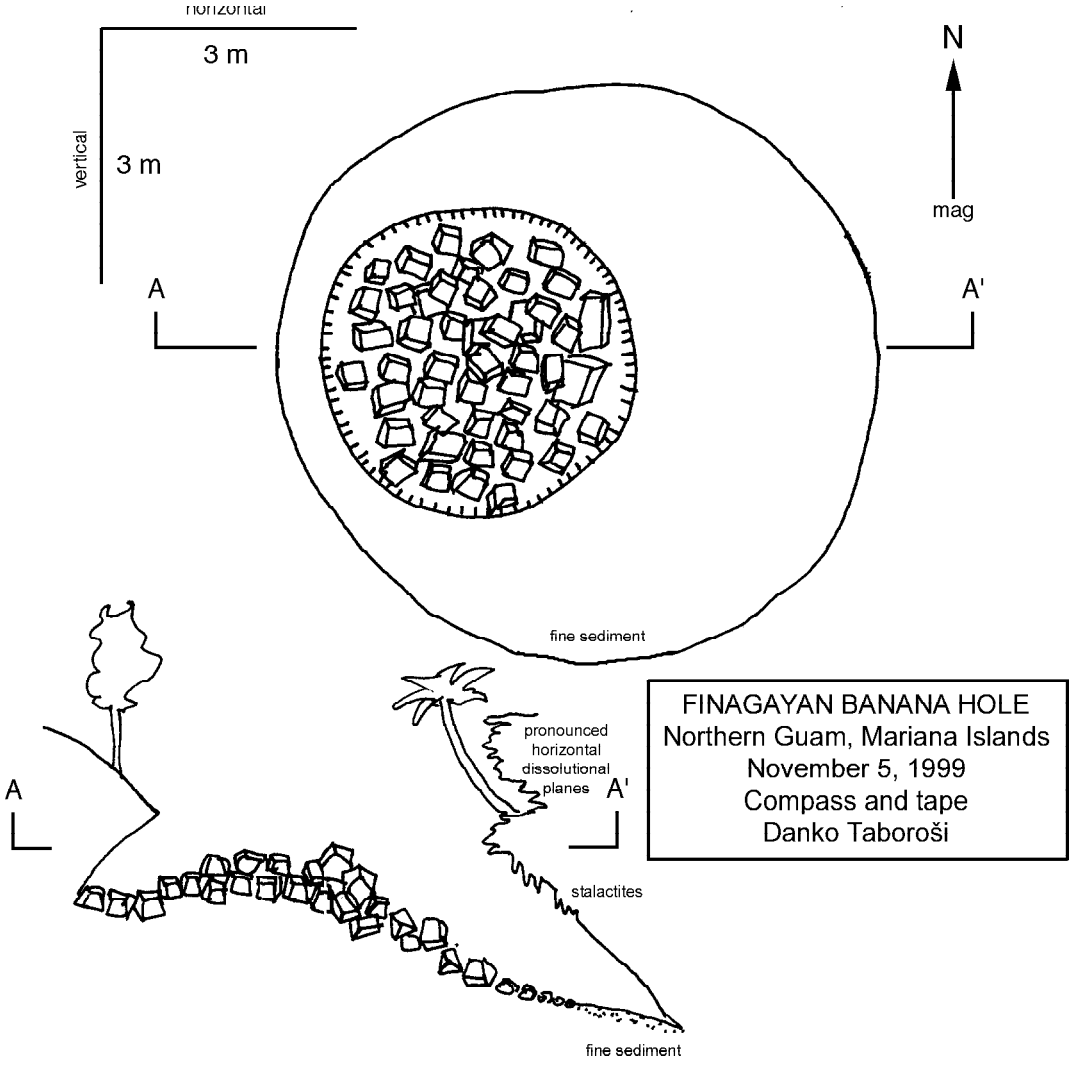

Fig. 7. 10: Map and profile of Finegayan banana hole.

A unique collapse feature exists near the Hilton Hotel in Tamuning and is known as the Devil's Punchbowl (Plate 15, photo 2). It is a dome shaped, single chambered room accessible though a collapse in the ceiling, but only by rappelling. This feature appears to intersect the freshwater lens in a shallow pool. The pool in the Devil's Punchbowl will be one of the Harmon Sink dye-tracing project monitoring locations (D. Moran, pers. comm.) There are no passages leading from the chamber. It appears to be a collapsed single-chambered phreatic void, possibly a flank margin cave and is described in more detail in section 9. 2. 10.

In addition to collapse of simple phreatic voids, flank margin caves (Mylroie and Carew, 1990) may also collapse to form closed contour depressions. On Guam, flank margin caves are almost always breached by cliff retreat or small scale ceiling collapse without creation of a closed depression, but there is at least one collapse feature in northern Guam resulting in a pronounced sinkhole. It is part of the Pagat Cave and is the sinkhole located between two sections of the cave. It is simply a collapsed room of a flank margin cave.

Other collapse features

There are reports of vertical-walled collapse dolines in the Y-sengsong area. Some of these were examined on aerial photographs and appear to be collapse features but were not investigated during this project due to access restrictions by land owners.

Collapse depressions may not be always recognized due to breakdown of walls and filling in of the bottom. Therefore, a number of dolines of presently unknown origin may be collapse features.

Finally, collapse features may originate from collapse of a deep cavity that stopes its way to the surface. Such collapse dolines or subsidence dolines look much like other dolines but the depressions may be underlain by tens or hundreds of meters of broken rock (White, 1988). No such collapse features have been identified in northern Guam because of lack of surficial expression of such mechanisms.

7. 2. 5. Valley dolines

Valley dolines form during the degradation of underdrained valleys (White, 1988). They are remnants of previous surface drainage which was diverted underground as soon as the karstification process becomes stronger and faster than the valley formation process (Bonacci, 1987). After all conditions necessary for surface flow are eliminated by dissolution, most flow over the surface ceases, but continued runoff creates sinkholes (White, 1988). These continue to deepen and widen, occupying the space where valleys used to be.

Valley dolines exist in the southern part of northern Guam, in the area mapped as Agana Argillaceous Member of the Mariana Formation (Tracey et al., 1964). This limestone facies has high clay content, derived from the southern volcanic highlands. There is evidence (see Chapter 6) that during the period following the emergence of northern Guam an integrated surface drainage network developed in southern part of northern Guam, where argillaceous limestone is impermeable enough to support some surface flow. Eventually, karstification processes caused the diversion of most flow underground, leaving as evidence a network of dry valleys punctuated by sinkholes. Four of these dry valleys contain at least nine well developed valley dolines, one of which is a compound valley sink, or uvala. The dry valley containing most valley dolines is Pulatar valley. It contains a string of valley dolines between Apusento Gardens and Flora Pago Gardens apartment complexes in Chalan Pago. Some of the dolines have been converted into ponding basins, making it impossible to deduce their origin based on geometry alone. A dry valley containing these dolines is perfectly outlined by the 100 ft topographic contour line and is shown on Fig. 7. 11-a.

Two dolines in the nearby Guacluluyao dry valley (Fig. 7. 11-b) were deemed representative of valley dolines in northern Guam. They are nestled in a dry valley, with valley walls rising about 30 meters. The northern doline (Plate 15, photo 3) is 350 meters long and 50 meters wide. Its floor is flat and covered by alluvium. The periphery of the doline has some exposed limestone and colluvium derived from valley wall collapse. Its profile is shown in Fig. 7. 11-c. The southern doline is smaller and has been modified by human activities. One part of it has been deepened and serves as a fish pond (Plate 15, photo 4). The two dolines are separated by a ridge indicating one-time elevation of a valley floor (prior to development of dolines).

7. 2. 6. Karst valleys

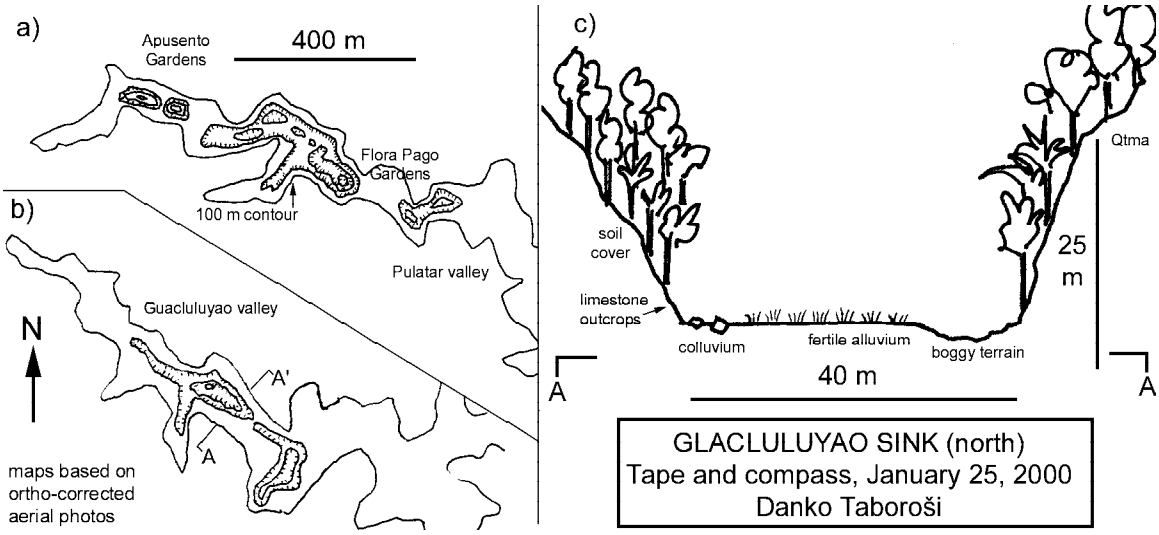

Fig. 7. 11: Valley sinks. (a) map of Pulatar dry valley sinks. (b) map of Guacluluyao dry valley sinks. (c) profile of Guacluluyao Sink (north).

A special type of a closed depression is known as karst valley and is not readily allocated to any of the basic categories of karst depressions (dolines, uvalas, poljes) (Jennings, 1985). They frequently contain valley dolines, but themselves form large elongated closed depressions (Jennings, 1985) and are nothing but deeply incised dry valleys.

The only such feature from northern Guam is the closed contour valley extending for more than a kilometer northwest of Maimai dry valley sink (Fig. 6. 4). It is only 20-30 meters wide but can easily be seen on USGS topographic maps.

7. 2. 7. Uvalas (compound dolines)

As individual dolines grow, they may coalesce and form large closed depressions with multiple ponors (White, 1988). Such compound dolines are known as uvalas (Cvijic, 1960).

There are large depressions that look like compound sinkholes scattered throughout the northern Guam plateau. However, as long as their origin is uncertain (i.e., depositional vs. dissolutional), it would be premature to classify them as uvalas.

However, real uvalas certainly exist in the Agana argillaceous member of the Mariana Limestone, which clearly exhibits some classical karst features.

The largest and the most complex internally drained depression here is the Chalan Pago uvala, with its steep and complex, deeply incised slopes. This uvala is clearly a result of surface dissolution (Fig. 7. 12). No ponor or cave passages associated with this feature could be identified.

A more typical uvala (clearly a compound feature) formed by coalescence of valley sinks exists in Pulatar dry valley, between Apusento Gardens and Flora Pago Gardens apartment complexes (Fig. 7.11-a).

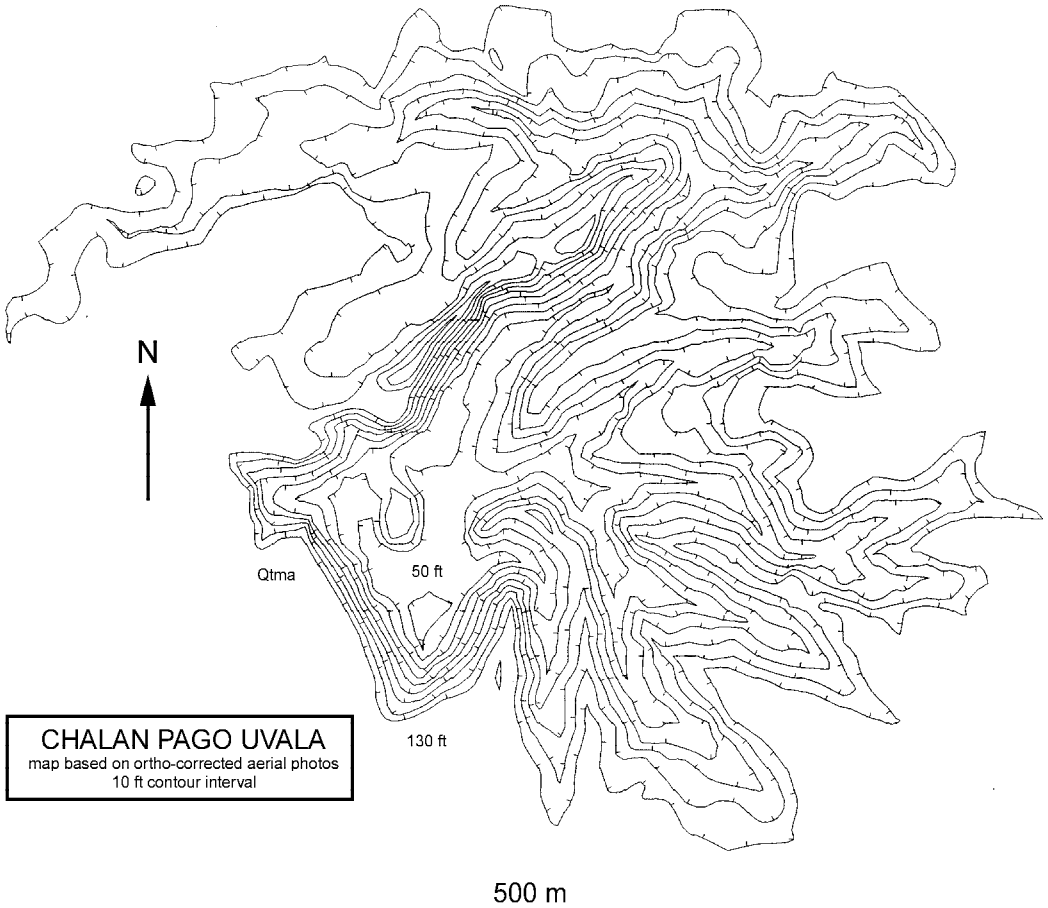

Fig. 7. 12: Map of Chalan Pago uvala.

7. 2. 8. Poljes

Poljes are large, flat-floored depressions in karst areas (Cvijic, 1960). There are a variety of mechanisms that may create a polje depression, and poljes are genetically classified as border poljes, structural poljes and base level poljes. They are a typical karst form in Dinaric karst and occur in other continental karst settings, such as France and Italy and tropical (continental-type) areas like in Malaysia and Cuba. Poljes have never been described from small carbonate islands such as Guam.

However, the presence of volcanic inliers in the northern Guam plateau has created unique conditions suitable for the development of a border polje. There are two depressions on the southeast flank of Mt. Santa Rosa, collectively known as the Gayinero Sink (Plate 15, photo 5). The depression to the north appears to be a small border polje. It satisfies all three criteria set forth by Gams (1978) to be considered a polje: 1) flat floor, 2) closed basin with steeply rising marginal slope on at least one side, and 3) karstic drainage. Reaching 400 meters in width, it even satisfies Gams' arbitrary requirement of 400 meters as the minimum width of a polje, although not that of 1 kilometer set by Cvijic (1893).

This polje covers an area of about 152,000 m^2 and is used exclusively for agriculture. At least four temporary allogenic streams enter the polje and converge on its alluvium-covered floor. The waters sink at a single ponor located at the polje's southwestern margin, some 500 meters away from the nearest volcanic terrane. This ponor almost certainly leads to a traversable cave, but which cannot be accessed without excavation of accumulated debris. The map and a schematic diagram of this polje's profile are shown in Fig. 7. 4-a.

Fairbridge (1968) stated that poljes appear to be associated with impeded underground drainage. According to anecdotal reports by local residents, Gayinero Sink was entirely flooded in early 1950s.

7. 2. 9. Depositional depressions

Many closed contour depressions on Quaternary carbonate islands are depositional in origin (Mylroie and Carew, 1995). They develop internal drainage and are modified by karst processes but the majority of their volume reflects initial topography instead of dissolution (Mylroie and Carew, 1995).

Mylroie et al. (1999) suggest that many depressions found in the pure limestone facies in northern Guam are depositional in nature. They write that depressions found in this area tend to be broad and shallow, which indicates origin from depositional topography and secondary structural modification. Depositional origin for depressions in northern Guam was proposed earlier by Ogden Environmental and Energy Services Co. (1995) who argued that there is no evidence that depressions in northern Guam are dissolutional because of lack of surface runoff. They wrote that the "development of solution sinkholes depends on the water flowing across the limestone surface." This, however, is not necessarily true, as sinkhole development can be a result of subcutaneous hydrology (Williams, 1983).

Although true sinkholes exist in northern Guam, both strictly dissolutional and collapse, the origin of any given broad, shallow depression in northern Guam remains problematical (Plate 15, photo 6). Their origin cannot be determined by field observations alone and could have both depositional or constructional components in any given case. A large number of small and deep depressions exist in the pure limestone facies in northern Guam and although many have been converted into ponding basins, they retain geometry unlikely to be a result of deposition (see section 7. 2. 10).

I have interpreted about 25% of the depressions in the pure facies in northern Guam to be dissolution or collapse, based on field observations. A further 10% seem to be directly related to faults and brecciated zones. The remainder are of unknown origin and could be a result of depositional topography.

Fig. 7. 13. shows distribution of closed contour depressions of various types in northern Guam, along with the depressions of unknown origin.

7. 2. 10. Human modification of depressions

Ponding basins

The northern Guam plateau contains many densely populated urbanized areas and continues to be subject to rapid development. This has resulted in human modification of landscape, which includes conversion of natural depressions into ponding basins and building of culverts to focus urban runoff into the depressions. A survey of ponding basins in northern Guam was an integral part of the karst inventory and locations of 71 ponding basins as well as their contour lines (10 ft interval) were mapped. Locations of all of these are shown in Fig. 7. 14, but only those ponding basins deeper than 10 feet were included in the inventory of closed contour depressions.

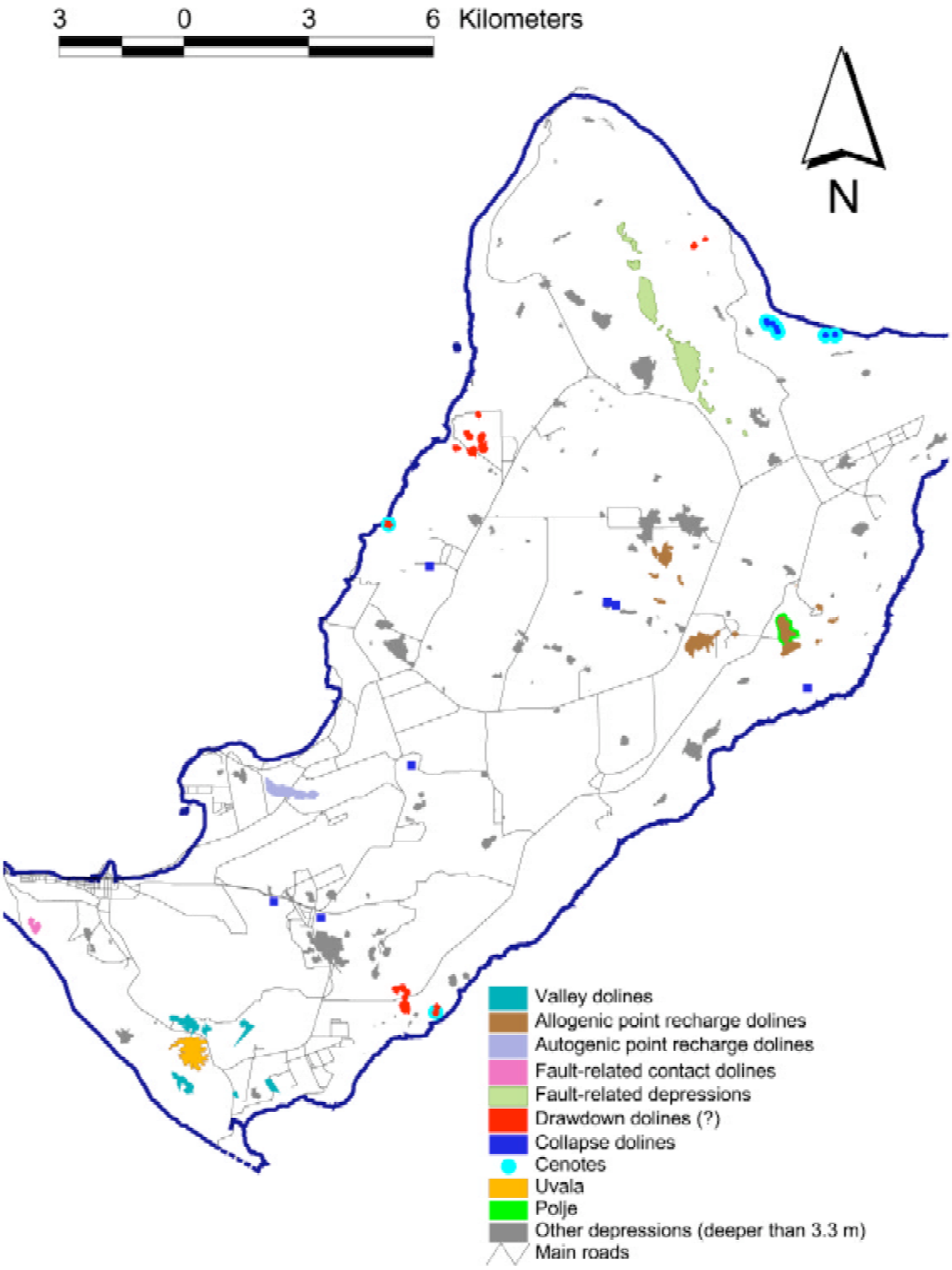

Fig. 7. 13: Types of karst depressions identified in northern Guam.

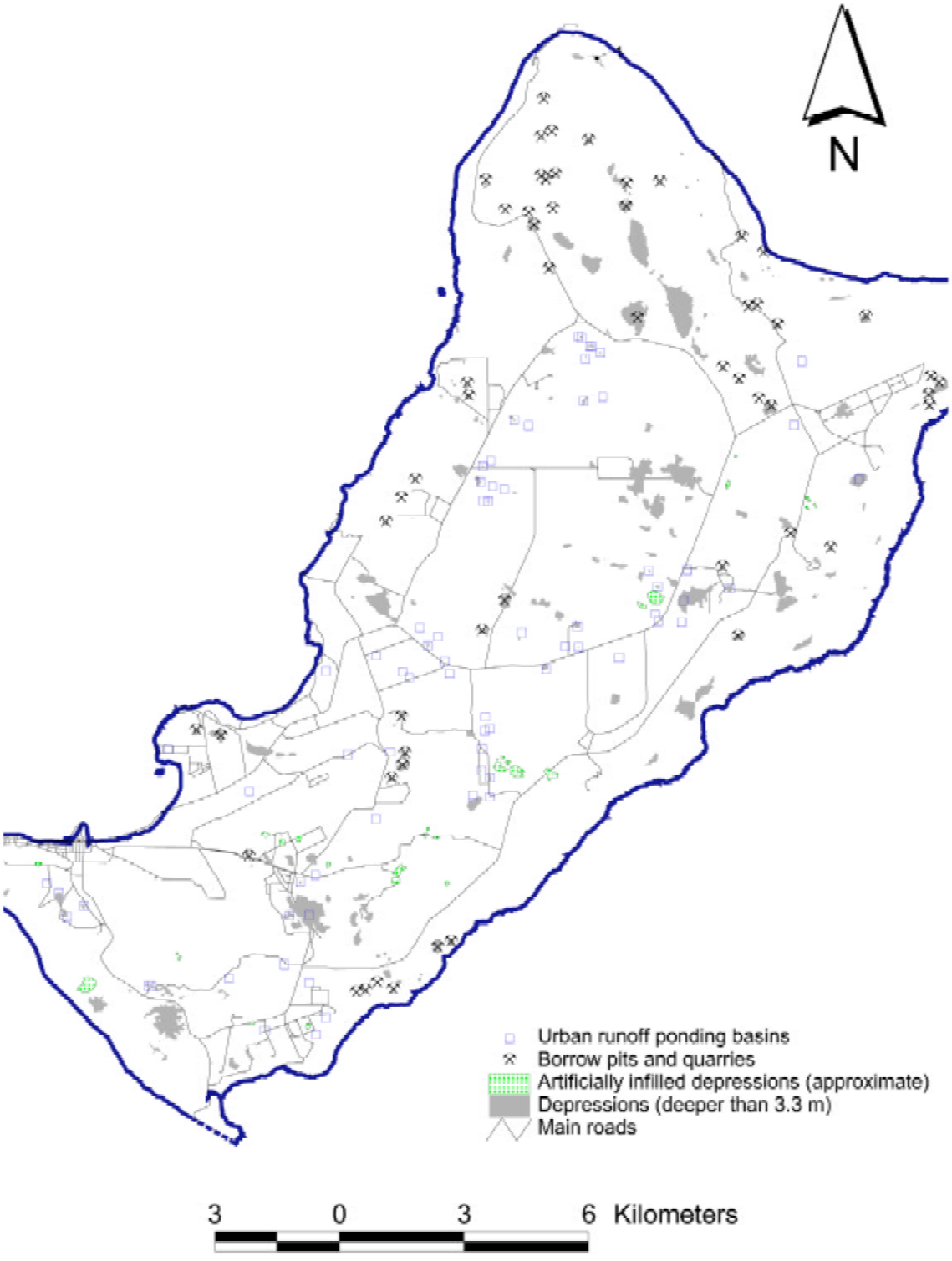

Fig. 7. 14: Closed contour depressions in northern Guam modified by human activities.

The ponding basins vary in geometry. Most have been modified to the extent of appearing completely artificial, having rectangular appearance, flat bottom and steep slopes (Plate 15, photo 7). They are, however, almost certainly modified natural depressions. The origin of these depressions cannot be established based on observations in the field. Once converted into ponding basins, various types of dolines are indistinguishable. A valley doline converted into a ponding basin at Apusento Gardens apartment complex in Chalan Pago, for example, appears the same as many ponding basins in Yigo and Dededo areas which were certainly not a result of valley-related processes.

An example of a ponding basin that is certainly a modified natural sinkhole is shown in Fig. 7. 15 and in Plate 15, photo 8.

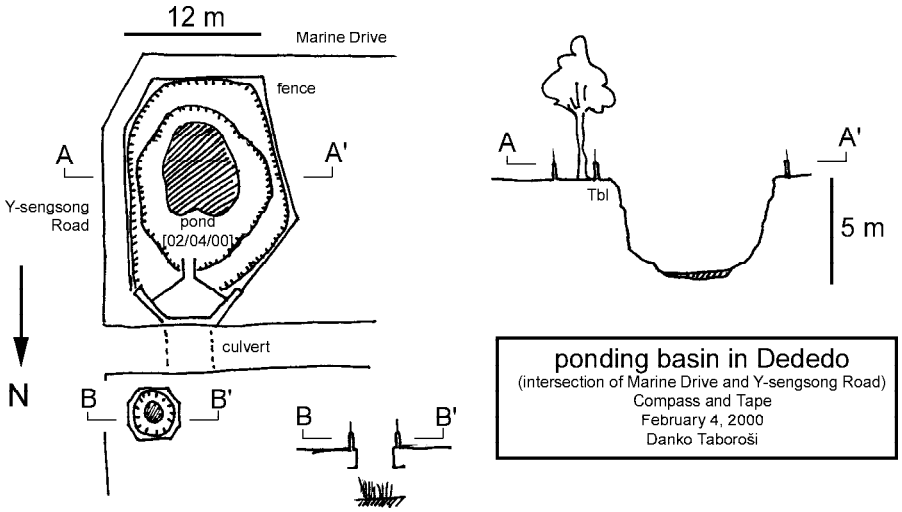

Fig. 7. 15: Map and profile of a natural doline modified into a ponding basin, located in Dededo, at the intersection of Marine Drive and Y-sengsong Road.

Quarries and borrow pits

Quarrying is another common human modification of natural depressions. A total of 56 locations of quarrying in northern Guam were identified from USGS topographic maps and are shown in Fig. 7. 14. This map shows locations of active as well as historical quarrying operations. Most borrow pits were limited operations in small natural depressions, mostly on military lands and original topography of depressions does not appear to have been significantly altered. In several instances, however, where major quarries were developed, no indications of initial topography remain (Plate 15, photo 9). Nevertheless, an old topographic map by U.S. Army Mapping Service used as a base map for the Water Resource Map of Guam (USGS, 1965) shows that quarries have frequently been developed in locations of prior natural depressions.

In the Northwest Field of Andersen Air Force Base, an unusual type of artificial depression looks surprisingly similar to small natural dolines. These depressions are made by explosive ordnance disposal, however, and should not be confused with true dolines (Plate 15, photo 10).

Infilled depressions

Urban development has often resulted in infilling of natural depressions. Current topography was compared to the old topographic base map for the Water Resource Map of Guam (USGS, 1965), and this indicated that at least 27 former natural depressions have been infilled. The true number is probably much higher, as the old map is at 1:50,000 scale and shows only the largest depressions. Small collapse depressions, which do not appear even on large scale maps, are probably often infilled by landowners to reduce hazards to life and property. A map of approximate locations and extent of known depressions which have been infilled is shown in Fig. 7. 14.

7. 3. Morphometric Analyses of Depressions in Northern Guam

Karst morphometry is a quantitative approach to the study of karst. Its founder was Cvijic (1893) who classified dolines according to their geometry. In addition to describing individual features, morphometry can also be applied to characterize the arrangement of karst features. Density of dolines can be analyzed and compared based on differences in terrain relief (Ford, 1964) as well as rock type (Kochanov, 1993). Distribution patterns as well as pattern disturbances (such as concentration along lineaments) can also be quantified (Williams, 1972). Finally, morphometry can be used to obtain clues to the genesis of depressions in a karst area (Kemmerly, 1982).

The reasons for applying such analyses to karst of northern Guam are numerous. Morphometric analyses aid in description of karst, they allow comparisons with other karst terranes and, ultimately, may answer questions about origin and nature of the karst features studied. It is presently not known whether many closed contour depressions scattered around the northern plateau are true karst depressions or simply depositional or constructional depressions, only subsequently modified by karst processes. Although fieldwork has revealed the existence of several types of solution dolines and collapse dolines, the majority of depressions in the pure limestone facies in northern Guam remain of unknown origin. Such depressions show no obvious ponors and are often entirely covered by soil. Urban development has made it even more difficult to directly evaluate the origin of these depressions as many have been converted into ponding basins, turned into quarries or destroyed by infilling. Clearly, the nature and origin of such depressions cannot be deduced by field observations alone. Karst morphometry provides an additional tool for acquiring clues to the genesis of depressions in northern Guam.

7. 3. 1. Data used

Field work for the study reported here was directed toward identifying various types of depressions, mapping representative individual sinkholes, and was focused on selected parts of the island. Therefore, data collected in the field were insufficient for morphometric analyses as they are incomplete and reflect a biased coverage. Because of these limitations, I restricted data for morphometric analyses to information derived from the ortho-corrected digital set of aerial photographs provided to WERI by the Government of Guam Bureau of Planning.

Data collected in the field were not used even to complement data used for morphometric analysis in order to avoid adding exploratory bias.

Commonly used sources of data for morphometric analyses are large scale topographic maps. USGS 7.5' quadrangles at 1:24,000 scale are a typical data source (Kochanov, 1993; Kemmerly, 1982; Troester et al., 1984). Maps, however, are of variable quality and, even at large scales, such as 1:10,000 may under-represent depression population by as much as 54% when compared to a field survey (Day, 1983). Nevertheless, maps are a common source of data for morphometric analysis and have been used for morphometric analysis even when large scale allowed identification of only large depressions (Matschinski, 1968; Troester et al., 1984). Topographic maps were not used for morphometric analyses on Guam because, when compared with field data, the maps appear to have selective coverages and often dramatically under-represent the real depression population.

The most practical medium for morphometric analyses are large scale aerial photographs. When viewed stereoscopically under magnification, such photos are preferable to topographic maps (Ford and Williams, 1989). Stereoscopic analysis of aerial photos was used to collect data for this project but primarily to locate features of interest and prepare for field work. Using stereoscopic images to gather data for morphometric analysis was attempted but abandoned due to several problems, including masking of topography by heavy forest, difficulty discerning broad shallow depressions as well as great difficulty of estimating depression depth and delineating boundaries.

Because of the problems described, data from the previously mentioned sources (field work, topographic maps and aerial photographs) were not used at all in the morphometric analyses of depressions. Instead, the sole data source was digitized topographic contour lines derived from ortho-corrected aerial photographs, as described in section 3. 3. 2. This data source proved to be superior to the others, due to its small contour interval, large scale, digital format, and availability of complementary digitized and ortho-corrected aerial photos.

When compared to 1:24,000 topographic maps, contours derived from digitized orthophotos show more than 10 times the number of depressions. When field checked, digitized orthophotos were inadequate only in locating small collapse sinkholes that could not be detected due to small area and heavy

canopy. Only about 15 such sinkholes are known from northern Guam. These are included in the karst inventory but excluded from the morphometric analysis to avoid bias.

To obtain usable data, the aforementioned digital GIS coverages were processed to eliminate all but closed contours. The new map revealed a total of 1252 closed contour depressions. Only 197 of those had two or more closed contour lines, indicating a depth of more than 10 feet. This arbitrary cutoff point provided a basis for creation of two data sets: all depressions and deep depressions (10+ feet). Most analyses were performed on deep depressions only. This is because the shallow depressions are frequently gentle undulations in terrain or a result of human activities, as artificial as sand pits in golf courses or military fuel storage facilities. Deeper depressions however, are more likely to be significant natural features. Troester et al. (1984) have demonstrated that the karst depressions in tropical regions are deeper than those in the temperate regions and even in the temperate regions the smallest average depth is 5.4 meters (Kentucky).

To avoid errors due to human modification of depressions into quarries and ponding basins, all depressions known to have had their shape altered were deleted from any tests evaluating geometry of individual features. However, because quarries and ponding basins were assumed to have been natural depressions at one time, all were considered in tests analyzing spatial distribution of depressions.

The following morphomeric analyses of depressions in northern Guam were performed:

a) geometry of depressions
    1) analysis of depression dimensions
    2) analysis of depth to diameter ratios of depressions
    3) analysis of depression depth frequency
b) areal analysis of depressions
    1) extent (number of features) in different lithologic or topographic settings
    2) variations in depression density
    3) variations in distance to nearest depression
c) analysis of spatial distribution of depressions
    1) nearest neighbor analysis
    2) evaluation of linear patterns

7. 3. 2. Geometry of depressions in northern Guam

Geometry of individual sinkholes was one of the first topics of morphometric studies in karst. Cvijic was the pioneer in this field and classified dolines based on their geometry (1893). The shape of a depression is outlined by a contour defining the break in slope at the depression's edge (White, 1988). Unless a depression is circular, a long axis can be drawn as the longest distance (L) across the depression, and the width (w) can be defined as the longest distance across the depression perpendicular to the long axis (White, 1988). Doline depth is usually defined as the difference in elevation between the lowest point in the depression and the highest elevated bounding contour (Ford and Williams, 1989). Various ratios have been developed to further analyze depression geometry. Area of a depression can be approximated by formula $A=(\Pi/4)*L*w$ (White, 1988).

Measurements of depressions were collected in Guam as part of the karst inventory. Length and width were calculated according to Williams (1971) criteria and distances were measured from digital maps using the "measure" function in ArcView software. Depths were defined as the number of closed contours delineating the depression multiplied by the contour interval of 10 feet. In a few cases, digitized topographic coverages contained elevation markers of 5 foot resolution at the bottoms of depressions and in those cases, depth assigned was a multiple of 5, rather than 10. Area of a depression was calculated by ArcView software as the area of the polygon defined by the highest closed contour. This method is more accurate than the use of area approximation formulas. Measurements for almost all inventoried depressions are included in Appendix 6. In addition to basic geometric measurements, other parameters were calculated, including azimuth of the long axis, distance to nearest neighbor and azimuth of the distance to nearest neighbor vector. These will be discussed in sections 7. 3. 8. and 7. 3. 9.

The following table (7. 1) represents the summary of geometric measurements for depressions in northern Guam and shows minimum, maximum and mean values for length, width, depth and area calculated for each known type of doline. Depressions of unknown type were grouped as a separate category. The last row shows overall values for all depressions in northern Guam. In addition to basic measurements, average values of length to width ratios and depth to diameter ratios for each genetic including unknown category of depressions are also provided. These ratios were calculated according to formulas from

Ford and Williams (1989).

The table shows that the length of depressions in northern Guam ranges from 30 to 1,353 meters, with the average value of 265 m. Average depth is 8 meters, with a maximum depth of 29 meters. Area of depressions ranges from 528 m^2 to 547,642 m^2, with the average being 40,672 m^2.

Table 7.1: Minimum, maximum and mean dimensions of depressions in northern Guam.

Identified types of	#	%	length (L) [m]			(W) [m]	depth (H) [m]			area (A) [m2]			mean ratios	
closed contour depressions	dep.	tot.	mean	min	max	w idth	mean	min	max	mean	min	max	L/W	H/diam.
Allogenic point recharge	14	7.0	318	60	948	189	9	6	14	59548	1075	269412	1.70	0.06
Autogenic point recharge	2	1.0	85	60	110	70	8	6	9	5122	1508	8735	1.21	0.10
Collapse dolines (all types)	15*	7.5												
Valley dolines	9	4.5	216	65	390	53	8	6	12	12595	1793	41941	4.39	0.08
Uvala	1	0.5	560			315	27			427460			1.78	0.06
Draw dow n dolines (?)	16	8.0	109	40	241	91	14	6	29	7416	1010	27682	1.25	0.15
Faulted contact	2	1.0	155	121	188	67	11	9	14	9895	5131	14659	2.33	0.10
Fault-related	15	7.5	360	100	1353	138	7	3	18	78571	5003	547643	2.32	0.04
Unknow n	127	63.2												
All depressions	201	100	265	40	1353	131	8	3	29	40672	528	547643	2.25	0.07

*no measurements due to muliple data sources (field work and orthophotos)

7. 3. 3. Depth to diameter ratios

Analysis of depth to diameter ratios of depressions has been used as means of determining the origin of depressions. Coleman and Balchin (1960) have argued that depressions of solutional origin would show a tendency toward dynamic equilibrium in their slopes, so a plot of depth to diameter ratios should give a cluster along a straight line. They analyzed depressions in Mendip plateau and obtained a widely scattered depth to diameter ratio plot. They suggested that the depressions are therefore of collapse origin, because such dolines would be variable in depth to diameter ratio. Jennings (1975) has analyzed dolines on the Craigmore plateau in New Zealand and found a strong correlation (r=0.87) between depth and mean diameter. This result argued against collapse origin and pointed to solutional origin or subsidence.

This technique was applied to depressions from northern Guam. The data set analyzed included only deep depressions, except those modified by human activities. The resultant depth to diameter ratio plot for northern Guam is shown on Fig. 7. 16.

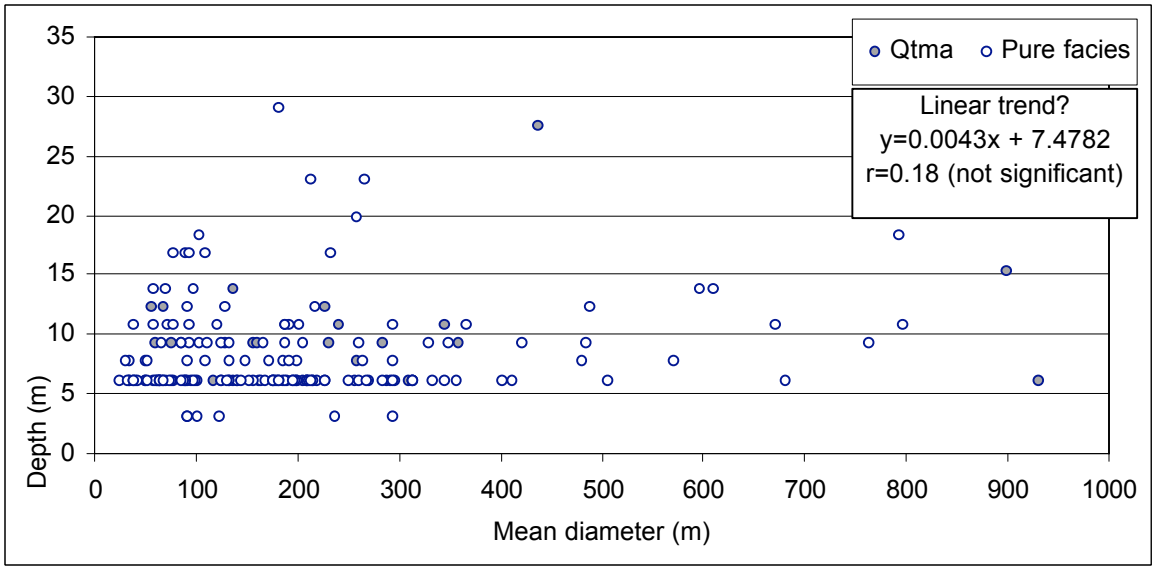

Fig 7.16: Depth to diameter ratio plot for northern Guam.

No significant linear correlation (at 0.05 level of probability) was found between depth and mean diameter (r=0.18, n=188). This result argues is compatible with collapse, depositional and constructional origins. Neither collapse, depositional nor constructional depressions would have a tendency to dynamic equilibrium in their slopes because they do not grow wider and proportionally deepen as is the case with solutional dolines.

7. 3. 4. Depression depth frequency

The rationale for applying this technique to Guam is to help characterize depression karst on Guam, allow comparisons with other karst regions and attempt to answer questions about the origin of closed contour depressions. Data used from northern Guam included all depressions found on digitized contour lines based on ortho-corrected aerial photos, including all shallow depressions. Those depressions known to have had their depth changed as a result of quarrying were eliminated from the data set. Troester et al. (1984) have observed that the exponential curve breaks down for very deep dolines as a consequence of small sample sizes. The Chalan Pago uvala, 27 meters deep, was thus eliminated from the data set because it is a uniquely deep feature that would heavily influence data for Agana Argillaceous Member area due to small sample size (n=29) of depressions there.

White and White (1979) have found that the frequency of occurrence of sinkholes in the Appalachians is independent of lithology and decreases exponentially with depth following the equation:

$$n=N_o * e^{(-Kd)}$$

where n is number of sinkholes, N_o is a constant coefficient that varies depending on the number of sinkholes, K is a constant, the inverse of which gives the characteristic depth of a sinkhole population, and d is sinkhole depth (White and White, 1979). Troester et al. (1984) have analyzed three other temperate karst areas and two tropical regions (parts of Puerto Rico and Dominican Republic) and also found an exponential decrease of sinkhole frequency with depth.

The number of depressions was plotted against depth, where the x axis was linear and y axis logarithmic. Data were fit to an exponential curve $n=N_o * e^{(-Kd)}$ using Microsoft Excel 97. This was done for the entire northern Guam, as well as separately for argillaceous limestone and pure limestones. The three resultant curves are shown on Fig. 7. 17., with best fit coefficients and correlation coefficients (R^2).

The best fit coefficients and correlation coefficients are compared with data from other karst regions in Table 7. 2.

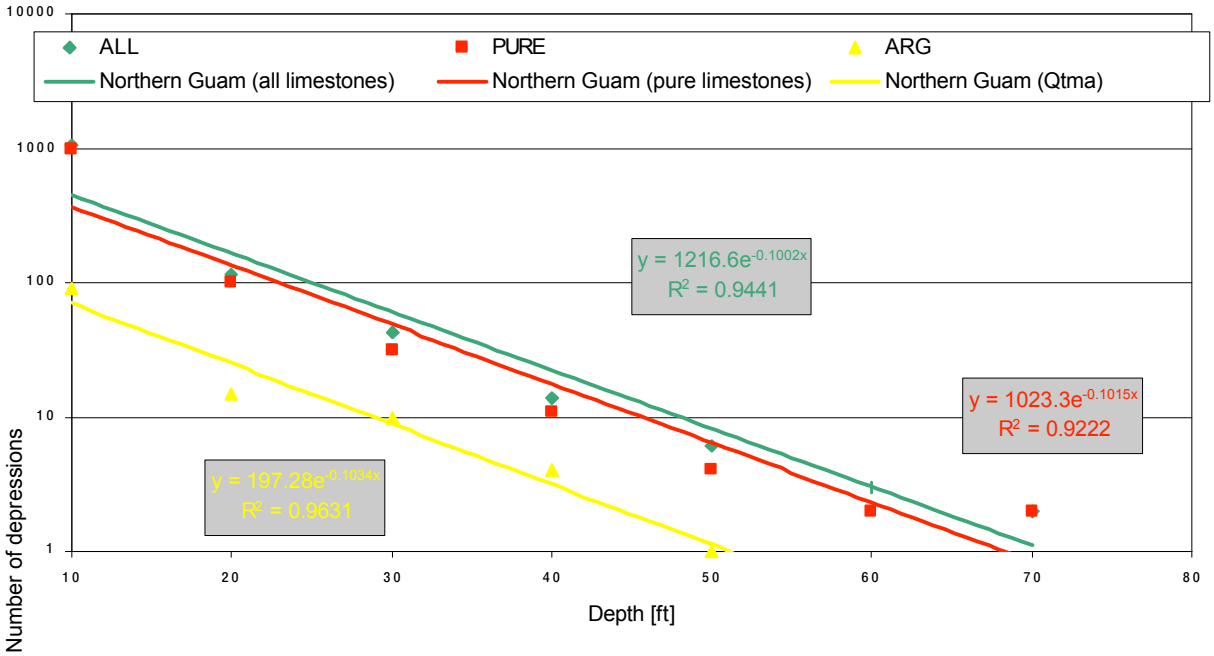

Fig 7.17: Depression depth frequency plot for northern Guam.

Table 7. 2: Best fit coefficients and correlation coefficients for exponential curves fitting depression depth frequency distributions of various karst terranes.

Karst Area	No	K(ft-1)	K(m-1)	r2	climate	source
Northern Guam -- Qtma	197	0.103	0.339	0.96	tropical	this study
Northern Guam -- pure ls.	1023	0.102	0.333	0.92	tropical	this study
Northern Guam -- all areas	1216	0.100	0.329	0.94	tropical	this study
Puerto Rico	6876	0.027	0.088	0.99	tropical	Troester et al. (1984)
Dominican Republic	69153	0.034	0.11	0.99	tropical	Troester et al. (1984)
Appalachians	12608	0.068	0.22	0.99	temperate	White and White (1979)
Kentucky	892	0.076	0.25	0.99	temperate	Troester et al. (1984)
Missouri	9789	0.094	0.31	0.99	temperate	Troester et al. (1984)
Florida	12299	0.362	1.18	0.99	temperate	Troester et al. (1984)

Correlation coefficients for Guam are significant at 0.01 level of confidence, although the actual values of r^2 are slightly lower than those of other investigated karst regions. This means that frequency versus depth of depressions from northern Guam fit of an exponential curve is not quite as strong as has been demonstrated for dolines in other karst regions. This could be explained by one or more of the following: 1) depressions in northern Guam have been modified by human activities, thus disturbing the natural exponential function of doline depth vs. frequency; 2) depressions in northern Guam are not all true dolines, and 3) depressions in northern Guam probably include a number of depositional depressions whose generally shallow depth would disturb the exponential depth distribution curve expected for dolines.

7. 3. 5. Areal analysis of depression distribution

Tracey et al. (1964) mapped Northern Guam in terms of six limestone formations and five facies of the Mariana Limestone. I have evaluated the distribution of depressions in various lithologies by counting the number of depressions found within a specific formation or facies. Number of depressions was then divided by total area of a mapped formation or facies to get average depression density for each unit (Table 7. 3). Additionally, total area of depressions and mean depression area in each lithologic unit, as well as all of northern Guam, were calculated in order to derive the index of pitting, as defined by Williams (1966). The reciprocal of this index is the doline area ratio (White, 1988). These values and ratios are shown on Table 7. 3 and are used to characterize and compare karst terranes.

Geol. Form.	Form. Area [km^2]	# of depr.	% of all depr.	# Depr. / km2	Total area of depr. [km2]	Mean area depr. [m2]	Index of pitting[1]	Doline area ratio[2]	L to near. neigh. [m] mean	min	max
Qtma	31.622	31	16.23	0.98	1.57	50734	20.1	0.04974	466	58	983
Qtmd	119.183	84	43.98	0.70	3.39	41325	35.2	0.02843	460	79	1724
Qtmm	17.199	12	6.28	0.70	0.55	45701	31.4	0.03189	611	202	1216
Qtmr	35.899	19	9.95	0.53	0.51	26924	70.2	0.01425	555	103	1376
Tbl	47.577	42	21.99	0.88	1.40	33451	33.9	0.02953	565	465	1655
Tal	1.782	2	1.05	1.12	0.03	15608	57.1	0.01752	470	145	475
Ta	2.003	1	0.52	0.50							
Tb	0.226	0	0								
Tj	0.044	0	0								
Qtmf	0.076	0	0								
Qrm	0.100	0	0								
Qrb/Qal	7.376	0	0								
N. Guam	263.087	191	100.00	0.73	7.46	39165	35.3	0.02835	500	58	1724

[1] Ford and Williams, 1989; [2] White, 1988

Table 7. 3: Different lithologies in northern Guam, their area and their respective number, percentage and density of depressions, total and mean depression area, index of pitting, doline area ratio and distances to nearest neighbors.

The proportion of total number of depressions in northern Guam found within a particular lithologic unit corresponds to the proportional area of that unit in northern Guam (Fig. 7. 18). This implies that lithology does not play a major role in the development of depressions. This contrasts with studies done in continental karst of North America, which have shown significant lithologic control of depression density (Howard, 1968; Kochanov, 1993).

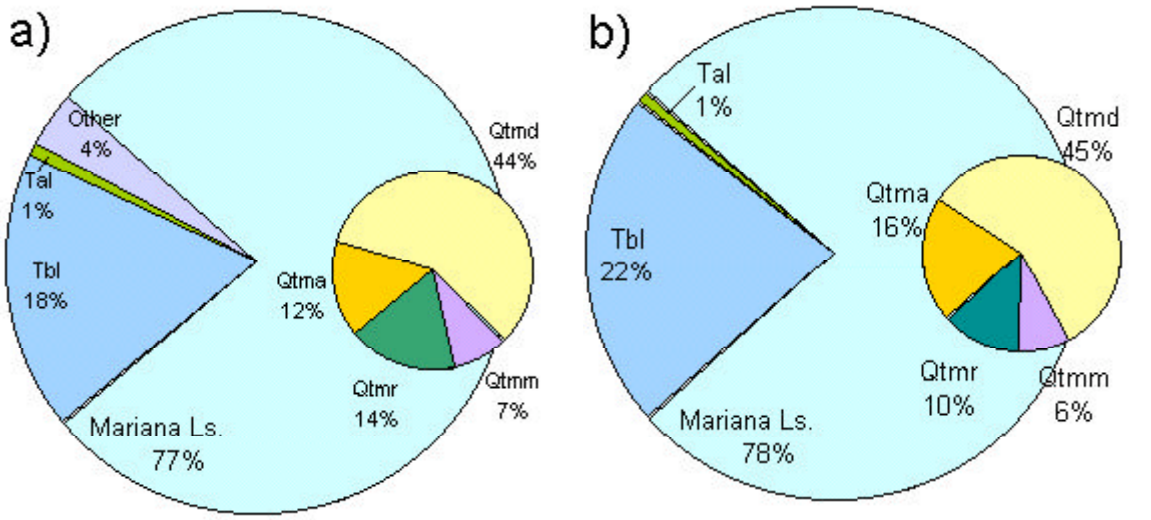

Fig. 7. 18: a) Areas of different lithologies in northern Guam compared to total area of northern Guam. b) Number of depressions found within different lithologies in northern Guam as a proportion of the total number of depressions.

Although lithology does not appear to influence density of depressions, topographic and structural differences appear to be consequential. During the inventory of closed contour depressions, topographic or structural setting of a depression was noted and described in terms of one of the following categories: plateau, plateau edge (<1 km away from cliffs), coastal terrace, valley, contact with volcanic units, and faulted contact between two limestone formations. As shown on the pie charts in Fig. 7. 19-a, 31% of depressions found in pure limestones in northern Guam are found on the plateau at less than 1 kilometer away from the coastal cliffs. Coastal terraces account for 4% of the total, 7% are found on contacts with volcanic units, 2% are found in a valley and 56% are found on the plateau, more than a kilometer inland from the coastal cliffs. Agana Argillaceous Member was evaluated separately, and 32% of depressions there are located within topographic valleys (Fig. 7. 19-b).

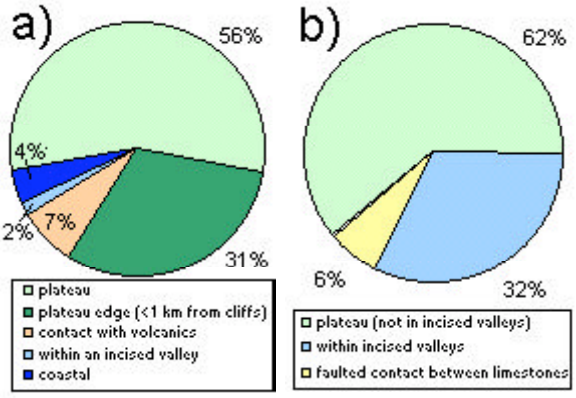

Fig. 7. 19: Percentage of depressions found in different topographic settings: a) pure limestones in northern Guam. b) Agana Argillaceous Member.

7. 3. 6. Density of depressions

Depression density in northern Guam was evaluated using ArcView's Spatial Analyst software. In order to calculate depression density, maps showing depressions as topographic contour lines were converted into maps where each depression is represented by a single point. The spatial location of a doline is usually represented by its lowest point (Ford and Williams, 1989). This conversion was done manually using ArcView by creating a point shape representing the deepest spot in each depression. For shallow depressions containing a single closed contour line, the deepest point could not be determined, so their location is represented by the mathematical center of a depression. The conversion was performed by Avenue language script for ArcView, "Polygon Centroid to Point Theme," by Tara Montgomery, 12/20/99, downloaded from esri.com.

Once a GIS point coverage was made, Spatial Analyst's "calculate density" function was applied, using "kernel density type" formula. This procedure was applied to a point coverage of all depressions from northern Guam regardless of depth and separately to a point coverage of only deep depressions. This resulted in contour maps showing variations in depression density throughout northern Guam (Figs. 7. 20. and 7. 21).

If all depressions are considered, the variations in density range from 0 depressions per km^2 to almost 19 per km^2. The distribution seems patchy, with numerous areas throughout northern Guam having 10 or more depressions/km^2 and several "hotspots" with 16 to 19 depressions per km^2. The hotspots are located in Dededo (south of Potts Junction and in Ipapao area) and in the Northwest Field area of the AAFB. A series of high depression density spots running parallel to the coastline from Ritidian to Tarague seems to indicate location of a yet unmapped fault, parallel to the large brecciated zone mapped by (Tracey et al., 1964). Another unmapped fault parallel to these two seems to run from Uruno Point to south of Potts Junction and is delineated by a series of high depression density spots (Fig. 7. 20). All areas showing depression density of 10 or more depressions per km2 are located north of the Tumon-Yigo trough.

If only depressions deeper than 3.3 m are considered, the distribution of high depression density areas is somewhat different. Two obvious "hotspots" are Mt. Santa Rosa and Mataguac Hill where numerous deep depressions occur due to availability of allogenic recharge. Several high depression density areas occur in the northwest field where depressions have probably developed associated with the geologic faults there. In Agana Argillaceous Member, high density of depressions is due to valley sink development. Several "hotspots" exist where the origin of depressions is still unknown. These include area inland from Haputo Beach that has depressions up to 30 meters deep and may be drawdown dolines, Ipapao area, and Fadian Point to Barrigada area.

7. 3. 7. Distance from depressions

The distance from any point in northern Guam to the nearest closed contour depression was calculated using ArcView's Spatial Analyst "find distance" function. Data was prepared in the same way as for calculating density and two separate data sets were evaluated again (all depressions and deep depressions).

The resultant maps have shown that there are just a few small areas north of the Tumon-Yigo trough that are more than 500 meters away from a closed contour depression (Fig. 7. 22). There are no points north of the Tumon-Yigo trough that are more than 700 meters away from a closed contour depression. In the southern part of northern Guam, the depressions are a bit less closely spaced with a no-depressions area from Sabana Magas to Agana Swamp (Fig 7. 22).

If only depressions deeper than 3.3 m are considered, most of northern Guam is within a kilometer from the nearest deep closed contour depression (Fig. 7. 23). North of the Tumon-Yigo trough, no area is more than 1200 m away from a deep depression.

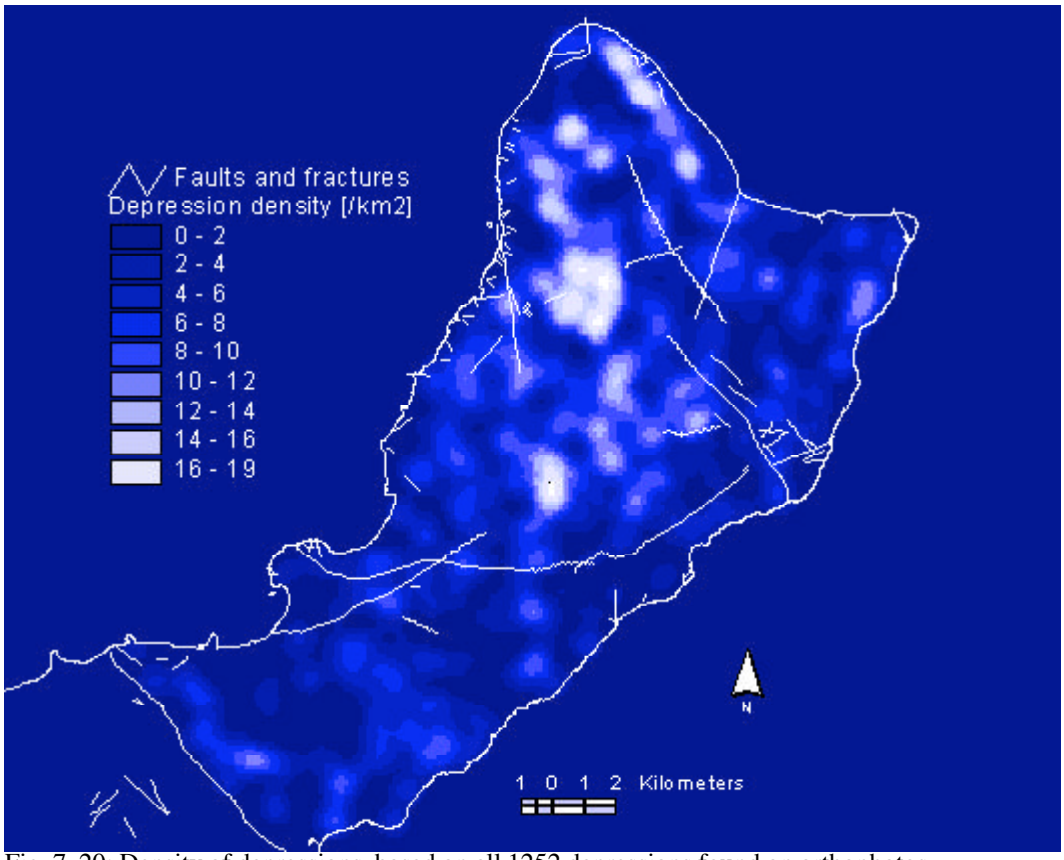

Fig. 7. 20: Density of depressions, based on all 1252 depressions found on orthophotos.

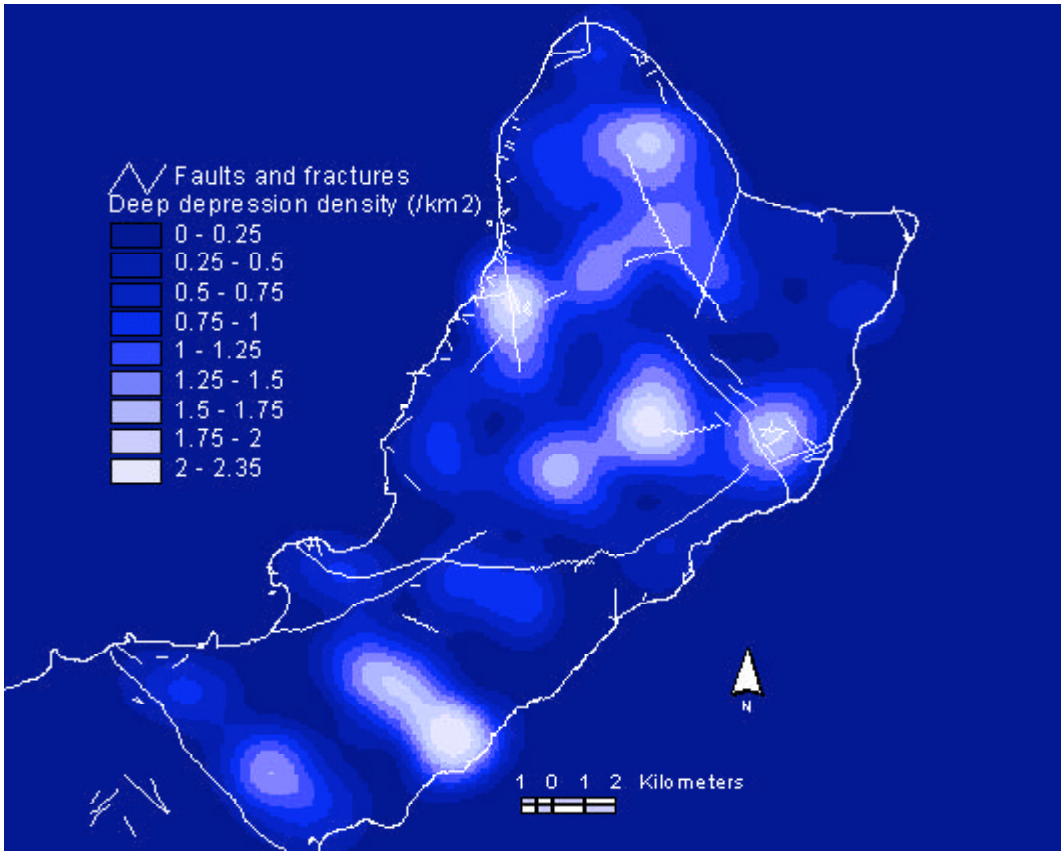

Fig. 7. 21: Density of deep depressions, based on 3.3+ m deep depressions, from orthophotos.

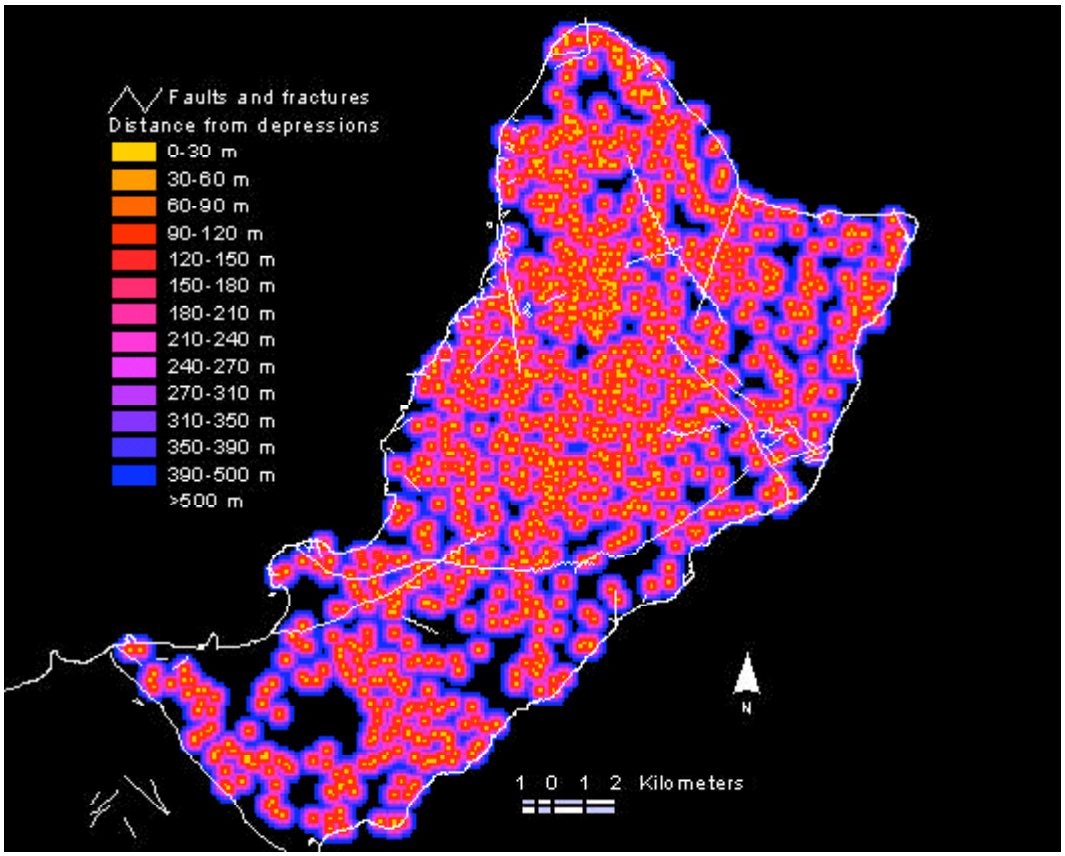

Fig. 7. 22: Distance from all 1252 known depressions found on orthophotos.

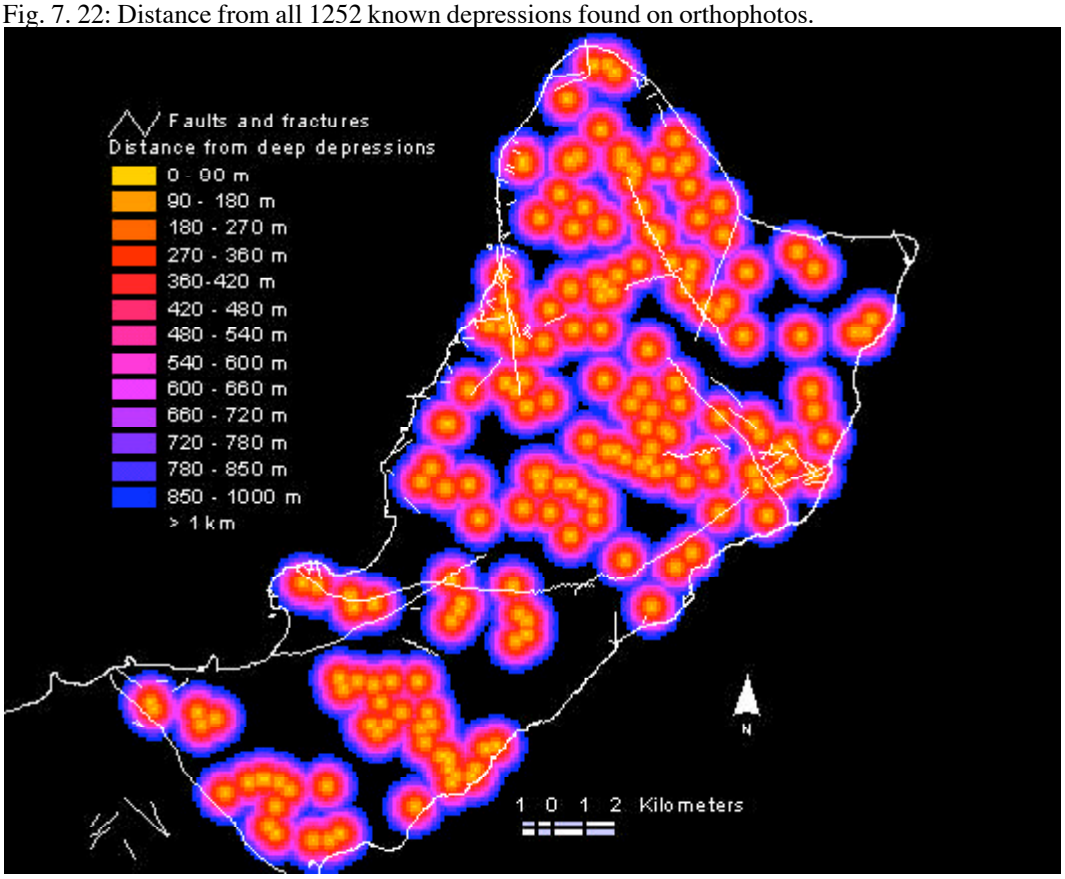

Fig. 7. 23: Distance from depressions deeper than 3.3 m, found on orthophotos.

7. 3. 8. Nearest neighbor analysis

The arrangement of dolines in a particular area can be as scattered isolated individuals, scattered clusters, or densely packed groups and irregularly spaced chains (Ford and Williams, 1989). All four patterns are apparent in maps of Guam (Fig. 7. 1., 7. 2., 7. 13., 7. 26., and 7. 27). Individual depressions and clusters are scattered throughout northern Guam as well as parts of southern Guam, densely packed groups exist in the central part of southern Guam and chains of depressions are found along dry valley floors immediately north of the Pago-Adelup fault as well as along allogenic recharge margins of northern volcanic inliers.

Two methods have been used to mathematically characterize distribution of points on a map: the quadrat method, and nearest neighbor analysis. The quadrat method is used to evaluate differences in density of points throughout the test area, but has some drawbacks associated with it. Quadrats are arbitrary sampling units and results vary with changing quadrat size (Williams, 1972). Nearest neighbor analysis examines spacing of points by measuring distance-to-closest-neighbor. Data analyzed consist of an empirical frequency distribution of distance (Williams, 1972). In order to acquire further clues to the genesis of closed contour depressions in northern Guam, the nearest neighbor analysis was used to determine their distribution pattern.

To perform the nearest neighbor analysis a map showing depressions as points (as described in section 7. 3. 6) was processed using "Nearest Neighbor Script, v. 1.8" for ArcView, by Colin Brooks, 04/10/98. This program compared the average actual distance (L_a) from each depression to its closest neighbor with the expected mean distance (L_e). Expected mean distance is based on an infinitely large random population with the same density (D) of points as in the study area and is calculated by the formula:

$$L_e = 1 / (2*\mathrm{SQRT}(D))$$

The ratio L_a/L_e is labeled R and forms the basis for conclusions. R ranges in value from 0 (maximum clustering) through 1 (random) to 2.1491 (uniform) (Williams, 1972).

R-values for the following data sets were calculated:

1) all 1252 depressions throughout northern Guam and its subsets of
   a) 1132 depressions found on pure limestone facies and
   b) 120 found in the area mapped as Agana Argillaceous Member

2) all 197 deep depressions (i. e. >3.3 m deep) in northern Guam and subsets of
   a) 168 deep depressions found on pure limestone facies and
   b) 29 found in area mapped as Agana Argillaceous Member

3) 197 computer generated randomly-scattered points plotted by "Generate randomly distributed points" Avenue script for ArcView by Stephen Lead, 20/10/99. This data set was used to control the procedure and software and should return an R value of 1.

Distribution of points (depressions) in the area mapped as Agana Argillaceous Member (Tracey et al., 1964) was evaluated separately because the nature of karst there is different from the rest of the northern Guam plateau presumably as a result of high clay content of limestone.

Results of the tests are shown in the table included in Fig 7. 24. This figure also shows map representation of actual data sets. A randomly-generated data set, which confirmed the validity of procedures and returned an expected R value of 1.0, is also included in this figure.

When all depressions were considered, R values were 0.929 for northern Guam in entirety, 0.951 for pure limestones and 0.831 for Agana Argillaceous Member. For depressions deeper than 3.3 m, the R value for all of northern Guam was 0.845, for pure limestones 0.869, and for the Agana Argillaceous Member 0.699. The divergence from random in all cases was on the side of clustering and its significance was evaluated by standard Z tests (Davis, 1986). All R-values are significantly different from random distribution at the 0.01 level of confidence. It may therefore be concluded that the dispersion pattern of depressions in northern Guam is not random.

Nevertheless, although there was divergence from random in all tests, the pattern is close to random when all depressions (n=1252) are evaluated for all of northern Guam. When all depressions are analyzed in the pure limestone facies only, divergence from random is even smaller but when all depressions are analyzed in argillaceous facies, divergence from random is greater.

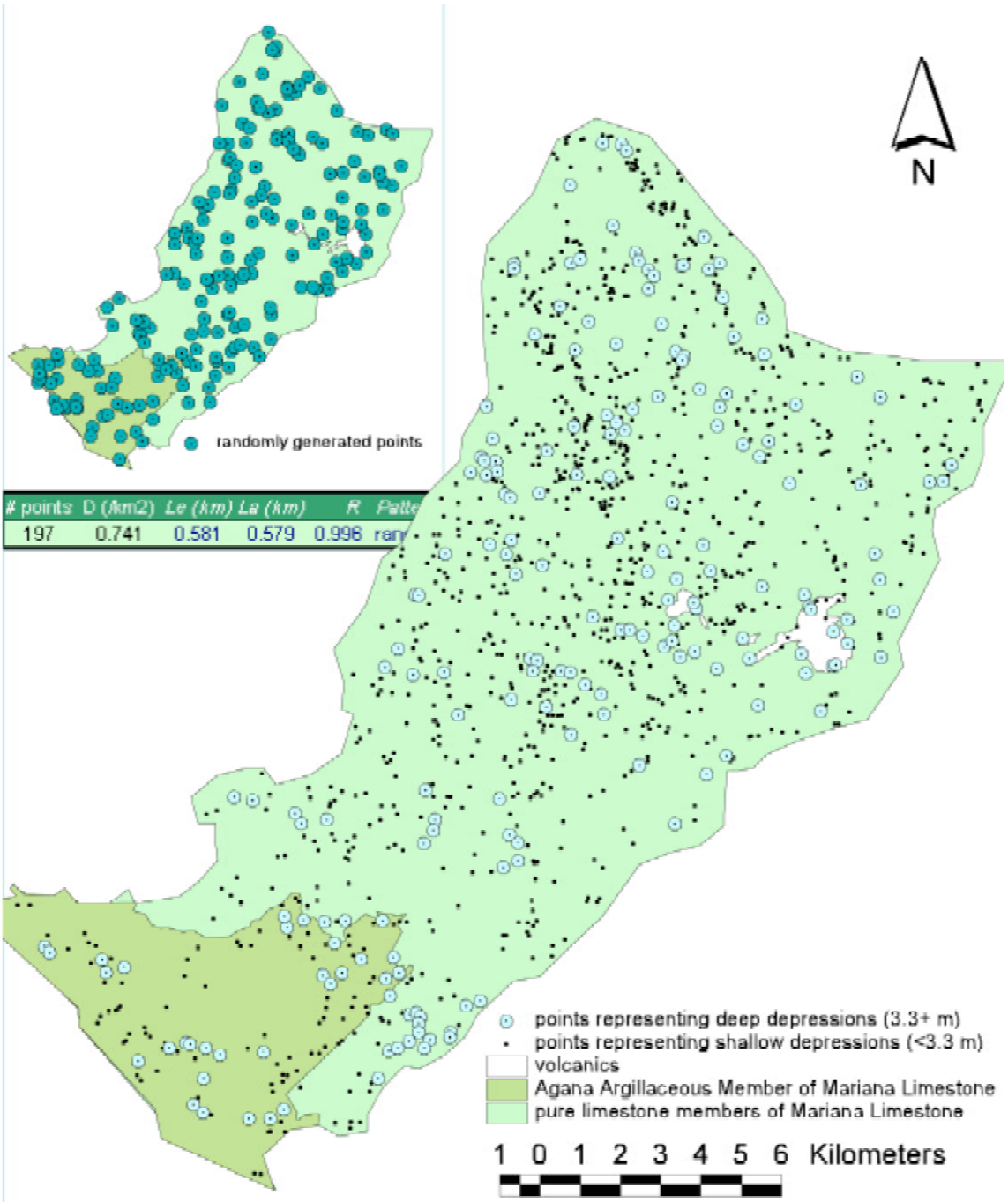

Locality	# depressions (all)	D (per km2)	Le (km)	La (km)	R	Pattern
Agana Argillaceous Member	120	3.105	0.284	0.236	0.831 *	clustered
Pure limestones in northern Guam	1132	5.045	0.223	0.212	0.951 *	near random
All limestones in northern Guam	1252	4.707	0.230	0.214	0.929 *	near random

Locality	# depressions (3.3+ m)	D (per km2)	Le (km)	La (km)	R	Pattern
Agana Argillaceous Member	29	0.750	0.577	0.404	0.699 *	clustered
Pure limestones in northern Guam	168	0.749	0.578	0.502	0.869 *	tending to cluster
All limestones in northern Guam	197	0.741	0.581	0.491	0.845 *	tending to cluster

Fig. 7. 24: Map representation of data and results of the nearest neighbor analysis of depressions in northern Guam. Inset shows a random data set used to control procedure and software.

When only those depressions deeper than 3.3 m are considered, overall divergence from random in the entire northern Guam is greater than for all depressions. This means that clustering of deep depressions is greater than that of all depressions. Again, when the dispersion pattern of deep depressions is evaluated separately for pure limestones and argillaceous facies, the pattern in pure limestones shows less of a departure from random while the pattern in argillaceous facies shows a greater departure from random. The distribution pattern of deep depressions in the argillaceous facies can thus be described as more clustered.

R values generated by nearest neighbor analysis in northern Guam were compared to those of other karst terranes. As an example of tropical karst, Williams (1972) provides data for eight New Guinea areas which range from near random to approaching uniform patterns of doline distribution. In continental karsts, Kemmerly (1982) analyzed terranes in Tennessee and Kentucky and concluded that their spatial distribution varies from random to clustered. Table 7. 4. shows some of these values alongside values from northern Guam.

Table. 7. 4: Results of nearest neighbor analysis for several continental karst areas and Caribbean islands compared to Northern Guam.

Locality	Spatial distribution	R value	N	Source
Oak Grove, KY	clustered	0.743*	887	Kemmerly (1982)
Bowling Green S, KY	clustered	0.793*	1302	Kemmerly (1982)
Hammacksville, KY	clustered	0.831*	1067	Kemmerly (1982)
Hopkinsville, KY	clustered	0.853	504	Kemmerly (1982)
Franklin, KY	random	0.925	241	Kemmerly (1982)
Johnson Hollow, KY	random	1.03	78	Kemmerly (1982)
Sango, TN	random	1.06	821	Kemmerly (1982)
Allensville, KY	random	1.18	1089	Kemmerly (1982)
Darai Directed karst 2, New Guinea	approaching uniform	1.226*	130	Williams (1972)
Darai Fluviokarst, New Guinea	approaching uniform	1.253*	185	Williams (1972)
Darai Directed karst 1, New Guinea	approaching uniform	1.328*	130	Williams (1972)
Darai Ridge karst, New Guinea	approaching uniform	1.333*	182	Williams (1972)
Darai Honeycomb karst, New Guinea	approaching uniform	1.404*	188	Williams (1972)
Antigua	clustered	0.533*	45	Day (1978)
Barbados	tending to cluster	0.874*	360	Day (1978)
Yucatan (Chichen Itza Fm.)	near random	0.987	25	Day (1978)
Puerto Rico (Aguada Fm.)	near random	1.124*	122	Day (1978)
Puerto Rico (Lares Fm.)	near random	1.141*	459	Day (1978)
Jamaica (Browns Town-Walderston Fm.)	approaching uniform	1.246*	301	Day (1978)
Jamaica (Swanswick Fm.)	approaching uniform	1.275*	273	Day (1978)
Northern Guam (pure limestone)	tending to cluster	0.869*	168	this study
Northern Guam (Qtma)	clustered	0.699*	29	this study

*significantly different from random, at 0.05 level

7. 3. 9. Evaluation of lineaments

The nearest neighbor analysis of deeper depressions in northern Guam indicates that the distribution pattern of depressions is not random (R=0.845) and the divergence from randomness is on the side of clustering. There are two approaches to the assessment of pattern disturbances: 1) examine orientation of individual depressions and 2) explore the possibility of alignment of neighboring depressions (Williams, 1972).

First step in the process was to depict as rose diagrams the orientation of mapped geologic faults and fractures in northern and southern Guam (and all of Guam combined) (Fig. 7. 25-a).

In order to examine orientation of individual depressions, depression long axes were viewed as vectors and the bearings of all elongate depressions were plotted on rose diagrams, separately for Qtma areas and pure limestones, as well as all of northern Guam combined (Fig. 7. 25-b).

To explore the possibility of neighboring depression alignments, vectors were drawn from the deepest point in each depression to the deepest point of the closest neighboring depression. Orientation of those lines (nearest neighbor vectors) was plotted on

rose diagrams as well, separately for Qtma and pure limestones and all of northern Guam combined (Fig. 7. 25-c).

A separate rose diagram was created to show orientation of valleys in the Agana Argillaceous Member area and Pago River basin because it has already been shown that a large number of depressions there lie within valleys. This was done to visually evaluate the possibility that orientation of streams and valleys is structurally controlled (Fig. 7. 25-d).

Finally, a rose diagram was made to show orientation of regional lineaments subjectively drawn based on apparent linear alignments of depressions in northern Guam (Fig. 7. 25-d).

It appears that the orientation of faults in northern Guam is bimodal, with a NW-SE and a NE-SW components. This pattern is reflected in the orientation of depression long axes as well as nearest neighbor vectors in the Qtma area and, to an extent, in the rest of northern Guam as well. Orientation of valleys in Qtma area and river channels of the Pago River basin seems to correspond very well to the orientation of faults in northern Guam.

This can be explained by the fact that a large number of depressions in the Agana Argillaceous Member area appear to be a result of surface dissolution where surface flow was guided by structural discontinuities. In the rest of northern Guam, however, where surface dissolution could not have been a main force in creation of depressions, orientation and alignment of depressions can be explained by subsurface processes, such as preferential infiltration along faults and fractures.

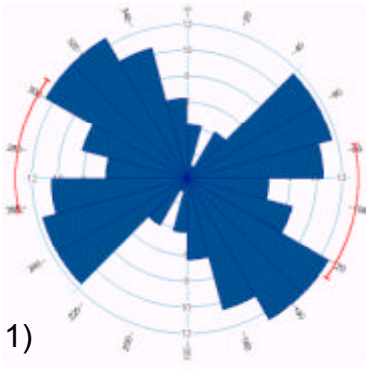

ORIENTATION OF FAULTS IN NORTHERN GUAM
Class Interval .....15°
Population 95
Maximum Percentage...12.6%
Mean Percentage 8.3%
Standard Deviation 3.76%
Vector Mean .....281.99°
Confidence Interval .....23.58°
R-mag 0.72

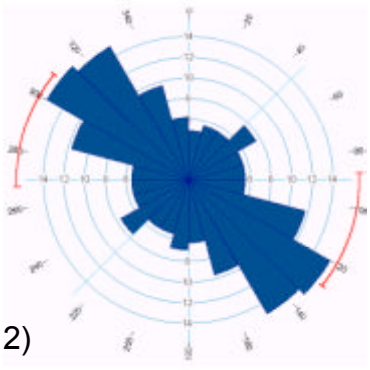

ORIENTATION OF FAULTS IN SOUTHERN GUAM
Class Interval .....15°
Population 146
Maximum Percentage...15.8%
Mean Percentage 8.2%
Standard Deviation 3.8%
Vector Mean .....288.18°
Confidence Interval .....20.48°
R-mag 0.69

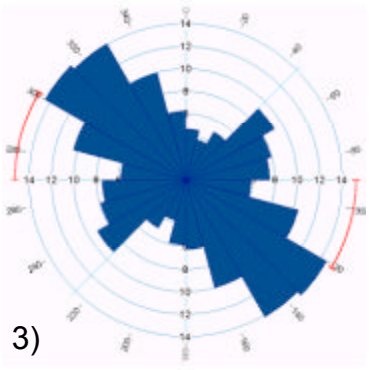

ORIENTATION OF FAULTS IN GUAM (North and South)
Class Interval .....15°
Population 241
Maximum Percentage...14.5%
Mean Percentage 8.3%
Standard Deviation 3.41%
Vector Mean .....285.65°
Confidence Interval .....15.54°
R-mag 0.70

Fig. 7. 25 (a): Rose diagrams illustrating orientations of faults in Guam: 1) Northern Guam only. 2) Southern Guam only. 3) All of Guam.

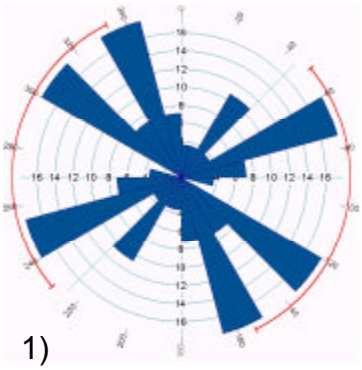

DEPRESSION LONG AXES IN Qtma AREA
Class Interval .....15°
Population 28
Maximum Percentage...17.9%
Mean Percentage 9.1%
Standard Deviation 5.91%
Vector Mean .....281.76°
Confidence Interval .....52.04°
R-mag 0.64

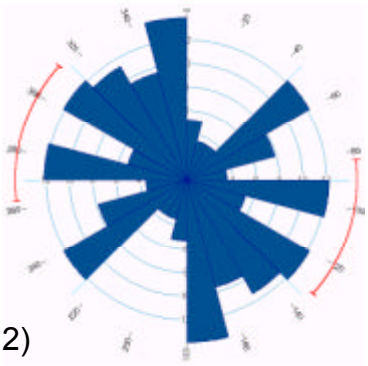

DEPRESSION LONG AXES IN ALL OF NORTHERN GUAM
Class Interval .....15°
Population 143
Maximum Percentage...13.3%
Mean Percentage 8.3%
Standard Deviation 3.59%
Vector Mean .....286.46°
Confidence Interval .....22.09°
R-mag 0.66

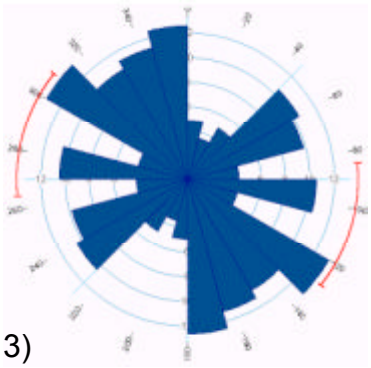

DEPRESSION LONG AXES IN PURE LIMESTONES
Class Interval .....15°
Population 115
Maximum Percentage...13.9%
Mean Percentage 8.3%
Standard Deviation 3.91%
Vector Mean .....287.56°
Confidence Interval .....24.54°
R-mag 0.66

Fig. 7. 25 (b): Rose diagrams illustrating orientations of long axes of depressions in northern Guam: 1) Agana Argillaceous Member of the Mariana Limestone. 2) All of northern Guam. 3) Pure limestones only.

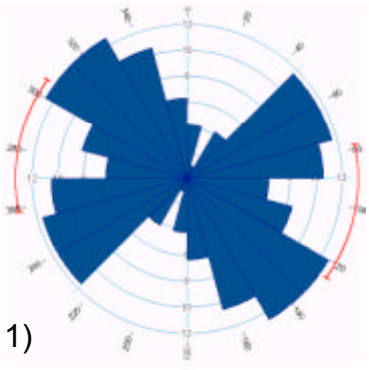

ORIENTATION OF FAULTS IN NORTHERN GUAM
Class Interval .....15°
Population 95
Maximum Percentage...12.6%
Mean Percentage 8.3%
Standard Deviation 3.76%
Vector Mean .....281.99°
Confidence Interval .....23.58°
R-mag 0.72

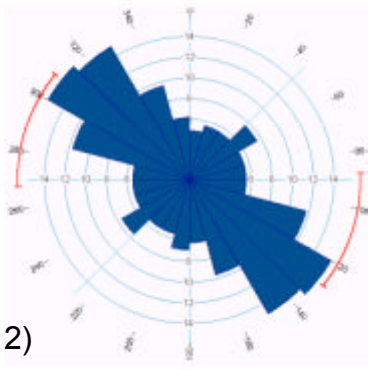

ORIENTATION OF FAULTS IN SOUTHERN GUAM
Class Interval .....15°
Population 146
Maximum Percentage...15.8%
Mean Percentage 8.2%
Standard Deviation 3.8%
Vector Mean .....288.18°
Confidence Interval .....20.48°
R-mag 0.69

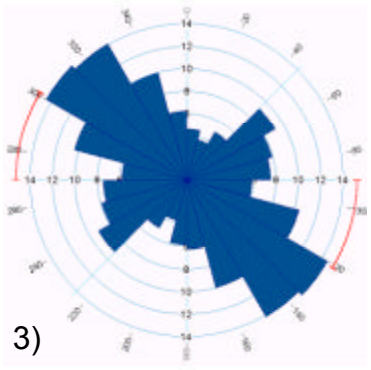

ORIENTATION OF FAULTS IN GUAM (North and South)
Class Interval .....15°
Population 241
Maximum Percentage...14.5%
Mean Percentage 8.3%
Standard Deviation 3.41%
Vector Mean .....285.65°
Confidence Interval .....15.54°
R-mag 0.70

Fig. 7. 25 (a): Rose diagrams illustrating orientations of faults in Guam: 1) Northern Guam only. 2) Southern Guam only. 3) All of Guam.

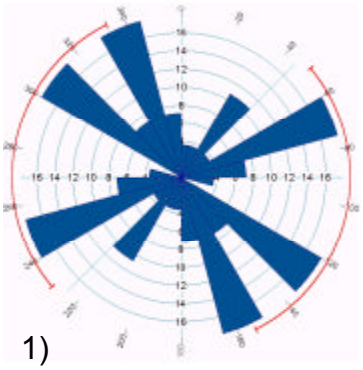

DEPRESSION LONG AXES IN Qtma AREA
Class Interval .....15°
Population 28
Maximum Percentage...17.9%
Mean Percentage 9.1%
Standard Deviation 5.91%
Vector Mean .....281.76°
Confidence Interval .....52.04°
R-mag 0.64

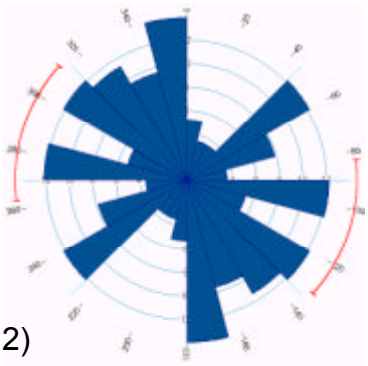

DEPRESSION LONG AXES IN ALL OF NORTHERN GUAM
Class Interval .....15°
Population 143
Maximum Percentage...13.3%
Mean Percentage 8.3%
Standard Deviation 3.59%
Vector Mean .....286.46°
Confidence Interval .....22.09°
R-mag 0.66

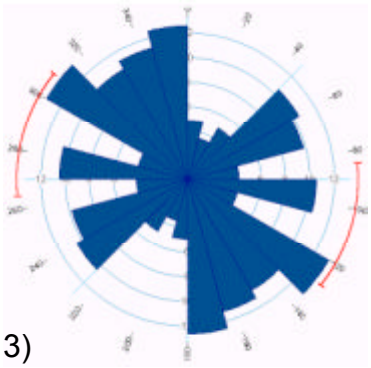

DEPRESSION LONG AXES IN PURE LIMESTONES
Class Interval .....15°
Population 115
Maximum Percentage...13.9%
Mean Percentage 8.3%
Standard Deviation 3.91%
Vector Mean .....287.56°
Confidence Interval .....24.54°
R-mag 0.66

Fig. 7. 25 (b): Rose diagrams illustrating orientations of long axes of depressions in northern Guam: 1) Agana Argillaceous Member of the Mariana Limestone. 2) All of northern Guam. 3) Pure limestones only.

7. 4. Types of Depressions in Southern Guam

After identifying and inventorying closed contour depressions in southern Guam (Fig. 7. 26., Fig. 7. 27., Appendix 7), the next step was to classify them into different genetic categories. Types of depressions identified in southern Guam vary with area and include:

1) in central part of southern Guam: cockpit karst, valley sinks and karst valleys
2) in the ridge from Mt. Alifan to Mt. Lamlam: dolines underdrained by volcanic contact conduits
3) along the east coast of southern Guam: point recharge and collapse dolines
4) small depressions in the Orote peninsula and limestone outcrops south of the Pago-Adelup fault

7. 4. 1. Cockpit karst and valley dolines

Numerous large and deep dolines have developed in Bonya Limestone in central part of southern Guam in the Naval Magazine area. They look like the cockpit karst described from Jamaica (Sweeting, 1958), but extend over a much smaller area. The main Bonya Limestone outcrop has an area of 2.15 km^2 and is located immediately northeast of the Fena Lake (Plate 16, photo 1). It contains at least 26 tropical cockpit dolines. The limestone outcrop is entirely surrounded by volcanic rocks and the clayey Talisay Member of the Alifan Limestone. Several small outcrops of pure Alifan Limestone are found scattered within the Bonya Limestone area and also contain cockpit dolines. Surrounding volcanic and Talisay Member terranes provide allogenic catchment and give rise to two surface streams, the Maemong River and the Bonya River. Maemong River flows at least 80 meters through the subsurface under a Bonya Limestone hill. It resurfaces and immediately joins the Bonya River to form the Tolae Yu'us River (also known as the Lost River). The Tolae Yu'us River flows at least 420 meters through the subsurface before it joins outflow from Fena Lake to make Maagas River. A network of dry alluviated valleys and alluvial deposits on the bottoms of dolines indicate that the rivers have frequently shifted their course.

The rivers provide local base level and underdrain the limestone as they travel through Bonya and Alifan outcrops. The result is the development of large dolines so close to each other that ridges separating them in some areas are less than a meter wide (Plate 16, photo 2). The elevation of the ridges reflects the position of the original land surface. The deepest of the dolines are about 30 meters deep. A map and profile through this cockpit karst area is shown in Fig. 7. 28. Some of the dolines have traversable cave passages at their bottoms, leading to the bottoms of neighboring dolines. At least one doline has been deepened enough to have exposed the volcanic basement at its bottom and at least two dolines support ephemeral lakes (Plate 16, photo 3).

In addition to cockpit dolines, several valley dolines exist in the area. They dot the course of Bonya River and are found even in areas mapped as the volcanic Bolanos Formation by Tracey et al. (1964) that in the past were covered by Bonya Limestone outcrops. The final portion of Bonya River and the entire surface course of Tolae Yu'us River flows in a deeply incised elongate closed contour depression. This karst valley is 90 meters wide at its maximum but more than 1.5 kilometers long and ends as a blind valley when the Tolae Yu'us River disappears underground.

7. 4. 2. Dolines in Alifan Limestone mountain ridge

Alifan Limestone caps the mountain ridge separating central southern Guam and Talofofo River basin from the Philippine Sea. The highest peaks on Guam are made of Alifan Limestone and include Mt. Lamlam, Mt. Almagosa and Mt. Alifan. This limestone cap is entirely underlain by volcanic units at lower elevations. It contains at least 5 large closed contour depressions, the deepest being about 20 meters deep and some containing notable alluvial deposits. They are densely forested and extremely difficult to traverse (Plate 16, photo 4).

Mylroie et al. (1999) write that the Alifan Limestone flanks of the mountain intercept flow from adjacent volcanic terrane and the resultant underflow has created the observed closed contour depressions. Depressions are also found overlaying major conduit flowpaths within the Alifan Limestone. No caves have been discovered within these dolines.

7. 4. 3. Depressions on the east coast of south Guam

A limestone band extends along the east coast of southern Guam, separating the Alutom and Bolanos formations from the Pacific Ocean. Most of the limestone is mapped by Tracey et al. (1964) as the Mariana Limestone Argillaceous Member, with several small Bonya and Alifan outcrops and a linear series of Mariana Limestone Reef and Forereef Facies outcrops parallel to the coast. The surface contact between limestone outcrops and inland volcanic

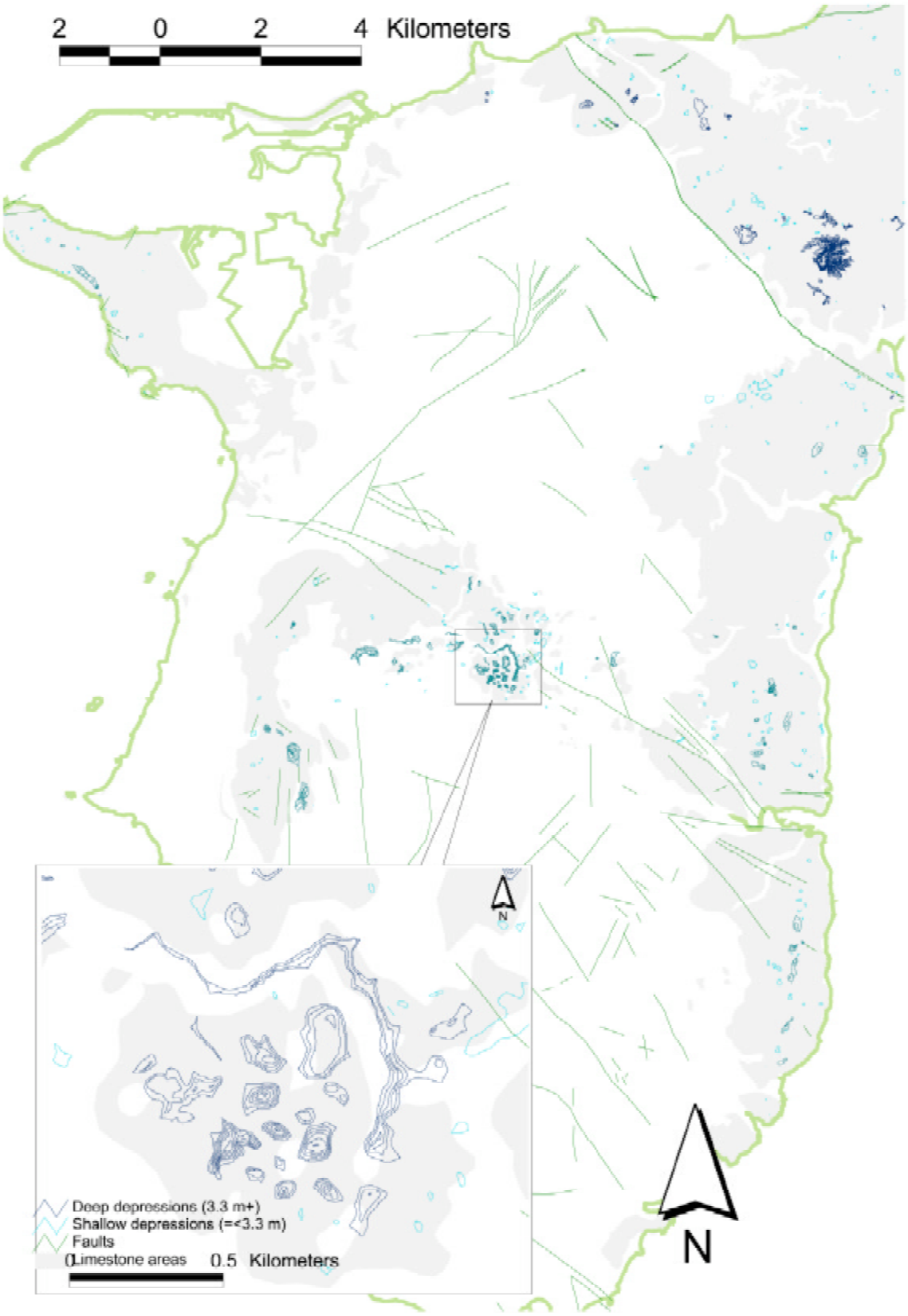

Fig. 7. 26: Map of closed contour depressions in southern Guam.

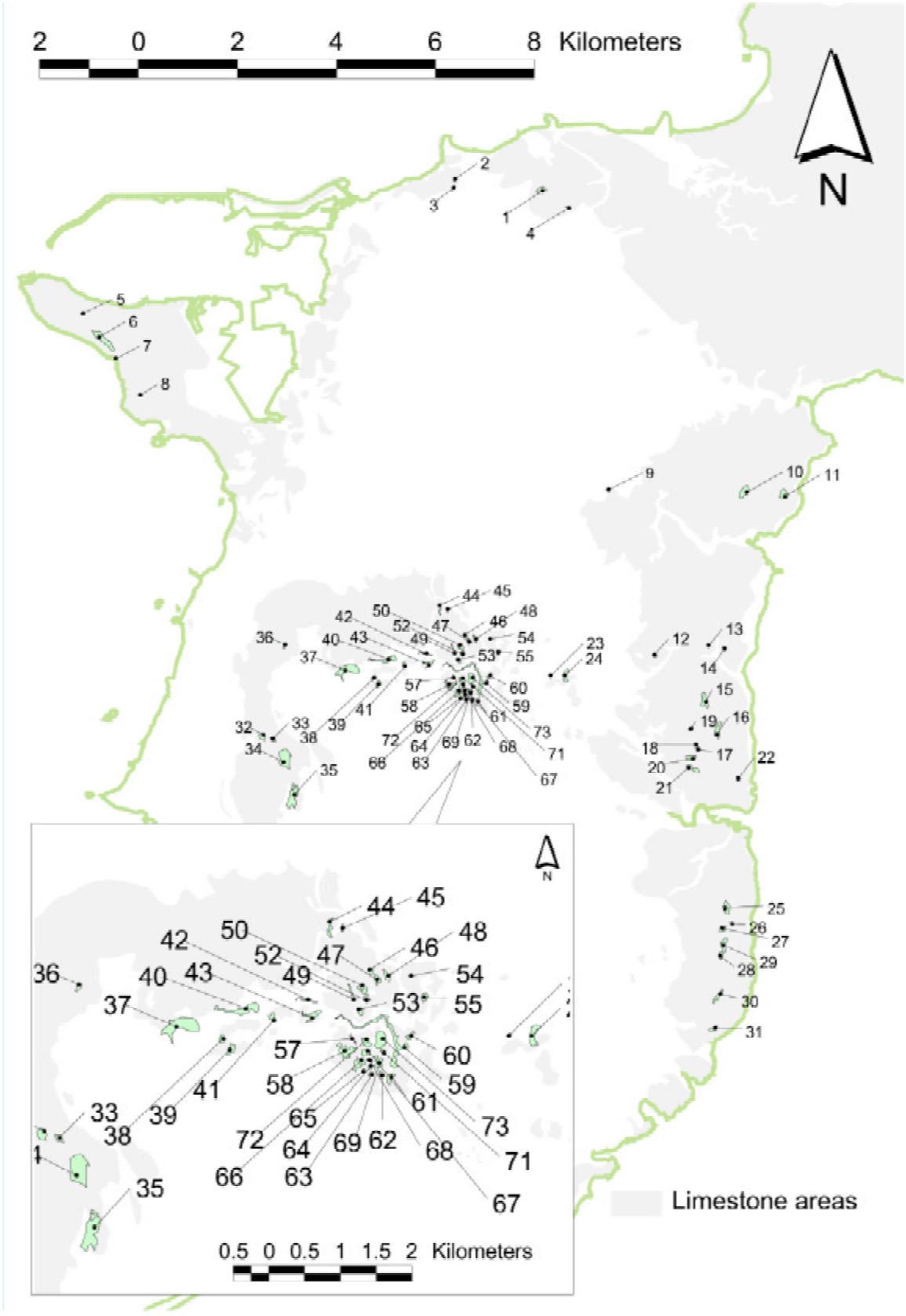

Fig. 7. 27: Inventoried closed contour depressions in southern Guam.

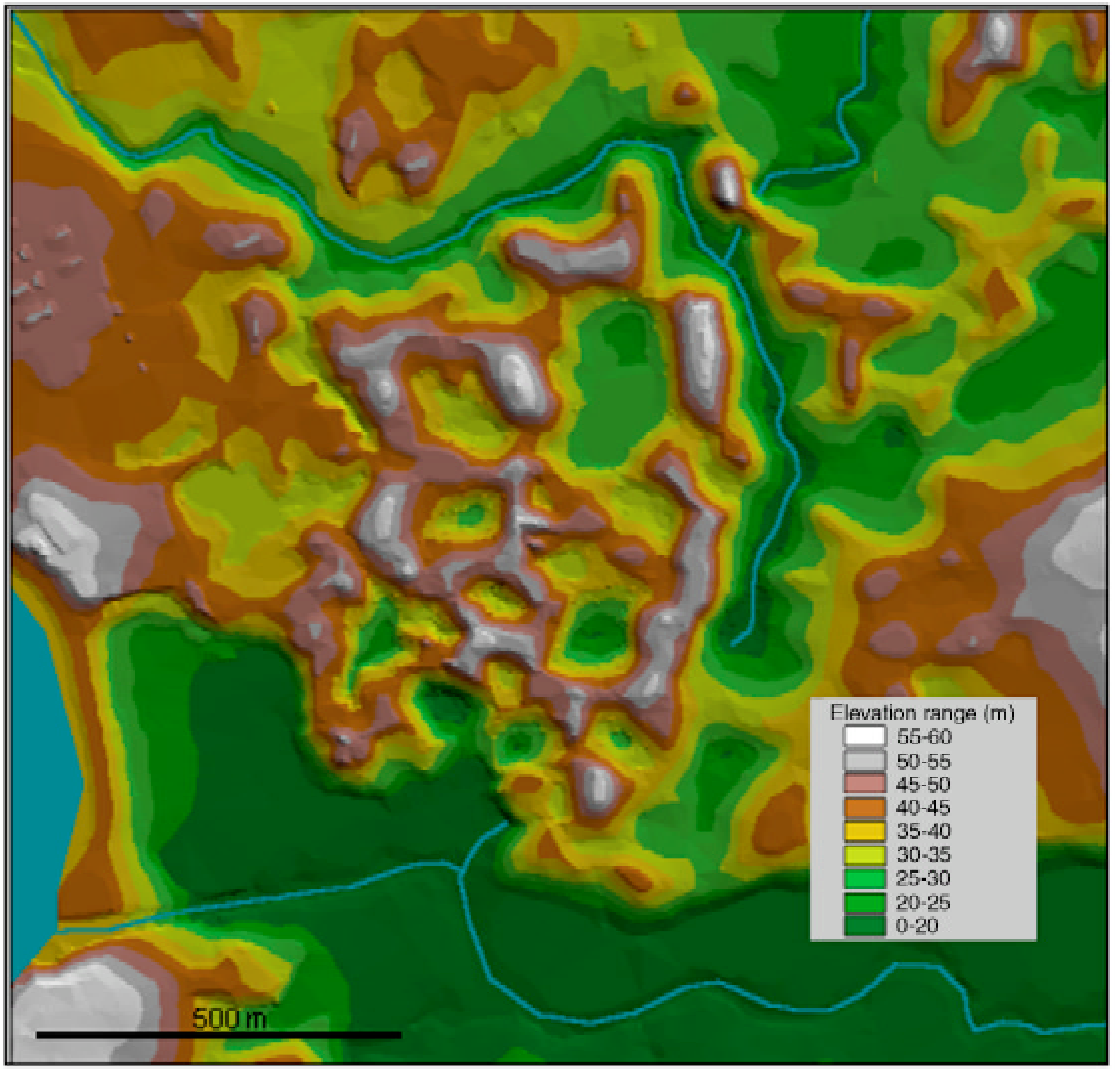

Fig. 7. 28: A map of cockpit karst in Naval Magazine area.

terrane is about 23 kilometers long and amazingly shows virtually no closed contour depression development. A single depression deeper than 10 feet located along the contact has been inventoried. This is probably because high clay content of Argillaceous Member supports perching of surface water. Further east, along the Pacific coast, most of the Argillaceous Member rocks are separated from the ocean by a paleo-reef, composed of pure Mariana Limestone Reef facies. The closed contour depressions have developed along the contact between Argillaceous and Mariana Reef facies. It is possible that Argillaceous Member rocks supported surface flow that disappeared into sinkholes upon reaching pure limestone facies. Out of 21 closed contour depressions inventoried within limestones of the east coast of southern Guam, 15 are found near the contact of Argillaceous Member and reef or forereef facies of Mariana Limestone. Additionally, there are several smaller collapsed sinkholes in the area, some of which lead to freshwater and may be collapsed conduits.

An interesting collapse sinkhole reminiscent of banana holes (Harris et al., 1995) occurs in a Bonya Limestone outcrop north of Togcha river (Fig. 7. 29). Known as Ito and Minagawa Sink (Plate 16, photo 5), it is about 10 meters deep and contains a shelter cave, infilled by collapse materials, gravel and sand. The cave was used as a shelter by two Japanese soldiers, Ito and Minagawa, following World War II. If this sinkhole is indeed a banana hole, it is a unique in sense that it has developed in a local water table within a small limestone outcrop surrounded by argillaceous rocks, and not in an extensive freshwater lens.

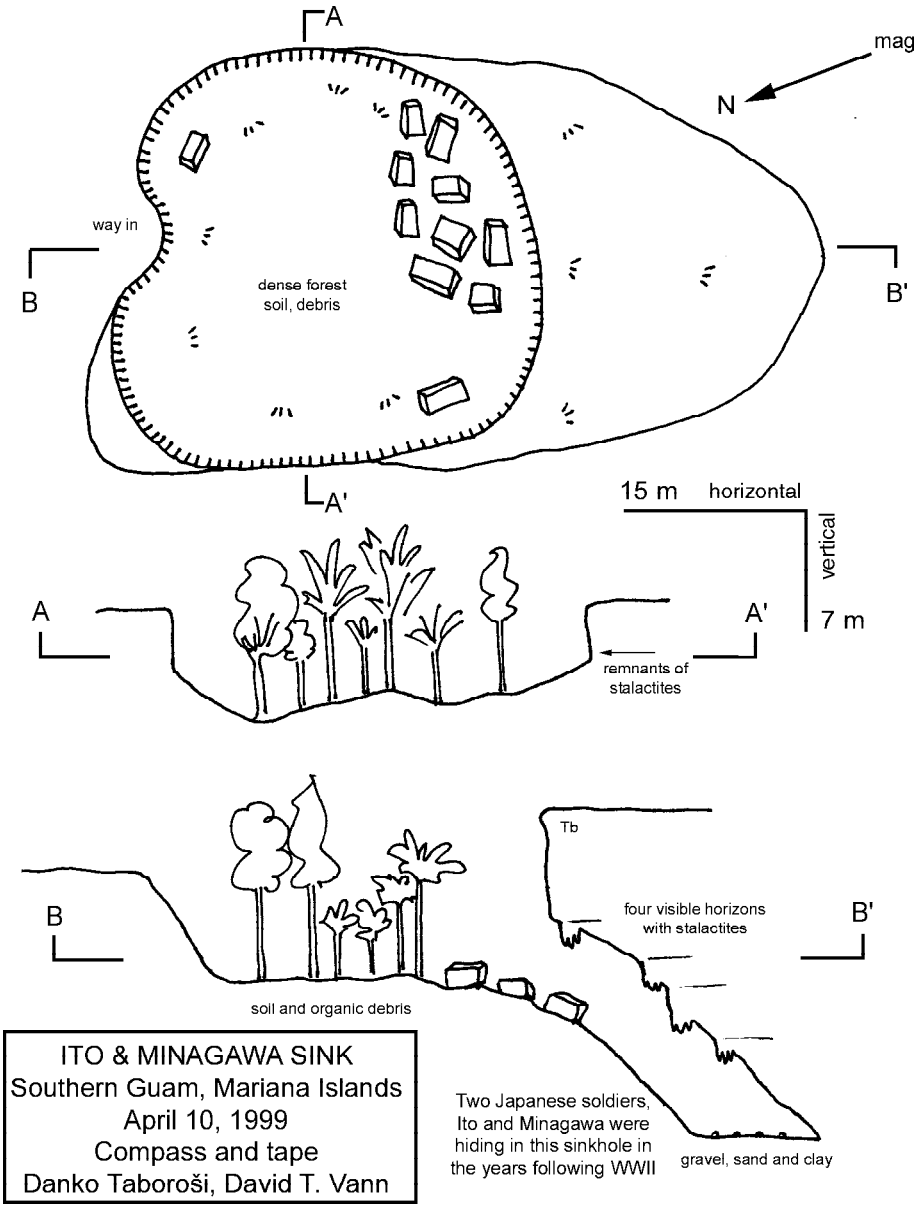

Fig. 7. 29: Map and profiles of Ito & Minagawa Sink.

7. 4. 4. Other depressions in southern Guam

Four depressions deeper than 10 feet were inventoried on Orote peninsula but were not investigated directly. Their origin is unknown, but likely to be collapse of phreatic voids given the purity of reef limestones there and lack of perched surface waters.

Two small depressions occur in the Argillaceous Member in Asan, on the contact with the volcanic Alutom Formation. They are probably a result of sinking of allogenic waters.

Two inventoried depressions and numerous other shallow depressions occur within the Alifan Limestone outcrop on Nimitz Hill, immediately south of the Pago-Adelup fault. Being adjacent to a major geologic fault, this area is heavily faulted and fractured and contains numerous traversable fracture caves. The alignment of caves and depressions along faults is evident in the field. Depressions here are collapse dolines whose walls are often part linear following orientation of faults and fractures (Fig. 7. 30a-b).

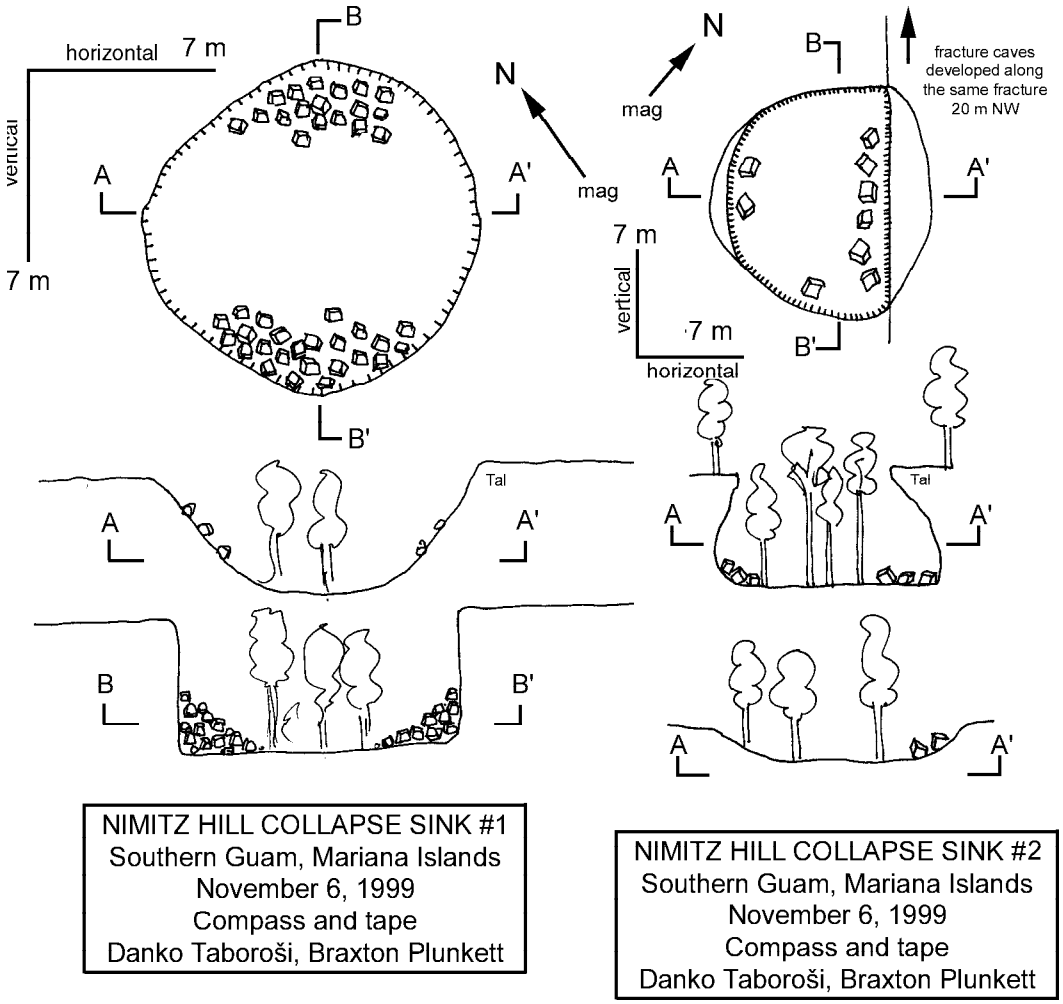

Fig. 7. 30: Maps and profiles of fracture-controlled sinkholes in Nimitz Hill. (left) Nimitz Hill collapse sink 1; (right) Nimitz Hill collapse sink 2.

— Chapter 8 —
VADOSE CAVES AND CONDUITS

This chapter investigates caves and groundwater conduits on Guam that were made by dissolution in the vadose (unsaturated) zone. Because of the glacioeustatic sea level changes Guam has experienced, it is common on Guam to find vadose caves in the phreatic zone and find phreatic caves in the vadose zone. However, selection of caves discussed in this and the next chapter are based on their genetic origin and not their present location with respect to the sea level. Therefore, many caves currently found in the vadose that have actually formed in the phreatic zone prior to uplift of the island are genetically phreatic and are discussed in the next chapter. Correspondingly, caves discussed in this chapter include only those actually made by vadose processes.

8. 1. Vadose Caves and Conduits

The defining characteristic of vadose caves (and conduits) is that they are formed by the action of underground streams flowing above or at the water table (White, 1988). It is thought that water infiltrating from the surface is aggressive and moves downward dissolving its way through the rock layers. The water does not necessarily descend directly to the water table; geological structures may influence its movement and guide development of caves (Waltham, 1981). A classic type of a vadose cave is a clean-washed, canyon passage occupied by a stream. Sinkhole drains, vertical shafts and solution chimneys are also types of vadose caves, although lacking streams in the classical sense.

It should be noted here that although speleologists and karst hydrologists often focus their research on conduits large and unobstructed enough to permit human entry, as is the case with this study as well, such conduits represent a tiny proportion of the totality in most cases (Ford, 1999). Non-traversable parts of conduit systems are usually not termed caves. In this chapter I discuss vadose conduits in general—accessible to people or not, active or inactive, with the focus being on caves, i.e. conduits that can be explored by people.

8. 2. Types of vadose caves in northern Guam

Traversable vadose caves are locally abundant in northern Guam but not numerous overall. There are many traversable caves currently in the vadose zone, but those actually made in the vadose zone are few. Out of 79 caves that have been inventoried in northern Guam, only 15 are vadose conduits or vertical vadose by-passes, all the rest being mixing zone and other phreatic voids that have been placed in the vadose zone by relative sea level drop. Such caves are discussed in the next chapter.

Types of vadose caves in northern Guam are vertical shafts and pit caves, solution chimneys and stream caves. Vertical shafts and pit caves are vertically extensive voids made by descending vadose water. Solution chimneys are fractures enlarged by solution, irregular in shape and ground plan (White, 1988). Vertical shafts, pit caves and solution chimneys are highly significant hydrologically as they provide by-pass routes for vadose waters through the epikarst and part of the vadose zone.

Stream caves are caves enlarged predominantly by free-surface streams eroding downward or laterally or both (Ford and Ewers, 1978). Such caves are rare in northern Guam because the young limestones there are unaltered by diagenesis and are too porous to allow flow and focusing of surface waters. Because of this, the only stream caves in northern Guam have developed on the flanks of volcanic inliers of Mt. Santa Rosa and Mataguac Hill, by focused allogenic input from volcanic surfaces.

Agana Argillaceous Member of the Mariana Limestone is less porous and I expected to find vadose stream caves there, associated with numerous fluviokarst features identified there (Chapter 6). However, no such caves were identified despite exhaustive fieldwork. This could be a result of close-to-sea-level elevation of dry valleys in the area, where associated caves are probably clogged by sediment. I also expected to find vadose caves associated with the numerous closed contour depressions in northern Guam but found that they are almost never associated with traversable cave passages. Rare exceptions are collapse sinkholes in Chalan Pago and Barrigada which provide access to extensive passages, but these are tubular and horizontal and are probably abandoned phreatic conduits.

Inventory of caves (in which the vadose caves are included) from northern Guam is given in Appendix 8. The map showing distribution and types of vadose caves in northern Guam is shown in Figure 8.1.

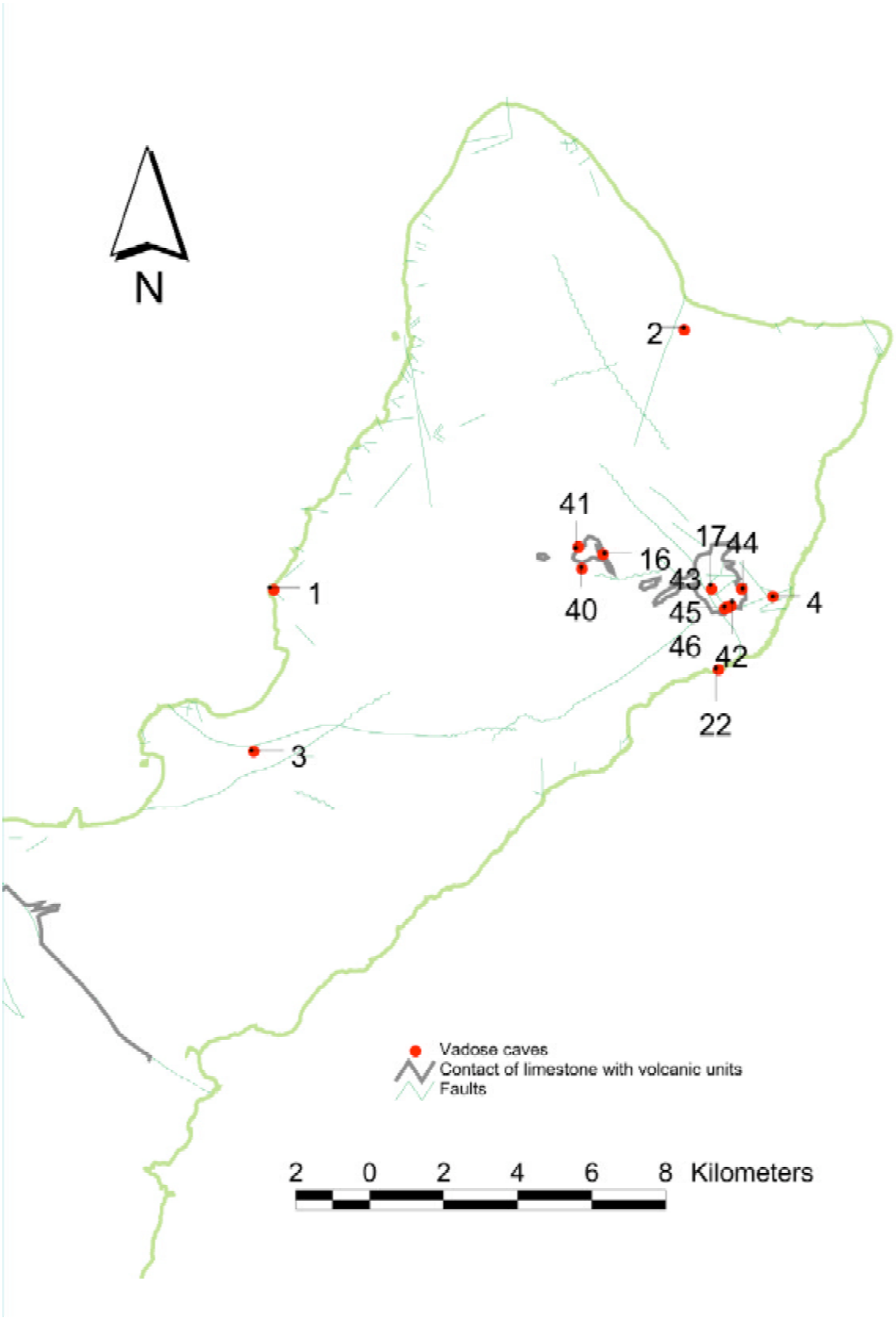

Fig. 8. 1: Locations of vadose caves in northern Guam.

8. 2. 1. Vadose shafts, pit caves and solution chimneys

Vadose shafts, pit caves and related features play an important role in transport of water via the vadose zone and provide the fastest routes, often allowing by-pass of thick sections of epikarst. These features are considered caves if they are traversable. They are usually quite difficult to explore and require rappelling gear. Because of their important hydrologic role as a part of the epikarst, they have been discussed in detail in section 5. 3. 3., with the discussion on epikarst and the subcutaneous zone.

8. 2. 2. Stream caves

The only accessible stream caves in northern Guam are found on the volcanic flanks of Mataguac Hill and Mt. Santa Rosa. Mataguac Hill has three such caves identified (Mataguac Spring Cave, Mataguac Mud Cave and North Mataguac Cave), while Mt. Santa Rosa area has five known so far (Awesome, Interesting, Piggy, Elvis' Pelvis, and Virgin caves). Janum Cave is a spring cave located near Janum Point, on the coast near Mt. Santa Rosa and is believed to be the terminus of a conduit system delivering allogenic water from Mt. Santa Rosa to the coast. Explorations of these caves should only be attempted during the dry season and sunny weather.

Mataguac Spring Cave (Fig. 8. 2, Plate 17, photo 1) is located at the bottom of Mataguac Spring Sink, on the southeast flank of Mataguac Hill. It is a ponor of a small stream fed by Mataguac Spring and allogenic runoff from the local volcanic terrain. Runoff from Mataguac Hill and water from Mataguac Spring flow a short distance over the alluviated floor of the sink to the entrance of the cave, which is about 6 meters wide and 3.5 meters tall. The entrance leads to a single passage traversable for 15 meters. The floor of the cave is mud (from erosion of volcanic saprolite) and limestone rubble. This cave follows the contact between the Alutom Formation and overlying Mariana Limestone detrital facies, and is a vadose-cut canyon. However, volcanic bedrock and the geologic contact are not visible due to the extensive mud deposits.

Mataguac Mud Cave (Fig. 8. 3, Plate 17, photo 2) is located in a sinkhole on the southwest flank of Mataguac Hill and is more complex. The active passage is traversable for 27.5 meters, with the floor entirely covered by mud, organic debris and limestone rubble. Contact between volcanic basement and limestone is discernible in the cave walls. This cave shows two levels of passage development: an active vadose cut canyon and a parallel dry phreatic tube above it. Interpretation of the top passage as a phreatic tube is based on the nearly perfect elliptical cross-section of the tubular passage, extensive fine sediment deposits throughout and smooth dissolution features in the walls. The two passages connect in several places where the phreatic tube floor has collapsed and opened it to the underlying vadose passage. There are two possible explanations for the presence of a phreatic tube in this typical vadose cave. It is likely that the initial horizon of cave development started out as a phreatic tube when flow was slow and the proto-passage full of water. As the passage enlarged and true conduit flow developed, down-cutting began and new vadose passages under-drained the initial phreatic system (J. Mylroie, pers. comm.). It is also possible that the phreatic tube is actually younger than the vadose passage underneath: since the cave is fed by allogenic recharge it is subject to occasional heavy flooding which may overwhelm the vadose passage and activate phreatic passage above (J. Mylroie, pers. comm.)

North Mataguac Cave is probably similar to the two described above, but was not explored. Unfortunately, the entrance to this cave was destroyed by infilling on April 9, 2000 during construction activities on the north slope of Mataguac Hill (Plate 17, photo 3). Because this cave is an active swallet for allogenic water captured by Mataguac Hill, its infilling causes obvious risks of flooding as well as collapse of structures built on the fill.

Piggy Cave (Fig. 8. 4, Plate 17, photo 4) has developed on the north side of Mt. Santa Rosa. Its main entrance is inside a small doline. The bottom of the doline is alluviated and supports dense wetland vegetation. A puddle few meters in diameter is present even in the dry season. Adjacent to this lowest point in the doline is the main entrance to Piggy Cave, located at the base of an Alifan Limestone hill. The entrance is about 4 meters wide and 2 meters tall, with scattered collapse boulders. A single passage leads from the entrance, following the bedrock-basement contact (Plate 17, photo 5). The passage floor is volcanic basement, with volcanic and limestone debris, including volcanic fragments cemented by calcite deposition (Plate 17, photo 6). The passage is an actively down-cutting vadose canyon incised in volcanic rock by an ephemeral stream. The passage contains numerous puddles and pools, even in the dry season. The largest of the pools is more than 2 meters deep (Plate 17, photo 7). The passage is generally 1-2 m wide and up to a few meters tall. Several steep drop-offs, up to 3 meters tall, become underground waterfalls during rain events.

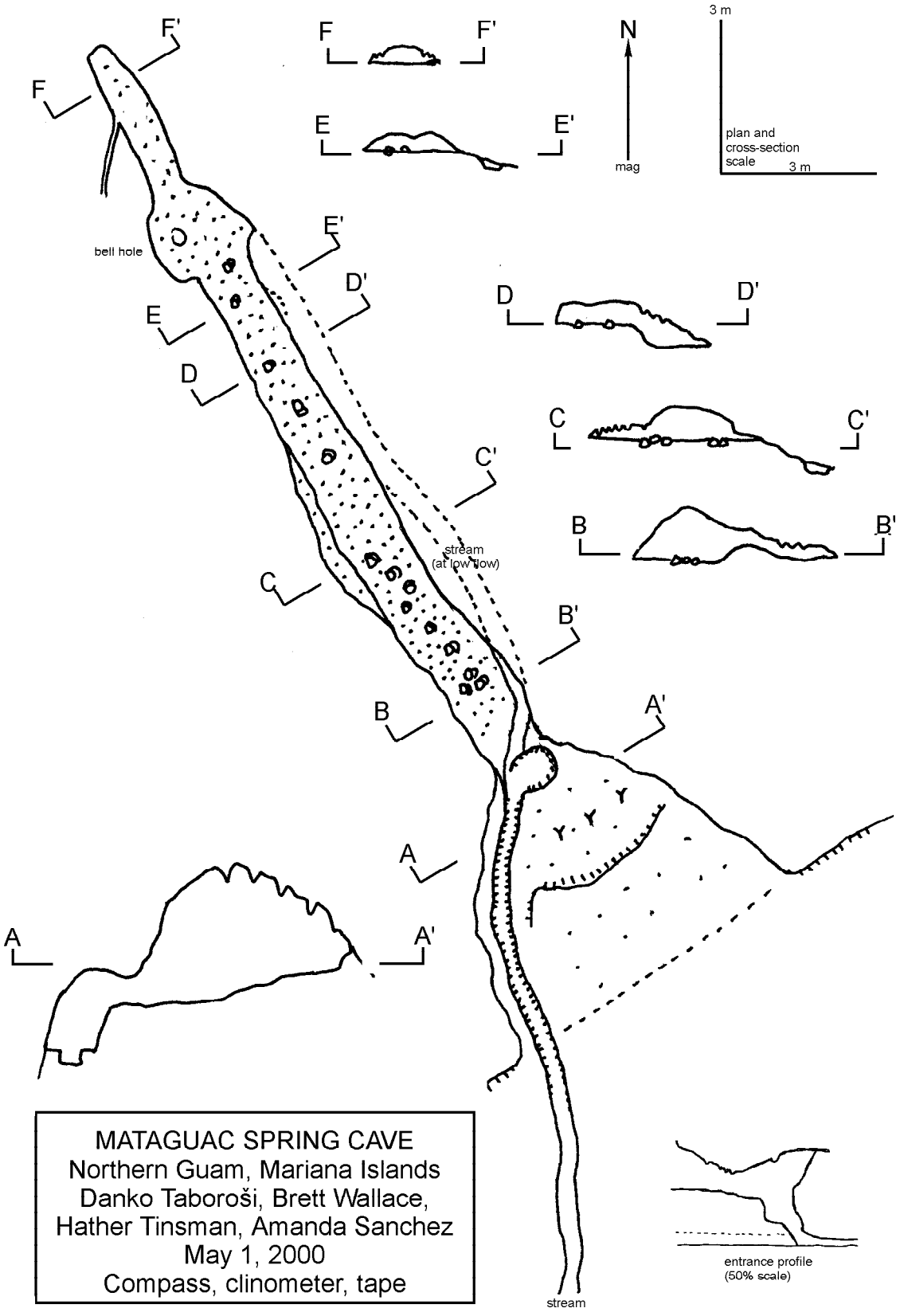

Fig. 8. 2: Map of Mataguac Spring Cave.

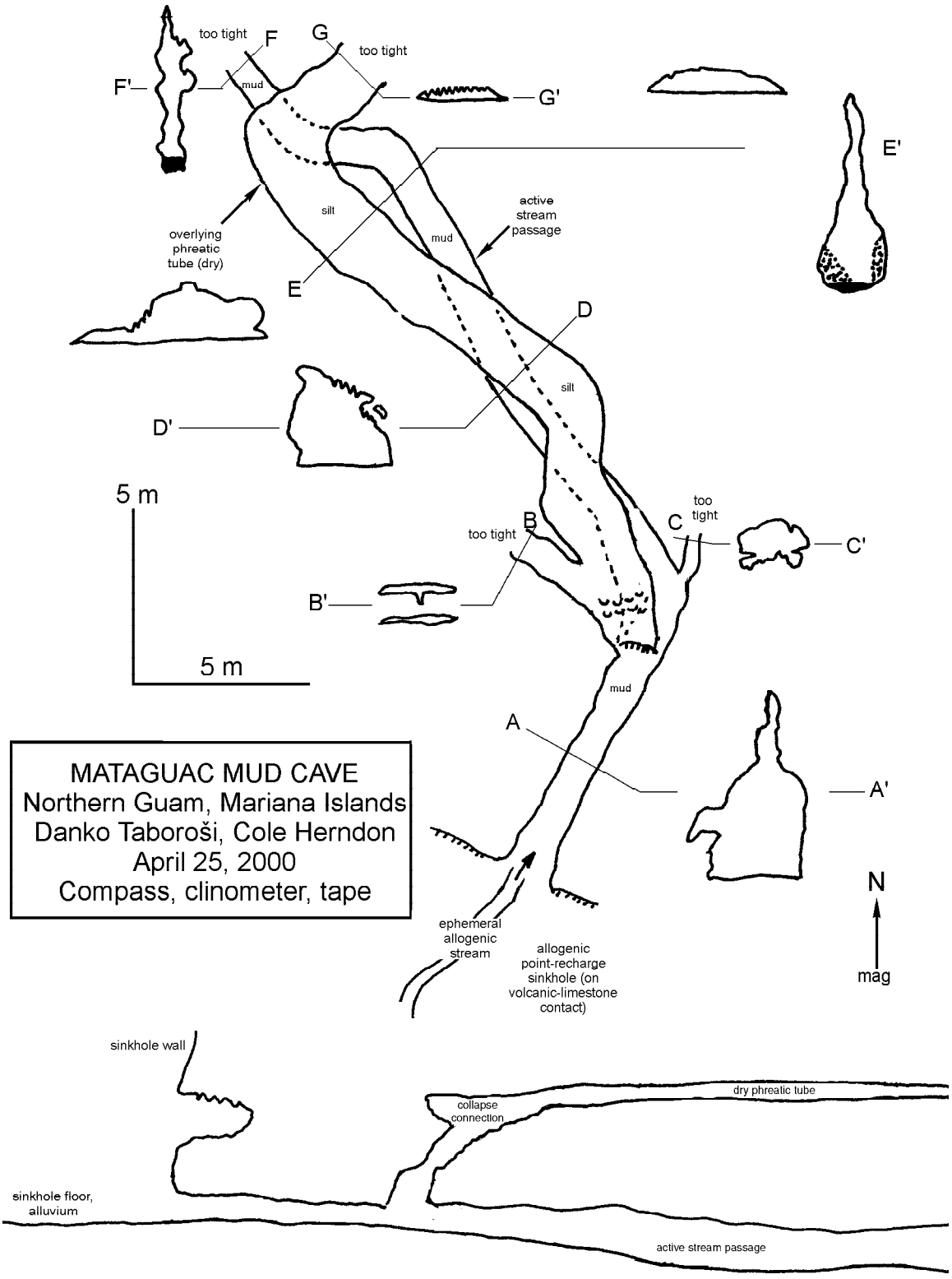

Fig. 8. 3: Map of Mataguac Mud Cave.

Physical erosion of volcanic bedrock is evident and the stream channel of the main passage has been cut to a meter below the contact with the limestone. The limestone-volcanic contact is clearly visible throughout the main cave passage. Most of this cave is a single narrow stream passage, but several larger rooms have been made by progradational collapse. In such places, it is necessary to walk over the rubble instead of following the vadose stream which has been buried by collapse, before rejoining the stream passage. In collapse rooms, several additional entrances and skylights have been made by ceiling collapse (Plate 17, photo 8). The stream passage becomes too small to follow after 120 meters from the entrance. The back entrance to the cave is located near the end of traversable stream passage. It is has developed by progradational collapse, to the top of a 9 meter tall vertical passage. This cave is beautifully decorated by stalactites and flowstone banks. Collapse rooms show very little stalactite development. A prominent feature in collapse rooms are vertical flutes in the boulders and walls, made by input of vadose waters flowing through the ceiling (Plate 17, photo 9). In the upper portions of the cave (the first two collapse rooms) some phreatic dissolution features are identifiable in the walls, but they are not as numerous as in Awesome Cave, discussed next.

Awesome Cave (Fig. 8. 5) is another stream cave fed by an allogenic stream originating on the slopes of Mt. Santa Rosa. Located in the southeast of Mt. Santa Rosa, on the volcanic-limestone contact, this cave is entered via a collapse entrance in an allogenic point recharge sinkhole (Awesome Sink). The active swallet of the cave is mud clogged and not traversable. The cave is a series of large chambers (up to 20 m wide and 8 m tall), descending in a step-like fashion. Underneath the chambers, a vadose canyon passage developed on the volcanic contact carries an ephemeral allogenic stream. Most of the ceiling of the large chambers is characterized by well developed phreatic dissolution surfaces. Only in the top chamber, at the cave entrance, is the ceiling collapse in nature, well decorated by small stalactites. The floor here is composed of collapse rubble. The ceiling of the lower (second and third) chambers is generally subparallel to the floor and contains phreatic cusps and smooth surfaces developed across paleosol infill materials. Paleosol infill exposed in the chamber ceiling include matrix-supported and clast-supported breccias, infill of joints and fractures in the bedrock, and soil pipes. Most of the cave floor of the second and third chamber is composed of mud, flowstone, and, along the eastern wall, a series of large rimstone pools. The lowest (fourth) chamber has a horizontal and an extremely flat ceiling, almost completely a result of phreatic dissolution. It also exposes numerous soil breccias and soil-infilled fractures. The floor of this room is mostly made of collapse boulders. In one place in the floor, the underlying vadose stream passage can be entered though an opening in its collapsed roof. The vadose stream passage follows the volcanic contact (Plate 18, photo 1). The high energy ephemeral stream has incised into the volcanic bedrock. Passage floor here contains volcanic and limestone fragments, rocks cemented by $CaCO_3$ and soil breccia (Plate 18, photo 2). The passage can be followed upstream towards the swallet for about 35 meters. Downstream, the passage joins Interesting Cave, another vadose stream coming from a point recharge sinkhole adjacent to Awesome Sink.

Unlike Piggy Cave, where large chambers appear to be a result of collapse, chambers in Awesome Cave appear to be flank margin caves. They could be associated with previous fresh-water lens positions and sea level still-stands. It is also possible that phreatic dissolution features in this cave have developed during flooding episodes when the drainage in the main vadose stream passage was impeded. This complex cave is one of the more spectacular caves in Guam, because of its size, unique speleothems (Plate 18, photo 3), and historical artifacts (Plate 18, photo 4) found in it.

A single stream cave, probably part of the Mt. Santa Rosa stream cave system, used to be traversable at its discharging end. On the east coast of Guam, the only known discharging cave is the now inaccessible Janum Spring Cave, located near Janum Point, on the coast south of Mt. Santa Rosa. The cave contains a large spring (Janum Spring) with excellent water quality. This cave is no longer traversable, having been closed by a landslide during the 1993 earthquake (H. G. Siegrist, pers. comm.). Rogers and Legge (1992) describe this cave as having a 9 m wide and 6 m tall entrance, 0.6 meters above mean sea level. The single chamber narrows to 6 meters wide at a point 21 meters from the entrance. A steady stream of freshwater runs across the cave floor and discharges at the beach. The cave floor is composed of limestone, but volcanic basement probably forms the base of much of the non-traversable part of this cave, thus preventing salt water intrusion and allowing excellent water quality of Janum Spring. This cave is certain to be a part of a vadose conduit system delivering allogenic water from the east side of Mt. Santa Rosa to the ocean. A large sediment plume has been observed in the ocean at Janum Spring following a heavy rainfall episode (J. Jenson and C. Wexel, pers. comm.).

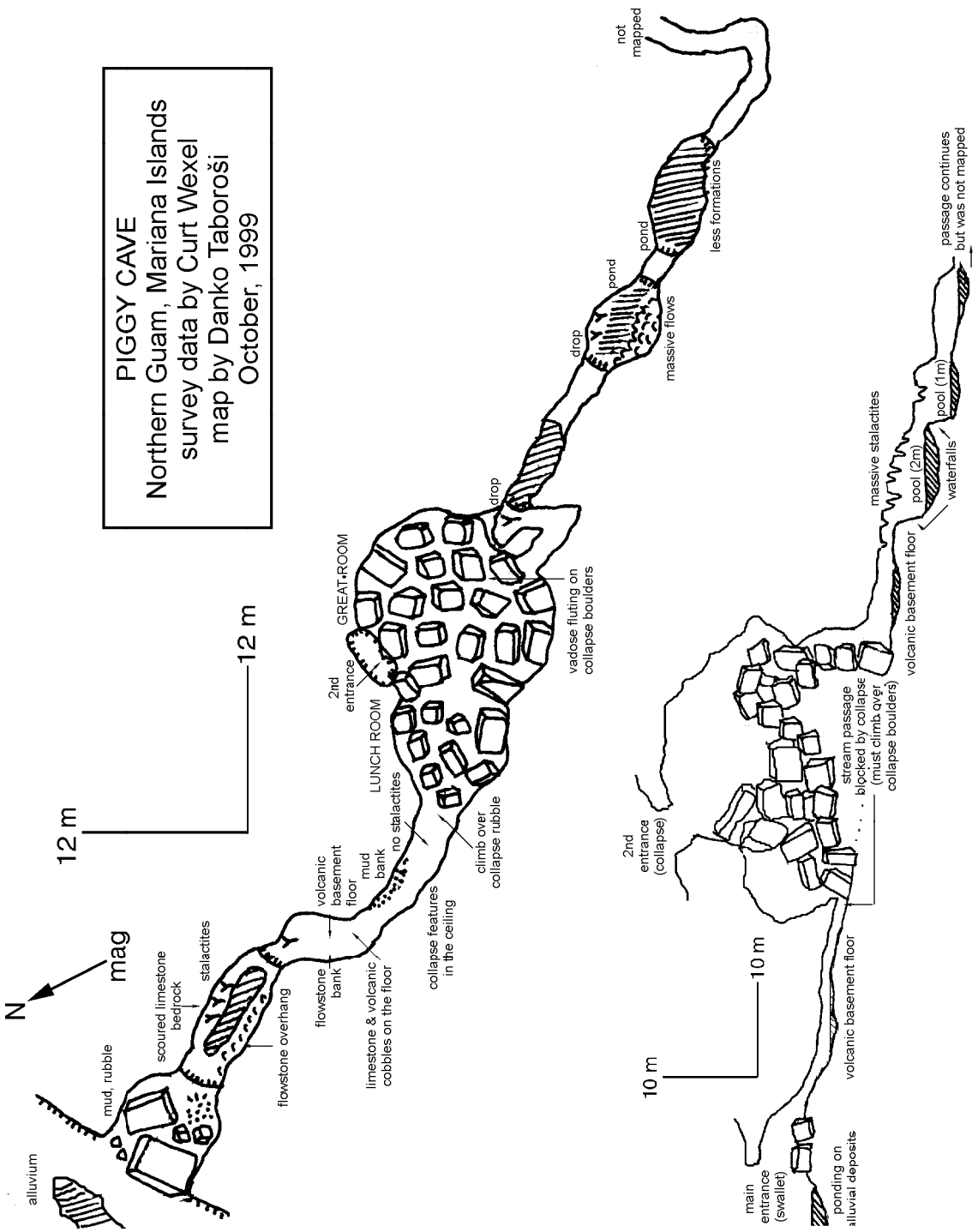

Fig. 8. 4: Map of Piggy Cave.

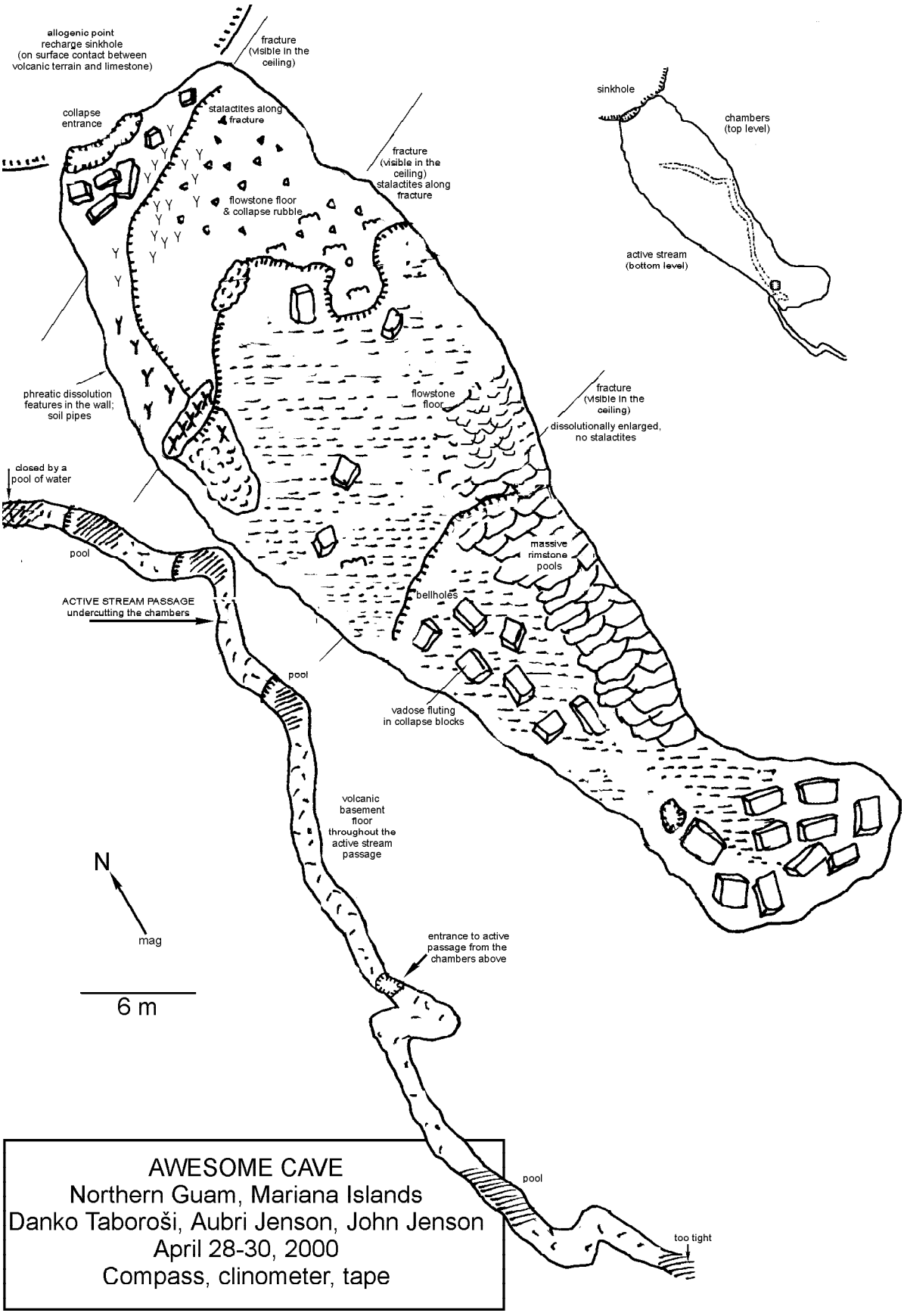

Fig. 8. 5-a: Map of Awesome Cave.

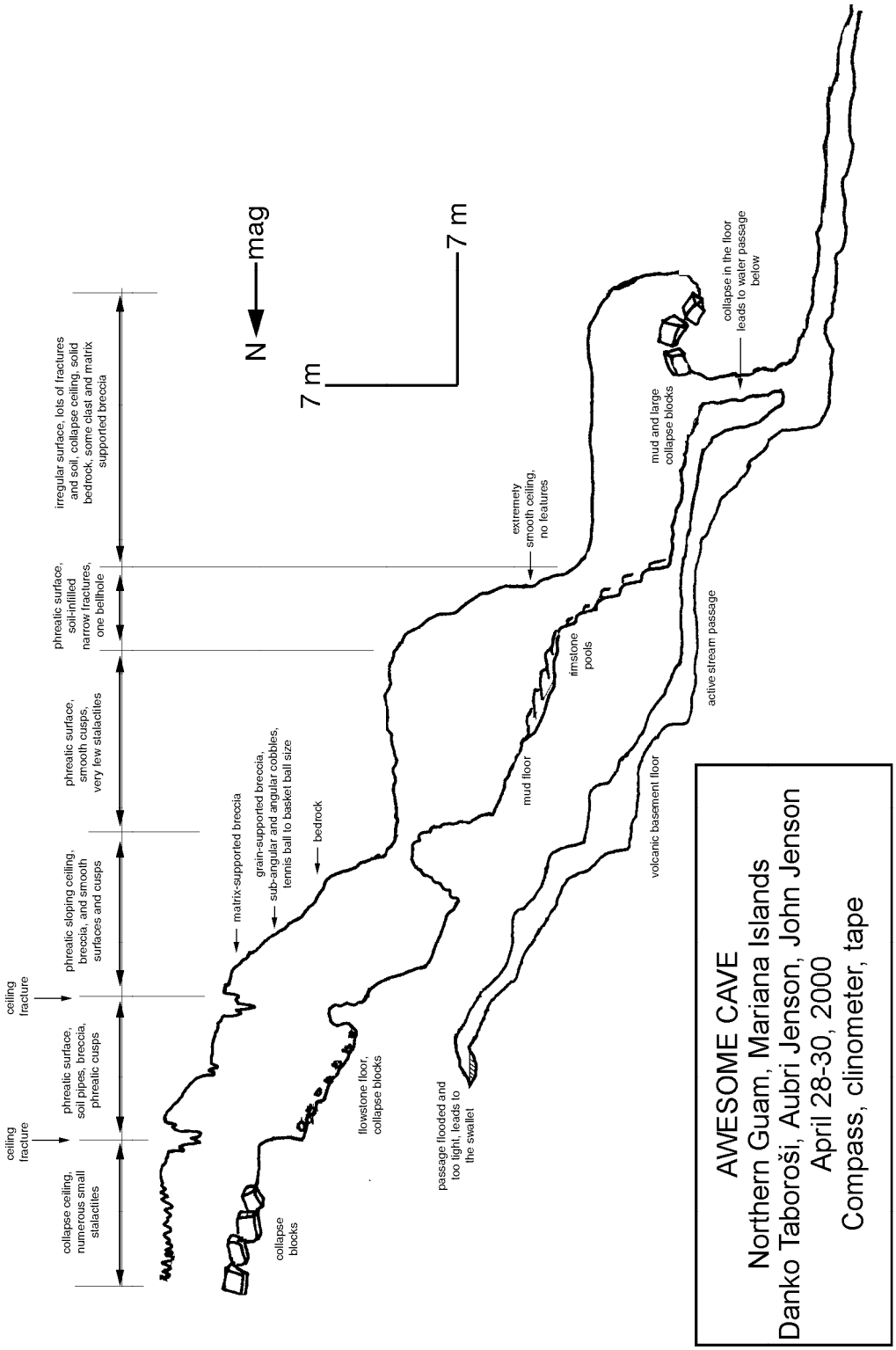

Fig. 8. 5-b: Map of Awesome Cave (profiles).

These stream caves have an established aquatic fauna. Shrimp (*Macrobrachium lar* and an unidentified atyid species) were found in Piggy Cave and a crab species (*Discoplax longipes*) appears common in Piggy and Mataguac Mud Cave (B. Tibbatts, pers. comm.), but were so far not recorded in the other stream caves. A brown tree snake (*Boiga irregularis*) was found inside Mataguac Mud Cave some 35 meters from the entrance. Tadpoles (*Bufo marinus*) are numerous in the stream flowing through Mataguac Spring Cave.

Delineation of allogenic drainage basins feeding known stream caves

Allogenic recharge to the Northern Guam Lens Aquifer comes from three non-carbonate areas: volcanic highlands on the south side of Pago-Adelup fault and volcanic inliers of Mataguac Hill and Mt. Santa Rosa.

Contrary to expectations, extensive exploration from 1998 to 2000 has revealed no stream cave development along the Pago-Adelup fault, despite a large allogenic catchment area of 21.79 km^2 (Fig. 6. 2.). It appears that all allogenic input from southern volcanic highlands is captured by Fonte and Pago rivers which flow over the argillaceous limestone in the southern part of northern Guam and discharge into Philippine Sea and Pacific Ocean respectively.

Mt. Santa Rosa has a total area of 1.31 km^2. It contains at least 9 distinct drainage basins (Fig. 8. 6). The largest drainage basin in the Gayinero Sink basin covers an area of 0.66 km^2 of volcanic terrain and 0.29 km^2 of alluvium, on the southwestern slopes of Mt. Santa Rosa. No caves were identified within this large basin, probably because they have been infilled by alluvium. This basin contributes water to the Tumon-Yigo trough, providing extensive recharge to the Northern Guam Lens Aquifer. The three largest known caves in the area, Piggy Cave, Awesome Cave and Interesting Cave have respective drainage basins of 0.05 km^2, 0.03 km^2 and 0.02 km^2. These data illustrate how extremely small allogenic recharge areas can produce major caves. Delineation of drainage basins can also be used to locate undiscovered caves, but none has been found so far. A significant cave is expected to occur some 350 meters northeast of Awesome Cave and 300 meters south of Piggy Cave, fed by the 0.04 km^2 drainage basin in the southeast of Mt. Santa Rosa, but exploration has yet to reveal it.

Volcanic basement exposed over an area of .32 km^2 forms the Mataguac Hill. The three caves associated with this inlier are Mataguac Spring Cave and Mataguac Mud Cave and North Mataguac Cave, draining southeastern, northern and southwestern slopes respectively. Due to small area of Mataguac Hill and lack of small-scale topographic data, drainage basins of these caves could not be accurately delineated.

8. 3. Non-traversable Vadose Conduits in Northern Guam

Caves described in the previous section represent the small portion of karst conduits in northern Guam that are at least partially accessible to people and can therefore be directly explored. Most conduits, however, are inaccessible and cannot be explored directly. Such preferential flow paths in the aquifer have to be investigated by methods other than cave mapping, such as dye-tracing, natural potential survey, down-hole video, etc.

8. 3. 1. Basement conduits

Stream caves that have developed on the flanks of volcanic inliers in northern Guam follow the volcanic-limestone contact and act as basement conduits for freshwater. Each of the Mt. Santa Rosa caves are traversable for less than 200 meters, after which the passages become too tight or obstructed by collapse. Although inaccessible and not called caves anymore, these passages continue as preferential flow paths delivering freshwater to the sea level. The area underlying the northern Guam plateau where volcanic basement lies exposed above the modern sea level is shown on Fig. 8. 7 (Vann, in prep., Mylroie et al., submitted). This area makes up about 21% of the total area of the northern Guam plateau and supports active vadose conduits at the bedrock-basement contact.

Submarine terraces mapped by Emery (1962) suggest that the lowest long-term glacioeustatic stillstand was 95 meters (315 ft) below the modern sea level. At that time, up to 58% of the volcanic basement underlying northern Guam limestone plateau was located above the sea level (Vann, in prep.). Bedrock-basement conduits could therefore have developed extensively (Fig. 8. 7). Such conduits would have become flooded by relative sea level rise but may continue to operate to a certain extent as phreatic conduits.

8. 3. 2. Other conduits in the vadose zone

A dye trace study conducted at Andersen Air Force Base in 1992, following Typhoon Omar,

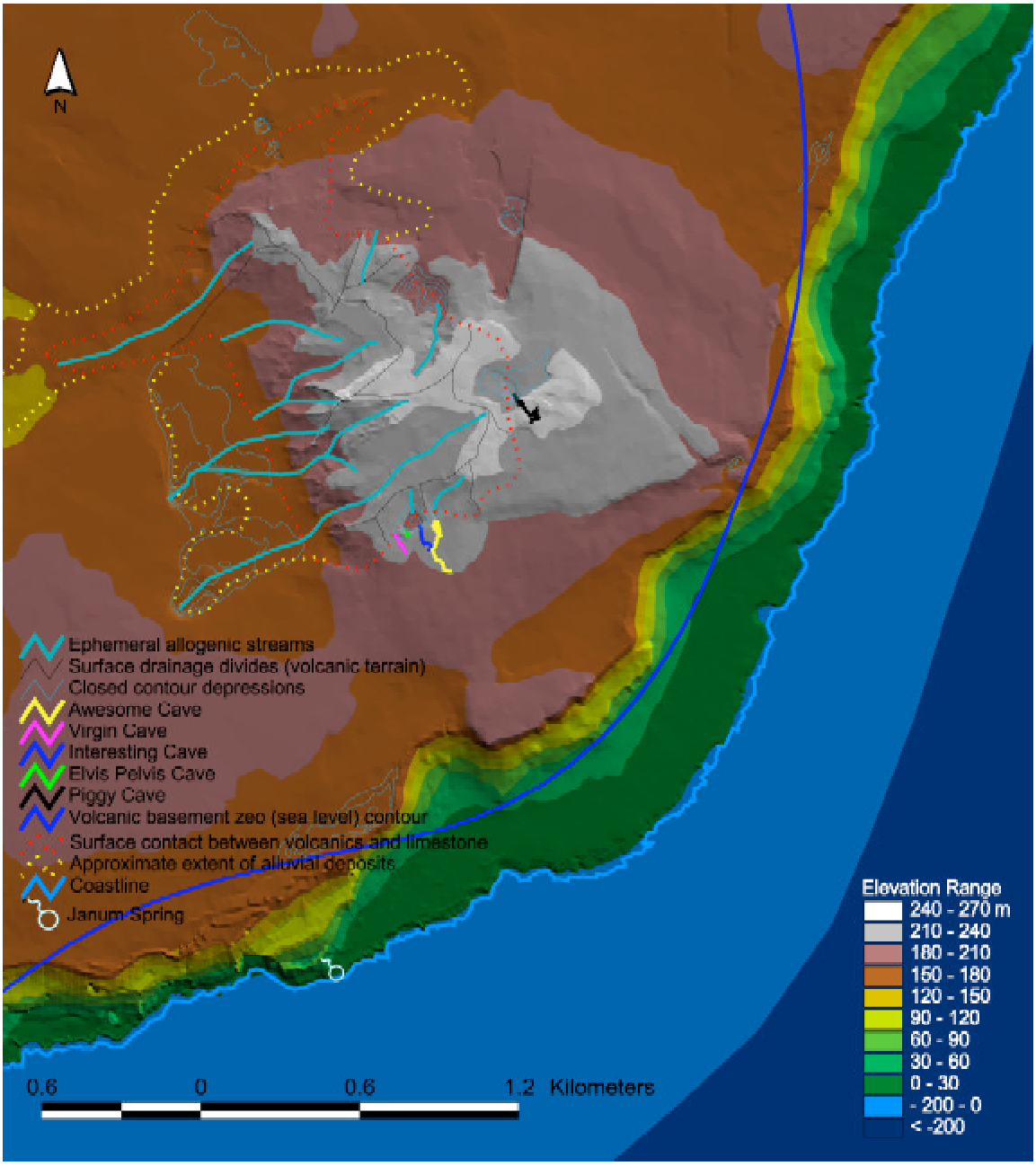

Fig. 8. 6: Map of Mt. Santa Rosa and Mataguac Hill areas, showing locations and extent of known caves, allogenic surface drainage divides and drainage basins. (Approximate extent of caves at Mt. Santa Rosa was provided by Curt Wexel).

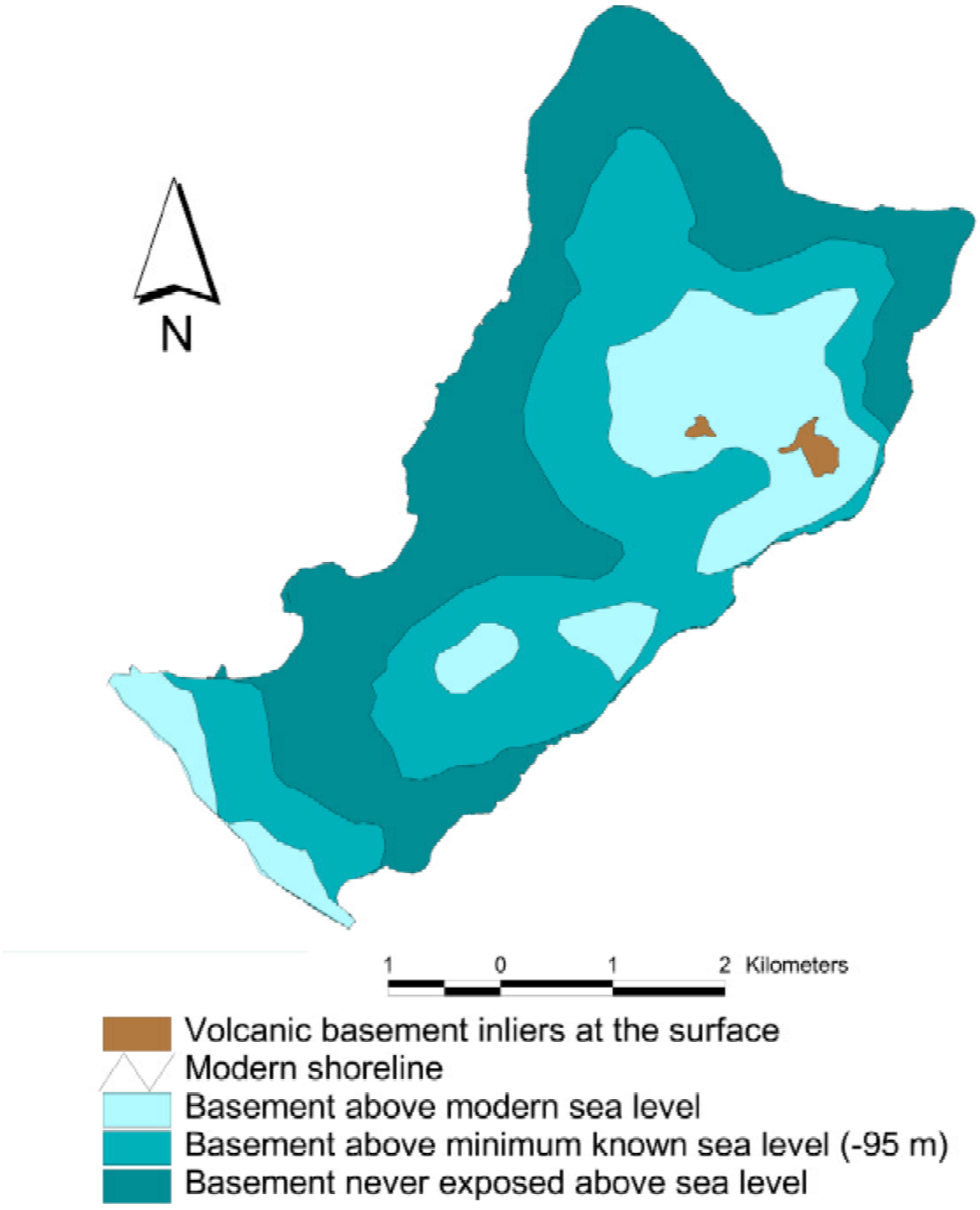

Fig. 8. 7: The extent of basement volanic units located above the modern sea level and the lowest known sea level still stand.

documented combined vadose and saturated flow transport rates of up to 91-244 m/day, along linear paths consistent with major fracture orientations (Barner, 1995 and 1997).

Another dye trace study was conducted at Navy housing area in Finagayan, in 1994. Dye injected in the vadose zone was not intercepted by the monitoring wells placed around the injection site and was finally detected about a year later in Hilaan Pool (Lost Pond), a small cenote on the coast (OEESCI, 1995). In a second trial, dye was injected in Finagayan Banana Hole, a small collapse sinkhole. It was chased by large amounts of water, which carried the dye to the coast some 1.7 km away in only 4 hours (OHM, 1999).

Observations of well hydrographs by Jocson et al. (1999) indicate that water table responses during the wet season, particularly from heavy storms, are immediate, indicating rapid movement through the vadose zone.

Vertical flow through the vadose zone may be extremely rapid, with water traveling through 60-180 meters of vadose zone bedrock in a matter of hours or even minutes (Jocson et al., 1999). Vadose zone conduits capable of such rapid movement of water are probably shafts, pit caves and enlarged joints and fractures, discussed in sections 5. 3. 3. and 8. 2. 1.

The conclusions regarding the flow in the vadose zone based on these studies are thus that vadose flow can occur within a rapid-flow conduit system with water traveling in difficult-to-predict, multiple directions.

8. 4. Types of Vadose Caves in Southern Guam

Stream caves are much more numerous in southern Guam than in the north. This is to be expected due to the presence of older and diagenetically more mature limestones in southern Guam interacting with a surface drainage network developed on adjacent volcanic rock areas. The Alifan and Bonya Limestones in the Fena Reservoir area host the majority of caves in southern Guam, all of them being in some way associated with underground stream flow, permanent, ephemeral or abandoned. On the east coast of southern Guam, no active stream caves are known but several paleo-stream caves are found in the Mariana and Bonya Limestones. Orote peninsula, comprised of young reef limestone isolated from any surface drainage, has no developed stream caves.

Alifan Limestone block (Nimitz Hill area) on the south side of Pago-Adelup fault is the site of a large number of complex caves. For the purposes of this report, these caves are termed “fracture caves” as fractures play a major role in their development. The caves do not fit into typical island karst classification scheme (pit caves, stream caves and flank margin caves) and show evidence of being modified by several processes, including vadose enlargement of fractures, collapse, and dissolution in the phreatic zone.

My inventory of caves (in which the vadose caves are included) from southern Guam is given in Appendix 9. Figure 8.8 is a map showing distribution and types of vadose caves in southern Guam.

8. 4. 1. Active stream caves

The only known active stream caves in southern Guam are found on the Navy Magazine, in Fena Lake area and are associated with groundwater conduits in Alifan Limestone capping mountains to the west or with allogenic surface streams originating on surrounding volcanic terrain. There are two distinct types of stream caves in southern Guam: those carrying and discharging groundwater stored in limestone inliers (spring caves) and those carrying underground portions of already developed surface streams (flow-through caves).

Spring caves

The best example of this type is Almagosa Cave, located on the eastern slope of Mt. Almagosa west of the Fena Lake (Plate 18, photo 5). The cave entrance is at Almagosa Spring, a flashy spring discharging water collected by the Alifan Limestone mountain ridge. Nearby Chepak Spring, about 65 meters away, provides an additional entrance to this cave (C. Wexel, pers. comm.). A low, muddy, active stream passage leads from the Almagosa Spring entrance. It is up to a 1.5 meters high, up to few meters wide. The floor of the passage is comprised of limestone bedrock and not volcanic rocks, although they must be quite shallow. Limestone on the floor of the stream passage is extremely jagged, shaped by mechanical erosion as well as dissolution (Plate 18, photo 6). Small, non-traversable tributary conduits join the main stream passage at a right angle, their ephemeral flows cutting well-developed vertical flutings in the main passage walls. This portion of the stream passage almost certainly becomes completely flooded during high discharge episodes. After about 10 meters from the cave entrance, the passage becomes high enough to allow walking (Plate 18, photo 7). Further upstream, the main passage

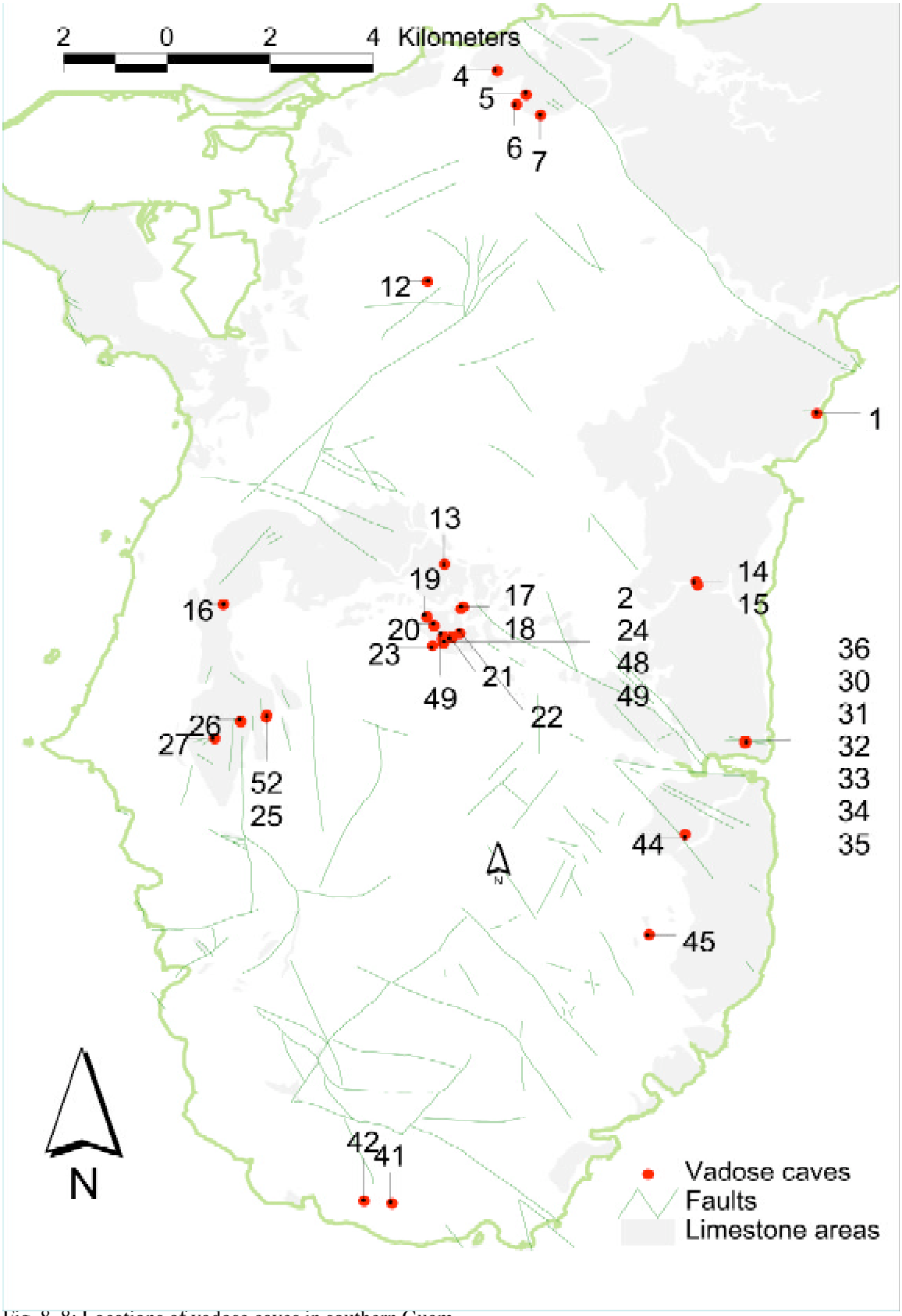

Fig. 8. 8: Locations of vadose caves in southern Guam.

continues as a large phreatic tube (Plate 18, photo 8) up to a total length of 65 meters where it is sealed by a siphon. By swimming through the siphon (a practice not recommended due to murky water and risk of disorientation) it is possible to reach the beautifully decorated and rarely visited continuation of the main passage. This stream passage ends after 100 meters from the siphon, fully obstructed by an underwater mud plug. Total length of the main stream passage is thus about 165 meters, and total survey length that includes side passages is about 250 meters (C. Wexel, pers. comm.) It is likely that additional unexplored passages exist in this cave. This well decorated active stream cave is an unusual karst feature on a carbonate island, more typical of continental settings. It was not explored in detail due to time and access restrictions and the fact that the focus of the study was on northern Guam. A map of this cave is currently in preparation (Wexel, in prep.).

There are unverified reports of a similar cave leading from nearby Dobo Spring and connecting to Almagosa Cave (Rogers and Legge, 1992).

Liyang Almagosa Gelagu (also known as the North Almagosa Cave) is located some 30 meters north of Almagosa Spring. It is a dry cave, containing a few stalactites and flowstone deposits, with soil covering most of the floor. Tubular passages of this cave, some 20 meters long in total, are probably abandoned stream conduits, once part of the Almagosa Cave system.

Flow-through caves

The second type of stream caves are found in the Bonya Limestone, northeast of the Fena Reservoir. While Almagosa cave is a part of a basement contact conduit system draining vadose and phreatic water from Alifan Limestone, other stream caves in the area are underground portions of developed surface streams. The first of the two such caves carries Maemong River from its swallet on the northeast side of a Bonya Limestone hill to the resurgence on the opposite end, from a base of a 25-m-tall cliff. The minimum length of this cave is about 100 meters, it being the straight distance from swallet to resurgence. It is possible that this cave is permanently flooded, and not traversable. Rogers and Legge (1992) report that this cave is over 350 meters long but it is unclear how this was measured since the cave was not traversed. Another stream cave pirated the entire flow of Tolae Yu'us River (also known as the Lost River). It extends for at least 420 meters, it being the straight distance from Tolae Yu'us River swallet to rise. This cave could not be entered from the resurgence end because it is entirely flooded; it is unknown if the cave is traversable from the swallet end.

An abandoned cave, Lost River Rise Cliff Cave, was located about 4 meters above the Tolae Yu'us River resurgence (Plate 19, photo 1). It is entered through an opening in the cliff and could represent a former river resurgence before the local base level was lowered. The cave is traversable for about 20 meters. It shows indications of having contained extensive sediment deposits upon which layers of flowstone have developed. The sediment has been subsequently removed, and the flowstone deposits indicate previous sediment level (Plate 19, photo 2).

8. 4. 2. Ephemeral stream caves

A good example of an ephemeral stream cave is Fena Sinkhole Cave, located in a cockpit doline east of Tolae Yu'us River resurgence. The entrance to the cave is at the bottom of the doline. The cave passages contain thick alluvial deposits. Branches and other plant material and fresh organic debris were found in some of the passages in this cave, clear evidence of a recent storm water flow. Most of the main passage is large and tall enough to comfortably walk through. At its end, the passage becomes only about 0.5 m high, containing extensive stalactite development in a ceiling so low that the stalactites are partially embedded in floor mud deposits (Plate 19, photo 3). Passage on the other side of this crawlway leads to an entrance opening at the bottom of the neighboring doline. This cave is a connection between the bottoms of two cockpit dolines and runs through Bonya limestone ridge separating them. It conducts water from one doline to another during high rainfall events.

Additional similar caves probably exist and connect other dolines in the Fena cockpit karst area. A large number of caves have been reported from the Navy Magazine area but could not be investigated during this study due to access restrictions. These caves are discussed in section 8. 4. 6. and most of them are probably dry stream caves active during high rainfall events.

8. 4. 3. Abandoned stream caves

Several large caves in southern Guam are stream caves made by voluminous runoff that has since been diverted. Today these caves are dry, only occasionally receiving local rainwater input, but not runoff.

The best examples of this type are the Talofofo Caves (Fig. 8. 9), a popular hiking destination and an extensive cave system located in the Mariana Limestone reef facies cliff overlooking Talofofo Bay. The seven caves in the complex are high ground today and can receive water only from the rain that falls right on top of them, but their size and shape indicates that they were once receiving extensive stream input. The caves and one natural arch are clustered around two collapse sinkholes at the top of a limestone ridge. Four of the caves are small, single room or tube passages with soil floors and little or no decorations. These were listed by Rogers and Legge (1992) as Talofofo Caves #s 1, 4, 5 and 6. The remaining three are more significant and include a well-decorated cave containing several large connected chambers (Talofofo Cave #2), a long tubular cave extending through the limestone ridge and terminating in an opening in the face of the cliff overlooking the ocean (Talofofo Cave #3), and a large 32 m pit cave with two entrances and additional horizontal passages half way down the pit (Talofofo Pit Cave). This last cave is the largest in the complex but was curiously not mentioned by Rogers and Legge (1992) in their compendium.

Talofofo Cave #2 (Fig. 8. 10) is a series of four adjacent chambers. Entrance to the cave is through a steep 10 m long tube containing an additional small entrance and leading to a circular room, 8 m in diameter. This first room is dominated by six massive columns that nearly partition it. The floor is covered by cobbles, soil and flowstone, with the latter being a false floor collapsed in two places. Space below the false floor is not traversable. This chamber opens to the north, connecting to the second circular room, about 7 meters in diameter. The second room has few speleothems, small bell holes in the ceiling and a collapsed flowstone false floor revealing mud floor underneath. A single column in the northeast end marks the entrance to the third room. This room is oval in plan (9 m by 12 m) and well decorated by flowstone deposits. It is nearly split into two by three columns. The first portion of the room leads to a steep, flowstone covered passage, sloping about 36^{o} upward to the cave's third entrance. This passage appears to have developed along a fracture and probably received significant inflow. The portion of the room behind the column partition leads to a 13-m long, down-sloping, narrow passage 1.5-2 m wide, and well decorated by stalactites and columns. An additional elongate room (15 m by 4-6 m) can be accessed beyond the third chamber through a very tight squeeze through a column/flowstone partition in the north wall. The back of the cave contains a shallow pool of perched water, numerous small stalactites and a short flowstone floored passage.

Talofofo Cave #3 is a tubular passage starting from a collapse sinkhole on the southeast side of the limestone ridge. The passage leads through the ridge and opens in the cliff face on the opposite end, overlooking the ocean. Curiously, the passage steeply slopes towards the northwest, indicating flow of water from the direction of the present coastline towards the island interior. The water used to come from the cave entrance presently in the cliff, lacking any surface whatsoever that could capture the flow.

The largest in the complex is the Talofofo Pit Cave, a 32 meters deep pit, completely roofed over, containing two high entrances on its opposite ends. This extremely large cave probably contains the largest single open chamber on Guam and can only be accessed on rope. A small terrace and some horizontal cave passages are found about half way to the bottom of the pit.

Rogers and Legge (1992) write that Talofofo Caves had a "relatively simple history" and interpret them as phreatic dissolution features, made by diffuse flow. However, there is no evidence to support this interpretation. No phreatic dissolution features are visible anywhere in the caves; long and steep tubular passages are indicative of conduit flow; and finally, a 32 meters deep pit cave is certainly an unlikely result of phreatic dissolution. Interpretation as stream caves is more supported by cave morphology, although the source of enough focused discharge is not obvious. It is possible that the caves developed as conduits draining central Guam volcanic areas, through the limestone ridge, into the ocean. Central Guam terrain was subsequently lowered and runoff pirated by Talofofo River, leaving the caves as dry high ground. Gumayas Caves, located in the Togcha River gorge may be another example of abandoned stream caves.

8. 4. 4. Natural bridges

Natural bridges are made by weathering and partial collapse of stream caves. Bridges are often discussed in conjunction with natural arches and "karst windows" because they are all karst features through which daylight penetrates. However, bridges are features through which a river runs or has run, whereas arches are limestone spans not associated with stream flow (Cleland, 1910). There are a few examples of natural bridges in southern Guam. Arches and "karst windows" are more common, both in the north and south, but are made by collapse of sea caves or flank margin caves and are discussed in the next chapter.

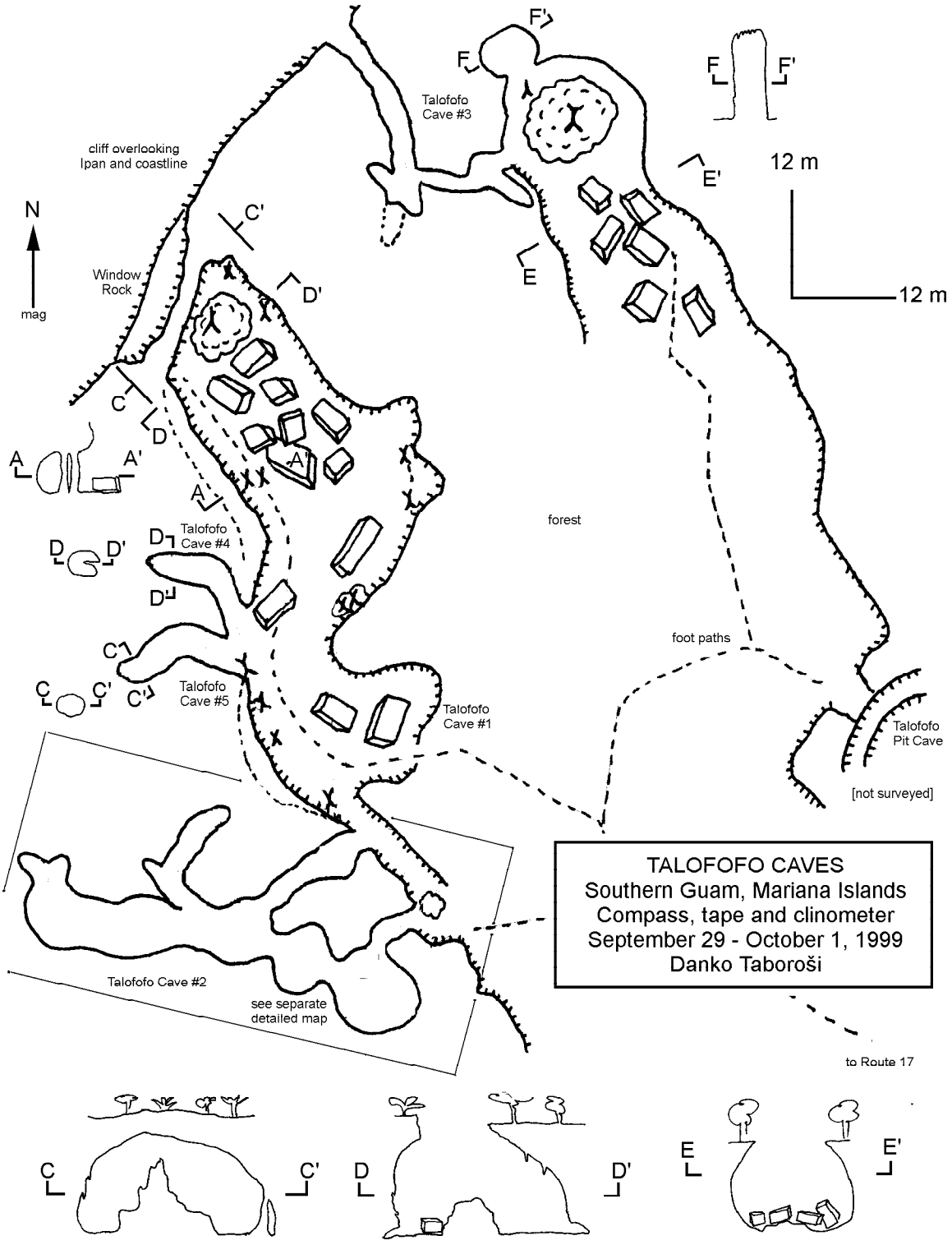

Fig. 8. 9: Map of the Talofofo Caves.

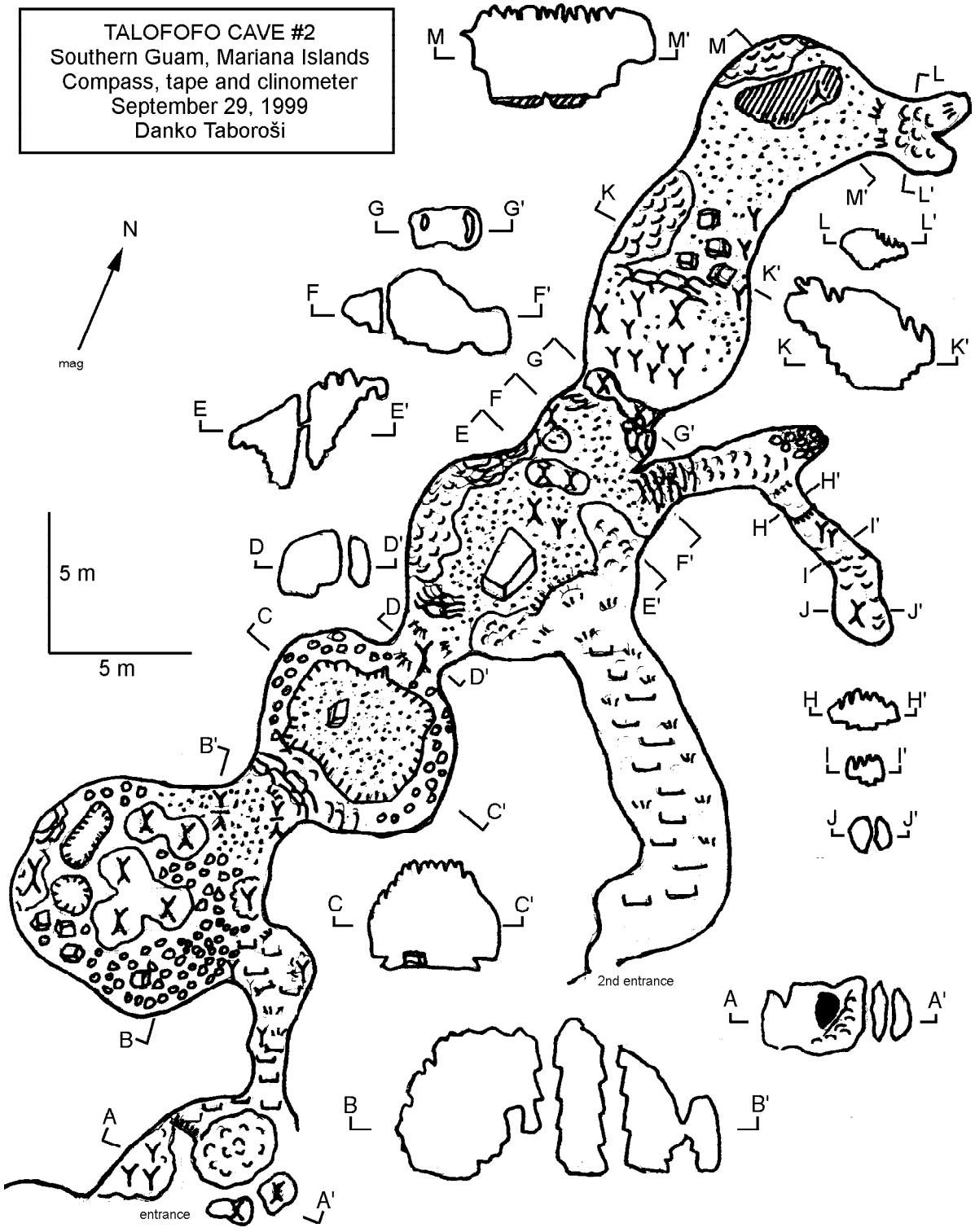

Fig. 8. 10: Map of Talofofo Cave #2.

The most famous natural span in Guam must be the Window Rock in the Talofofo Caves complex (Plate 19, photo 4). Although not necessarily remnant of a stream passage, it is a remnant of a collapsed stream cave room and possibly a natural bridge. It is located in Mariana Limestone reef ridge overlooking the village of Ipan. The bridge is about 12 meters tall, several meters wide and spans a distance of about 20 meters. Another such feature, Bonya River Arch, is in the Navy Magazine area. It also does not span an active waterway but is probably a remnant of a collapsed and abandoned river cave and may be an old natural bridge.

Two indisputable natural bridges are found in the Bonya Limestone karst in central southern Guam, and span across two channels of Maemong River, 10 meters away from each other. One of the bridges possesses stalactites and flowstone, evidence of being a remnant of a stream cave. The U.S. Navy has built a road across Maemong River, utilizing these natural bridges.

Natural bridges are common in karst valleys (Jennings, 1985) and some probably occurred along the east coast of southern Guam, particularly the Togcha River gorge, where a collapsed remnant exists. An inventory of natural bridges from Guam is included in Appendix 10.

8. 4. 5. Fracture caves

The Alifan Limestone block south of the Pago-Adelup fault, known as Nimitz Hill, is extremely rich in caves. This is a tectonically active, heavily faulted and fractured area. Although Tracey et al. (1964) mapped only two joints in this area, there are many more. A simple walk over this terrain reveals a large number of joints, often dissolutionally enlarged and appearing as 2-3 meter deep fissures, large enough for a person to move through (Plate 19, photo 5). Faults are also common and have not yet been mapped. Fractures, also, are often dissolutionally enlarged and frequently contain shelter caves. Some

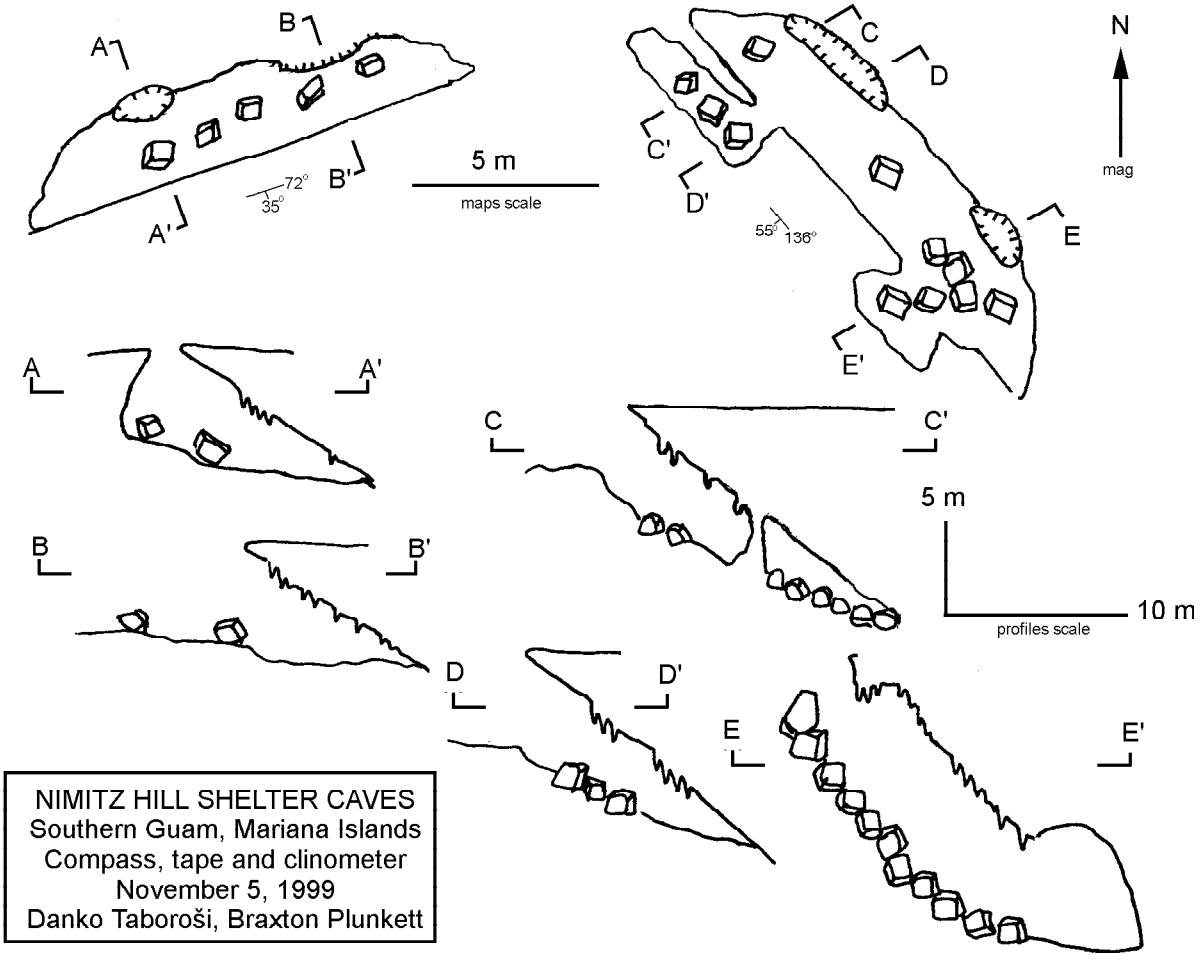

Fig. 8. 11: Maps of Nimitz Hill Shelter Caves.

examples of such shelter caves are illustrated by Fig. 8. 11. Numerous large and more complex caves in the area also show strong control by fractures and are presumably made by extensive enlargement of fractures.

Since enlargement of fractures seems to be the strongest genetic factor, these caves, very different from caves elsewhere on Guam, are discussed here under the designation of "fracture caves." They may or may not be related to "fracture caves" described by Mylroie and Carew (1995). The development of fracture caves on Guam seems to be much more complex than simple modification of sites of mechanical failure by groundwater. Development of fracture caves in Guam's Nimitz Hill area is probably influenced by shallow volcanic basement, allogenic catchment from nearby volcanic terrane, collapse events, past sea level and groundwater lens positions (as indicated by rare wall cusps and other phreatic dissolution features in some caves) in addition to enlargement of fractures.

Japanese Cave (Fig. 8. 12, Plate 19, photo 6), located in the jungle across from the Department of Defense High School on Nimitz Hill, can be considered representative of caves found in Nimitz Hill area because it shows all complexity and variety of genetic factors involved in their making. It is a small but genetically complex cave showing evidence of vadose and phreatic dissolution as well as collapse. The cave has two entrances, both results of collapses

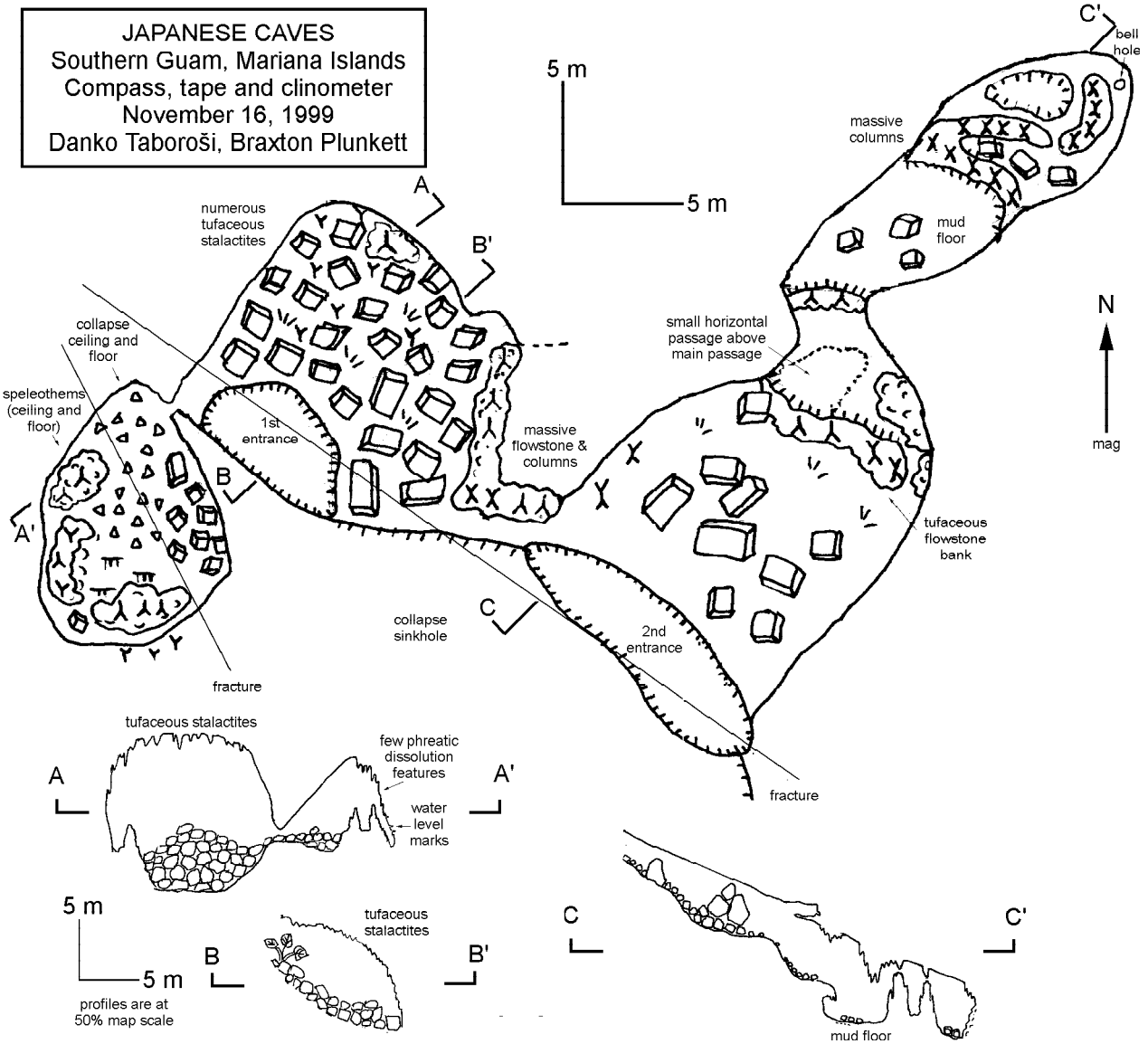

Fig. 8. 12: Map of Japanese Cave.

along a NW-SE trending fault.

The northwest entrance leads to a large day-lit collapse chamber. The chamber contains numerous boulders and rubble, all the result of collapse, and has abundant but small tufaceous stalactites. The second room is smaller and deeper and is entered through a short passage in the west part of the large chamber. The northeastern half of the ceiling in this room is flat and follows a fracture, while the other half has been stable longer and shows extensive stalactite development. Consequently, the floor in the northeast end is covered by rubble, while the opposite side of the room has several large stalagmites. Interesting phreatic dissolution features found in the southwestern wall are evidence of this cave's complex history and modification in a phreatic environment. Enlargement of this room and cave in general as a result of phreatic dissolution, possibly flank margin type, cannot be excluded.

The cave's southeast entrance leads to a large passage clearly developed along a fault, dipping about 30°. The cave appears as a series of small chambers, due to extensive stalactite/stalagmite partitions, but is really a single large planar passage, developed along a fault. Low portions in the cave show accumulations of fine sediment. A short horizontal plane passage leads from the ceiling and possibly indicates a stable former water table level.

Numerous other larger caves exist in the area and have been explored by local cavers. Most of them show strong control by faults and fractures, are well decorated by calcite deposits and show vadose and phreatic dissolution features as well as collapse features. At least six additional caves are known to local cavers and include Birthday Cake Cave and its 25-m long un-named neighbor, Six Wiggles Cave, Skylight Cave, Admirable Cave and Geiger Field Cave (C. Wexel, pers. comm.). Only the last two were visited during this project. Numerous smaller caves were encountered in this area virtually every time jungle was traversed. It is recommended that Nimitz Hill area be surveyed in more detail, because of the high concentration of caves here and their unique character. Locations of Nimitz Hill caves inventoried during this project are shown on Fig. 8. 8, but are approximations only. Determining precise locations of caves in this area was uniquely difficult because heavy canopy prevented the use of a GPS device and lack of features recognizable from the air prevented pinpointing of caves on aerial photos.

8. 4. 6. Other vadose caves reported from southern Guam

A large number of caves have been reported from the Naval Magazine area. No extensive field work took place there during this project and only a few caves were investigated. Rogers and Legge (1992) give a detailed description of Bay Rum Cave (a.k.a. Bay Leaf Cave) which appears to be a 172 m long, fracture guided cave, developed in Alifan Limestone. They further mention unexplored Hoyu Sabana Lamlam, Mt. Almagosa Cave and Pinnacle Cave (in the Alifan Limestone ridge) and Ibaba Cave, Liyang Namu Kanutu Cave and Hoyu Fena (in Bonya Limestone northeast of the Fena Lake). Approximate locations of these caves are given in the cave inventory (Appendix 9) and are shown on a map (Fig 8. 8).

Small caves have been reported from south Guam areas with no mapped limestone strata, namely Mt. Alutom and Merizo. A small cave reported from Mt. Alutom probably occurs in a small, unmapped limestone lens in the volcanic Alutom Formation. Caves from Merizo are reported from Gumoje and Suma river areas and have probably developed in limestone lenses in volcanic Bolanos units. Their approximate locations are provided in cave inventory (Appendix 9) and map (Fig. 8. 8)

— Chapter 9 —
PHREATIC CAVES AND CONDUITS

This chapter investigates caves and conduits made by dissolution in the phreatic (saturated) zone. Selection of caves discussed in this chapter is thus based on their presumed genetic origin and not their present location with respect to the sea level. Types of phreatic caves and conduits on Guam are discussed and selected features are described in detail.

9. 1. Phreatic Caves and Conduits

In their classic paper on the development of limestone cave systems, Ford and Ewers (1978) described three common types of caves: vadose caves, phreatic caves and shallow-phreatic (water-table) caves. They defined the phreatic caves as having evolved under conditions of total and permanent water fill until a rapid event causes them to be abandoned by their genetic waters. The shallow-phreatic caves are defined as having developed along or just beneath a piezometric surface that is of extent greater than the cave. Ford and Ewers (1978) also list a number of special case caves, one of which is an unintegrated cave (vug or room). Because caves are commonly defined as openings large enough to admit a human being (White, 1988), extensive parts of the karst drainage network are not designated as caves. Instead, such openings are considered conduits, if they are capable of supporting turbulent flow. White (1988) suggests that there is value in separating caves, which are objects that can be explored, and "conduits," which are parts of the underground drainage system.

This chapter investigates all voids made in the saturated groundwater zone (at or below the groundwater level)—whether phreatic or shallow-phreatic caves, phreatic conduits or unintegrated voids. Phreatic passages that develop in vadose caves as part of the proto-cave development or under flood conditions have already been discussed in the previous chapter as they are an integral part of vadose zone cave systems.

9. 2. Types of Phreatic Caves in Northern Guam

Most caves inventoried in northern Guam have been interpreted as phreatic caves. Out of the 79 caves I inventoried in northern Guam, 64 show evidence that they developed at or below the groundwater level.

Types of phreatic caves in northern Guam include collapsed abandoned phreatic conduits, flank margin caves (Mylroie and Carew, 1990), lens voids and possibly halocline caves (Palmer and Williams, 1984). Additionally, there are conduits in the phreatic zone that are too small to be directly explored but are evident from dye-trace and geophysical studies. Finally, collapse of phreatic caves may form other karst features, including natural arches, large collapsed rooms, banana holes (Harris et al., 1995) and massive collapse areas on the sides of cliffs. The various types of caves are discussed below. Representative examples of each on Guam are described in detail.

The complete inventory of caves (in which the phreatic caves are included) from northern Guam is given in Appendix 8. The map showing distribution and types of phreatic caves in northern Guam is shown in figure 9. 1.

9. 2. 1. Collapsed abandoned conduits

Only two traversable horizontal caves thought to be paleo-phreatic conduits have been identified in the interior of northern Guam away from volcanic inliers. The first is entered via 20 m-deep collapsed Carino Sink in Chalan Pago, and consists of 3 cave passages, surveyed by local cavers to a total length of about 100 meters (C. Wexel, pers. comm.) The surveying effort was abandoned after a portable gas monitor indicated oxygen content below safe limit (<18%).

The second such cave is entered through a 10 m deep collapsed Barrigada Sink (a.k.a. Appealing Sink) in Barrigada and also has a traversable length of about 100 meters (C. Wexel, pers. comm.)

Both of these karst features are probably abandoned conduits. Their horizontal orientation and circular cross-sections suggest origin as phreatic conduits developed at or near the water table, subsequently inactivated by the drop in sea level. Sea level drop may also have triggered the collapse and opening of the passages to the surface, once buoyant support by water was removed. Both Carino Sink and Barrigada Sink are presently used for disposal of household waste. Organic decay may be the cause of "bad air" in the passages of Carino Sink Cave.

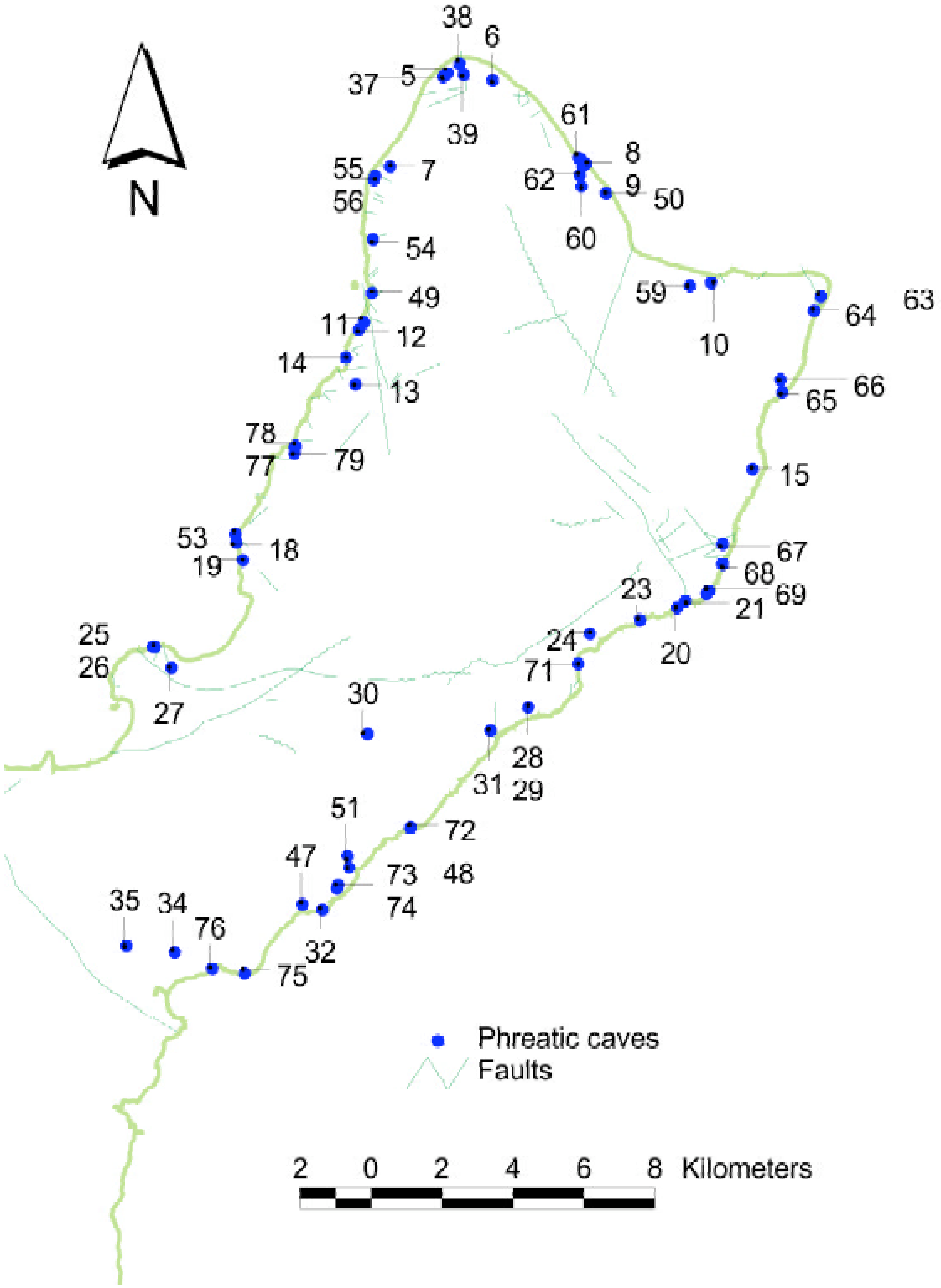

Fig. 9. 1: Locations of phreatic caves in northern Guam.

9. 2. 2. Flank margin caves

Flank margin caves are large phreatic dissolution voids, forming preferentially along the margin of the discharging freshwater lens, as a result of mixing of freshwater and saltwater (Mylroie and Carew, 1990). Distal margin of the freshwater lens is where the two primary areas of dissolution in a freshwater lens converge: top of the lens where vadose and phreatic waters mix, and the bottom of the lens where freshwater and marine water mix (Raeisi, 1995). This preferential dissolution reflects "mixing corrosion," first recognized by Bögli (1964). He defined it as the effect produced by mixing of two waters from different sources, both saturated with $CaCO_3$ and acting alone incapable of dissolution, which become aggressive and capable of dissolution upon mixing. This phenomenon has been recognized as the cause of major cave development in the Bahamas (Mylroie, 1988), Isla de Mona, Puerto Rico (Frank et al., 1998), the Yucatan (Back, 1986) and Guam (Mylroie et al., 1999). In addition to mixing zone corrosion, carbonate dissolution may be intensified by oxidation of organics in the water (Mylroie and Carew, 1995).

Typical morphology of flank margin caves, as described from the Bahamas (Mylroie et al., 1995) and Isla de Mona (Frank et al., 1998), includes large globular chambers, bedrock spans and thin bedrock partitions between the chambers, passages that end abruptly, and phreatic dissolution surfaces. The caves are horizontally broad but vertically restricted. One of the defining characteristics of flank margin caves is that they are not true conduits—they receive and discharge water via diffuse flow, and as such represent mixing chambers rather than conduits (Mylroie and Carew, 1990). Flank margin caves develop with no external opening and become exposed only by cave breaching from collapse or erosion (Mylroie and Carew, 1995).

Flank margin caves occur in a variety of settings on Guam and show diverse morphologies, as presented in sections 9. 2. 3. through 9. 2. 7. Most common setting is coastal cliffs where cliff retreat has breached the caves and formed cliff face entrances. In certain locations, the cliff may have retreated far enough that only the smallest portions of former flank margin caves still remain, and in such cases cave remnants are hardly distinguishable from bioerosional notches. Flank margin caves are also found on coastal terraces and slopes, where they are breached by ceiling collapse. Many occur at the bases of cliffs, where they have been subject to extensive collapse and their floors are usually entirely composed of collapse materials. Such caves often intersect the freshwater lens and are apparently associated with conduit flow. Such caves could have developed as flank margin caves and subsequently captured conduit flow. Finally, collapse of flank margin caves, in various stages and magnitudes may produce natural arches, large collapsed voids, and massive collapse areas in coastal cliffs.

Flank margin caves and dolomite

Formation of dolomite has long been a subject of debate and remains poorly understood (White, 1988). Some dolomitization models consider the mixing zone of fresh and marine waters an environment conducive to replacement of calcite and aragonite by dolomite. Because mixing zone is also the environment where enhanced dissolution produces flank margin caves, occurrence of dolomite and flank margin caves together could be expected. This is certainly the case with Isla de Mona in Puerto Rico, where the extremely large flank margin caves have developed along the contact of Lirio Limestone and underlying Isla de Mona Dolomite. It is not clear if the caves have preferentially formed along the contact with dolomite or if the caves are just another manifestation of the process that has created dolomite (Frank et al., 1998).

On Guam, the presence of flank margin caves, particularly in the northern part of the island, may be somewhat puzzling considering that no dolomite is known to occur there. Lack of dolomite on Guam could be explained by dynamic sea level changes Guam has experienced. Flank margin caves may have had enough time to form, but dolomite did not. Flank margin caves can form rather quickly and in the Bahamas are thought to have formed in 15,000 years or less (Mylroie et al., 1995).

It is also possible that a brackish lens favors dolomitization. In that case, the climate may be another factor: Guam's modern mean annual rainfall (1957-1992) is 2587 mm (Lander, 1994). Combined with the presence of allogenic recharge, high rainfall may keep Guam's freshwater lens not brackish enough to drive dolomitization, assuming that paleo-climates have been at least as humid as the modern climate. Semiarid Isla de Mona, for example, only receives 968 mm (31 years on record) of annual rainfall (Kaye, 1959), less than 40% of Guam's.

9. 2. 3. Breached flank margin caves in coastal cliffs

Dynamic relative sea level fluctuations that Guam has experienced have caused repeated vertical

movement of vadose, freshwater phreatic, mixing zone and marine phreatic zone. The top of the freshwater lens in northern Guam was as high as +200 m (as evidenced by carbonate deposition) and as low as -95 m (as evidenced by submerged platforms identified by Emery, 1962). It is, therefore, not surprising that flank margin caves are found at elevations as high as 150+ meters above the modern sea level. In fact, the majority of caves inventoried in northern Guam and interpreted as flank margin caves are located well above the modern sea level and freshwater lens.

Cave entrances can be identified in the cliffs all around the perimeter of northern Guam, from Amantes Point on the west coast to Iates Point on the east coast. The cliffline of Tamuning peninsula, between Agana and Tumon bays, also has several cave entrances but these are at the modern sea level and appear to be wave-eroded sea caves. Further north, in the Double Reef area, small but clearly visible cave entrances in cliff faces seem all but impossible to reach (Plate 20, photo 1). The most accessible cliff-side flank margin caves are in Ritidian and Tarague areas, where several can be entered by free-climbing of cliffs. Numerous flank margin caves, throughout northern Guam, occur at the bases of cliffs and are easily accessible.

Tarague Copra Cave (Fig. 9. 2) is a single-chambered cave breached by cliff retreat. It is located in the Tarague embayment and is entered by climbing the breakdown talus at the base of the cliff. The large entrance, almost 20 m by 6 m, is almost entirely blocked by large collapse boulders. The floor of the cave is comprised of soil and when I visited it, contained a large pile of coconut husks, probably accumulated there by coconut crabs (*Birgus latro*). The cave ceiling appears to be entirely a result of phreatic dissolution, with large cusps being the only visible feature. Cusps are thought to be phreatic dissolution features and their origin is discussed in detail in Frank et al. (1998). Virtually no vadose depositional features are present. The cave shows typical flank margin morphology, and early stages of development of secondary smaller rooms that end abruptly along with bedrock partitions, inland from the main chamber.

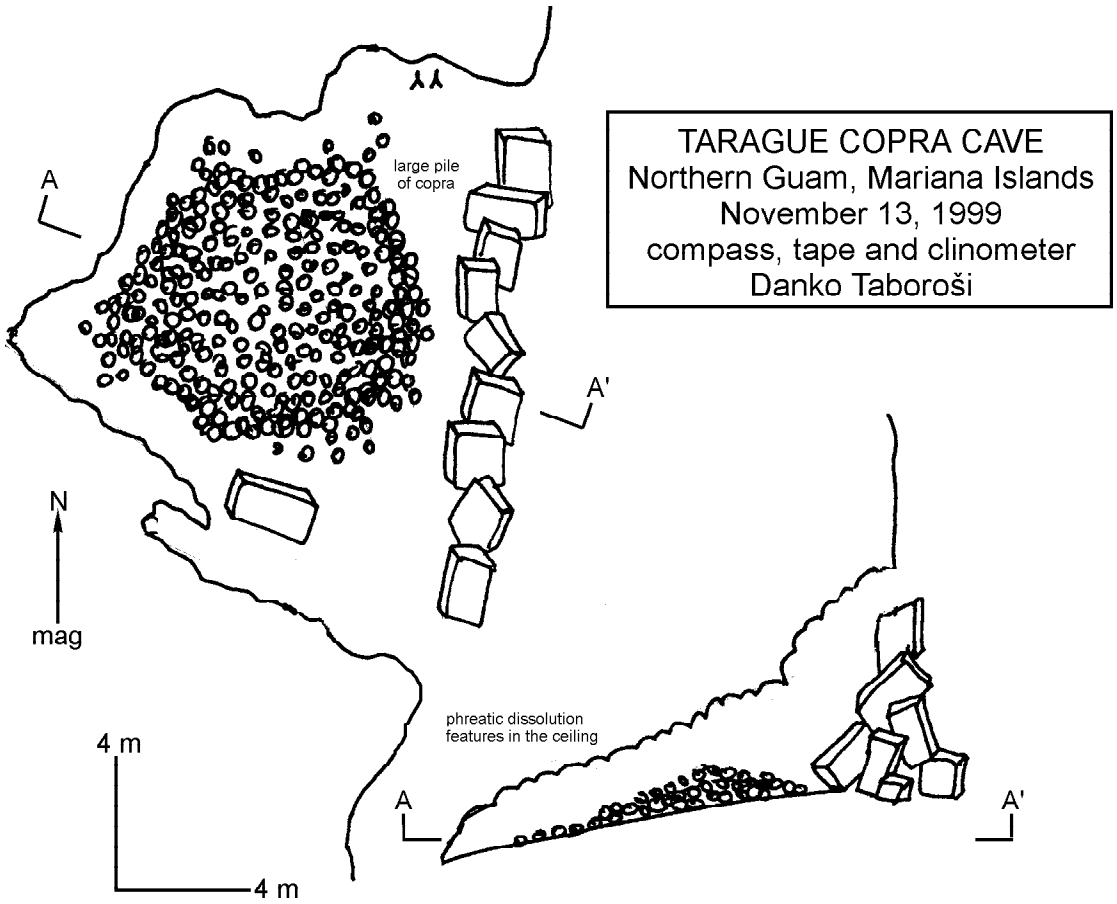

Fig. 9. 2: Map of Tarague Copra Cave.

Tarague Beach View Cave (Fig. 9. 3) is more typical of Guam's flank margin caves with cliff-side entrances. The entrance is located about 15 meters up the coastal cliff, just west of Mergagan Point, where a large tension dome remains of another flank margin cave (Mergagan Point Cave, Plate 20, photo 2), collapsed in a recent earthquake. Tarague Beach View Cave has one long room, about 16 m by 2-6 m, nearly partitioned into two by a group of large columns. The cave exhibits massive stalactite and column development, many of which have been grotesquely dissolved by subsequent phreatic dissolution. Dissolutional sculpturing of speleothems is reminiscent of that in the flank margin caves of Isla de Mona, Puerto Rico. The ceiling and walls show phreatic cusp development, which has been overprinted in the back portion of the cave by vertical vadose fluting. Vadose input is evident in the back portion, from numerous small stalactites and soda straws in the ceiling, dripstone on the floor, along with thick organic soil deposits, which have probably been brought by vadose water through the epikarst. The cliffline walls outside of the cave show phreatic cusp development, indicating that cave development was much more extensive before destruction by cliff retreat. Horizontal notches showing beads-on-a-string morphology (Vogel et al., 1990) and massive grotesquely dissolved speleothems extend along the cliff at the level of the cave entrance and another level some 15 m above (Plate 20, photo 3).

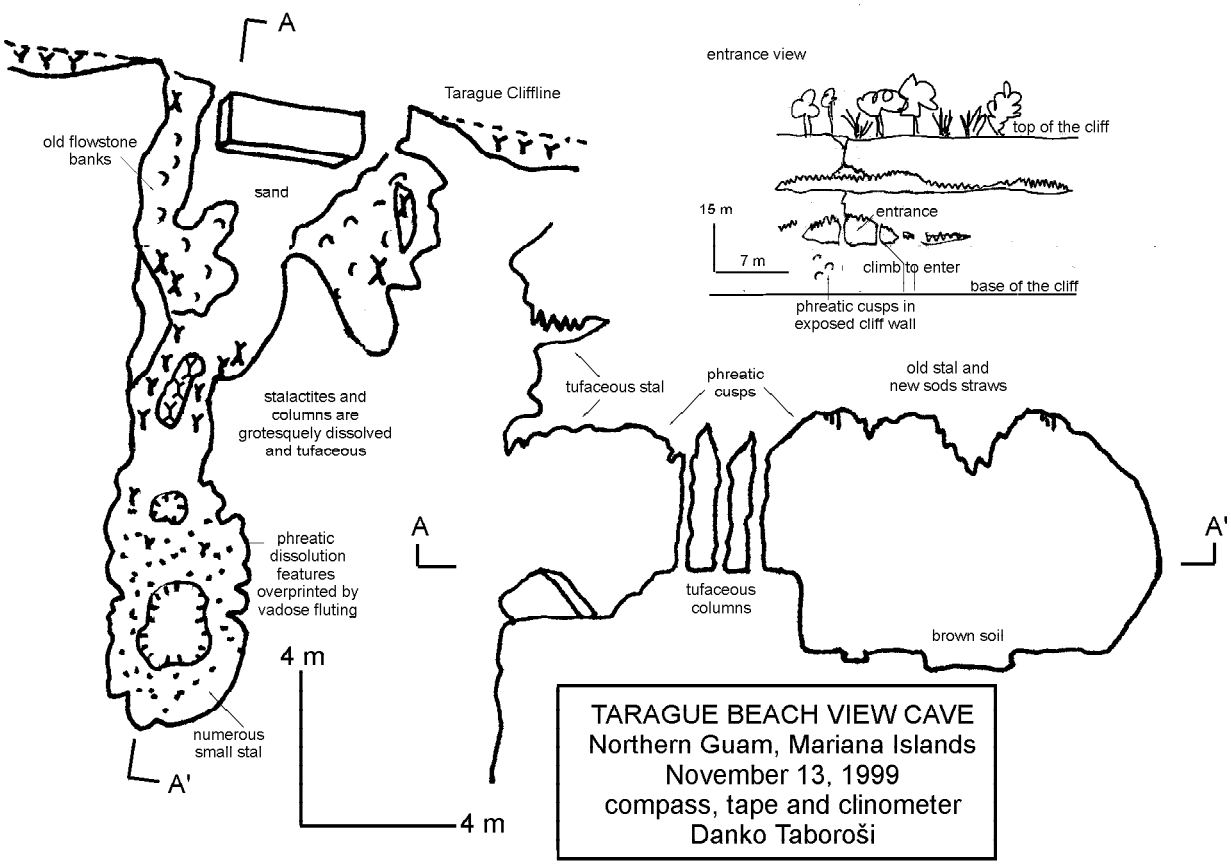

Fig. 9. 3: Map of Tarague Beach View Cave.

Ritidian View Cave (Fig. 9. 4, Plate 20, photo 4) is similar to the Tarague Beach View Cave. It is entered via a cliff-side entrance, nearly 20 meters wide and 8 m tall, located about 10 meters up a cliff overlooking Ritidian Beach (Ritidian Cliff). The large entrance and massive stalactites are visible from the beach and especially the Ritidian access road. The cave has one large room, divided into several sections by column partitions. Most of the speleothems are grotesquely sculptured by phreatic dissolution. The back part of the cave has a black soil-infilled pit, about 2 meters deep. Another large cave (Ritidian Gate Cave, Plate 20, photo 5) is located at the base of the cliff, on the right-hand side of the road just by the gate at Ritidian Wildlife Refugee.

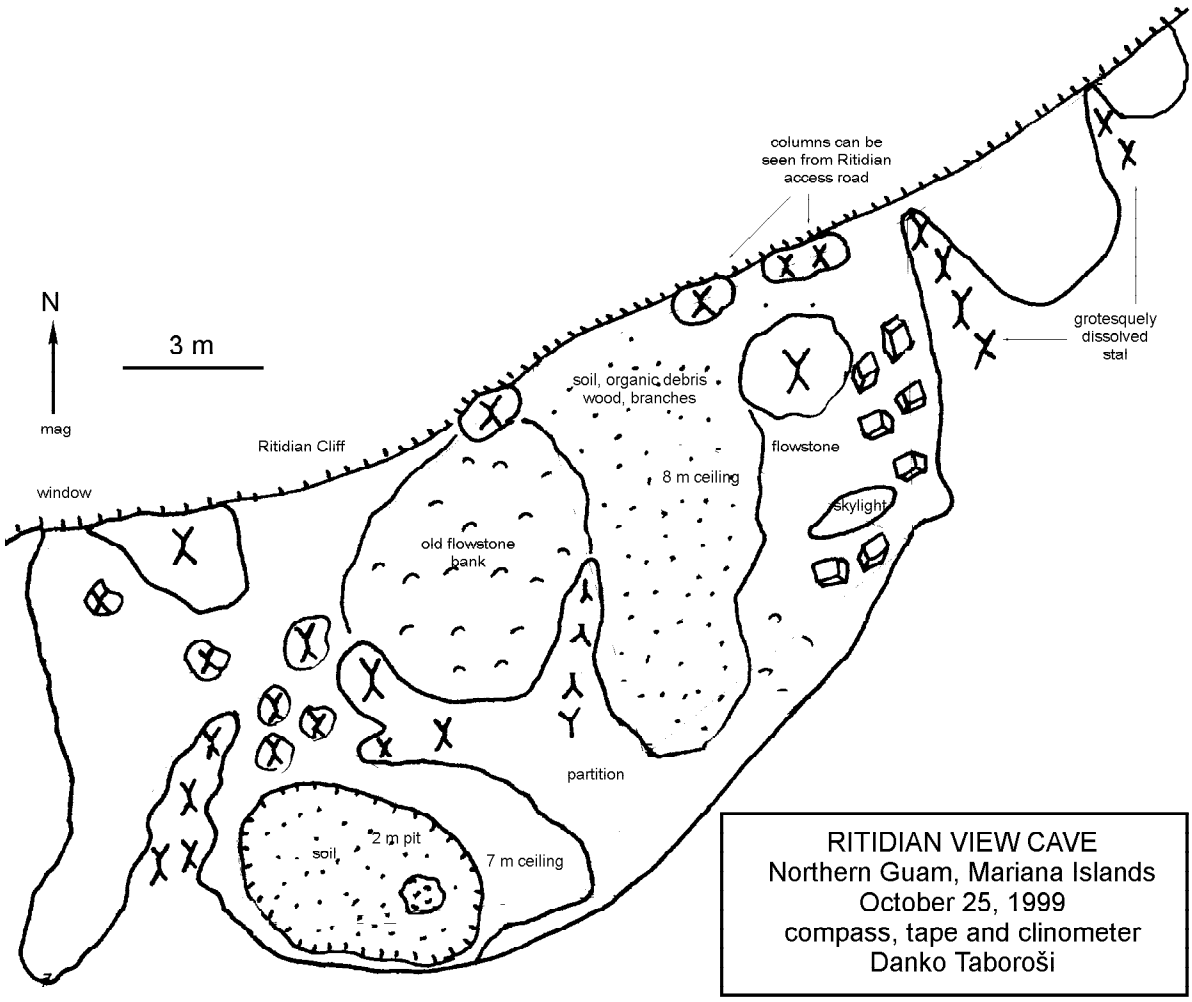

Fig. 9. 4: Map of Ritidian View Cave.

Ritidian Beach Cliffline (Fig. 9. 5) is perhaps the most accessible place to observe extensive flank margin caves that appear to have been breached by cliff retreat. This low cliff is located between Ritidian access road and Ritidian beach and is subparallel to the beach (see location map inset in Fig. 9. 5). After a surface survey of more than 400 meters of this cliffline, five caves and extensive cave features on the outside cliff walls were identified. Going from northeast to southwest along the cliffline, the first cave encountered is the Ritidian Beach Cave (Fig. 9. 5). It is a flank margin cave, single chambered and elongate in shape, apparently developed along a fracture visible in the ceiling. Most of the cave is undecorated with few stalactites and vadose fluting in the walls. The southwest part of the room, however, is separated from the rest of the cave by several column partitions; this part is well decorated and contains numerous cusps in the ceiling, and dissolved speleothems. A smoothly dissolved stalagmite (Plate 20, photo 6) and a sharply dissected stalagmite cut by phreatic dissolution (Plate 20, photo 7) are striking features, indicating a relative sea level rise and submergence of vadose features into the phreatic zone. Evidence of phreatic dissolution on vadose features in flank margin caves implies the following sequence of events:

1) formation of large cavities by the dissolution in the mixing zone
2) relative drop of sea level and placement of caves in the vadose zone where speleothems could be deposited
3) relative rise of sea level and re-placement of caves in the phreatic zone where dissolution of speleothems took place
4) relative drop of sea level and another vadose episode

The actual number of sea level changes and vadose

and phreatic episodes at any given site is impossible to evaluate, since evidence from previous episodes is obliterated by the most recent one.

The second cave in the cliffline at Ritidian Beach is a void opening just below the top of the cliff and penetrating about 7 meters into the cliff. It is decorated by tufaceous speleothems (for discussion of tufaceous speleothems see section 4. 4. 3). The third cave is the Ritidian Pictograph Cave (Fig. 9. 5., Plate 20, photo 8). Most of this cave's ceiling has collapsed so that only parts immediately adjacent to the cliff are roofed. These contain extensive speleothems and massive column partitions, forming several small chambers. Ancient Chamoru pictographs and pottery are found in this cave. Some 15 m further along the cliffline is another small cave, opening about 5 meters above the ground level and penetrating about 3 meters into the cliff. At the southwest end of the surveyed area is the Ritidian Double Arch, a remnant of yet another collapsed flank margin cave. Cave features, such as tufaceous speleothems, many of which are massive columns and extensive flowstone deposits, are found all over the cliff walls, indicating that they were once walls of caves or a large single cave, destroyed by cliff retreat. The five caves that exist today may merely be the only remnants and small chambers of the once large cave.

A similar interpretation can be applied to massively decorated notches found on the cliffs at Amantes (Two Lovers) Point at four distinct horizons (Plate 21, photo 1). The origin of these cave-like features on the outside of the cliff is debatable (flank margin caves vs. bioerosional notches). Several additional true caves are found in the Amantes cliffs and are probably flank margin. Several cave entrances are clearly visible in the cliff and have not yet been explored. Flank margin caves at different elevations appear to be breached and connected by vertical dissolution features (pit caves) (Plate 21, photo 2).

9. 2. 4. Beads-on-a-string morphology notches in coastal cliffs

Observations of Guam's coastline and cliffline have revealed the presence of narrow linear notches originally interpreted as paleo-bioerosional grooves (Jenson et al., 1997). While many coastal notches are clearly bioerosional (Plate 21, photo 3), the presence of stalactites in some notches was reason for re-interpretation of grooves as remnants of breached margin caves, because it was thought that speleothems could develop only in a closed cave atmosphere. However, a closer look at some of the speleothems found in the coastal cliffs revealed that they are commonly soft and crumbly, made by algal tufa deposits. Apparently, humid tropical climate may allow growth of speleothem-like tufaceous deposits in the outside atmosphere.

Currently, a number of inventoried features found along the coastline of northern Guam, suggestive of both flank margin cave remnants and bioerosional notches, await interpretation. Numerous notches in Guam's cliffs are unquestionably bioerosional, showing typical morphology and no speleothems, and, at sea level, active grazing by limpets (*Patelloida chamorrorum*) and chitons (*Acanthopleura gemmata*) (L. Kirkendale, pers. comm.), as well as boring by *Lithothrya* sp. barnacle (G. Paulay, pers. comm.) and possibly grazing by grapsid crabs as evidenced by fecal pellets nearly 100% $CaCO_3$ (B. Smith, pers. comm.). However, the notches in question are different from obvious bioerosional notches. They exhibit the "beads-on-a-string" morphology (Vogel et al., 1990) and often extensive speleothem development. In one case (just west of Mergagan Point, Plate 21, photo 4), notch development appears coupled with several cliff-side flank margin caves. Most notches in the Bahamas, previously thought to be paleo-bio-erosional grooves, have been reinterpreted by Mylroie (1991) as remnants of flank margin caves. Such a statement cannot be made for Guam as of yet, but the problem is being studied (Mylroie and Carew, 2000). Beads-on-a-string morphology may be a diagnostic feature for differentiating flank margin cave development from paleo-bioerosional notches (Mylroie et al., 1999).

The most impressive and extensive notches exhibiting beads-on-a-string morphology and speleothems are found in Tarague area (west of Mergagan Point), several discontinuous segments between Latte and Lafac points and some in coastal limestone remnants in Uruno Beach area. Additional impressive notches, deeply incised and narrow, but without many speleothems and probably bioerosional in nature, are found at Anao and Fadian points.

9. 2. 5. Breached flank margin caves in coastal terraces and slopes

Unlike flank margin caves in cliffs that become breached by cliff retreat, caves that form in coastal terraces and sloping parts of the coastline develop entrances by ceiling collapse. Because of their location near the modern sea level, they often intersect the freshwater lens.

Representative of this type, though not typical of the diverse flank margin caves on Guam, is

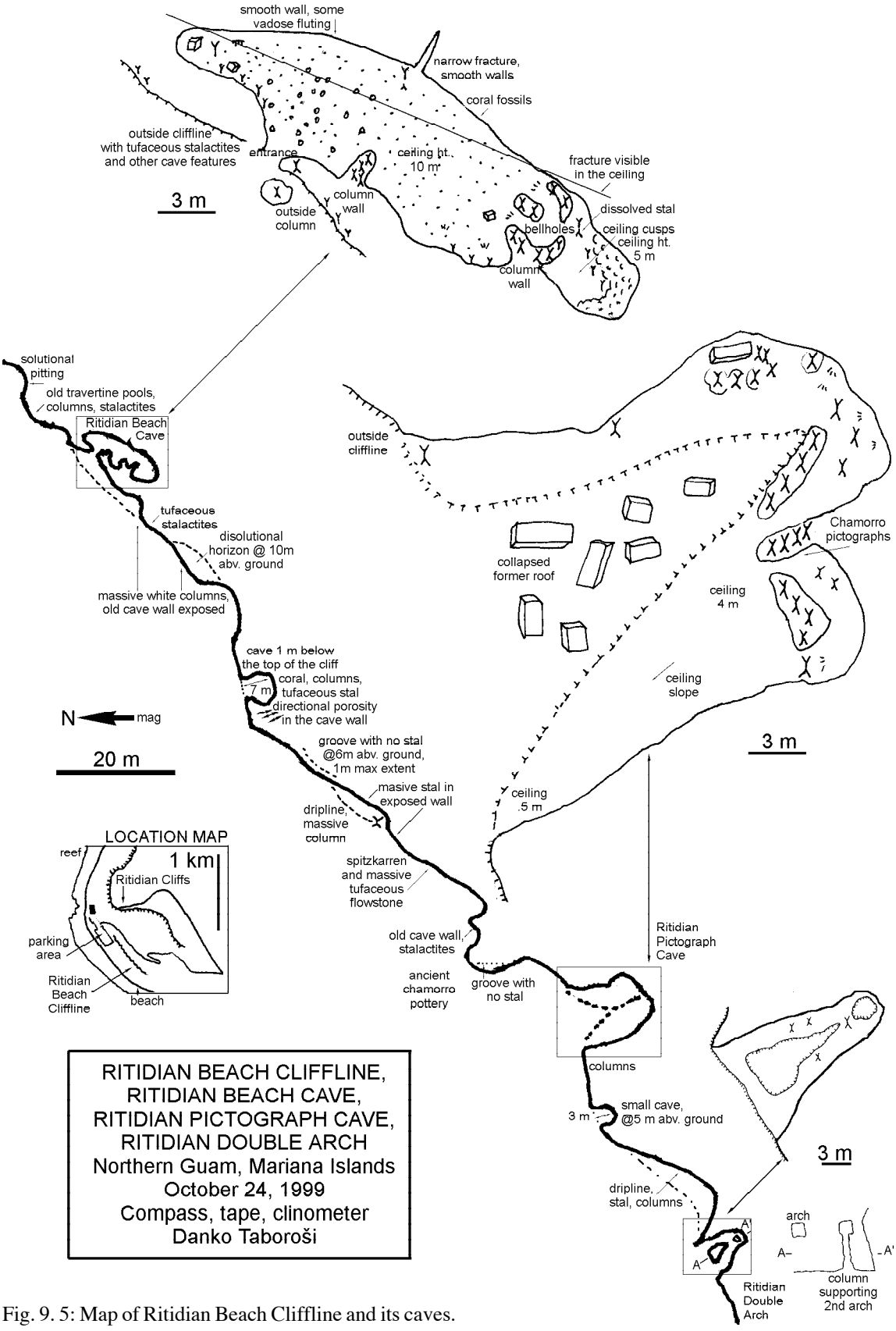

Fig. 9. 5: Map of Ritidian Beach Cliffline and its caves.

Pagat Cave (Plate 21, photo 5), located on a sloping coastal bench on the east coast of Guam, about half way between Pagat and Campanaya points, 300 m inland from the coast. It is entered through a central collapse sinkhole, leading to two caves: Pagat Cave on the north side and Haya Pagat Cave on the south. The two caves were connected prior to collapse of the central sink. Pagat Cave entrance is about 4 meters wide and leads to a sloping passage containing extensive flowstone deposits and a large column. The passage widens to a narrow chamber containing a 0.5 m-deep freshwater pool, flowstone bank and several large stalagmites, and leads further north to the cave's only room. The room is about 15 m by 15 m, and its eastern half is entirely covered by a freshwater pool gradually deepening toward the north end and reaching a maximum depth of 3.5 m at the north wall. Narrow submerged passages lead from the north and east part of the water-filled room. They are not wide enough to accommodate a person. The pool's floor is mostly made of collapse rubble, partially cemented in places. Extensive submerged flowstone and partially submerged stalagmites are found in the southeast and north end of the pool. The eastern half of the room is covered by soil, sloping up toward the west, presumably derived from ceiling collapse. The cave ceiling shows excellent phreatic cusp development, indicating phreatic dissolution. Stalagmites have smooth surfaces and also show evidence of dissolution under phreatic conditions, which is expected given dynamic sea level changes experienced by Guam. Shrimp (*Macrobrachium lar* and *Atyoida* sp.) were found in the cave's pool.

Haya Pagat Cave entrance is 10 meters south of Pagat Cave entrance, on the south end of the central collapse sink. It contains a single chamber, approximately the size of Pagat Cave's only room, covered by soil and collapse rubble. The south wall of the room is an extensive flowstone partition which can be negotiated in several high places to reach the back of the room. The deepest portion of the room, behind the flowstone partition, reaches freshwater at the same level as Pagat Cave's pool. Water in Haya Pagat Cave, however, does not form a pool and is barely visible among rubble blocks.

Pagat and Haya Pagat Caves fit the flank margin model for cave development (Mylroie and Carew, 1990) but differs from most of Guam's other flank margin caves or coastal freshwater caves in the significant respect that it is one of only three water table caves (Castro's, Joan's and Pagat) where no additional submerged passages could be identified by snorkeling. A map of Pagat and Haya Pagat caves was prepared by Mylroie et al. (submitted).

Probably the largest flank margin cave on Guam is Ritidian Cave (Fig. 9. 6, Plate 22, photo 1), located on the coastal terrace about 950 m east-southeast of Ritidian Point, at the base of a cliff 360 meters away from the coast in Guam National Wildlife Refuge. It is entered through a very small opening (1 m diameter) made by ceiling collapse. The antechamber of the cave, separated from the main room by a massive flowstone partition, is steeply sloping, with a decorated ceiling subparallel to the floor. The floor is made of flowstone, partially covered by collapse rubble and soil. The massive flowstone partition can be negotiated in one place to enter the cave's large room. This room is circular in plan (~36 m across), with a high (10 m), flat ceiling. The ceiling is relatively undecorated suggesting frequent breakdown. It is also heavily fractured, and massive stalactites have developed along some of the fractures (Plate 22, photo 2). The floor, however, shows few collapse features. The central part of the room contains a large collapse block. Most other collapse blocks have been cemented by flowstone, visible in the peripheral parts of the room. The distal end of the room contains a freshwater pool (Plate 22, photo 3), with collapse rubble floor and extensive submerged vadose deposition features. Submerged passages can be seen by snorkeling in the pool but cannot be explored without SCUBA. The most impressive features about this cave are its spacious main room and numerous massive stalagmites (Plate 22, photo 4). Most speleothems, however, are covered by black material (Plate 22, photo 5). Speleothems are white underneath the thin black layer, suggesting that the deposition of this layer was a recent event. The cave's ceiling appears to be quite thin, with plant roots penetrating it in places, and it is possible that the black coating of the cave may be from organic material transported from the epikarst above, although this is only a speculation, as I had no time for detailed investigation of its origin.

Another cave in a similar setting is nearby Castro's Cave (Plate 22, photo 6), located on the coastal terrace, at the base of a cliff, about 1100 meters southeast of Ritidian Cave and 2.3 km northwest of Mergagan Point, 400 meters inland from Castro's Beach. It is entered through a very small opening (<1 m diameter) made by ceiling collapse. It contains one large, steeply sloping room, with the floor and ceiling subparallel. The room is heavily partitioned by extensive flowstone walls which give impression of several rooms and passages. The floor of the cave is made of flowstone and rubble; no bedrock can be seen. Rubble is dominant in the lowest portion of the cave where there is a freshwater pool (Plate 22, photo 7).

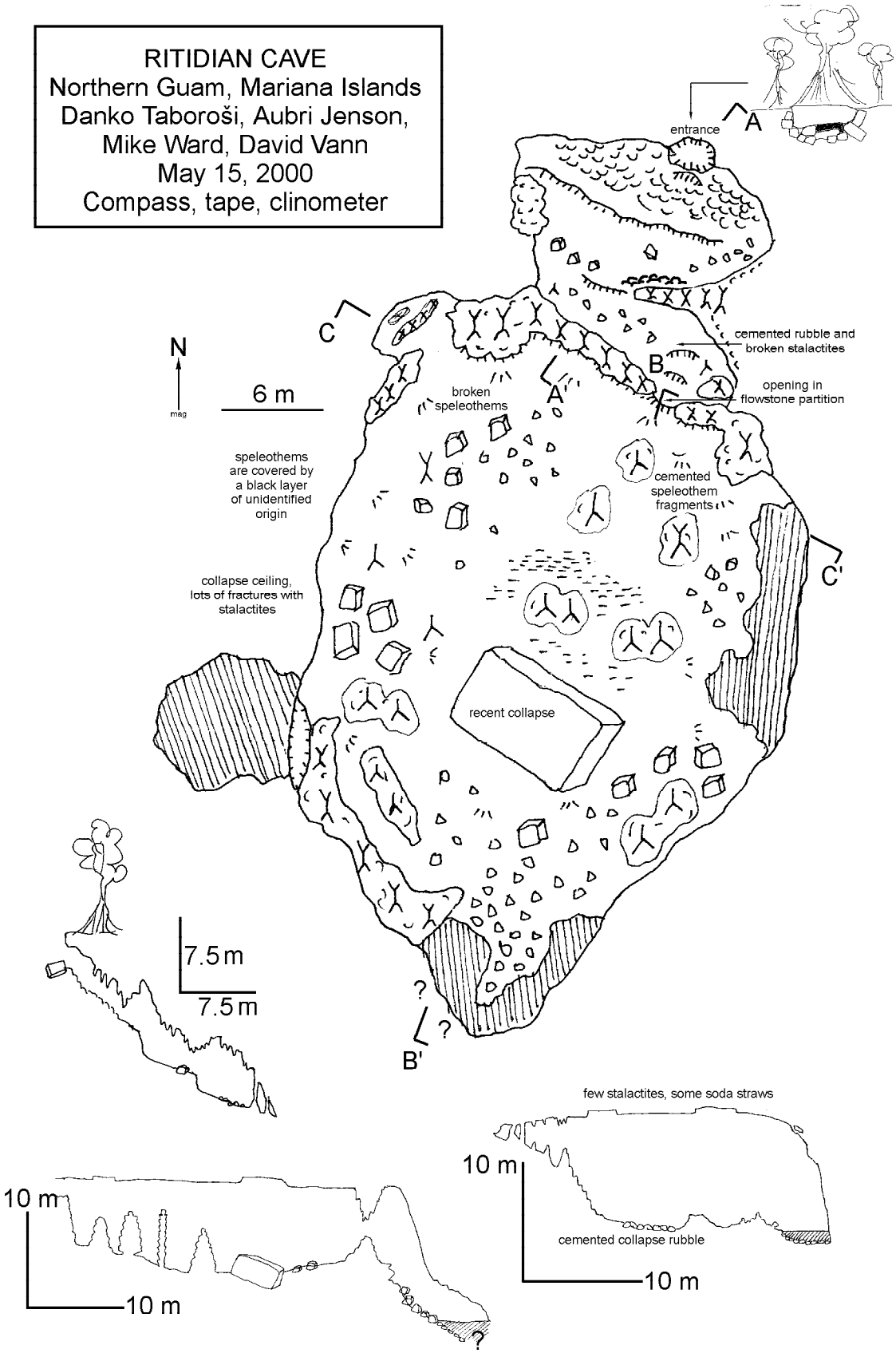

Fig. 9. 6: Map of Ritidian Cave.

Underwater observations of the pool revealed extensive rubble deposits and no submerged passages. This cave is extremely beautifully decorated, containing hundreds of massive stalactites, stalagmites and columns. Like in the nearby Ritidian Cave, speleothems here are stained by black deposits, but to a lesser extent. The steep slope of this cave's floor is unusual for coastal water-table caves in Guam and is probably a result of collapse events.

Joan's Cave (Hilaan Natural Well #1) is located at the foot of the cliff about 130 meters north from the Lost Pond, in Hilaan area on the Philippine Sea. The cave is entered through a small collapse in the ceiling, and leads down about 12 meters to the freshwater level. The floor of the cave is mostly comprised of collapse rubble with some flowstone deposits. This cave is in latter stages of collapse, with the heavily fractured ceiling still containing few in-situ stalactites. The cave is a series of irregularly shaped small rooms at several levels. Several passages are obstructed by collapsed boulders. There are four freshwater pools in the lowest room, two of which are about 2 m deep and the other two less than 0.5 meters deep. No traversable submerged passages were identified by snorkeling.

Another freshwater cave, Tarague Well #5, has a similar entrance and could be a flank margin cave breached by ceiling collapse. Located just 70 m inland from Tarague Beach, it is almost entirely flooded. A narrow, steeply inclined, soil-floored tube leads to the freshwater level, exposed as a small pool, less than 1 m in diameter. Sub-aqueous extent of the cave is unknown.

It should be noted that, with the exception of shrimp in Pagat Cave, no aquatic vertebrates or invertebrates were recorded in any of the previously discussed caves.

9. 2. 6. Collapsed flank margin caves with extensive submerged portions

Cave development in northern Guam is the most extensive along the coastline. Most of these caves are breached flank margin caves (Mylroie and Carew, 1995). Some of those caves are significantly different from flank margin caves as described by Mylroie and Carew (1990, 1995) from the Caribbean. Typical flank margin caves are dominated by large globular chambers, broad in horizontal plane but vertically restricted and receive and discharge water by diffuse flow (Mylroie et al., 1995). Many coastal caves from Guam are vertically extensive, floored by collapse rubble and have no bedrock floors exposed, and can be followed downward below the sea level into extensive submerged portions that include fracture-oriented linear passages. Finally, such caves often show indirect evidence of conduit flow, something not associated with typical flank margin caves.

According to J. Mylroie (pers. comm.), it is not unexpected for former flank margin caves to become part of the present conduit network and capture conduit flow, as they represent former spots of preferred diffuse flow as well as shortcuts to the coast. Fracture-oriented passages may be a secondary dissolutional result, after the cave had already begun to from by other mechanisms (J. Mylroie, pers. comm.) and large vertical extent of some caves can be a result of dynamic sea level changes that Guam has experienced. Therefore, such unusual coastal caves are probably flank margin caves modified as a result of unique geologic and hydrologic conditions on Guam. However, it is also possible that those caves are made by progradational collapse, similarly to the caves described in Bermuda (Mylroie et al., 1995). Bermuda's collapse caves are explained as a result of progradational collapse of large voids formed in the vadose zone at the contact of limestone and basement volcanic rock during sea level low-stands (Mylroie et al., 1995). According to topography of basement volcanic units in northern Guam (Fig. 8. 7) modeled by Vann (in prep.), the volcanic basement in eastern coastal areas, where some collapse-type caves on Guam occur has very likely spent time in the vadose zone during sea level low-stands, associated with submerged terraces documented by Emery (1962). Bermuda-type vadose voids could indeed have progradationally collapsed to the surface from the shallow basement-limestone contact to form caves on the east coast of Guam, Marbo Cave, Fadian Fish Hatchery Cave and Joe Quitigua's Water Cave in particular. Similar caves in other parts of Guam, where volcanic basement was never in the vadose zone, could be a result of progradational collapse of deep phreatic voids and include Fafai and Frankie's Cave on the west coast, submerged portions of Tarague Well #4, and probably the other Tarague cenotes on the north coast.

Marbo Cave (Fig. 9. 7-a), also known as Campanaya Cave or Campanaya Spring, is a popular picnic spot, located at the base of a cliff on the north end of Sasajyan embayment. This cave was used as a water source by the Japanese Military forces from about 1942 to 1944 and by the U.S. Army from 1947 to 1950 (Randal and Holloman, 1974). A large collapse entrance at the base of a cliff leads into cave's only subaerially exposed room. The room is some 20 meters across and contains a freshwater pool. The

entire floor of the cave is covered by collapse rubble. No bedrock floors are visible. A small part of the cave floor, adjacent to the entrance, is taken up by a concrete platform. A large collapse boulder to the left of the platform separates the cave into two portions. The part between the boulder and the platform (shallow pool) is up to 2 meters deep, while the part on the far side of the boulder (deep pool) is about 6 meters deep. Few calcite depositional features, no phreatic dissolution features and extensive algal (purple) coating are visible in the subaerially exposed walls of the cave. Prior studies have described this cave as a single chamber containing a freshwater pool and no evident outlet (Lange and Barner, 1995). However, SCUBA investigation of this cave revealed additional rooms and passages. An 8 m long tubular passage, elliptical in cross-section, starts at the bottom of the deep pool in the west portion of the cave and extends upwards at a ~45° angle. The passage terminates above the water level and contains a small air pocket, penetrated by plant roots. The walls and ceiling of the air pocket are made of soil, not limestone. Also at the bottom of the deep pool, another narrow passage leads to a small room containing hundreds of small stalactites, now completely flooded at a depth of about 4 meters. Salinity in the deep pool was measured to be 1.9 ppt at the surface and 2.6 ppt at a depth of 6 m. The temperature was uniform, at 26.2°C (08/11/1999).

The most extensive passages start from the shallow pool end, at the southeast end of the main room. A nearly vertical flooded passage leads into a large room, some 20 meters across. Its floor is at a depth of about 7 m and is covered by collapse blocks; room walls are made of bedrock. Additional narrow passages extend deeper. A few calcite deposition features (mostly broken flowstone fragments and several isolated in-situ stalactite deposits) are visible, especially just below the cave water level (Plate 23, photo 1). Deeper passages are all made by collapse rubble and boulders and contain some silt and clay deposits. The collapse boulders show extremely jagged mixing zone dissolution features (Plate 23, photo 2). Some of these passages appear large enough for a diver to pass but were not further investigated due to high risks of collapse and disorientation.

Rogers and Legge (1992) write that a stream with a discharge of approximately 113,600 liters per day traverses the freshwater pool from west to east, but it is unclear how this was measured or observed. No movement of water is detectable by casual observation. However, indirect evidence for conduit flow in this cave is based on the cave's fauna and geophysical investigations.

Adult *Eleotris fusca* fish and *Macrobrachium lar* shrimp were recorded in the cave on several occasions. These organisms are amphidromous, meaning that their reproductive cycle involves a marine larval stage. Larvae complete their development in the ocean and migrate back into freshwater (cave) habitat to mature and reproduce (B. Tibbatts, pers. comm). Therefore, for amphidromous species to inhabit a cave, there have to be direct connections between the cave and the ocean large enough for larvae to swim through. Larvae of *Eleotris fusca* are about 18-22 mm long during recruitment; shrimp larvae are about 4-5 mm long (B. Tibbatts, pers. comm).

A study by Lange and Barner (1995) found a significant natural potential anomaly (Fig. 9. 7-b) immediately seaward from the cave leading them to conclude that the anomaly overlies "the conduit carrying water from the cave system toward the sea," based on their assertion that the natural potential method is the only geophysical technique that responds to the movement of fluids, rather than their mere presence (Lange and Barner, 1995).

About 7.1 kilometers southwest of Marbo Cave is the very similar Fadian Fish Hatchery Cave (Fig. 9. 8, Plate 23, photo 3). It was also opened by collapse at the base of a cliff and appears as a single chambered cave containing a large freshwater pool. With SCUBA, however, one additional submerged passage becomes accessible. It is a linear passage developed along a NW-SE trending fracture, visible in the ceiling, in the southwest part of the cave. This passage is vertically extensive at least to a depth of 8 meters below water level and is oriented toward the coast, 150 meters away. The lower parts of this passage are characterized by extremely jagged mixing zone dissolution features. No SCUBA investigation beyond this passage took place due to high risk of collapse and extreme clouding of water by easily disturbed silt deposits. The origin of silt (limestone-derived or non-limestone) was not determined. Only *Macrobrachium lar* shrimp was found inhabiting this cave.

Rogers and Legge (1992) mention two additional caves in Fadian area, named Fadian Point Cave and Fadian Stream Cave, and describe them as having freshwater streams that flow across the chambers' floors and disappear into "low bedding plane tube[s]." Neither of these two caves could be located during this project. Descriptions by Rogers and Legge (1992) are unusual, as my study has not identified any inland caves with streams flowing over limestone floor anywhere in northern Guam. These caves were also not mentioned in the very thorough

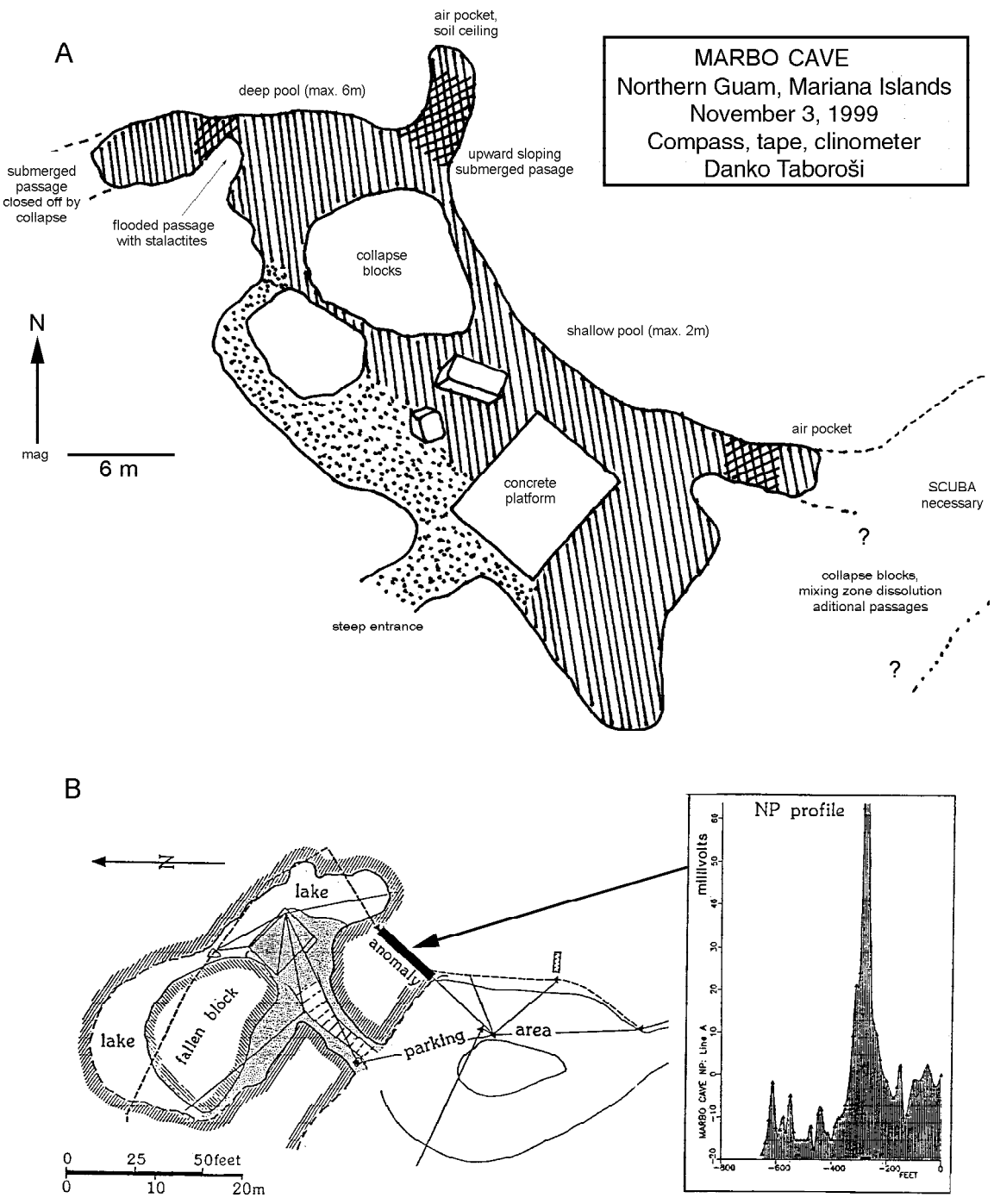

Fig. 9. 7: (a) Map of Marbo Cave; (b) results of natural potential survey of Marbo Cave area by Lange and Barner (1995).

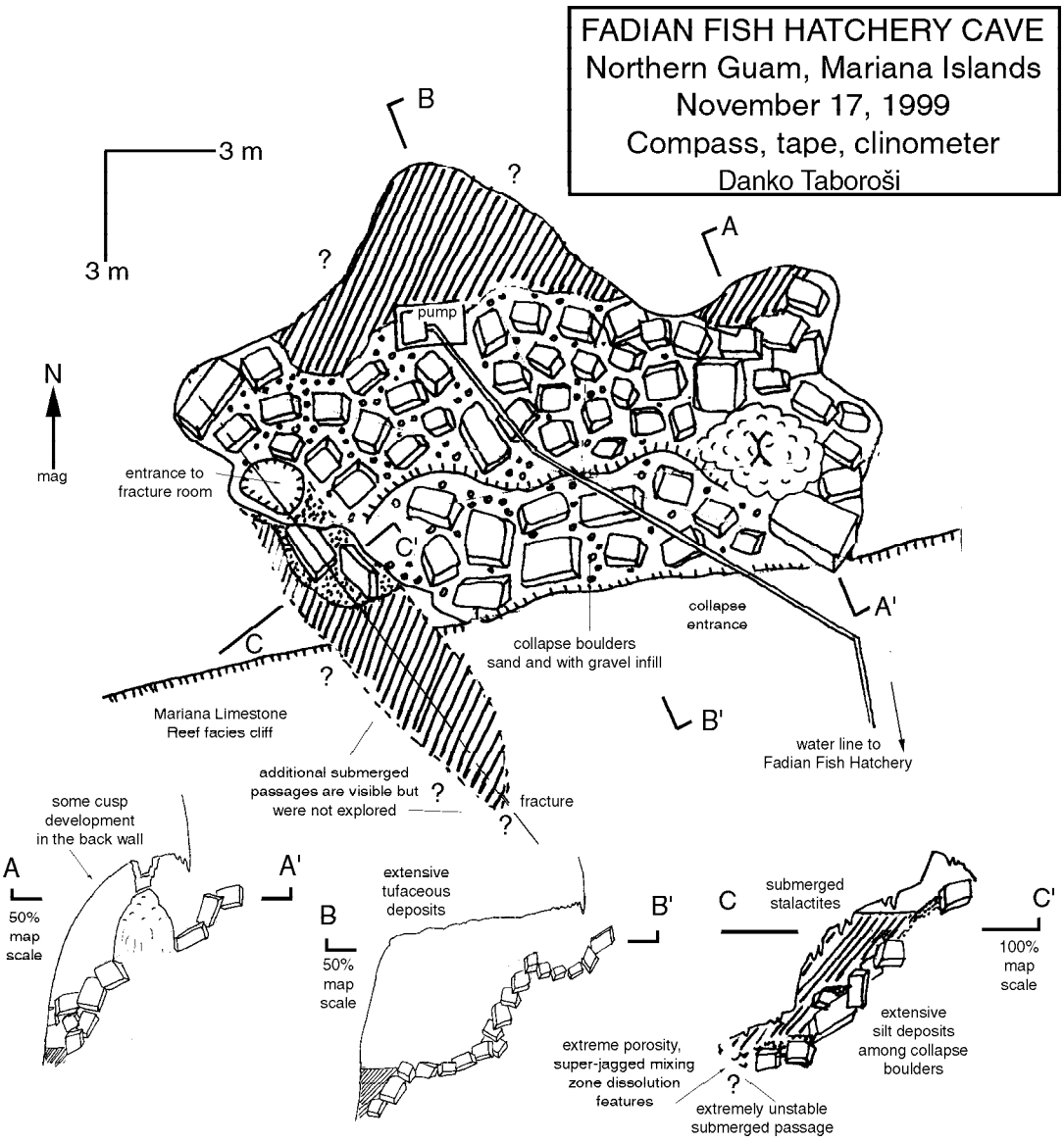

Fig. 9. 8: Map of Fadian Fish Hatchery Cave.

"Reconnaissance survey for new fresh water sources on the northern section of Guam" (Robert and Company, 1948).

Joe Quitigua's Water Cave (Plate 23, photo 4) is another example of a collapsed cave, acting as a shallow phreatic conduit. It has no above-water component and from the outside appears as a small shallow perched water pond, breached by excavation in the Hawaiian Rock quarry in Mangilao. At the northwest edge of the pond, a small hole about 0.5 m in diameter leads to an entirely water-filled room, without any air pockets. The room appears to be oriented along a fracture, easily visible in the ceiling. A single stalactite and some flowstone deposits can be seen but most of the walls, floor, and ceiling of this chamber are a result of collapse. SCUBA exploration of this cave was attempted but aborted because exhaled air bubbles disturbed the ceiling and caused a "rain" of limestone chips in the water column. A fracture of NW-SE orientation is visible in the cave's ceiling. Its northwest end points inland, towards the cliffs and an unusual large tube-like cave (Hawaiian Rock Quarry Cave, Plate 23, photo 5) and the southeast end towards the ocean and a small bay with documented freshwater discharge (Hawaiian Rock Quarry Beach Springs). The Hawaiian Rock Quarry Tube Cave has developed in

poorly cemented coarse rubble facies and shows no depositional or dissolutional features. The orientation of the cave is perpendicular to the modern coastline. The cave's location and orientation suggest that it may have developed as a preferential flow path to the coastline and may be an abandoned part of the system now containing Joe Quitigua's Water Cave and Hawaiian Rock Quarry Beach Springs, but this is only speculative. This pond and cave is inhabited by *Macrobrachium lar* shrimp and an endemic *Orcovita mollitia* crab (G. Paulay, pers. comm.)

Frankie's Cave (Fig. 9. 9), located in the Double Reef area on the west coast of the island, is accessible through a collapsed ceiling. It is a single-chambered cave with a fresh water pool, located 18 meters from the shoreline south of Double Reef Beach. Most of the cave's floor is covered by collapse rubble except for a single narrow subaerial passage leading from the main room, which seems to be floored by bedrock. The passage opens to a cliff overlooking the beach, about 5.6 m meters above the mean sea level. This passage may be a paleoconduit inactivated by relative sea level drop. In the submerged portions of the cave, existence of additional passages has been documented by snorkeling, but has not been further investigated using SCUBA due to difficulties of bringing equipment to this remote location. The coastline seaward of the cave forms a small cove with freshwater discharge estimated to be about 7.5 million liters per day (Jocson et al., 1999).

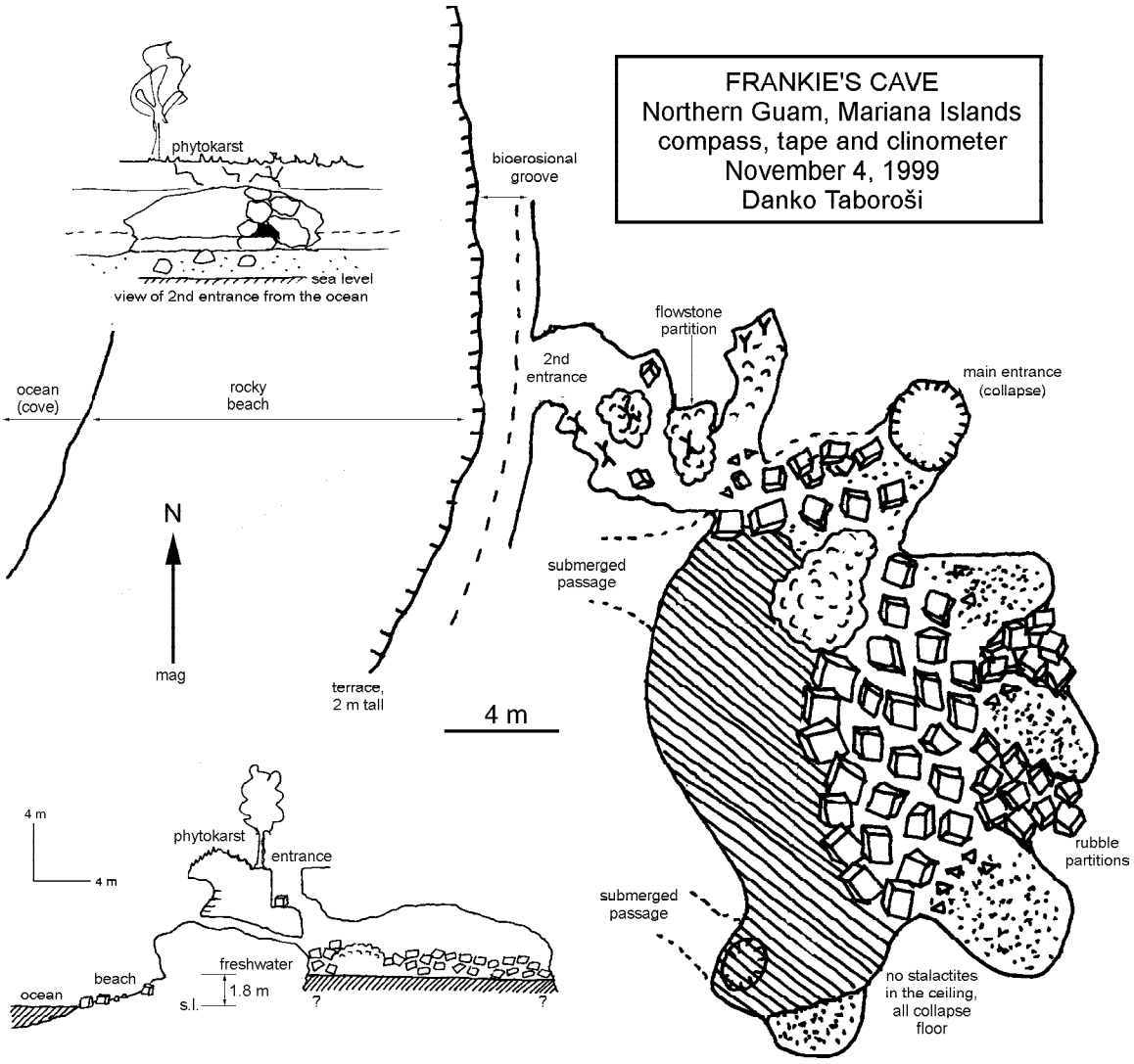

Fig. 9. 9: Map of Frankie's Cave.

Southward on the west coast, just north of Bijia Point is Fafai Cave (Fig. 9. 10, Plate 23, photo 6). It is entered through an opening in the cliff about 6 meters above sea level, about 85 meters inland from the coast. It is a single-chambered cave with a pool of fresh water. The entire cave is floored by collapse blocks or sediment and flowstone deposited on top of the collapse blocks. Peripheral parts of the cave contain a freshwater pool. The extent of the cave under water is unknown but may be extensive as observed by snorkeling. Snorkeling among the large collapse blocks in the center of the room has revealed that they are extremely corroded by mixing zone dissolution, at the cave water level (Plate 23, photo 7). As in the case of Frankie's Cave, it is possible that this cave is a part of a conduit that got elevated so that its flow was diverted to lower channels, as suggested by Lange and Barner (1995). A crab (*Discoplax longipes*) is common in this cave.

On the north coast of the island, in Tarague Embayment, a number of collapsed sinkholes intersect the freshwater lens. These cenotes are described in detail in section 7. 2. 4. At least one of the cenotes (Tarague Well #4) leads to extensive submerged cave passages. SCUBA investigation of this cave has revealed that the main chamber that collapsed to form the cenote extends to a depth of 15 meters below water level. In the northeast part of the submerged portion is a narrow fracture-like passage that leads to the second room, some 15 meters in diameter and about 10 meters tall, reaching a depth of 21 m. No depositional features are visible anywhere in the submerged portions of this cave. Walls, ceiling and the floors are all indicative of extensive collapse. Collapse blocks in the lower portions of the cave have been attacked by aggressive dissolution and show characteristic extremely jagged mixing zone features. Additional smaller passages probably lead from this

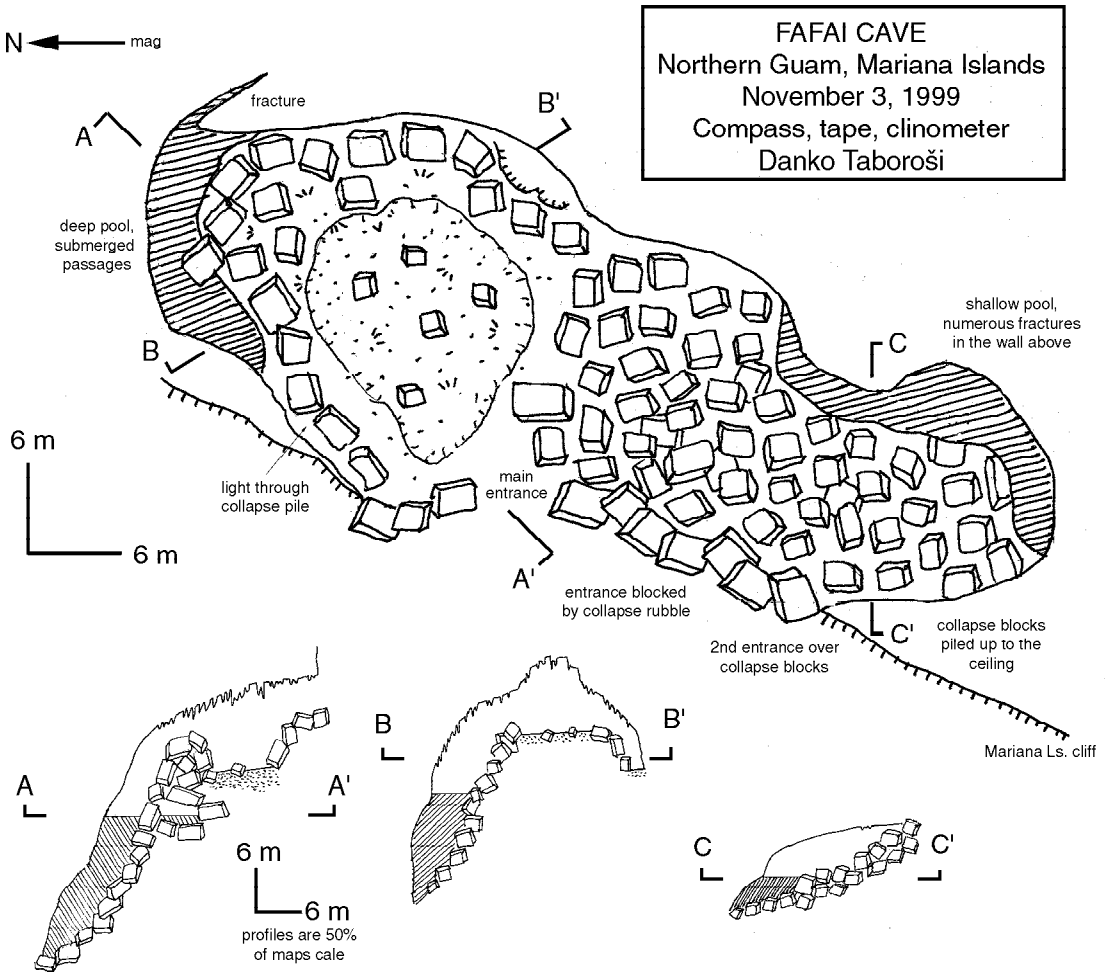

Fig. 9. 10: Map of Fafai Cave.

large, insufficiently explored room. This investigation has confirmed earlier reports by U.S. Navy divers (Hogan, 1959). The cenote is inhabited by shrimp (*Macrobrachium lar*) and crab (*Discoplax longipes*) (Lange and Barner, 1995).

Lange and Barner (1995) conducted a natural potential survey along transects between the Tarague cenotes and the coastline. Significant natural potential anomalies led the authors to conclude that Tarague area is the site of "groundwater movement toward the sea... concentrated within solutionally enhanced permeable zones or karst conduits." The cenotes themselves are not actual conduits but may be offset "standpipes" of the conduit system. Water movement at the surface of the pools in the cenotes is indicative of diffuse transport with rates ranging from 6 m/day (Tarague Well #3) to 11 m/day (Tarague Well #6) (Barner, 1995).

It should be noted that all previously described caves are located inland from coves, embayments and/or coastal discharge points. Marbo Cave is located at the extreme northeast end of a Sasayvan, a large coastal embayment. Fadian Cave is located in the vicinity of Fadian Cove, a prominent small bay devoid of any fringing reef growth and the site of a small coastal spring. Joe Quitigua's Water Cave is inland from Hawaiian Rock Quarry beach, also a small cove with documented freshwater discharge. Frankie's Cave is a few meters inland from a cove with exhibiting significant freshwater discharge (Jocson et al., 1999). Fafai Cave is located inland from well-documented freshwater seeps (Jocson et al., 1999). Tarague cenotes are found within an embayment where a conspicuous channel has developed in the fringing reef. Emery (1962) has observed that the present reefs are locally transected by channels related to freshwater streams in the volcanic areas in southern Guam. It is possible that analogous channels develop in the fringing reefs in northern Guam as a result of concentrated freshwater discharge from karst conduits.

Exploratory SCUBA-diving investigations of the caves described in this section reveal that some of Guam's freshwater caves lead to additional submerged passages and rooms that are much more extensive than previously recognized. What have been previously described as 1 m or 0.5 m deep freshwater pools (Fafai Cave) and small and shallow pool (Marbo Cave) by Rogers and Legge (1992) and "small body of freshwater" (Fadian Fish Hatchery Cave) by Robert and Company (1948), all lead to submerged passages at least 7 meters deep. These cavernous, fresh-water reservoirs are resources more extensive than has been thought. Considering some of these caves are easily accessible to picnickers and some are used for routine garbage disposal, this new information should increase the concerns about protecting them from pollution.

9. 2. 7. Unbreached flank margin caves

Voids are commonly intercepted by well drilling. Unbreached flank margin caves however, developing along the perimeter of the island, are not encountered because no well drilling usually takes place at the coastline. In an isolated incident, a large void (5.5 meters vertical extent) was encountered during the drilling of saltwater supply well for the University of Guam Marine Laboratory. The void starts at 6.25 m and ends at 11.6 m measured from the land surface (UOG-1 well log). This large void is located in the present mixing zone environment and could be a flank margin cave.

9. 2. 8. Other coastal caves

A group of interesting caves are located on the east coast of Guam, in the vicinity of Lujuna Point. They have developed preferentially along the bedding planes and their entrances are elongated and parallel to the dip of the inclined beds (Plate 24, photos 1 and photo 2). The cave development seems to be controlled by sea level and the caves are either flank margin caves or sea caves (see section 10. 3. 2. for discussion of sea caves). These caves were seen and photographed from a boat and were not directly investigated.

Several small caves have developed on the contact between Janum Formation and overlaying Mariana Limestone, just south of the Janum exposure near Catalina Point (Plate 24, photo 3). Located a few meters above the sea level, their origin is unclear. They could be small flank margin caves, sea caves, or caves associated with former coastal discharge. A brief survey of the caves' immediate vicinity produced no evidence of present freshwater discharge.

Also in Janum area, North and South Catalina Beach Caves (Plate 24, photo 4) are two groups of three and four small caves respectively, located at the beach level, between Lujuna and Catalina points. They were identified from aerial photographs and were not directly investigated. They could be sea caves or small flank margin caves.

9. 2. 9. Arches

Natural arches are made by weathering and partial collapse of caves. Arches are karst features

through which light penetrates, but unlike natural bridges, they are not associated with stream flow. Arches are common along the coastline of northern Guam and are made by collapse of flank margin caves, discharging caves and sea caves. Arches that were made by collapse of sea caves are difficult to distinguish from arches made by collapse of karst caves but are all discussed here, irrespective of their origin. An inventory of arches from northern and southern Guam is included in Appendix 10.

A good example of a collapsed flank margin cave forming a double arch is the Ritidian Beach Double Arch (Fig. 9. 5) formed in the cliffline parallel to the beach at Ritidian. The larger of the two is about 3 meters wide and spans 10 meters. The smaller arch is about 2 meters wide, spans 6 meters and is supported by a massive column. Just below Lafac Point, another impressive double arch was formed by collapse of what appears to have been a large phreatic void (Lafac Grotto).

Double Reef Arch is a natural arch, probably formed by collapse of a discharging cave similar to nearby (not collapsed) Coconut Crab Cave. A coastal spring estimated to be discharging up to 7.5 million liters per day (Jocson et al., 1999) is located underneath the natural arch.

An example of a natural arch formed by collapse of a sea cave can be seen just south of Haputo Beach. It is a low arch and is best seen from the land. Several other natural arches, whose origin (flank margin cave vs. sea cave) is not clear, are located on the east coast, between Pagat and Anao. A typical representative of these is Pagat Arch (Plate 24, photo 5) at the coastline near Pagat Cave.

9. 2. 10. Large collapsed chambers

Collapse of flank margin caves and other phreatic voids is a common occurrence. Because such voids develop with no opening to the surface, those that collapse are the only ones we can directly explore. Collapsed flank margin caves have already been discussed in section 9. 2. 5. There appear to be several special cases—large spherical phreatic voids that have developed in coastal, flank margin environments, but are morphologically distinct among flank margin caves. These puzzling voids have been opened to the surface by roof collapse.

Located about 300 meters away from the coast in Tamuning, Devil's Punchbowl is one of the most impressive karst features on the island (Plate 25, photo 1). This fishbowl-shaped cavern occupies a hill overlooking the Hilton Hotel. The opening made by roof collapse is cylindrical, approximately 20 meters in diameter (Plate 25, photo 2). The roof of the cave shows typical tension dome collapse. The drop from the edge of the collapsed roof to the top of the breakdown pile in the pit is about 21 meters, with an additional 10 meters to the base of the pile. The cavern is 60 meters in diameter and contains a shallow freshwater pool. The pool was reported to be 2 meters deep and 27 meters in diameter by Robert and Company (1948) but was less than half that size on May 7, 2000, when I explored it. There are no fissures or passages leading from this spherical cavern. In August 1948, Robert and Company (1948) have calculated the elevation of the pool to vary between 0.61 and 0.95 meters above the Mean Lower Low Water Datum. They have also determined that the tidal fluctuations lag time of the pool in the cavern is about 4 hours at high tide and 2 to 4 hours at low tide. This lag indicates a considerable resistance to tidal movement and a lack of conduits connecting this cavern to the ocean. The pool in the Devil's Punchbowl will be one of the Harmon Sink dye-tracing project monitoring locations (David Moran, pers. comm.) The Devil's Punchbowl is also known as Ypao Natural Well, as it was named by Robert and Company (1948). Rogers and Legge (1992) reported that this feature may have been destroyed, but fortunately this was not the case.

Another impressive collapsed phreatic chamber is the Lafac Grotto (Plate 25, photo 3). This massive void was breached by roof collapse and, in two additional places, by wave erosion and cliff retreat. It contains two natural arches and possibly several short cave passages. It is quite similar to The Grotto on Saipan. Connections to the ocean in Saipan's Grotto are submarine, and in Lafac Grotto above the sea level.

9. 2. 11. Large collapses in coastal cliffs

Lacking protective reef and containing a large number of flank margin caves and sea caves, the east coast of northern Guam is riddled by wave-breached and collapsed voids. At least 10 massive collapse areas are readily identifiable in eastern cliffs, most being between Lafac and Anao points and between Lujuna and Pagat points. Some of them may be a simple result of cliff retreat unrelated to caves but many were probably initiated by cave collapse assisted by wave erosion. Mylroie et al. (1999) believe that some of the collapses on the east coast are clearly associated with cave roof failure.

The largest collapse area is the Lafac-Anao Collapse #3 (see Appendix 14 for location), which is 150 meters tall and 300 meters wide and extends to

the top of the coastal cliff. This collapse area has several cave entrances at its northern end. In Lujuna area, there are two major collapse areas (southern one being 60 meters tall by 230 meters wide (Plate 25, photo 4) and the northern one 95 meters tall by 120 meters wide (Plate 25, photo5)). Both have remnants of caves at the coast immediately adjacent to them. Dimensions of major collapse areas are given in Appendix 10. The collapse scars, some very recent some partially vegetated, in the cliffs are easily visible on aerial photos of the cliffs in Appendix 14.

9. 2. 12. Lens voids

The occurrence of cavities without entrances, such as phreatic caves postulated to develop at the water table on carbonate islands (Mylroie and Carew, 1995), is confirmed by evidence from well drilling and direct observation in quarry walls. Such cavities, described as non-integrated caves by Ford and Ewers (1978), are, in this paper, referred to as lens voids. According to Mylroie and Carew (1997), there are two geochemical environments in the freshwater lens where carbonate dissolution may be extensive: top of the lens (water table) where vadose and phreatic waters mix, and the bottom of the lens where fresh and marine groundwater mix. Voids can also develop at random places, anywhere within the freshwater lens (Mylroie et al., 1995). Therefore, voids intercepted by drilling on Guam are likely to be lens voids that have preferentially developed at the top and the bottom of the freshwater lens as well as random places within the lens. However, voids can also be primary in origin and not karst features at all.

Careful examination of well logs collected by David Vann and Mauryn Quenga as part of the Guam Hydrologic Survey program and several additional well logs (UOG-1, Tarague wells- Lange and Barner, 1995) has revealed nearly 300 voids, cavernous zones and clay pockets encountered during drilling of 119 wells in northern Guam. All of these have been inventoried and are included in Appendix 11.

Most wells in northern Guam are drilled using direct rotary drilling units with air and/ or mud circulation capability (CDM, 1982). Occasionally, during the drilling the drill fails to fit tightly against the borehole walls, allowing air to escape (Ogden Environmental and Energy Services Co., 1995). Such zones are marked as zones of "lost circulation" on well logs and are interpreted as cavernous areas, large cavities or zones with numerous small pores. In rare cases, the well logs record a drop of the drill of up to 2 meters (Well A-21) indicating large cavities. Smaller drops, of .3 to 1 m or so, are more common (Wells A-21, D-18, Y-5, Y-16, IRP-12). Downhole videos (such as those of IRP wells on Andersen Air Force Base) provide a direct view of some of the voids encountered during well drilling.

Lens voids can be directly observed in the walls of quarries. Perez Brothes quarry has several isolated lenticular voids (Plate 25, photo 7); they are scattered and do not form visible horizons. In Hawaiian Rock quarry, the voids are not as large but are more numerous and are arranged along a distinct horizon (Plate 25, photo 8). The latter observation indicates probable development of voids along the top of the freshwater lens; the former may be a result of isolated void development at random places within the lens. Unlike in Perez Brothers quarry, some of the voids in Hawaiian Rock quarry contain speleothems. Development of voids at the top of the freshwater lens has already been suggested by Mink (1976) who stated that during well drilling "it is not unusual to encounter cavernous limestone and the saturated zone simultaneously".

Because voids in limestone are not necessarily solution voids and could be primary in origin, the nature of voids intercepted by drilling is debatable. Future research should focus on identifying horizons of void development, if any, and correlating the elevations with other paleo-sea level indicators, such as coastal notches and terraces.

9. 2. 13. Collapsed lens voids (banana holes)

Voids that have developed at the top of the freshwater lens may collapse, particularly if located close to the land surface, and form small closed contour depressions known as banana holes. Banana holes are broad, vertical-walled depressions, described from the Bahamas, and reaching dimensions of 2 to 10 meters in diameter and 5 meters in depth (Harris et al., 1995). A feature in northern Guam most reminiscent of banana holes is located near the navy housing area in Finagayan. It is presently unknown whether this feature is truly a banana hole, made by collapse of a shallow phreatic void, or a sinkhole made by progradational collapse from a greater depth. The question could perhaps be answered by use of a ground penetrating radar as described by Harris et al. (1995). A description of this feature and a map (Fig. 7. 10) are given in section 7. 2. 4. with the discussion on collapse sinkholes.

9. 2. 14. Halocline caves

Voids developing along the halocline have been reported by divers in the Bahamas (Palmer and Williams, 1984). The halocline (at the bottom of the freshwater lens) is a zone of enhanced dissolution, caused by the mixing of fresh and marine ground waters. Dissolution can occur in the halocline mixing zone even if both waters are saturated with respect to calcium carbonate (Plummer, 1975). Although some of Guam's caves and especially lens voids intercepted by drilling could have formed along the halocline, no specific features could be associated with the halocline with any certainty.

9. 2. 15. Non-traversable phreatic conduits in northern Guam

Flow in the phreatic zone was also evaluated by the previously mentioned dye trace studies. In the 1992 Andersen Air Force Base study, transport rates (6-11 m/day) in the phreatic zone were consistent with diffuse transport (Barner, 1995). The 1994 Navy study found that water traveled through vadose and phreatic zones over a distance of at least 1.7 km within 4 hours but velocity in the phreatic zone only could not be determined (OHM, 1999). The same study concluded that groundwater flow in their study area "may not be characteristic of diffuse flow, but rather, it may follow specific flow paths to the discharge points on the coast" (OHM, 1999).

Data are not sufficient to allow generalizations regarding conduit flow in the phreatic zone. Jocson et al. (1999) state that if vadose flow can be controlled by conduits, as indicated by Air Force dye trace study, the possibility of similar conduits in the phreatic zone cannot be ruled out. They argue that if vadose conduits are relicts developed under phreatic conditions they should be present in the current phreatic zone. Conversely, if vadose conduits are products of vadose processes then the modern phreatic zone would contain relict vadose conduits formed during Pleistocene sea level lows (Jocson et al., 1999). Data from Emery (1962) and Tracey et al. (1964) indicate that all bedrock in the current phreatic zone was previously exposed to vadose conditions.

Ashton (1966) wrote that the top of the phreatic zone is hydrologically and morphologically different from both the vadose and the phreatic zones and termed it the epiphreatic zone. This zone may develop discrete passages to accommodate water coming in flood waves from the vadose zone causing an increase in head until increased flow rates restore equilibrium. Bonacci (1987) called this zone the high water stand zone or zone of horizontal circulation, distinct from the vadose and phreatic zones. It should be noted that shallow parts of the modern phreatic zone in northern Guam have spent the longest time in the vadose zone during previous sea level lows and would hence have the best developed remnants of vadose conduits. The existence of well-developed shallow phreatic conduits could explain rapid transport in the phreatic zone following rainfall pulses despite the relatively much slower diffuse flow documented in the phreatic zone.

9. 3. Phreatic Caves in Southern Guam

Unlike in the north, where phreatic caves are clearly a majority among inventoried caves, in the south they do not account for a large portion of known caves. They are, nevertheless, common along the entire eastern coastline of southern Guam and in Orote Peninsula.

Types of phreatic caves in southern Guam include flank margin caves, natural arches, collapsed phreatic conduits, and probably a banana hole. Additionally, there are probably conduits in the phreatic zone that are too small to be directly explored but are hypothesized based on the arrangement of inland collapse features and channels in the reef.

Inventory of caves (in which the phreatic caves are included) from southern Guam is given in Appendix 9. The map showing distribution and types of phreatic caves in southern Guam is shown in figure 9. 11.

9. 3. 1. Flank margin caves

There are numerous flank margin caves along the east coast of southern Guam. Most known caves are located in the cliffs on the north side of Talofofo Bay (Adjoulan Point Cave, Asquiroga Cave, four Matala Caves and three caves at Tres Botsas). Entrances to all of these single-chambered caves are located in cliff faces (elevations up the cliff are given in Appendix 9). On the south side of Talofofo Bay, a prominent massive stalagmite overhanging the Gayloup Cove is probably a leftover of a flank margin cave all but destroyed by cliff retreat.

The Matala and Asiga areas are also rich in caves. Several cave entrances can be seen in the coastal cliffs, and anecdotal information from local residents points to many more. The coastal plain as well contains a large number of caves, including some that intersect the groundwater level and contain permanent pools. The most accessible of the caves in

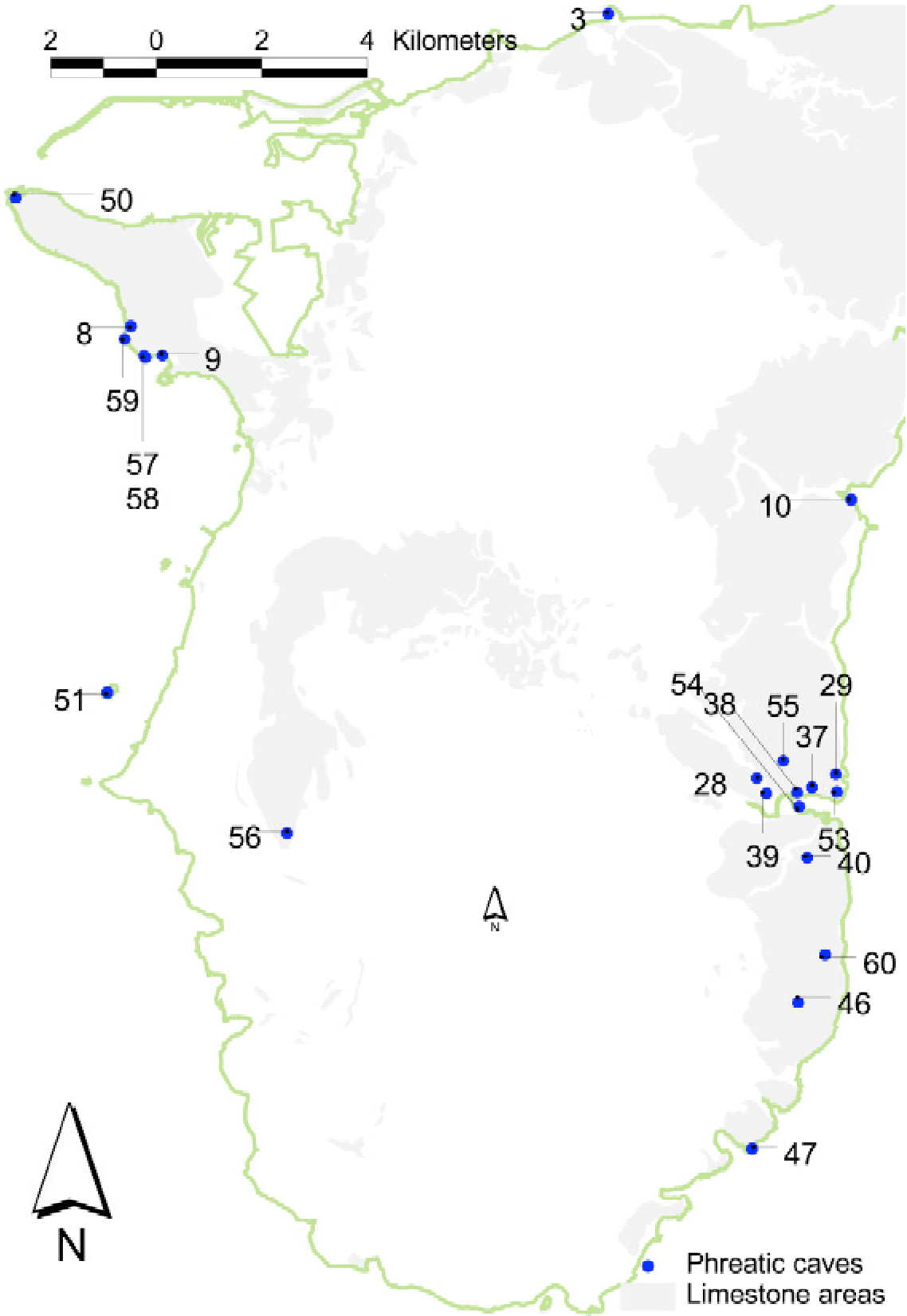

Fig. 9. 12: Locations of phreatic caves in southern Guam.

this area is Asiga Cave, located at the top of the coastal cliff in Malojloj.

Cliffs in Anaga area, behind the village of Ypan probably have several flank margin caves. Mata Cave and the nearby shelter caves behind Notre Dame School in the Mata area of Talofofo are probably also of flank margin origin.

Cliffs of Orote Peninsula also show several cave entrances, probably flank margin in origin. The largest phreatic voids in Orote Peninsula are the Orote Grottos (Plate 25, photo 6). Located at the south end of the south side of Orote Peninsula, these two adjacent, extremely large phreatic chambers were breached by wave erosion and probably expanded by partial collapse.

Among the small off-shore islands in southern Guam, the best example of a flank margin cave is a single-chambered cave on Anae Island, opened by roof collapse. The cave intersects the groundwater lens and has a small brackish water pool. The cave is most easily accessed from the northwest side of the island. Additional remnants of caves breached by cliff collapse can be seen in the vertical cliff at the southernmost point of the island.

9. 3. 2. Arches

There are several natural arches made by collapse of flank margin caves (or sea caves) in southern Guam. None are as spectacular as the examples from the east coast of northern Guam. A small arch has developed on the small reef island near Tipoco cemetery in Inarajan. Another small arch, Orote Window, made by partial collapse of a flank margin cave, is visible near the top of the cliff on the south side of Orote Peninsula.

9. 3. 3. Collapse flank margin caves with extensive submerged portions

Asanite Cave is located at the base of the cliff at Asanite Point. The cave has no limestone bedrock and is floored entirely by a steep pile of collapse blocks and some flowstone developed over the collapse. Located near the sea level, the cave intersects the groundwater and has extensive submerged passages. Snorkeling in the cave revealed a depth of submerged chambers of at least 8 meters. This cave is very similar to Marbo and Fadian Fish Hatchery caves from northern Guam. Like in the case of similar northern caves, Asanite Cave is located just inland from a conspicuous cove developed between Asanite and Ypan Points. Two undescribed species of atyid shrimp have been recorded in Asanite Cave. They are red or pink in color, up to 18 mm long and blind (B. Tibbatts, pers. comm.) There are additional collapsed caves and sinkholes located in the village of Ypan and in the forest west of it.

9. 3. 4. Banana holes

A single example of a potential banana hole is located in a Bonya Limestone outcrop in the Country Club of the Pacific golf course in Ypan. This sinkhole, named Ito and Minagawa Sink, is deeper than banana holes from the Caribbean (Harris et al., 1995). Description and a map of this feature is given is section 7. 4. 3. about the sinkholes from southern Guam.

9. 3. 5. Non-traversable phreatic conduits in southern Guam

Although five incised allogenic rivers transit the entire width of limestone and flow into the Pacific ocean, there are indications of karst conduits draining areas between the rivers. No significant freshwater discharge has been observed along the beaches but conspicuous channels exist in the reef and may be a result of submarine freshwater discharge impeding coral growth. Collapse sinkholes and caves intersecting the freshwater lens, documented in the area between Togcha Point and Ypan Point, may represent collapsed portions of these conduits. Observed groundwater discharge in the area is limited to seep fields along the Ypan beach and a spring in Ylig River mouth area (N. Hendricks, pers. comm.).

— Chapter 10 —
COASTAL DISCHARGE FEATURES

This chapter investigates coastal discharge features on Guam. Varying in type from beach seeps and springs to solution-widened fractures and discharging caves, coastal discharge features on Guam have been inventoried and examined in detail along the east coast of northern Guam. Due to heavy surf and lack of a coastal terrace, discharge features along the west coast of Guam were not comprehensively surveyed.

10. 1. Coastal Discharge Features in Northern Guam

Coastal discharge features in northern Guam belong to several types that appear to be associated with the coastal morphology (Jenson et al., 1997). Freshwater discharge from sandy beaches is from beach springs and seeps. In areas without beaches, where sheer cliffs dominate the coast, the groundwater discharges from the cliff faces, most commonly from dissolution-widened fractures, and in several cases from caves that open to the sea (Mylroie et al., 1999). Additionally, submarine seepage zone and springs have been identified in depths from just below the mean sea level to about 12 meters below sea level.

Coastal discharge features have been mapped in detail in a part of Guam's coast from Tumon Bay to Double Reef (Jocson, 1998; Jocson et al., 1999), but have not yet been systematically mapped elsewhere. I have found several new springs in Jocson's study area and additional springs elsewhere along Guam's coast. These new finds and all previously documented springs are included in the inventory of coastal discharge features (Appendix 12). In the area mapped by Jocson (1998) estimates of significant discharge from fractures range from about 200 m^3/d (0.05 mgd) to 7,500 m^3/d (2 mgd); estimated discharge from the caves ranges from about 2,300 m^3/d (0.6 mgd) to 20,000 m^3/d (5 mgd) (Mylroie et al., 1999). Discharge was not estimated for any of the new springs identified during this study.

The coastal discharge features in northern Guam belong to several types: beach springs and seeps, seepage from shallow water from the modern reef, discharging fractures, discharging caves and submarine vents. Additionally, small bays reminiscent of caletas (Back et al., 1984) occur in several places in northern Guam and may be related to coastal discharge.

10. 1. 1. Beach springs and seeps

Permanent springs and seeps are common discharge features on the beaches in northern Guam. They are ubiquitous and more or less continuous along the beaches in embayments, such as Tumon and Agana bays, with rarely more than a 100 meters separating each major spring or seepage zone (Jenson et al., 1997). The springs are best viewed at low tide, when channels, parallel rills, and mini-deltas are made in the beach sand by the effluent (Plate 26, photo 1). Prolific growth of green algae seems to be associated with some of the springs in Tumon Bay (Plate 26, photo 2). In Tumon and Agana bays, Jocson (1998) has identified about six major springs, ranging in discharge from 20 to 180 l/s (0.5 to 4 mgd). Similar discharge features are common in other beaches in embayments, such as Haputo Beach and Double Reef Beach. Most of the beach springs become submerged during high tides and are difficult to observe. The larger springs, however, are visible even at high tides (Plate 26, photos 3 and 4). During an earthquake on February 27, 2000, a conduit feeding one of the springs collapsed and formed a small "sinkhole" in the beach sand in Tumon Bay (Plate 26, photo 5).

Beach springs are also common on "linear" beaches, where the cliffs are recessed from the coastline and the shoreline typically contains long beaches parallel to the edge of the lowermost of the uplifted marine terraces and the cliffs behind them. Springs and seeps on such beaches are common but do not appear as numerous as in the beaches in large embayments. Typically, springs emerge from under the beach rock deposits and are easily visible at low tide (Plate 26, photo 6). The best examples of this type can be seen on Uruno Beach, Ritidian Beach, and the beaches between Ritidian and Mergagan points. In the area between Ritidian and Tarague, there are no linear beaches and the uplifted terrace is immediately adjacent to the ocean. Beach sediments accumulate only in small bays (10-20 m across), where seeps and springs are visible in the sand at low tide.

10. 1. 2. Seepage zones on the reef platform and reef front

Jenson et al. (1997) report that the single largest spring located during their study of Agana Bay is associated with a fracture in the reef platform, located below the sea level, even at the lowest tide. More commonly, exact sites of freshwater discharge on the reef platform are difficult to identify and volumes cannot be accurately estimated. Freshwater discharge, however, is evident based on temperature changes and visible mixing of waters that can be observed while snorkeling in Agana and Tumon bays and most of the reefs of west and northwest coastline of northern Guam, particularly in the Double Reef area. Freshwater discharge was also documented at the reef front. Jenson et al. (1997) have identified three locations on the reef margin outside of Tumon Bay where brackish water discharges at depths of up to 4 meters.

10. 1. 3. Discharging fractures

Most of the shoreline of northern Guam is occupied by shear cliffs of the limestone plateau rising about 60 to 200 meters above sea level. In places, tall cliffs are immediately adjacent to the ocean, but in most, there are local terraces extending a few meters from the cliff face at the waterline. The coastal cliffs are incised by semi-circular bioerosional grooves to a radius of up to 2 meters. Small fringing reefs are common on the west and part of the north shore of northern Guam, but the east coast is generally devoid of reefs because the water deepens abruptly along the steep slopes. In rocky shorelines, where no beach deposits have accumulated, the most common freshwater discharge features are dissolutionally enlarged fractures.

The fractures range in size and exist on a variety of scales, from enlarged joints less than a centimeter wide (Plate 26, photos 7 and 8) to large vertical fractures several meters wide. The small springs emerging from joint and small fractures are the most common. Several good examples can be seen in the rocky coastline on the north end of Double Reef Beach. Most significant discharge is from much larger fractures, clearly a subject to dissolutional enlargement and often large enough to be entered.

The large discharging fractures are typically open vertical fractures in the cliff face, solution-widened to 0.5 to several meters at the widest points, at and below the modern sea level. They typically close within five meters above the water line. Sharp stratification of fresh water flow in these fractures is readily observable, both from the refraction of light at the ~0.5-meters-deep contact of freshwater and the underlying seawater as well as the temperature contrast. According to estimates by Jenson et al. (1997), the linear surface flow velocity at the center of the largest of the fractures is about .5 m/s and the discharge volumes in the largest fractures range from 10 to 90+ l/s (0.25 to 2+ mgd). The three largest discharging fractures identified in northern Guam so far are all located in coastal cliffs between Double Reef Beach and Falcona Beach and are known as Menpachi Fracture, Scott's Fracture and No Can Fracture (south to north).

Menpachi Fracture (Fig. 10. 1, Plate 27, photos 7 and 8) is located about 100 meters north of the north end of Double Reef Beach. It is the widest discharging fracture identified so far. The mouth of the fracture is about 5 meters wide and interrupts the coastal algal reef terrace. It is not clear whether freshwater discharge dissolved the coastal terrace away or prevented its growth. Orientation of the fracture is normal to the coastline, east-northeast. The first 25 meters from the mouth appear as a canyon, having no roof and discharging a steady stream of water. After the 25 meters, fracture abruptly narrows and closes about 5 meters above the waterline. It is traversable for another 15 meters beyond that point, after which is becomes too narrow. In the un-roofed portion of the fracture, bottom is covered by carbonate sand deposits. In the final 15 meters, bottom of the fracture is limestone bedrock, without any sediment. Menpachi fracture receives flow from two large and one small tributary fracture, and shows evidence of another, now abandoned tributary. Estimated discharge from this fracture is 40 l/s (0.9 mgd) (Jocson, 1998).

Scott's Fracture (Plate 27, photos 1, 2, and 3) is located 150 meters north of Menpachi Fracture. The cliff-face at this location is about 7 meters away from the ocean, behind an algal terrace at the sea level. The fracture cuts through the terrace and forms a 0.5-m-wide, slightly-meandering channel opening to the sea. The fracture is about 3 meters deep, widening to about a meter at the bottom, which is covered by sand deposits. Inland from the 7-m-long channel through the algal terrace, the fracture continues into the coastal cliff and is traversable for six additional meters. Freshwater appears to be coming from two smaller fractures feeding the large fracture. Estimated discharge is 11 l/s (0.25 mgd) (Jocson, 1998).

No Can Fracture (Fig. 10. 2, Plate 27, photos 4, 5, and 6) is located about 650 meters north of Double Reef Beach. Oriented normal to the coastline, it extends east into the coastal cliff. It is 0.5 meters

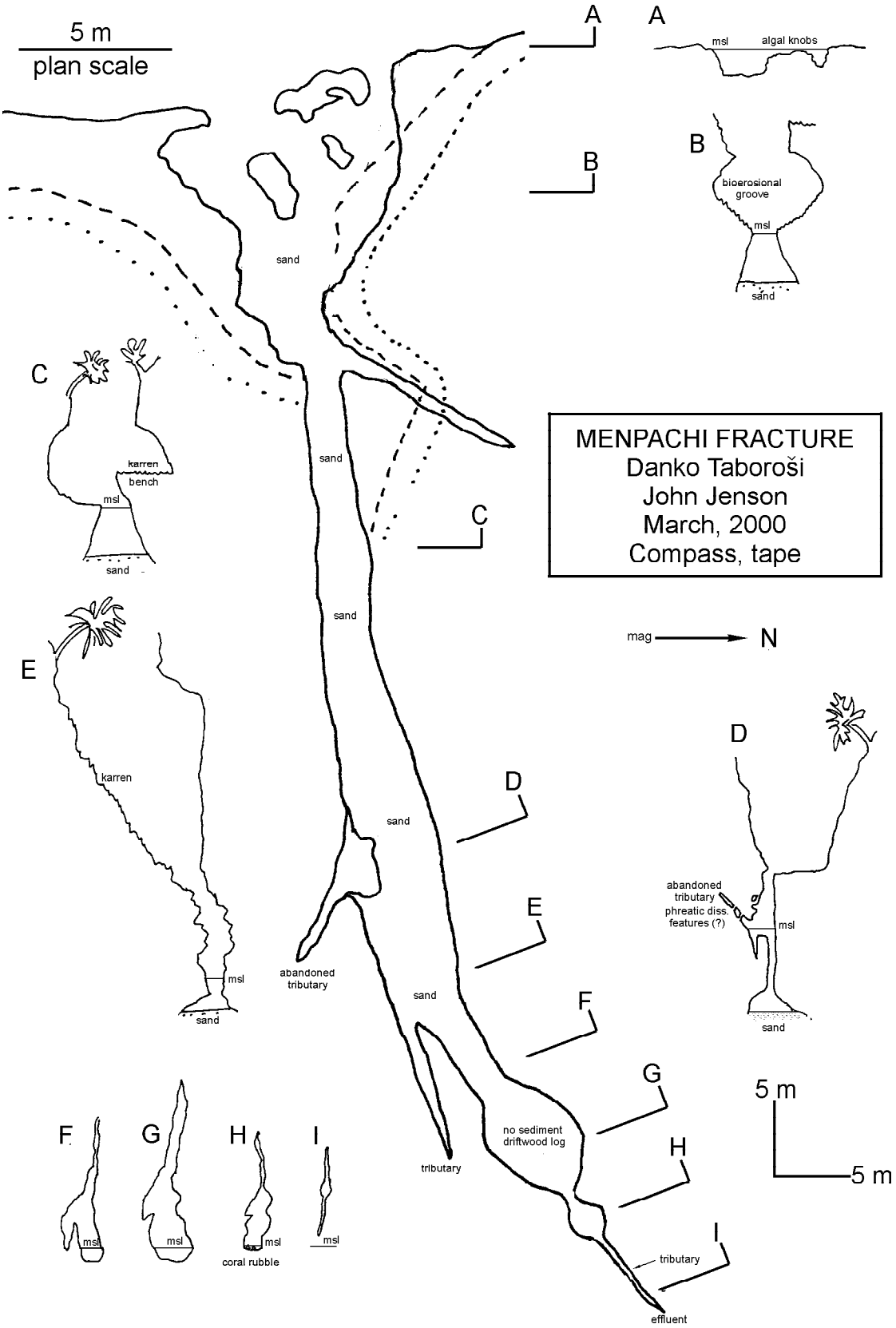

Fig. 10. 1. Map of Menpachi Fracture

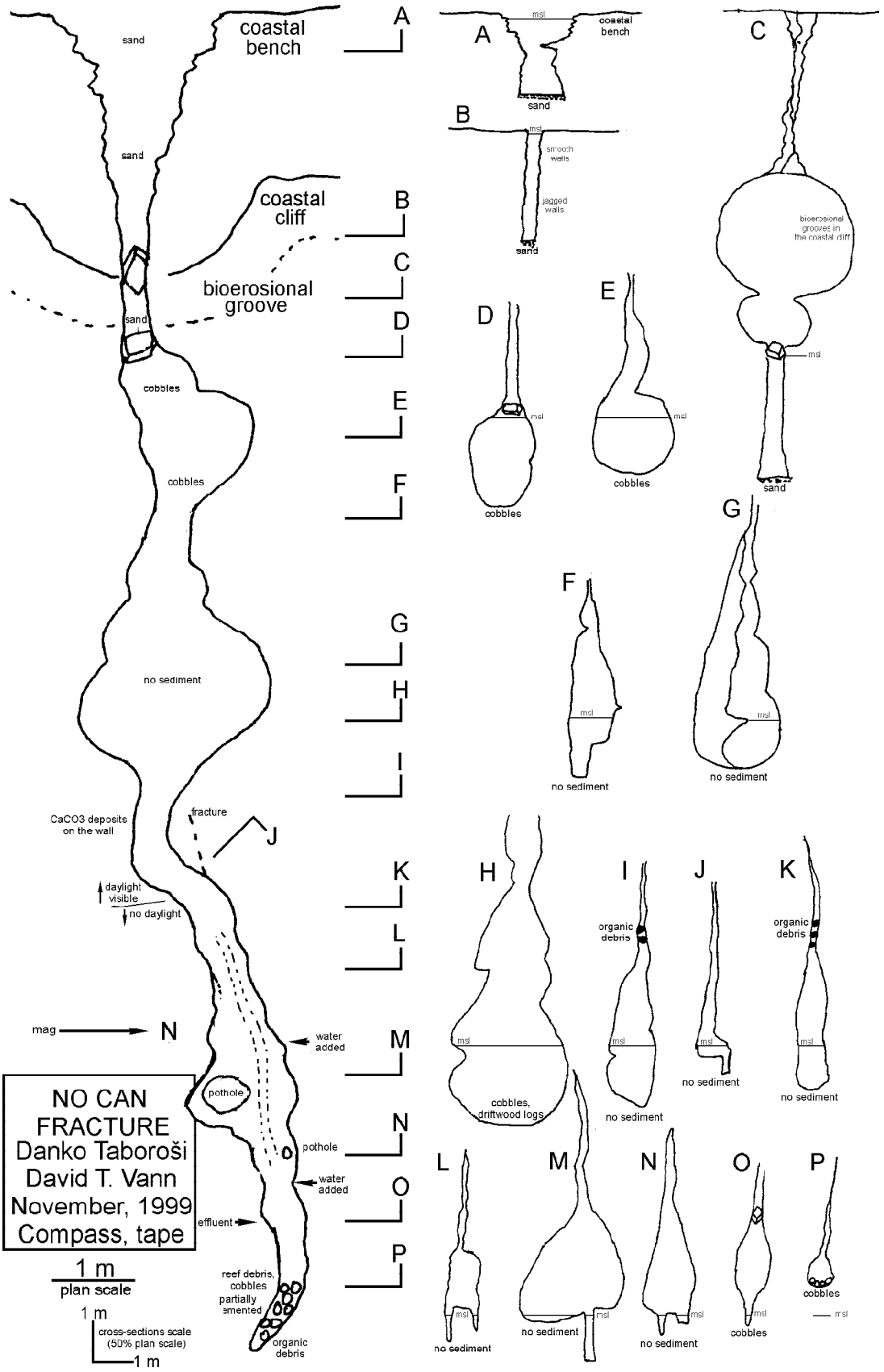

Fig. 10. 2. Map of No Can Fracture

wide at its entrance in the coastal cliff. Seaward of the entrance, the fracture forms a 3-m wide disruption in the coastal algal reef bench. By immersing oneself in the water flowing through the fracture, it is possible to swim through the 0.5-wide opening in the coastal cliff into the fracture which, after 2.5 meters, widens to 1.5 meters. The fracture then narrows to about a meter wide, before it widens again to form a small chamber almost 3 meters wide. The fracture then narrows to less than a meter wide before reaching the final wide chamber, about 2 meters wide. At this point, the floor of the fracture emerges above sea level and the fracture can be further traversed by walking instead of swimming. Only 5 meters further, 35 meters from the entrance, the fracture becomes too tight to traverse. The back end of the fracture contains partially cemented reef debris and organic debris, pushed there by storm waves. Most of the fracture floor, however, is limestone bedrock, lacking sediment. The fracture is vertically extensive but closes at 8-9 meters above waterline. Organic debris, such as driftwood and coconuts, are often found wedged in the narrow upper parts of the fracture, a result of storm waves. Discharge is estimated to be 18 l/s (0.4 mgd) (Jocson, 1998). Two small fractures in the walls of No Can appear to be tributaries.

10. 1. 4. Discharging caves

Some of the largest springs on the northwest coast of Guam are associated with coastal caves. The largest single point discharge feature identified so far in northern Guam is the Coconut Crab Cave (Fig. 10. 3, Plate 28, photo 1). This cave is located about 300 meters south of Double Reef Beach. The entrance is at sea level, in a small cove containing several large boulders. A steady stream of freshwater emerges from the cave at the waterline, best seen at low tide. The cave has one large chamber, about 30 m by 20 m, no more than 4 meters tall. The room is partitioned by several flowstone divides, giving impression of passages. The floor is entirely made of flowstone or covered by coral rubble, with several scattered large collapse boulders and flowstone mounds. The back wall of the cave is made of large collapse boulders. The cave appears to extend further inland but is entirely filled by boulders and was not explored. Coconut Crab Cave was estimated to discharge 225 l/s (5 mgd) by Jocson (1998). Another example of a discharging cave is Arch Spring (Plate 28, photo 2). This cave has collapsed, leaving only a part of its roof, now a natural arch.

10. 1. 5. Submarine vents

During his survey of coastal discharge points along the northwest coast of Guam, Jocson (1998) documented a group of three submarine vents (Plate 29, photos 1 and 2) discharging an estimated 18 l/s (0.4 mgd) combined. Freshwater discharges from small cavernous openings located at the base of the coastal cliff, at a depth of 4 meters.

Additional submarine vents along the northwest coast were located during this project, the deepest and largest being Matt's Freshwater Cave (Plate 29, photos 3, 4, and 5). This cave discharges a significant amount of freshwater but the discharge volume is difficult to estimate. Located at a depth of 11 meters, the cave has a single oval chamber, extending into the cliff. Freshwater discharges from several points in the cave, all dissolutionally enlarged fractures, about 10 cm wide. In addition to submarine discharging caves, there are also submerged fractures similar to No Can Fractures that discharge freshwater (Plate 29, photo 6).

10. 1. 6. Caletas

Small coves and bays reminiscent of caletas (Back et al., 1984), occur throughout the northern Guam. On the west coast of northern Guam, the most prominent caleta-like coves are Ague Cove, Frank's Cove, and Patinian Cove, all of which are associated with significant freshwater discharge. On the east coast of northern Guam, there are two additional such coves at the Hawaiian Rock quarry and Fadian Cove (Plate 28, photo 3) a kilometer further south. There are freshwater springs on the beaches of these coves as well. On a much smaller scale, there are a few beaches formed in very small coves along the north coast of Guam between Ritidian and Tarague. Each of the small beaches in this area exhibits freshwater discharge easily observed at low tides (Plate 28, photo 4). Larger embayments, such as Double Reef Beach (Plate 28, photo 5) and Haputo Beach (Plate 28, photo 6), as well as Tumon and Agana bays, may also be coastal features shaped by freshwater discharge.

10. 2. Coastal Discharge Features in Southern Guam

The limestone belt along the east coast of southern Guam was mapped (Tracey et al., 1964) as the Argillaceous Member of the Mariana Limestone, separating the inland volcanic highlands from the Pacific Ocean. Sheer cliffs dominate in some places, but most of the coastline is composed of uplifted

marine terraces with few linear beaches. Six allogenic rivers cross the limestone belt to discharge into the Pacific Ocean. The streams have incised steep-walled valleys through the limestone. Coastal bathymetry verifies that the incisions continue down to depth of the lowest glacio-eustatic sea level still-stand. The nature of groundwater discharge from the limestone terrain on the southeastern coast has not been studied. Only a few isolated beach springs have been identified on the beach in Ipan.

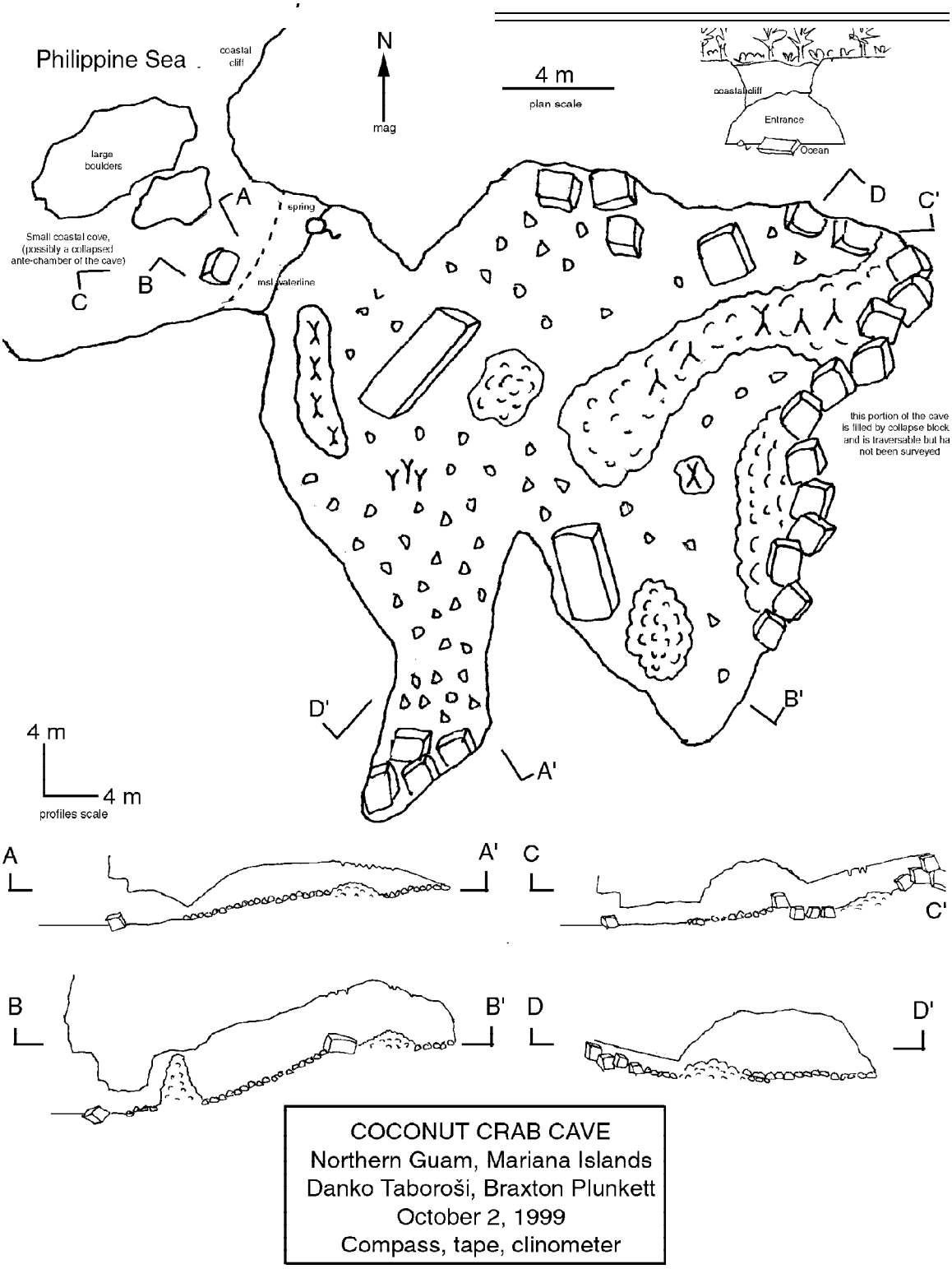

Fig. 10. 3. Map of Coconut Crab Cave

— Chapter 11 —
Submarine Karst Features

This chapter investigates karst features found below the modern sea level. Although not actively involved in the circulation of freshwater in Guam's karst areas, submerged features can provide important clues about geologic history of karst on Guam. Because of the difficulties involved in exploring submarine karst and because the scope of this project was on the hydrologically significant features, no comprehensive submarine survey was undertaken. Only a limited discussion of some examples of submarine karst features and an inconclusive inventory are presented here.

11. 1. Intertidal Karst

Intertidal reef rocks are affected not only by seawater but also by rainwater (Huang, 1981). On beaches, the characteristic intertidal karst form is beach rock. It occurs locally on all beaches along the west and north coast of northern Guam. It usually dips seawards, like the unlithified beach surface, and its composition appears identical to the composition of surrounding calcareous sand. The importance of dissolution in the formation of beach rock on Guam is unknown, but beach rock does appear to be modified by dissolution processes. A distinct type of karren (reminiscent of small potholes) occurs on beach rock deposits. Contribution of bioeroders is unknown and none were observed on beach rock.

In areas without beach deposits, elevated reef rocks are in contact with the ocean. Semi-circular bioerosional grooves, usually about 2 meters in diameters, have been cut into much of the coastal cliff line. Bioeroding organisms contributing to the formation of coastal grooves include limpets (*Patelloida chamorrorum*) and chitons (*Acanthopleura gemmata*) (L. Kirkendale, pers. comm.), as well as boring by *Lithothrya* sp. barnacle (G. Paulay, pers. comm.) and possibly grazing by grapsid crabs as evidenced by fecal pellets nearly 100% $CaCO_3$ (B. Smith, pers. comm.). Contribution of dissolution to the formation of bioerosional grooves is debatable. Solution by slightly undersaturated seawater in the area of wave action has been suggested as the cause of coastal grooves. Lack of such grooves in non-soluble ocean cliffs in suggested as evidence of solutional origin (Aley, 1964).

In parts of the rocky coastline in northern Guam, from Amantes Point to Tanguisson, from Hilaan to south of Haputo Beach and from Haputo Beach to Double Reef area, a narrow elevated bench in the inter-tidal zone separates the coastal cliffs from the modern reef. This terrace often contains shallow basins separated by a network of small algal ridges (up to 20 cm tall and wide). It is unknown whether these features are a result of construction of dissolution. Similar features can be seen on the modern fringing reefs in the intertidal zone. They are algal ridges rising up to 35 cm above the fringing reef flat, separating the reef into a series of large pools. The pools are arranged in a step-like pattern, so that the seawater pushed onto the reef by waves cascades over the ridges from one pool on the reef to another. Some of the best examples of this type of feature are from the eastern coastline of southern Guam (Plate 30, photo 1). These pools have been described in more detail by Emery (1962) who termed them "rimmed terraces." The origin of the pools is debatable, and can be a result of biological construction, bio-erosion, chemical dissolution or a combination of processes.

Further seaward, at the reef margin, the fringing reefs of Guam show typical spur and groove morphology. The spurs are *Porolithon* algal ridges, of different dimensions, normal to the reef front. The grooves are channels separating the ridges. Virtually no sediment is present in this area and encrusting algae and colonies of *Acropora* are the dominant organisms. The shallow portions of this zone are subaerially exposed only during the lowest tides of the year. Being permanently below the sea level, spurs and grooves are not influenced by freshwater and are not karst features. They have been incorrectly referred to as karst features and grikes (Huang, 1981).

Inland from the reef margin, spurs are packed closer together, and grooves are thinner. Further towards the shore, spurs come together and the grooves become roofed. Grooves thin out further but may still open to the reef terrace above resulting in blowholes. The best examples of blowholes in Guam can be seen on the intertidal reef terrace from Campanaya to Pagat points.

11. 2. Submerged Depressions and Caves

Emery (1962) has identified several submerged terraces associated with sea level low-stands, the lowest of which is located 95 meters below the modern sea level. Thus, karst features that have

developed in the vadose or phreatic zone associated with previous sea level low-stands are not completely submerged in the marine phreatic zone. Submerged karst features identified in Guam so far include pit caves (vadose shafts), caves and sinkholes.

11. 2. 1. Submerged pit caves

The best know submerged pit cave and one of Guam's most popular dive sites is the Blue Hole (Plate 30, photo 2), located off the southern coast of Orote Peninsula. It is a vertical shaft, opening on a reef flat at a depth of 20 meters. The shaft extends to about 95 meters below sea level. At a depth of 40 meters, a large window opens in the outer wall of the shaft allowing the diver to exit that way. Additional submerged shafts have been reported from northern Guam but none could be confirmed during this study.

11. 2. 2. Submerged caves

Perhaps the best know submarine caves on Guam are Anae Caverns. A popular diving destination, Anae Caverns are located at a depth of about 10 meters, at Anae Island off the coast of Agat. These shallow and open caves are probably submerged flank margin chambers.

Just north of Ague Cove is another submerged cave, entered at a depth of 12 meters, at the base of coastal cliff line. This cave is also a likely example of a submerged flank margin cave, possibly associated with ephemeral fresh water discharge.

An unusual submarine cave is located south of Haputo Beach. It is unique because it is the only submarine cave that continues to an inland cave intersecting the freshwater lens. This cave is entered at a depth of about 12 m. A passage continues into the coastal cliffs, and connects to a larger chamber. This chamber contains the halocline and the freshwater floating on the sea water, as well as a subaerial portion and a dry entrance made by roof collapse. This cave was filmed by Micronesian Divers Association and appears in their Aquaquest Micronesia video.

The deepest submarine cave documented during this study is Matt's Cave (Plate 30, photo 3), entered through an opening 2 meters in diameter at a depth of 50 meters in the Palace Wall (reef at the Palace Hotel in Tamuning). This cave consists of a long tubular passage and at least one room, and has been explored to a total distance of 200 meters, to a maximum depth of 65 meters (M. Howes, pers. comm.) Three additional caves are located at a similar depth, on the reef wall between the Palace and Hilton hotels. Another cave may exist below Matt's Cave, at a depth of 110 meters, in the second wall that starts seaward of the Palace Wall, at a depth of 90 meters (M. Howes, pers. comm.)

Additional submarine caves have been reported from Adelupe (~60 meters depth), vicinity of Piti Channel (~60 meters depth), Orote Peninsula and Pati Point.

11. 2. 3. Submerged sinkholes and depressions

Piti Bomb Holes (Plate 30, photo 4), located on the reef platform in Piti, are not really bomb holes but flooded sinkholes, the deepest of which is 11 m deep.

Another depression on a reef, possibly submerged karst or constructional in nature, is Shark's Hole in Hilaan (Plate 30, photo 5). This depression on a fringing reef is a sand-filled pit, about 3 meters deep.

Two submerged sinkholes on the coast in Inarajan are a popular picnic spot known as Inarajan Pools (also known as Saluglula Pools, Plate 30, photo 6). They are two adjacent sea water pools, approximately 80 m in diameter and about 10 meters deep. The pools are separated from the ocean by a fringing reef and may be submerged sinkholes. There are unverified reports of a submerged passage leading from the northern pool to the ocean.

A unique feature on Guam is Orote Pond. This flooded depression is located at the tip of Orote Peninsula, opposite Orote Island, adjacent to the cliff line. Located just a few tens of meters from the beach, this marine lake has limited circulation with the ocean. When I explored it, it showed a distinct halocline and freshwater at the surface, but it was unclear if the brackish nature of the water was a result of groundwater or just temporary influence of rainwater. The depth of the lake is unknown, but is at least 3 meters. The bottom is composed of fine sediment. A small bivalve and an unknown species of shrimp are the only fauna observed in the lake during my fieldwork there. There are reports of silver tarpon (*Megalops cyprinoides*) living in the lake (B. Tibbatts, pers. comm.)

11. 3. Marine Pseudokarst

Karst-like landforms produced by processes other than solution (or corrosion-induced subsidence or collapse) are known as pseudokarst (Ford and Williams, 1989). In addition to man-made caves of World War II era, two types of non-karst caves exist on Guam: primary caves (made by reef growth) and sea caves (made by wave scouring and erosion).

11. 3. 1. Reef caves

Reef caves develop on the reef margin by growth of the spur-and-groove *Porolithon* algal ridge. As the algae grow adding deposits to the spurs, the spurs may roof over the grooves. In such cases, a system of small rooms and passages may develop. Such features on the reef front resemble true caves and many recreational divers on Guam consider them caves. Good examples of this type can be found along the reef northeast of Pago Point, in Double Reef area (Plate 31, photo 1), at the reef front off shore from Togcha cemetary, at the reef front at Aga Point and elsewhere. The most complex reef caves have developed on the reef margins of fringing reefs of Merizo and Umatac, in Toguan Bay, Bile Bay and Fouha Bay. Reef caves there are impressive, vertically extensive features. They appear as vertical slits in the reef, extending from the sandy bottom at the base of the reef (10+ meters depth) to the ceiling (formed by the reef flat) just below the sea level. These roofed slits in the reef occasionally converge, giving impression of a complex cave system. In places, no daylight penetrates into the "passages." These "caves" are popular dive sites.

11. 3. 2. Sea caves

Sea caves can develop in shorelines that fulfill the following conditions: presence of a sea cliff in direct contact with the waves and currents, cliff must contain geologic structures allowing differential erosion, and the rock of which the cliff is composed must be sufficiently resistant to prevent quick development of a protective beach (Moore, 1954). Because sea caves are made predominantly by physical erosion by waves, they are not karst features strictly speaking, although contribution by dissolution by slightly undersaturated wave-agitated sea water and groundwater has been recognized (Moore, 1954).

Because sea caves develop in zones of weaknesses (joints, fractures) more easily eroded then the rest of the cliff, and such features have been observed on Guam to preferentially discharge groundwater at the coast, it is expected that dissolution by groundwater may play a role in development of sea caves. Presence of sea caves may therefore be an indication of concentrated groundwater discharge, difficult to directly observe in heavy surf areas.

Nevertheless, solution is not necessary in the development of sea caves and such caves are common in non-carbonate coastlines, such as southern California. They have been, however, described from carbonate islands as well, such as Jamaica, where wave pounding and collapse are suggested as primary genetic factors but contribution of solution by groundwater is recognized (Aley, 1964). In coastal karst of western Jamaica, orientation of sea caves has shows that development is controlled by dissolutionally-widened joints and fractures, which can be "followed inland on the surface for hundreds of feet beyond the termination of sea caves" (Aley, 1964). Area described is similar to northern Guam in that it has no surface drainage and fractures provide preferential flow paths for the movement of groundwater.

Sea caves are common on Guam, although distinctions between sea caves and true karst caves are difficult to make (Plate 31, photo 2). Typically, walls and ceilings of sea caves are blocky, showing evidence of wave pounding and collapse with few, if any, dissolutional features (Plate 31, photos 3 and 4). Most caves on Guam interpreted as sea caves are located on the east coast of northern Guam, where absence of fringing reefs and beaches warrants no protection from the waves. Reefs have been recognized as providing important protection from the waves. The Marquesas Islands, for example, unlike most Pacific islands, have no protective reefs and show extensive sea cave development (Varnedoe, 1973). Storm waves, as opposed to constant pounding of routine waves, occur in short time intervals but play an important role due to enormous pressures they exert on the cliffs (Moore, 1954). It has even been suggested that joints and fractures are widened by air compressed by storm waves (Kuenen, 1950).

In addition to sea caves, waves can preferentially erode the raised coastal terrace along structural weaknesses, resulting in deeply incised and enlarged fissures. Excellent examples of this type can be found on the east coast of Guam, just south of Pati Point (Plate 31, photo 5).

REFERENCES

Agassiz, A. (1903). The coral reefs of the tropical Pacific: Harvard College Museam Comp. Zool. Mem., v. 28, p. 410.

Aley, T. (1964). Sea Caves in the Coastal Karst of Western Jamaica: Cave Notes, v. 6, p. 1-3.

Allen, J. R. L. (1977). Physical Processes of Sedimentation. London: Allen & Unwin.

Andersen Air Force Base. (1995). Groundwater dye trace program and sell cluster proposal for the landfill area.

Ashton, K. (1966). The analysis of flow data from karst drainage systems: Trans. Cave. Research Group, G. B., v. 7 (2), p. 161-203.

Ayers, J. F. (1981). Estimate of Recharge to the Freshwater Lens of Northern Guam. University of Guam, Water and Energy Research Institute of the Western Pacific. Tech. Report No. 21 March.

Back, W., Hanshaw, B.B., and Van Driel, J.N. (1984). Role of groundwater in shaping the eastern coastline of the Yucatan Peninsula, Mexico, in LaFleur, R., ed., Groundwater as a Geomorphic Agent: Boston, Allen and Unwin, p. 281-293.

Back, W., Hanshaw, B. B., Herman, J. S., Van Driel, J. N. (1986). Differential dissolutionof a Pleistocene reef in the ground-water mixing zone of coastal Yucatan, Mexico: Geology, v. 14, p. 137-140.

Barner, W.L. (1995). Ground water flow in a young karst terrane developed along a coastal setting, northern Guam, Mariana Islands, Int. Res. Appl. Cen. Karst Water Res., Karst Waters Institute, Seminar field course: Beldibi/Antalya, Turkey, p. 12.

Barner, W.L. (1997). Time of travel in the fresh water lens of northern Guam, Proceedings of the Eighth Symposium on the Geology of the Bahamas and Other Carbonate Regions: Bahamian Field Station, Bahamas, p. 1-12.

Barrett Consulting Group (1992). Groundwater in Northern Guam, Sustainable Yield and Groundwater Development, prep. in assoc. with John F. Mink, for Public Utility Agency of Guam, Agana, Guam.

Barrett, Harris & Associates (1982). Northern Guam Lens Study, Summary Report, Guam Environmental Protection Agency, Harmon Guam.

Beddows, P.A. (1999). Conduit Hydrogeology of a Tropical Coast Carbonate Aquifer: Caribbean Coast of the Yucatan Peninsula: Hamilton, Ontario, McMaster University.

Blumenstock, D.I. (1959). Climate, Military Geology of Guam, Mariana Islands, Intelligence Division, Office of the Engineer, Headquarters, U.S. Army Forces Pacific.

Bögli, A. (1960). Kalklosung und karrenbildung. Z. Geomorph. Supp/bd. 2, 4-21.

Bögli, A. (1964). Mischungkorrosion; ein Beitrag zum Verkarstungsproblem.: Erdkunde, v. 18 (2), p. 83-92.

Bögli, A. (1980). Karst hydrology and physical speleology. Berlin: Springer-Verlag.

Bonacci, O. (1987). Karst Hydrology, with special reference to the Dinaric karst. Springer-Verlag, Berlin.

Bridge, J. (1948). Mineral Resources of Micronesia Volume 3 — 1, U. S. Commercial Company, Economic Survey of Micronesia, Honolulu.

Brook, D., Waltham, A. C. (1978). Caves of Mulu. Royal Geographical Society. 44p. Nottingham: Sherwood Press.

Brucker, R. W., Hess, J. W., White, W. B. (1972). Role of vertical shafts in the movement of ground water in carbonate aquifers. Ground Water, v. 10, n. 6., pp. 5-13.

Bull, P. A., Laverty, M. (1982). Observations on phytokarst. Z. Geomorph. 26. 437-57.

Carroll D., Hathaway, J. C. (1963). Mineralogy of selected soils from Guam. U.S. Geol. Survey Prof. Paper 403-F: 42 p.

Casanova, J. (1981). Morphologie et biolithogenese des barrages de travertins. "Formation carbonates externes, tufs et travertins." Ass. Francaise de Karstologie, Mem. 3, pp. 45-54.

CDM (1982). Final Report, Northern Guam Lens Study, Groundwater Management Program, Aquifer Yield Report, Camp, Dresser and McKee, Inc. in assoc. with Barrett, Harris & Associates for Guam Environmental Protection Agency.

Chafetz, H. S., Folk, R. L. (1984). Travertines: depositional morphology and the bacterially constructed constituents. J. Sed. Pet. 54 (1), 289-316.

Cleland, H. F. (1910). North American natural bridges, with a discussion of their origin. Bull. Geol. Soc. Amer., 21, 313-38.

Cloud, P. E. Jr. (1951). Reconnaissance Geology of Guam and Problems of Water Supply and Fuel Storage: Military Geology Branch, U.S. Geol. Survey.

Cole, W. S. (1963). Tertiary larger foraminifera from Guam. U.S. Geol. Survey Prof. Paper 403-E: 28 p. & 11 plts.

Coleman, A.M., and Balchin, W.G.W. (1960). The origin and development of surface depressions in Mendip Hills: Proceedings of the Geologists' Association, v. 32, p. 291-309.

Contractor, D. N. (1981). A two-dimensional, finite element model of salt water intrusion in groundwater systems. University of Guam, Water Energy Research Institute of the Western Pacific. Tech Report No. 26.

Contractor, D. N., Ayers J. F., and Winter, S. J. (1981). Numerical Modeling of Salt Water Intrusion in the Northern Guam Lens. University of Guam, Water Energy Research Institute of the Western Pacific. Tech Report No. 27: 3-5.

Contractor, D. N., Srivastava, R. (1990) . Simulation of Saltwater Intrusion in the Northern Guam Lens using a Microcomputer. Journal of Hydrology, 118. Pp. 87-106. Elsevier Science Publishers, Amsterdam.

Contractor, D. N., Jenson, J. W. (in press.) Simulated Effect of Vadose Infiltration on Water Levels in the Northern Guam Lens Aquifer. Journal of Hydrology.

Cvijic, J. (1893). Das Karstphaenomen. Versuch einer morphologischen Monographie.: Geog. Abhandl. Wien, p. 218-329.

Cvijic, J. (1925). Types morphologiques du terrains calcaires. Le holokarst. Le merokarst. Types karstique du transicion. C. R. Acad. Sci., 180, 592-4, 757-8, 1038-40.

Cvijic, J. (1960). La géographie des terraines calcaires: Belgrade, Classe des sciences mathématiques et naturelles, Acad. Serbe. Sci. Arts Mon. Monographie, tome CCCXLI.

Dasher, G. R. (1994). On Station — a Complete Handbook for Surveying and Mapping Caves. National Speleological Society, Huntsville, Alabama

Davis, J. C. (1986). Statistics and data analysis in geology: New York, John Wiley & sons.

Day, M. J. (1983). Doline morphology and development in Barbados: Anns. Assoc. Amer. Geogr., v. 73 (2), p. 206-19.

Dumaliang, P. P., Guard, C. P., and Taboro_i, D. S. (1998). Meteorological Data, in Jenson, J.W., and Jocson, J.M.U., eds., Hydrologic Data Collection on Guam: FY 1998 Report, Volume WERI Technical Report 83: Mangilao, Guam Hydrologic Survey Program, Water and Environmental Research Institute of the Western Pacific, p. 5-10.

Emery, K. O. (1962). Marine Geology of Guam, U.S. Geol. Survey Prof. Paper 403-B.

Fairbridge, R. W. (1968). The Encyclopedia of Geomorphology: New York, Reinhold Book Corporation.

Folk, R. F., Roberts, H. H., Moore, C. H. (1971). Black phytokarst from Hell (abstract). Geol. Soc. America Abstr. With Programs 3, 7: 569-570.

Folk, R. F., Roberts, H. H., Moore, C. H. (1973). Black phytokarst from Hell, Cayman Islands, British West Indies. Geol. Soc. America Bull., 84: 2351-2360.

Ford, D. C. (1964). Origin of the closed depressions in the central Mendip Hills, 20th International Geographical Congress, Abstracts of Papers: London, p. 105-106.

Ford, D. C. (1999). Perspectives in karst hydrology and cavern genesis, in Palmer, A.N., Palmer, M.V., and Sasowsky, I.D., eds., Karst Modeling Symposium: Charlottesville, VA, p. 17-29.

Ford, D. C., and Ewers, R. O. (1978). The development of limestone cave systems in the dimensions of length and depth: Can. J. Earth Sci., v. 15, p. 1783-1798.

Ford, D. C., Williams, P. W. (1989). Karst geomorphology and hydrology. Cambridge: University Press, Cambridge.

Frank, E. F., Mylroie, J., Troester, J., Alexander, E. C., and Carew, J. L. (1998). Karst development and speleologenesis, Isla de Mona, Puerto Rico: Journal of Cave and Karst Studies, v. 60, p. 73-83.

Gams, I. (1978). The Polje: Problem of Defintion: Zeits. Geomorph., p. 170-181.

Ginés, A. (1995). Deforestation and karren development in Majorca, Spain. Acta Geographica Szegediensis 34, Homage to László Jakucs special issue:25-32, Szeged, Hungary.

Ginés, A. (1996). An environmental approach to the typology of karren landform assemblages in a Mediterranean mid-mountain karst: the Serra de Tramuntana, Mallorca, Spain. In: Fornós, J. J. and Ginés, A. (eds): Karren Landforms, Universitat de les Illes Balears. Palma de Mallorca, 1996.

Goudie, A. S. (1983). Calcrete. In Chemical Sediments and Geomorphology. A. S. Goudie and K. Pye (eds), 93-131. London: Academic Press.

Gunn, J. (1978). Karst hydrology and solution in the Waitomo district, New Zealand. Ph.D. Thesis, University of Auckland, Auckland.

Gunn, J. (1981). Hydrological processes in karst depressions. Z. Geomorph., 25, 313-31.

Gunn, J. (1983). Point-recharge of limestone aquifers — a model from New Zealand karst. J. Hydrol., 61, pp. 19-29.

Harris, J. G., Mylroie, J. E., and Carew, J. L. (1995). Banana holes: Unique karst features of the Bahamas: Carbonates and Evaporites, v. 10, no. 2, p. 215-224.

Hogan, P.C. (1959). Memo. Subject: Underwater survey of sub-surface fissions eeding Tarague springs and well. 16 March 1959.

Howard, A.D. (1968). Stratigraphic and structural controls on landform development in the central Kentucky karst: Bull. Natl. Spel. Soc., v. 30, p. 95-114.

Huang, J. (1981). Karst features of cays (coral reef) in China. Fourth International Coral Reef Symposium, vol. 1. Manila, Philippines.

Jennings, J. N. (1975). Doline morphometry as a morphogenetic tool: New Zealand examples: New Zealand Geog., v. 31, p. 6-28.

Jennings, J. N. (1985). Karst geomorphology. Oxford: Basil Blackwell.

Jenson, J., Jocson, J., and Siegrist, H.G. (1997). Groundwater discharge styles from an uplifted Pleistocene island karst aquifer, Guam, Mariana Islands, in Beck and Stephenson (Eds.), The Engineering Geology and Hydrology of Karst Terranes, Balkema, Rotterdam, p. 15-19.

Jenson, J. W., Siegrist, H. G. (1994). Bedrock hydrologic features influencing internal transfer in the Northern Guam Lens Aquifer System. Eos Transactions, 75 (43): 257.

Jocson, J. M. U. (1998). Hydrologic Model for the Yigo-Tumon and Finegayan Subbasin of the Northern Guam Lens Aquifer, Guam. Unpub. MS Thesis, University of Guam.

Jocson, J. M. U., Jenson, J. W., Contractor, D. N. (1999). Numerical Modeling and Field Investigation of Infiltration, Recharge and Discharge in the Northern Guam Lens Aquifer. WERI Technical Report No. 88. Water and Environmental Research Institute of the Western Pacific, University of Guam. Mangilao, Guam.

Johnson, J. H. (1964). Fossil and recent calcareous algae from Guam. U.S. Geol. Survey Prof. Paper 403-G: 40 p. and 15 plts.

Julian, H. E., Young, S. C. (1995). Conceptual model of groundwater flow in a mantled karst aquifer and effects of the epikarst zone. In Karst GeoHazards, Beck (ed.), Balkema, Rotterdam.

Kaye, C. A. (1959). Geology of Isla Mona, Puerto Rico, and Notes on Age of Mona Passage: US Government Printing Office, Washington, D.C., U.S. Geological Survey Professional Paper, p. 178.

Kemmerly, P. R. (1982). Spatial analysis of a karst depression population: Clues to genesis: , v. Geological Society of America Bulletin, p. 1078-1086.

Kirkaldy, J. F. (1950). Solution of the chalk in the Mimms Valley, Herts. Proc. Geol. Assoc., vol. 61.

Klappa, C. F. (1978). Biolithogenesis of Microcodium: Elucidation. Sedimentology 25

Kochanov, W.E. (1993). Areal analysis of karst data from the Great Valley of Pennsylvania, in Beck, B.F., ed., Applied Karst Geology: Rotterdam, Balkema.

Kogov_ek, J., Habic, P. (1980). Preucavanje vertikalneg prenikanja vode na primerah Planinske in Postojnske Jame. (The study of vertical water percolation in the case of Planina and Postojna Caves). Acta Carsol 9, pp. 133-148.

Kuenen, P. P. (1950). Marine Geology: New York, Wiley and Sons.

Lander, M. A. (1994). Meteorological factors associated with drought on Guam: Mangilao, Guam, Water and Energy Research Institute of the Western Pacific, University of Guam, p. 39.

Lane, E. (1993). Subsurface karst features in Florida, in Beck, ed., Applied Karst Geology: Rotterdam, Balkema.

Lange, A. L., Barner, W. L. (1995). Application of the natural electric field for detecting karst conduits on Guam, in Beck, ed., Karst GeoHazards: Rotterdam, Balkema.

Macaluso, T., Sauro U. (1996). The karren in evaporitic rocks: a proposal of classification. In: Fornós, J. J. and Ginés, A. (eds): Karren Landforms, Universitat de les Illes Balears. Palma de Mallorca, 1996.

Matschinski, M. (1968). Alignment of dolines northwest of Lake Constance, Germany: Geological Magazine, v. 105, p. 56-61.

Matson, E. A. (1993). Nutrient Flux Through Soils and Aquifers to the Coastal Zone of Guam (Mariana Islands), American Society of Limnology and Oceanography, Inc.

McLean, J. S. (1977). Factors altering the microclimate in Carlsbad Caverns, New Mexico. U.S. Geol. Survey, Open-file Report, 76-171., 56 pp.

Miller, T. (1987). Fluvial and collapse influences on cockpit karst of Belize and eastern Guatemala. 2nd Multidisciplinary Conference on Sinkholes and the Environmental Impacts of Karst, 9-11 February, 1987. Orlando, Florida.

Mink, J. (1976). Groundwater Resources of Guam: Occurrence and Development. University of Guam, Water Energy Research Institute of the Western Pacific. Tech Report No. 1- Sept.

Mink, J. F., Vacher, H. L. (1997). Hydrogeology of northern Guam, in Vacher, H.L., and Quinn, T., eds., Geology and Hydrogeology of Carbonate Islands. Developments in Sedimentology 54: Amsterdam, Elsevier Science, p. 743-761.

Monroe, W. H. (1964). The zanjon, a solution feature of karst topography in Puerto Rico. U. S. Geol. Surv. Prof. Paper 501-B, 126-129

Moore, D.G. (1954). Origin and Development of Sea Caves: Bulletin of the National Speleological Society, p. 71-76.

Mylroie, J. E. (1988). Karst of San Salvador, in Mylroie, J.E., ed., Field guide to the karst geology of San Salvador Island, Bahamas: Ft. Lauderdale, Florida, Bahamian Field Station, p. 17-44.

Mylroie, J. E., Carew, J. L. (1990). The flank margin model for dissolution cave development in carbonate platforms: Earth Surface Processes and Landforms, v. 15, p. 413-424.

Mylroie, J. E., Carew, J. L. (1991). Erosional notches in Bahamian Carbonates: bioerosion or groundwater dissolution?, in Bain, R.J., ed., Proceedings of the Fifth Symposium on Geology of the Bahamas: Port Charlotte, Florida, Bahamian Field Station, p. 85-90.

Mylorie, J. E., Carew, J. L. (1995). Karst development on carbonate islands. In: Unconformities and porosity in carbonate strata, Budd, D. A., Saller, A. H., Harris, P. M. (eds). American Association of Petroleum Geologists Memoir 63, p. 55-76.

Mylroie, J. E., Carew, J. L. (1995). Geology and karst geomorphology of San Salvador Island, Bahamas. Carbonates and Evaporites, v. 10, no. 2, p. 193-206.

Mylroie, J. E., Carew, J. L. (1997). Land use and carbonate island karst, in Beck, B.F., and Stephenson, J.B., eds., The Engineering Geology and Hydrogeology of Karst Terranes: Rotterdam, Balkema.

Mylroie, J. E., Carew, J. L. (1999). Speleogenesis in young limestones in coastal and oceanic settings, in Klimchouk, A.B., Ford, D.C., Palmer, A.N., and Dreybrodt, W., eds., Speleogenesis: Evolution of Karst Aquifers: Huntsville, AL, National Speleological Society, p. 496.

Mylroie, J. E., Carew, J. L., Frank, E. F., Panuska, B. C., Taggart, B. E., Troester, J. W., and Carrasquillo, R., (1995). Comparison of flank margin cave development: San Salvador Island, Bahamas and Isla de Mona, Puerto Rico, in Boardman, M. R., ed., Proceedings of the Seventh Symposium on the Geology of the Bahamas: San Salvador, Bahamian Field Station, p. 49-81.

Mylroie, J. E., Carew, J. L., Moore, A. I., (1995). Blue holes: Definition and genesis: Carbonates and Evaporites, v. 10,no. 2,p. 225-233.

Mylroie, J. E., Carew, J. L., and Vacher, H. L. (1995). Karst development in the Bahamas and Bermuda, in Curran, H. A. and White, B., eds., Terrestrial and Shallow Marine Geology of the Bahamas and Bermuda: Geological Society of America Special Paper 300, p. 251-267.

Mylroie, J. E., Jenson, J. W., Jocson, J. M. U., and Lander, M. (1999). Karst Geology and Hydrology of Guam: A Preliminary Report: Mangilao, Water & Environmental Research Institute of the Western Pacific, University of Guam.

Mylroie, J. E., Jenson J. W., Taboro_i, D., Jocson, J. M. U., Vann, D. T., Wexel, C. (Submitted). Karst features of Guam in terms of a general model of carbonate island karst. Journal of Cave and Karst Studies.

Mylorie, J. E., Panuska, B. C., Carew, J. L., Frank, E. F., Taggart, B. E., Troester, J. W., Carrasquillo, E. (1995). Development of flank margin caves on San Salvador Island, Bahamas and Isla de Mona, Puerto Rico, in Boardman, M., ed., Seventh Symposium on the Geology of the Bahamas: San Salvador Island, Bahamas, Bahamian Field Station, p. 49-81.

OEESCI (1995). Remedial Investigation Report for Construction Battalion Landfill Site, Vol. I: Honolulu, Ogden Environmental & Energy Services Co., Inc.

Ogden Environmental and Energy Services Co., Inc. (1995). Remedial Investigation Report (Final) for Construction Engineer Battalion Landfill Site, Public Works Center, Guam: Comprehensive Long-Term Environmental Action Navy (CLEAN) for Pacific Division, Naval Facilities and Engineering Command, Pearl Harbor, Hawaii.

OHM (1999). Construction Battalion Landfill Remediation Site, Navy.

Pace, M. C. (1992). Investigation and review of dissolution features on San Salvador Island, The Bahamas, Mississippi State University.

Pace, M. C., Mylroie, J. E., Carew, J. L. (1993). Petrographic analysis of vertical dissolution features on San Salvador Island, Bahamas. In Proceedings of the Sixth Symposium on the Geology of the Bahamas, White B. (ed). San Salvador, Bahamas. Bahamian Field Station, p. 17-21.

Pacific Islands Engineers (1950). Geology of Middle Guam, Island of Guam, Mariana Islands, Vol. 1 (out of 2), prepared for Department of the Navy Bureau of Yards and Docks, April 1950

Pacific Islands Engineers (1950). Geology of Middle Guam, Island of Guam, Mariana Islands, Vol. 2 (out of 2), prepared for Department of the Navy Bureau of Yards and Docks, April 1950

Pacific Islands Engineers. “Historical Review of the Geology of Guam with References.” Contract Noy-13626. Prepared for the Department of the Navy.

Palmer, R., and Williams, D.W. (1984). Cave development under Andros Island, Bahamas: Cave Science, v. 13, p. 79-82.

Piper, A. M. (1946). The Water Resources of Guam and the Ex-Japanese Mandated Islands in the Western Pacific. U. S. Commercial Company, Economic Survey, Honolulu.

Pluhar, A., Ford, D. C. (1970). Dolomite karren of the Niagara escarpment, Ontario, Canada. Z. Geomorph. 14(4), 392-410.

Plummer, L. N. (1975). Mixing of sea water with calcium carbonate ground water, in Whitten, E.H.T., ed., Quantitative studies in geological sciences, Volume 142, Geological Society of America Memoir, p. 219-236.

Pohl, E. R. (1955). Vertical shafts in limestone caves. Natl. Speleol. Soc. Occasional Pap. No. 2, 24 pp.

Quenga, M. (in prep.) Salwater intrusion in the Northern Guam Lens Aquifer. University of Guam MSc thesis. Mangilao, University of Guam.

Raeisi, E., Mylroie, J. E. (1995). Hydrodynamic behavior of caves formed in the fresh-water lens of carbonate islands. Carbonates and Evaporites, v. 10, no. 2. p. 207-214

Randal, R.H., Holloman, J. (1974). Coastal Survey of Guam: Mangilao, Marine Laboratory, University of Guam.

Reagan, M.K., Meijer, A. (1984). Geology and geochemistry of early arc-volcanic rocks from Guam: Geological Society of America Bulletin, v. 95, p. 701-713.

Robert and Company, Inc. (1948). Reconnaissance survey for new fresh water sources on the northern section of Guam, M. I.: Atlanta, Georgia, p. 28.

Rogers, B. W., Legge, C. J. (1992). Karst features of the territory of Guam. Submitted to Department of Parks and Recreation. Bulletin 5. Pacific Basin Speleological Survey. National Speleological Society. Ring of Fire Press. San Francisco, California.

Sasowsky, I. D. (1997). Conceptual models of groundwater flow and contaminant transport in carbonate aquifers: Past, present and future: Geological Society of America Abstracts and Programs, v. 29, no. 6, p. 181-182.

Schlanger, S. O. (1964). Petrology of the limestones of Guam with a section on petrography of the insoluble residues by J. C. Hathaway and D. Carroll. U.S. Geol. Survey Prof. Paper 403-D: 52 p. & 21 plts.

Scoffin, T. P., Stoddart, D. R. (1983). Beachrock and intertidal cements. In Chemical Sediments and Geomorphology. A. S. Goudie and K. Pye (eds), 93-131. London: Academic Press.

Siegrist, H. G. (1992). Selected bibliography of 20th century geoscience and related scientific literature of Micronesia, part I: Mariana island arc. Micronesian Area Research Center, University of Guam, Mangilao, Guam.

Stark, J. T., Tracey, J. I., Jr. (1963). Petrology of the volcanic rocks on Guam. U.S. Geol. Survey Prof. Paper 403-C: 32 p.

Stearns, H. T. (1937). Geology and Water Resources of the Island of Guam. U. S. Department of the Interior, Geological Survey.

Stensland, C. S. (1963). Description of soil profiles. In, D. Carroll and J. C. Hathaway, Mineralogy of selected soils from Guam. U.S. Geol. Survey Prof. Paper 403-F: 43-49.

Sweeting, M. M. (1958). The karstlands of Jamaica: Geogr. J., p. 184-99.

Todd, R. (1966). Smaller foraminifera from Guam. U.S. Geol. Survey Prof. Paper 403-I: 41p. U.S. Army. Chief Eng., Intellig. Div., Headg. U.S. Army Pacific, Tokyo.

Tracey, J. I., Schlanger, S. O., Stark, J. T., Doan, D. B., May, H. G. (1964). General Geology of Guam. U. S. Geol. Surv. Prof. Paper 403-A: 104p.

Tricart, J. and DaSilva. (1960). Un example d'evolution karstique en milieu tropical sec; le mourne de Bom Jesus de Lapa (Bahia, Brasil). Zeitschrift fuer Geomorphologie 4; 1, 29-42.

Troester, J. W., White, E. L., and White, W. B. (1984). A comparison of sinkhole depth frequency distributions in temperate and tropic karst regions, Proceedings of the First Multidisciplinary Conference on Sinkholes: Orlando, Florida.

United Nations University (1995). Small islands, big issues. World Development Studies 1, World Institute for Development Economics Research, 156 p.

Vandegrift, A. (1958). Fallout shelters list. US Marine Corps, Guam [unpublished]

Vann, D.T. (in prep.) Revision of basement volcanic contour lines for northern Guam. University of Guam MSc thesis. Mangilao, University of Guam.

Varnedoe, B. (1973). The Marquesan Cave Survey: The Huntsville Grotto Newsletter, v. XIV.

Viles, H. (1984). Biokarst: review and prospect. Progress in physical geography 8(4), 523-42.

Vogel, P. N., Mylroie, J. E., and Carew, J. L. (1990). Limestone petrology and cave morphology on San Salvador Island, Bahamas: Cave Science, v. 17, p. 19-30.

Wall, J . R. D., Wilford, G. E. (1966). Two small scale solution features in limestone outcrops in Sarawak, Malaysia. Z. Geomorph. N. F. 10: 91-94.

Waltham, A. C. (1981). Origin and development of limestone caves: Progress in physical geography, v. 5.

Ward, P. E., Brookhart, J. W. (1962). Military geology of Guam. Water resources supplement.

Ward P. E., Hofford, S. H., Davis, D. A. (1965). Hydrology of Guam, Mariana Islands. U.S. Geol. Survey Prof. Paper 403-H: 25 p. and map.

Wexel, C. T. (in prep.) Almagosa Springs watershed model. University of Guam MSc thesis. Mangilao, University of Guam.

White, W. B. (1988). Geomorphology and Hydrology of Karst Terrains: New York, Oxford Press, 464 p.

White, E. L., White, W. B. (1979). Quantitative morphology of landforms in carbonate rock basins in the Appalachian highlands: Geol. Soc. of Amer. Bull., v. Part I, Vol. 90, p. 385-396.

Wilford, G. E., Wall, J. R. D. (1964). Karst topography in Sarawak. J. Tropical Geography 18: 44-70.

Williams, P. W. (1966). Morphometric analysis of temperate karst landforms: Irish Speleology, v. 1, p. 23-31.

Williams, P. W. (1971). Illustrating morphometric analysis of karst with examples from New Guinea.: Z. Geomorph., v. 15, p. 40-61.

Williams, P. W. (1972). The Analysis of Spatial Characteristics of Karst Terrains, in Chorley, R.J., ed., Spatial Analysis in Geomorphology: London, Methuen, p. 135-163.

Williams, P. W. (1983). The role of the subcutaneous zone in karst hydrology. Journal of Hydrology, 61, pp. 45-67.

Williams, P. W. (1985). Subcutaneous hydrology and the development of doline and cockpit karst: Z. Geomorph., v. 29 (4), p. 463-82.

Zambo, L., Ford, D.C. (1997). Limestone Dissolution Processes in Beke doline, Aggtelek National Park, Hungary: Earth Surface Processes and Landforms, v. 22, p. 531-543.

Zolan, W. J. (1982). A Preliminary Study of Natural Aquifer Discharge on Guam. University of Guam, Water Energy Research Institute of the Western Pacific. Tech Report No. 34.

MAPS

U.S. Geol. Survey (1964). Geologic Map and Sections of Guam, Mariana Islands: U.S. Geol. Survey Prof. Paper 403-A. U.S. Gov. Printing Office, Wa

U.S. Geol. Survey (1965). Water Resource Map of Guam, Mariana Islands: U.S. Geol. Survey Prof. Paper 403-H. U.S. Gov. Printing Office, Wa

U.S. Geol. Survey (1968). Agana Quadrangle, Mariana Islands- Island of Guam, 1:24,000 Series (Topographic)

U.S. Geol. Survey (1968). Agat Quadrangle, Mariana Islands- Island of Guam, 1:24,000 Series (Topographic)

U.S. Geol. Survey (1968). Apra Quadrangle, Mariana Islands- Island of Guam, 1:24,000 Series (Topographic)

U.S. Geol. Survey (1968). Dededo Quadrangle, Mariana Islands- Island of Guam, 1:24,000 Series (Topographic)

U.S. Geol. Survey (1968). Inarajan Quadrangle, Mariana Islands- Island of Guam, 1:24,000 Series (Topographic)

U.S. Geol. Survey (1968). Merizo Quadrangle, Mariana Islands- Island of Guam, 1:24,000 Series (Topographic)

U.S. Geol. Survey (1968). Pati Point Quadrangle, Mariana Islands- Island of Guam, 1:24,000 Series (Topographic)

U.S. Geol. Survey (1968). Ritidian Quadrangle, Mariana Islands- Island of Guam, 1:24,000 Series (Topographic)

U.S. Geol. Survey (1968). Talofofo Quadrangle, Mariana Islands- Island of Guam, 1:24,000 Series (Topographic)

U.S. Geol. Survey (1968). Topographic Map of Guam, Mariana Islands, 1:50,000

VIDEOS

Andersen Air Force Base. IRP wells down-hole videos, a collection of VHS tapes, deposited at the Water and Environmental Research Institute of the Western Pacific, University of Guam, Mangilao, Guam.

Micronesian Divers' Association. Aquaquest Micronesia, VHS tape. Piti, Guam.

OTHER

Aerial photographs of Guam. Stereoscopic set, deposited at the Water and Environmental Research Institute of the Western Pacific, University of Guam, Mangilao, Guam.

Bureau of Planning, Government of Guam. Digitized ortho-corrected aerial photographs of Guam. Set of TIF files, 1 through 70.

Well logs. Collected by Guam Hydrologic Survey program, deposited at the Water and Environmental Research Institute of the Western Pacific, University of Guam, Mangilao, Guam.

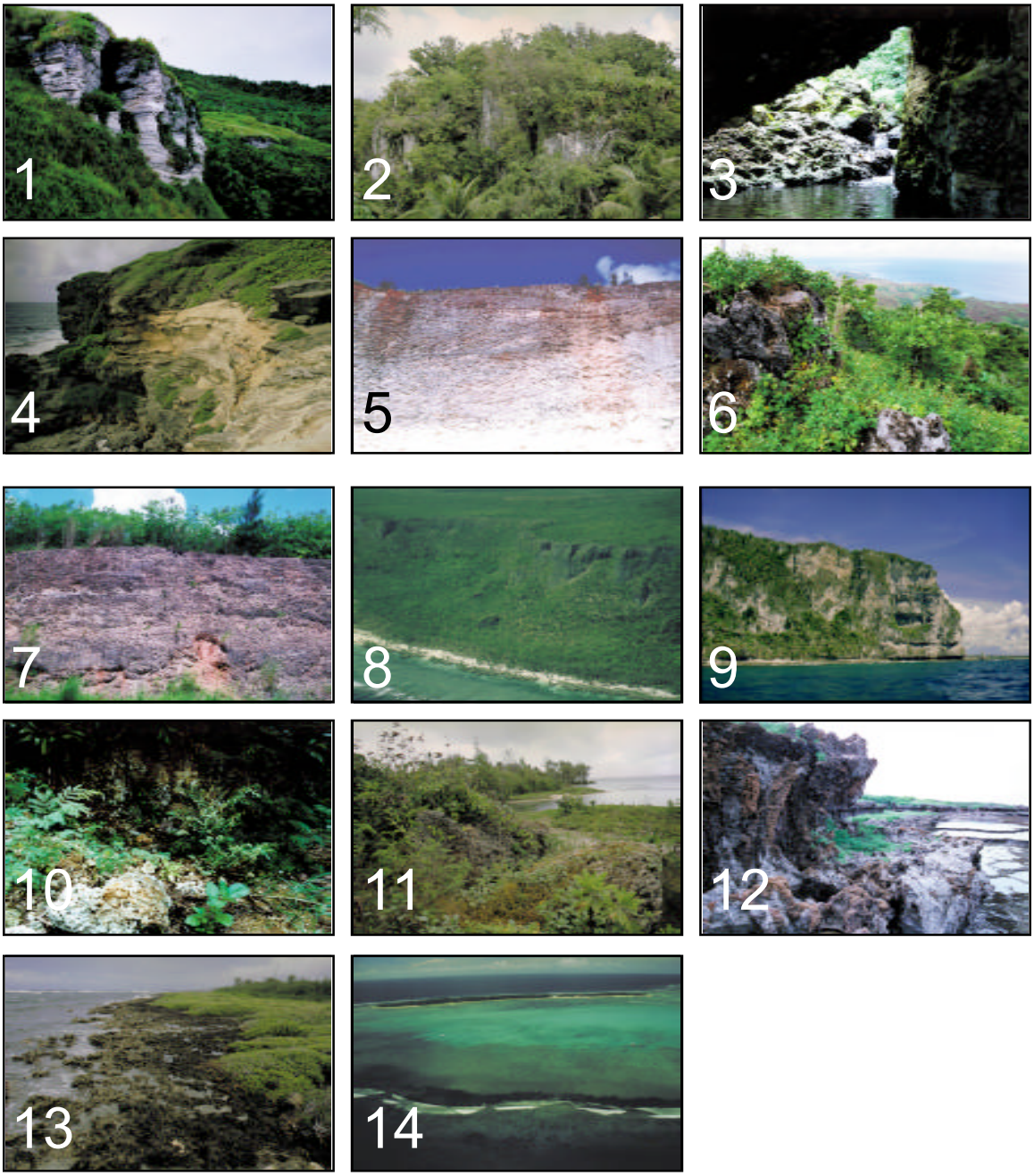

Plate 1: **Limestones in Guam:** 1) Outcrop of Maemong Limestone in the hills overlooking Sella Bay. 2) Outcrop of Maemong Limestone in central Guam, adjacent to Talofofo Golf Resort. 3) Bonya Limestone in Togcha River gorge. 4) Janum Formation in a small coastal embayment north of Catalina Point. 5) Barrigada Limestone exposed in the walls of Perez Brothers quarry. 6) Alifan Limestone at the top of Mt. Lamlam, the highest peak on Guam. 7) Talisay Member of Alifan Limestone, exposed in a roadcut along Route 2A in Piti. 8) Cliffs of Mariana Limestone Reef Facies in Ritidian. 9) Mariana Limestone Detrital Facies exposed in the cliff at Amantes (Two Lovers) Point. 10) Scattered boulders of Mariana Limestone Molluskan Facies in Yigo. 11) Outcrops of Mariana Limestone Forereef Facies just north of Togcha River mouth. 13) Merizo Limestone on the back side of Cocos Island. 14) Modern barrier reef encompassing the Cocos Lagoon.

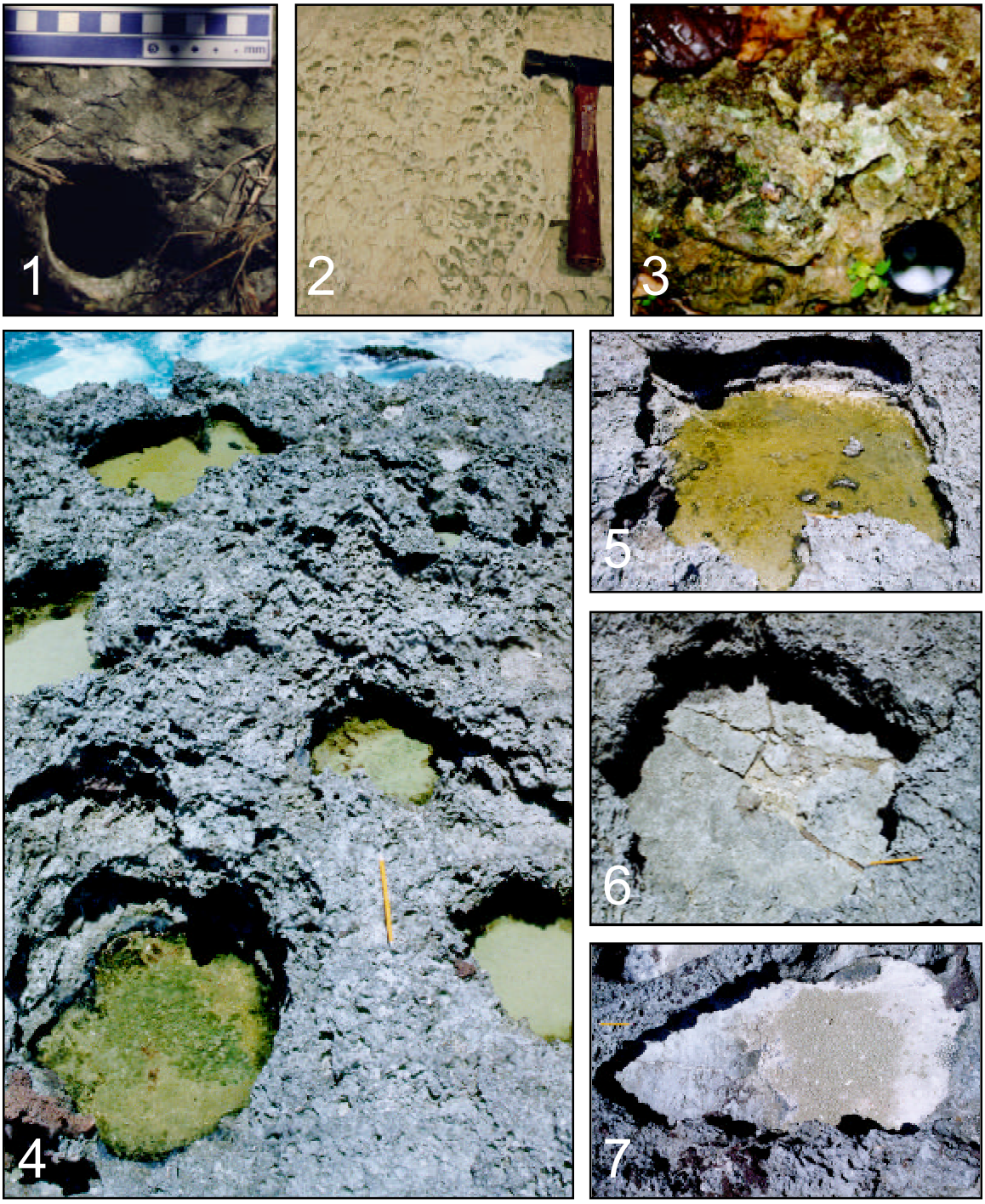

Plate 2. **Etched karren forms from solutional attack on massive bedrock:** 1) solution pit in a Mariana Limestone reef facies rock. 2) rain pits in Janum Limestone. 3) spitzkarren sculpturing in inland Mariana limestone rocks. 4) a cluster of littoral kamenitza-like solution basins on the coast at Campanaya Point. 5) a joint-controlled littoral solution basin (notice two joints intersecting at a 90° angle). 6) inactive solution basins due to widened joints. 7) an elongate solution basin developing along a single joint. 8) salt crystals in a coastal evaporation basin.

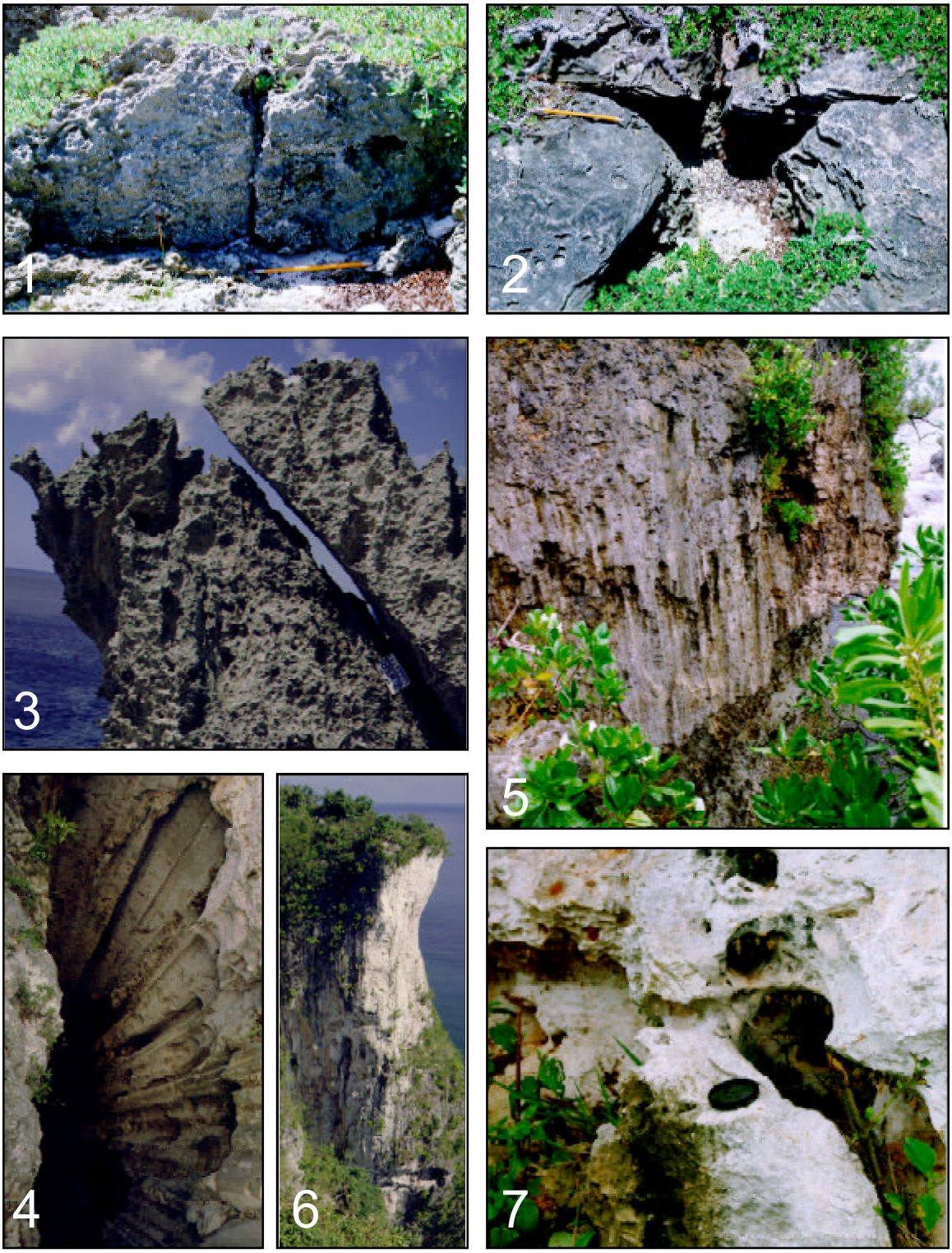

Plate 3. **Etched karren forms from solutional attack on structural weaknesses:** 1) kluftkarren and groovekarren in coastal rocks south of Taguan Point. 2) kluftkarren and star-shaped pit development at joint intersections, coastline south of Taguan Point. 3) splitkarren, in coastal rocks north of Haputo Beach. **Hydraulic karren forms:** 4) partial rillenkarren in coastal rocks in Double Reef area. 5) spectacular rillenkarren in the walls of Amantes Point pit cave. 6) decantation flutings on Amantes Point cliff. **Mixed hydraulic and structural control karren forms:** 7) pit and tunnel karren in an unearthed boulder of Mariana Limestone in Finagayan.

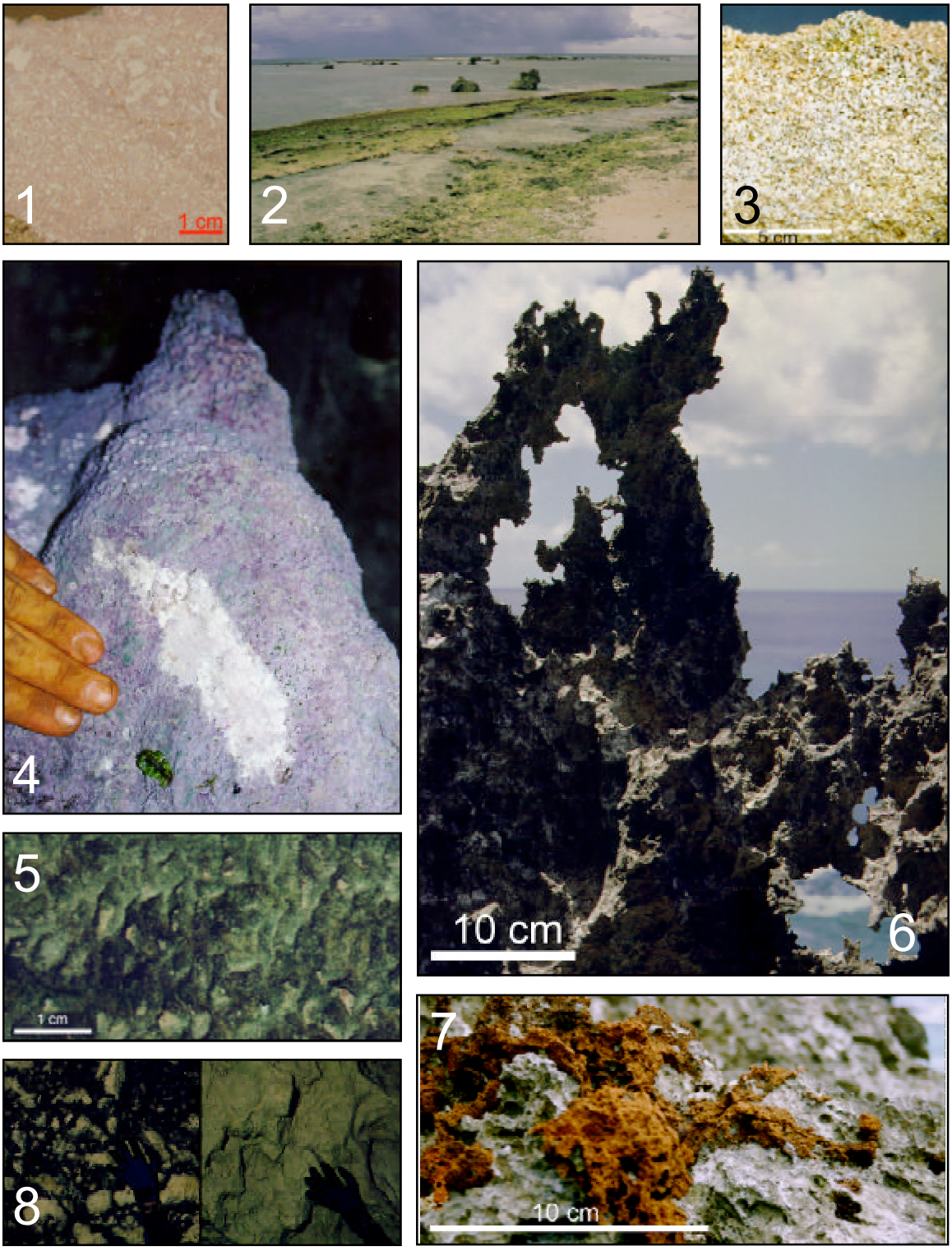

Plate 4. **Cementation phenomena in northern Guam:** 1) calcrete from a sinkhole in Tarague. 2) beach rock at Tarague. 3) cross-section of a beach rock. **Destructive phytokarst of northern Guam:** 4) amorphous phytokarst on a decaying speleothem. 5) grooves similar to directed phytokarst, covered by green algae, in a cave in Ritidian. 6) spectacular example of littoral phytokarst lacework morphology. 7) solutioned paleosol pockets in littoral phytokarst (note lack of algae-indicating dark color). 8) solution pits in Coconut Crab Cave with (left) and without (right) a black algal coating.

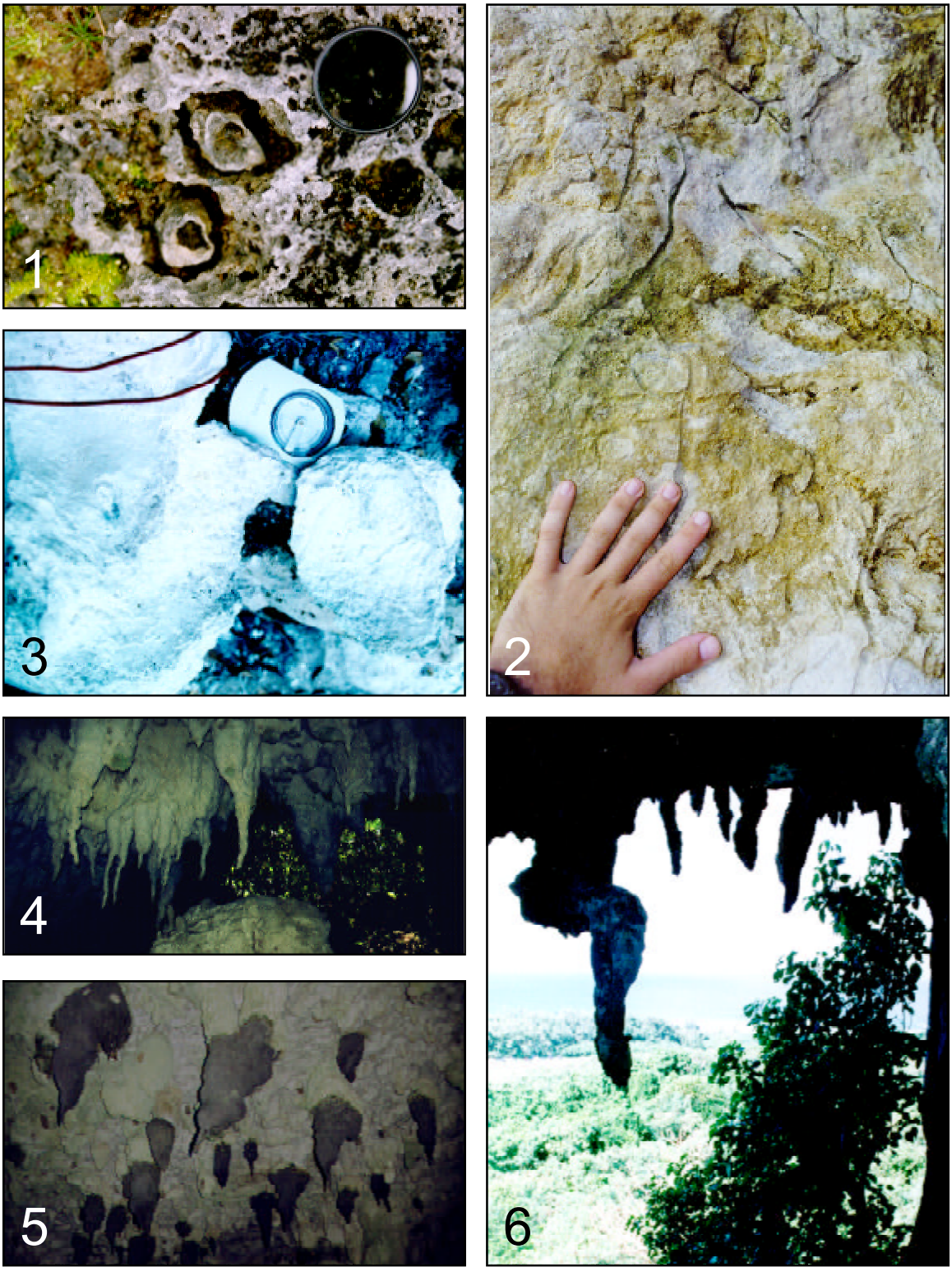

Plate 5. **Root-action phytokarst of northern Guam.** 1) possible root-action accretion features in reef rock near Double Reef. 2) root grooves from a collapse boulder wall at Mergagan Point. **Constructive phytokarst from northern Guam.** 3) cross-section of a tufaceous stalagmite from Ritidian. 4 and 5) directed mud-like speleothems from a low cave entrance in Ritidian. 6) non-vertical speleothems from a cliff-side cave entrance in Ritidian.

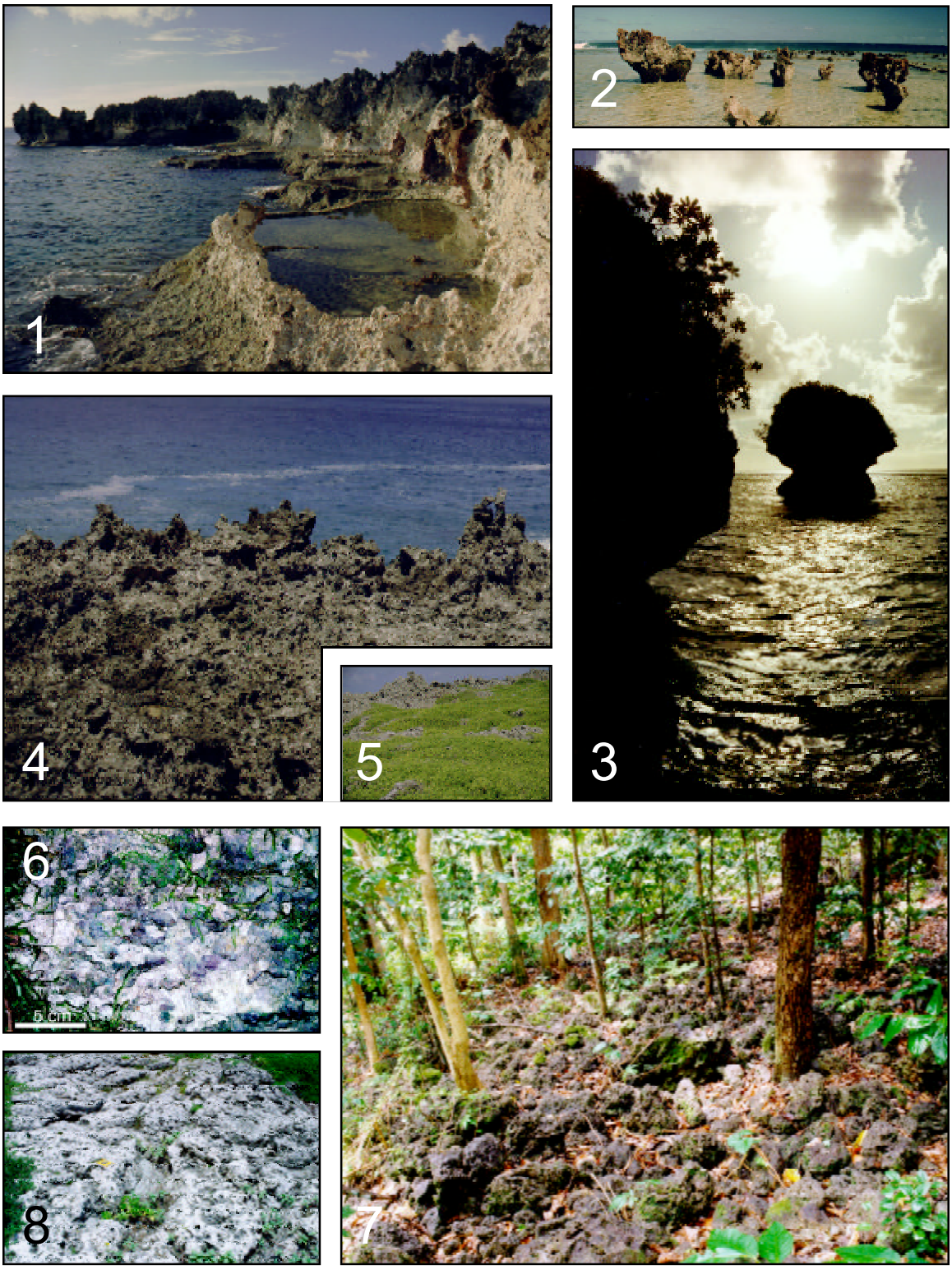

Plate 6. **Karrenfelds (karren assemblages of northern Guam):** 1) littoral karst at Ague point. 2) Pleistocene reef remnants on a modern reef. 3) mushroom rocks in Hilaan. 4) littoral phytokarst at Haputo Point. 5) vegetated phytokarst at Anao Point. 6) inland rainfall solution features from Mangilao. 7) stony grounds in the limestone forest at Double Reef. 8) karst pavement-like surface near Fadian Point.

Plate 7. **Karren and phytokarst features of southern Guam:** 1) groovekarren in foraminiferal Maemong limestone, in the outcrops overlooking Sella Bay. 2) "grike-canyon" in the same area. 3) ridges separating sinkholes in Fena area cockpit karst. 4) rinnenkarren runnels in Bonya limestone. 5) tufa deposits in small waterfalls. 6) karst pavement from Alifan Limestone mountain ridge, in the vicinity of Mt. Lamlam.

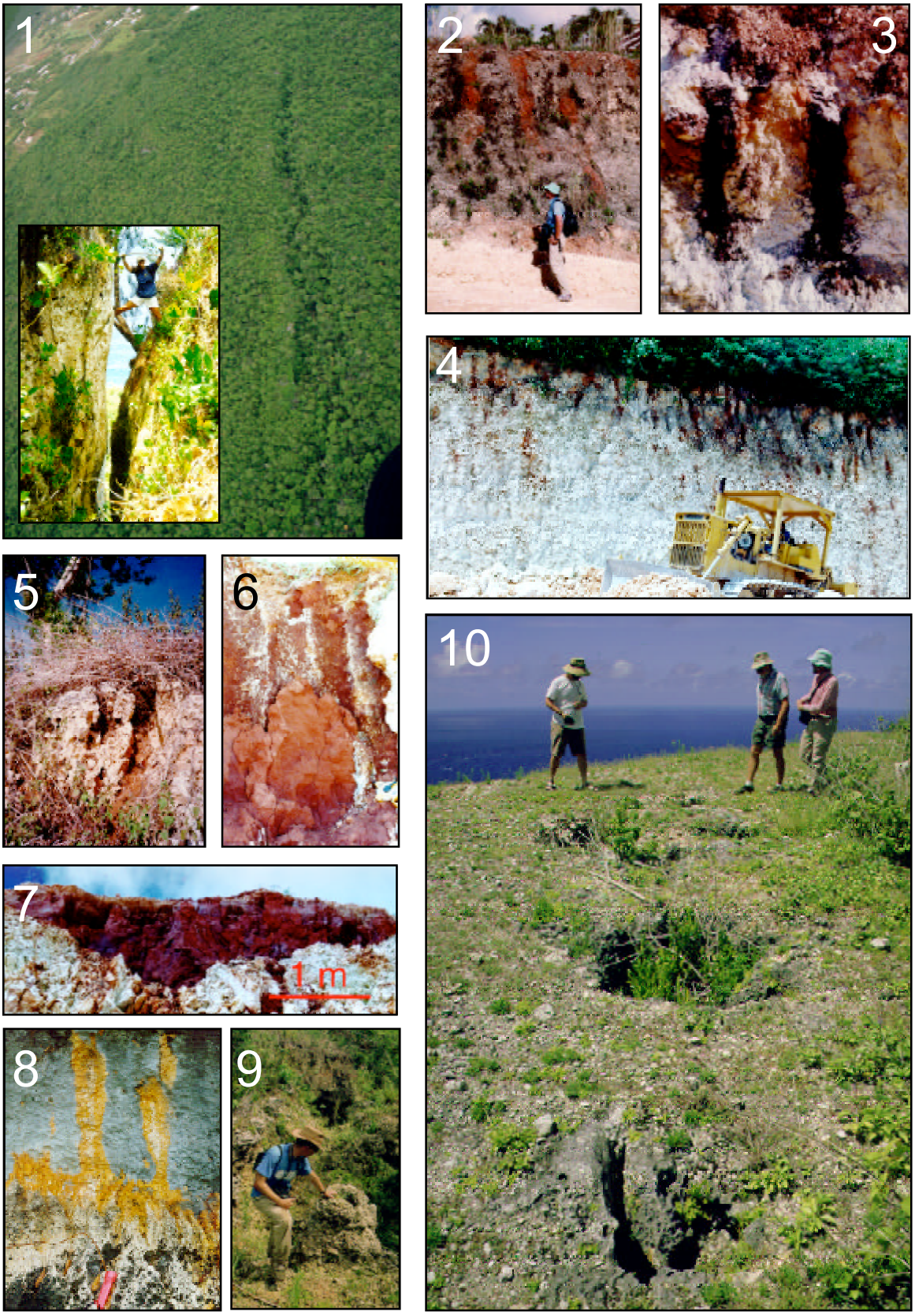

Plate 8: **Soil pipes and other features of the epikarst.** 1) Prominent fault east of Mt. Santa Rosa. Inset: Mati Point cliff where the same fault intersects the cliffline. 2) and 3) soil pipes in the walls of Perez Brothers Quarry. 4) soil pipes in quarry walls near Harmon Sink. 5) soil pipe in Mariana Limestone from Talofofo. 6) soil pipes made by soil infilling of adjacent vadose shafts, in Harmon. 7) soil-infilled basin in Perez Brothers Quarry. 8) paleosol in soil pipes in Qtma rocks in Inarajan. 9) a cast of a paleo vadose shaft, from Harmon Sink. 10) shallow shaft-like solution features from a cliff rampart overlooking Tarague Embayment.

photo by David T. Vann

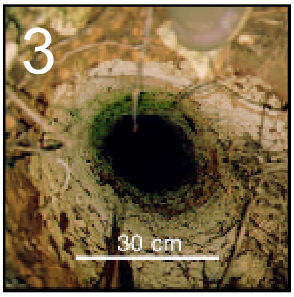

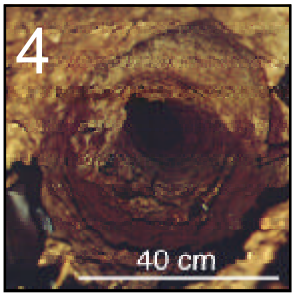

Plate 9: **Vadose by-passes.** 1) a vadose shaft in Agana Argillaceous Member of the Mariana Limestone (note previous soil infilling of the shaft, now paleosol). 2), 3) and 4) vertical shafts from Harmon sink (note soil walls in photo 3 and bedrock walls in photo 4). 5) remnants of a shaft cluster in a displaced boulder. 6) pit cave at Amantes (Two Lovers) Point. 7) pit cave at Taga'chang Beach. 8) a group of wells in a depression on Andersen Air Force Base.

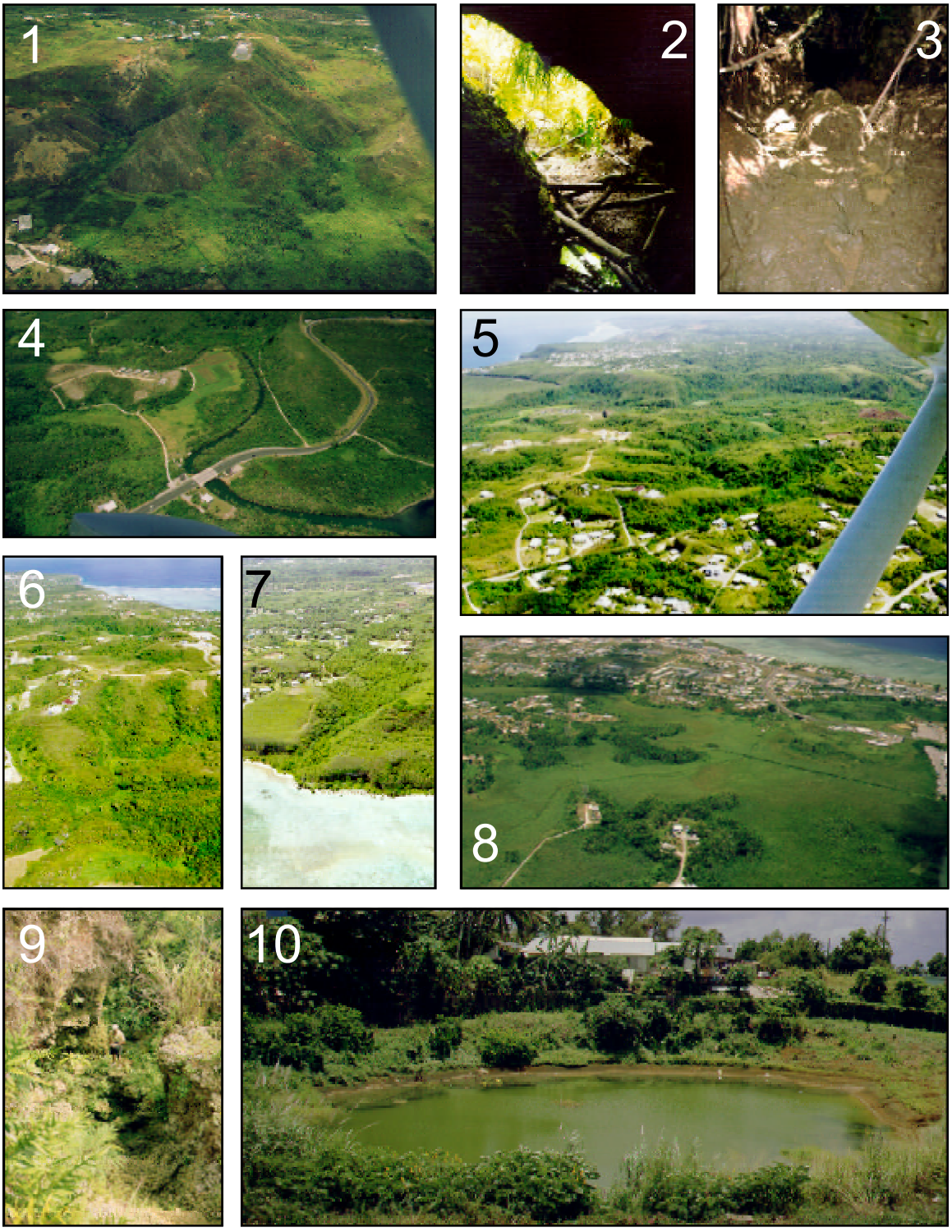

Plate 10: **Surface drainage karst features from northern Guam.** 1) An aerial view of Mt. Santa Rosa, a volcanic inlier in northern Guam (note incised ephemeral stream valleys). 2) entrance of Mataguac Spring Cave, a ponor of an ephemeral allogenic stream. 3) a sediment-clogged ponor of an ephemeral allogenic stream, leading to Awesome Cave. 4) an aerial view of a portion of Pago River, a developed allogenic stream flowing over karst. 5) an area in Chalan Pago deeply incised by dry valleys. 6) an aerial view of dry valleys in Guacluluyao area in Chalan Pago. 7) an aerial view of a small dry valley leading to Pago Bay. 8) One of the ponors in the blind valley terminating in Harmon Sink. 9) an aerial view of the Agana swamp. 10) Perching of water in a shallow closed contour depression in Mangilao.

Plate 11: **Surface drainage karst features from southern Guam.** 1) Talofofo and Asalonso bays, mouths of two large southern through streams. 2) Togcha River mouth and channel. 3) Togcha River gorge. 4) Upper portions of Togcha gorge, exhibiting significant flow on July 17, 1999. 5) Lower portions of Togcha valley, with no flow on the same date, July 17, 1999. 6) Resurgence of Tolae Yu'us river.

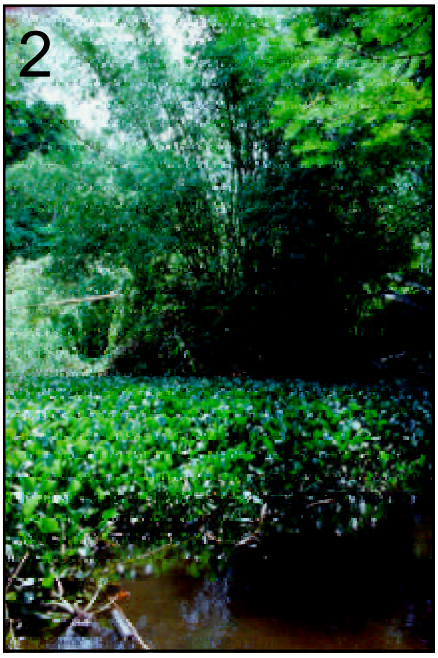

Plate 12: **High level springs in Guam.** 1) Mataguac Spring. 2) Pond at Agana Spring. 3) Concrete reservoir and gauge at Asan Spring. 4) Almagosa Spring and the entrance to Almagosa Cave.

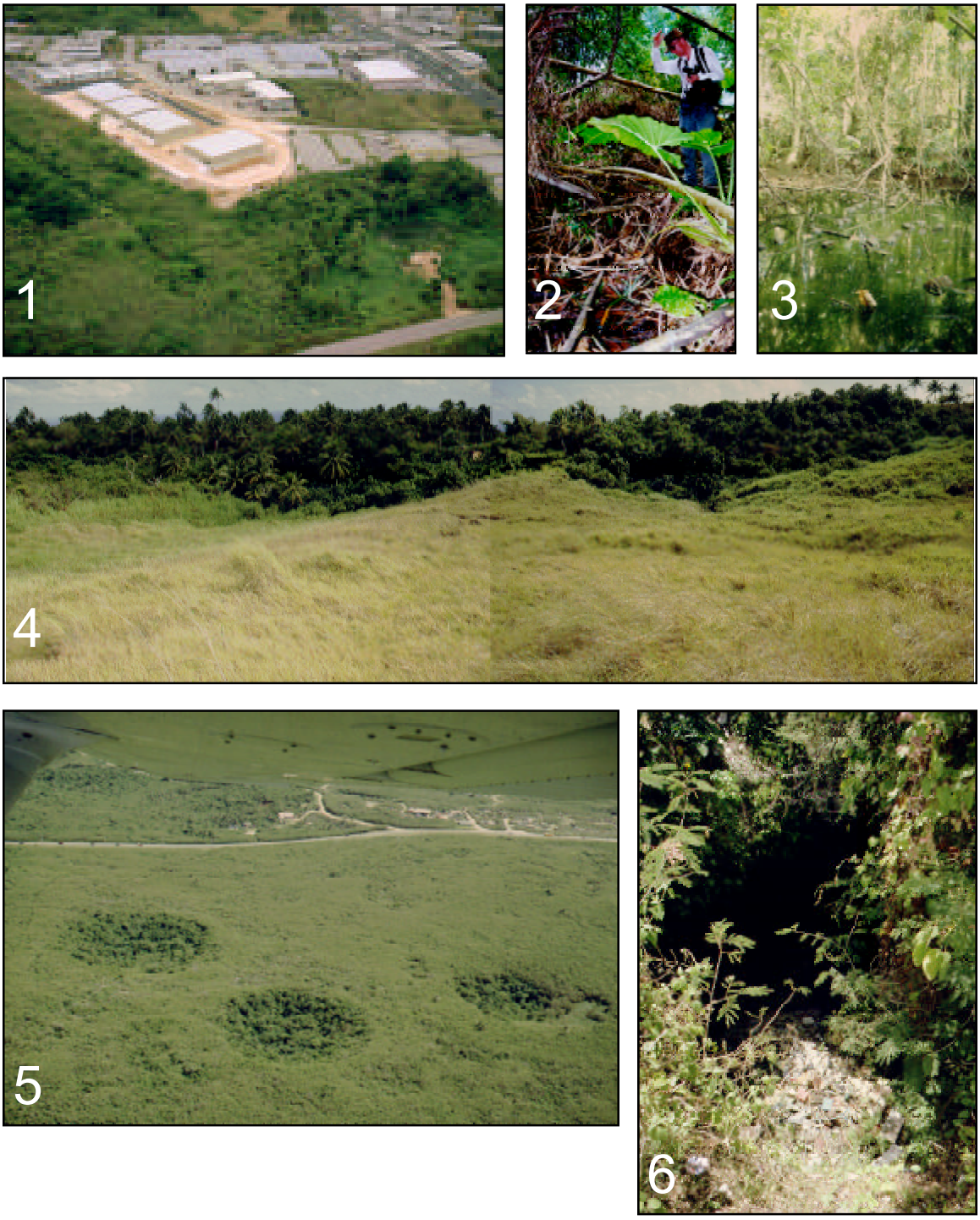

Plate 13: **Sinkholes from northern Guam.** 1) An aerial view of Harmon Sink. 2) bottom of Mataguac Spring Sink (note hydrophilic vegetation and a small stream accross the sinkhole floor). 3) an ephemeral pond forming in a sinkhole on the northern edge of Mataguac Hill. 4) Awesome and Interesting sinks and the volcanic rock ridge separating them. 5) an aerial view of Pinate sinkhole cluster. 6) collapsed Carino Sink in Chalan Pago.

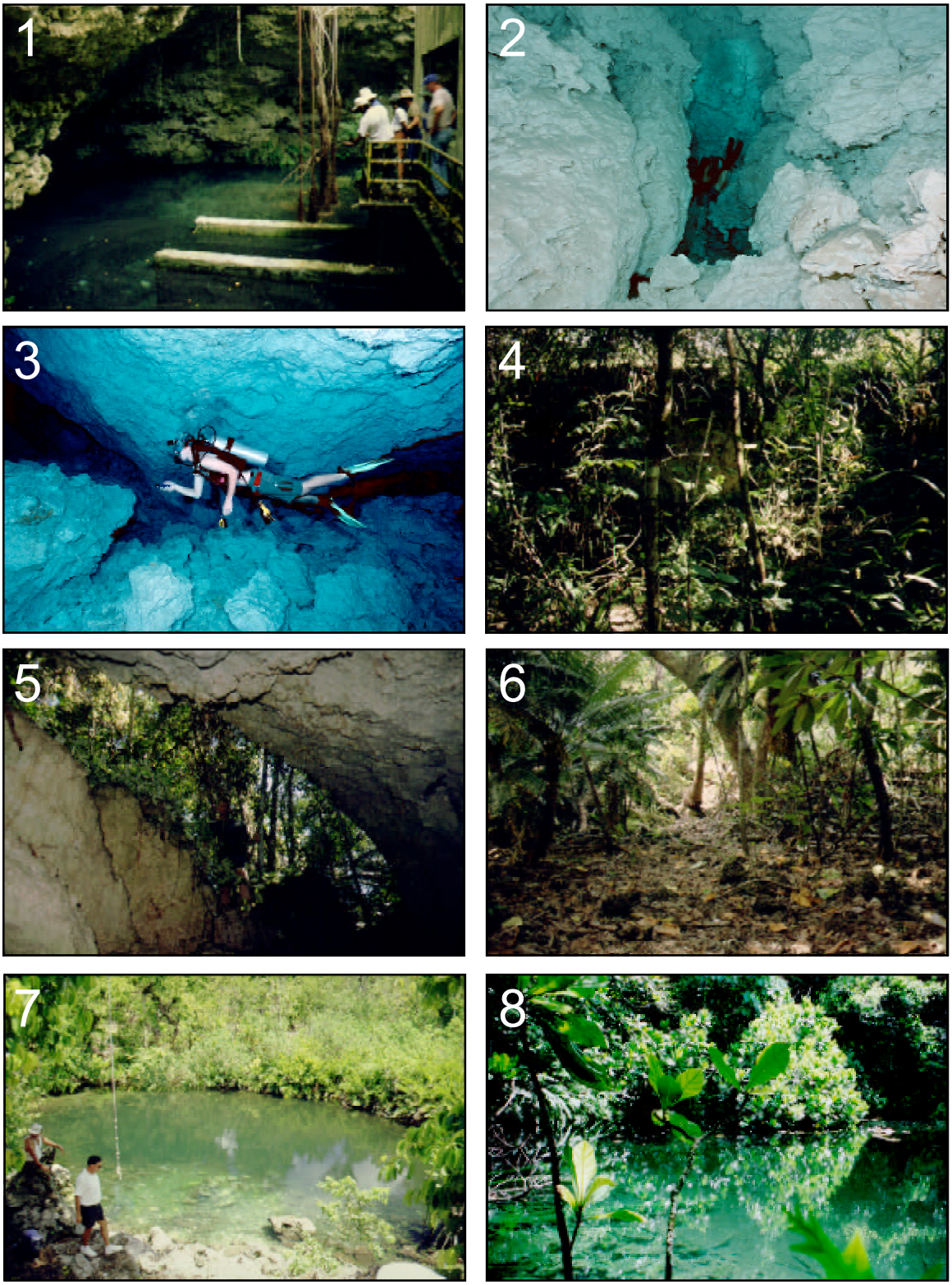

Plate 14: **Examples of cenotes from northern Guam.** 1) collapse sinkhole Tarague Well #4. 2) A fracture in the submerged portion of Tarague Well #4 leading to an additional submerged chamber, at a depth of 15 m. 3) submerged portion of Tarague Well #4; note collapse features in ceiling and floor of the cave. 4) collapsed vertical wall of Tarague Well #2. 5) A view from shelter cave in Tarague Well #3. 6) Flat, sediment-filled bottom of Tarague Well #3. 7) The Lost Pond (Hilaan Pool), a popular picnic spot. 8) Hawaiian Rock Sinkhole #2.

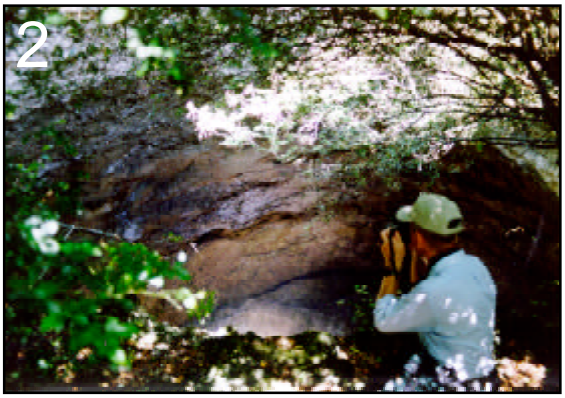

Plate 15: **Sinkholes and other depressions from northern Guam:** 1) Finagayan Banana Hole. 2) Devil's Punchbowl. 3) Guacluluyao valley sink (north). 4) fish pond made in Guacluluyao valley sink (south). 5) Gayinero Sink. 6) a probable depositional depression in AAFB NW Field. 7) a typical ponding basin. 8) a natural sinkhole modified into a ponding basin. 9) Perez Brothers Quarry. 10) EOD crater in AAFB Northwest Field.

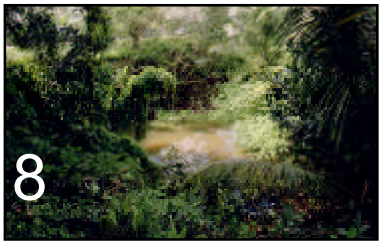

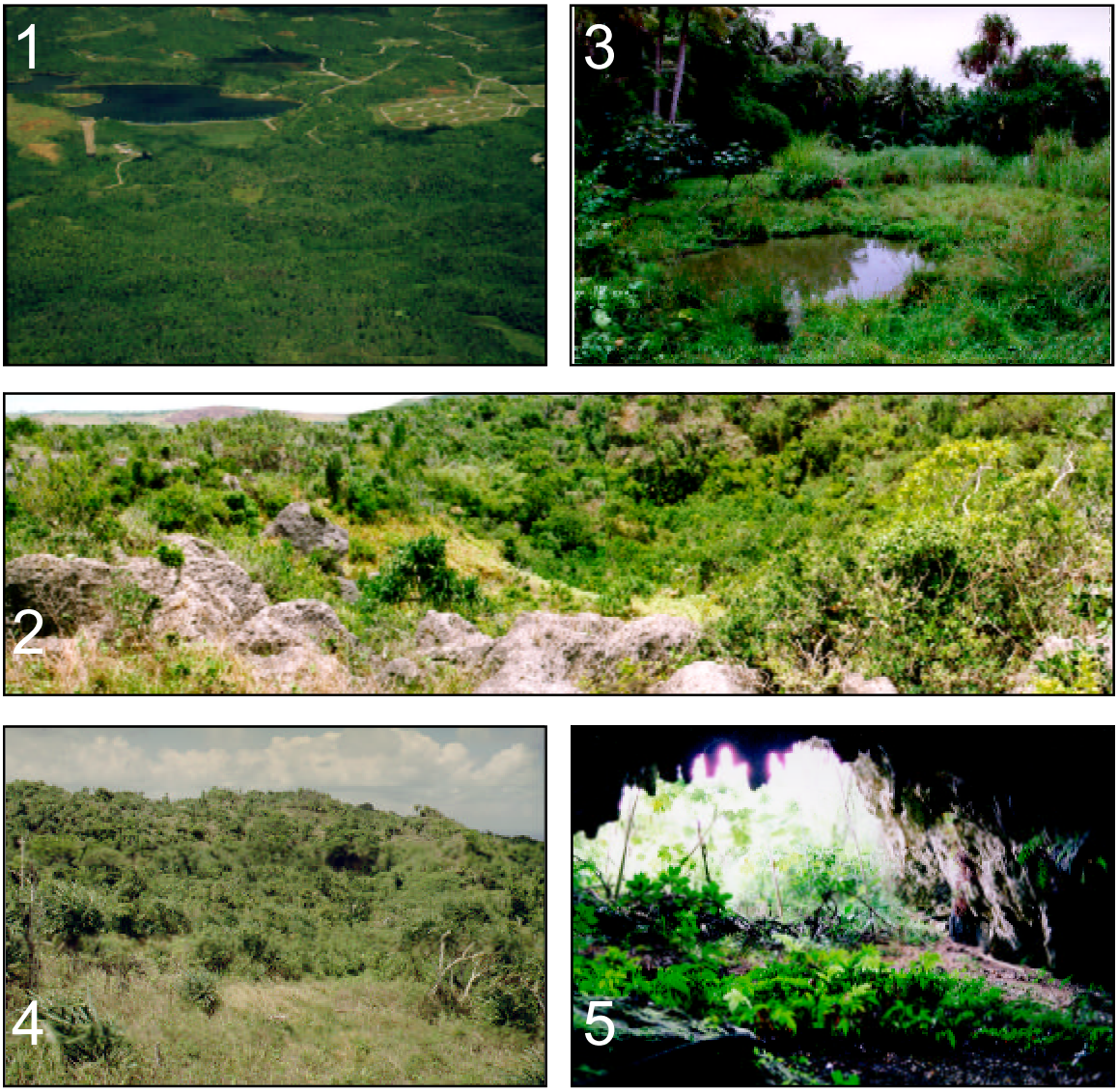

Plate 16: **Examples of sinkholes from southern Guam.** 1) Cockpit karst area northeast of the Fena Reservoir. 2) a typical cockpit sinkhole with a narrow limestone ridge separating it from its neighbors. 3) a pond in a cockpit karst sinkhole in Navy Magazine area, fed by a permanent stream. 4) a sinkhole on the Alifan Limestone mountain ridge. 5) shelter cave in Ito and Minagawa's Sink.

Plate 17: **Volcanic contact stream caves.** 1) entrance to Mataguac Spring Cave. 2) two passage levels in Mataguac Mud cave-- bottom is vadose, top is phreatic. 3) destruction of Third Mataguac Cave by infilling. 4) active stream passage in Piggy Cave. 5) contact between Alutom volcanic units and overlaying limestone in the walls of Piggy Cave. 6) volcanic fragments cemented by flowstone, Piggy Cave. 7) a pool in Piggy Cave stream passage. 8) room in Piggy Cave made by progradational collapse. 9) vadose flutes in Piggy Cave.

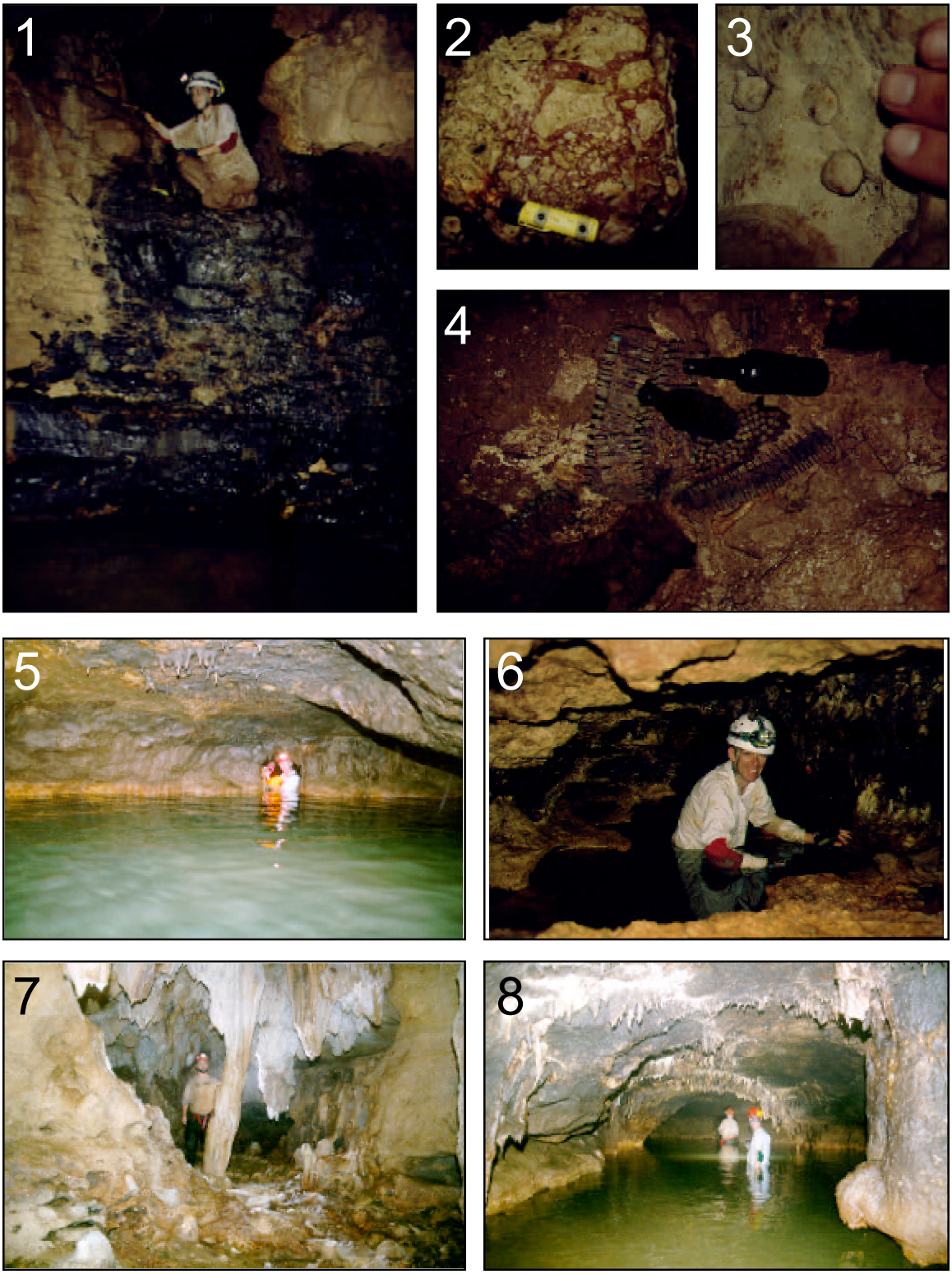

Plate 18: **Awesome Cave.** 1) actively downcutting vadose stream passage. 2) soil breccia. 3) cave pearls. 4) World War II artifacts. **Almagosa Cave.** 5) permanent stream passage feeding Almagosa Spring. 6) vadose passage that occasionally floods-- note solutional scallops and jagged features, result of dissolution and physical erosion. 7) one of the tributary passages in Almagosa Cave. 8) classic phreatic tube passage in Almagosa Cave.

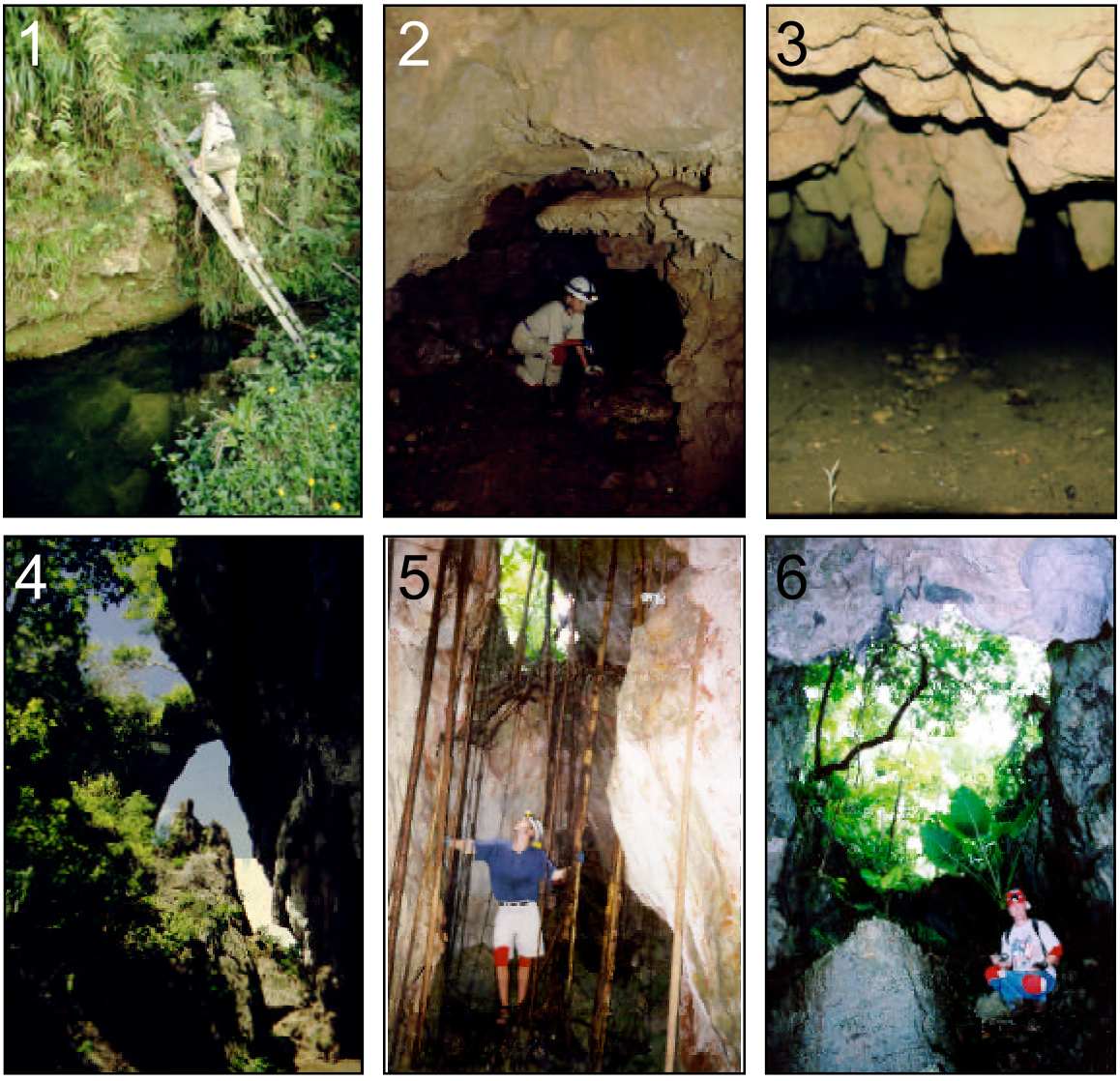

Plate 19: **Vadose caves from southern Guam.** 1) Entrance of the Lost River Rise Cliff Cave. 2) flowstone deposit indicating the level of previous sediment floor, in the Lost River Rise Cliff Cave. 3) Low passage in Fena Sinkhole Cave, with extensive mud deposits and organic material, an indication of ephemeral flow. 4) Window Rock in the Talofofo Caves complex. 5) a narrow passage developed along a fracture in one of the Nimitz Hill caves. 6) collapse entrance to Japanese Cave in Nimitz Hill.

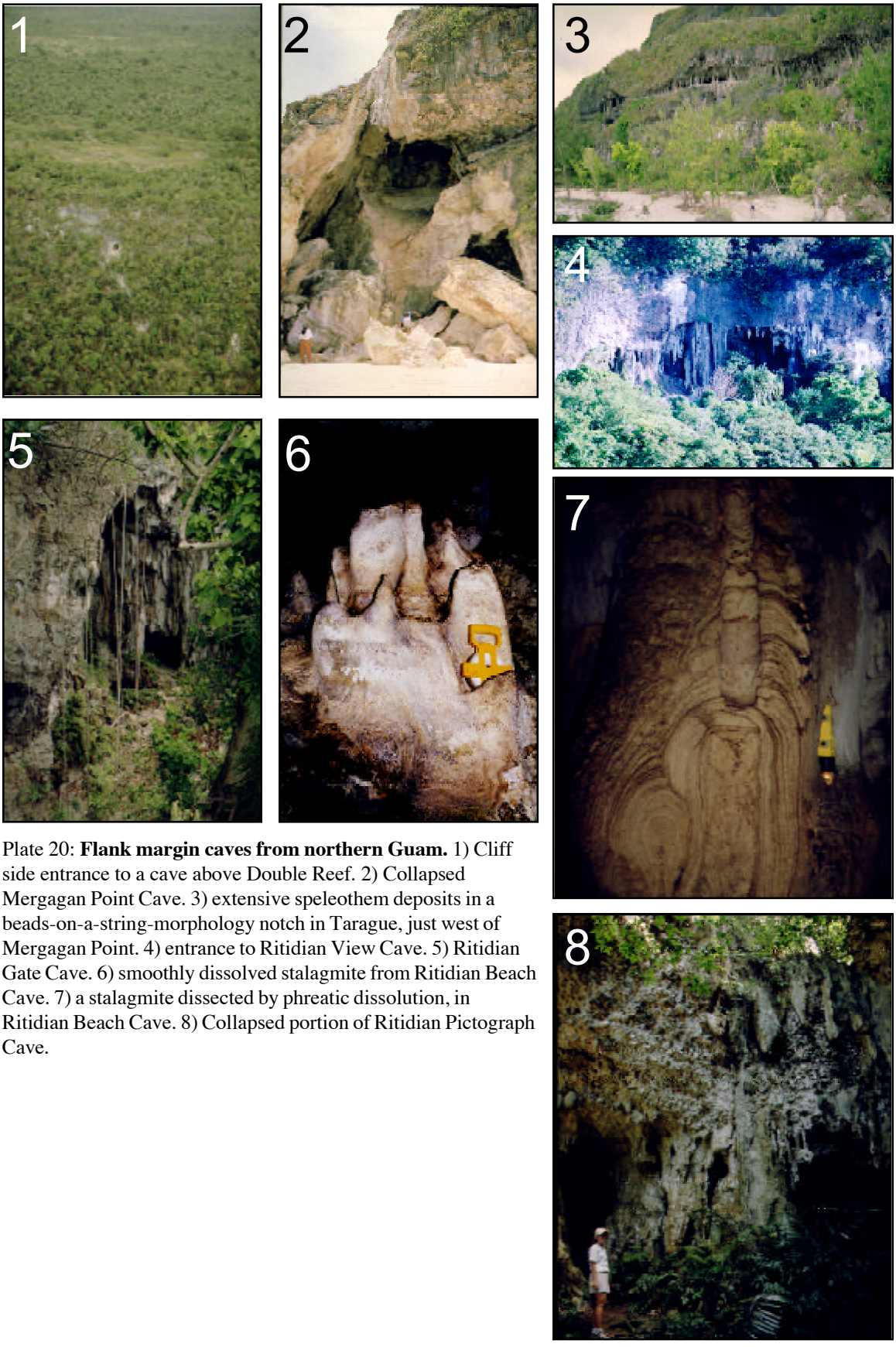

Plate 20: **Flank margin caves from northern Guam.** 1) Cliff side entrance to a cave above Double Reef. 2) Collapsed Mergagan Point Cave. 3) extensive speleothem deposits in a beads-on-a-string-morphology notch in Tarague, just west of Mergagan Point. 4) entrance to Ritidian View Cave. 5) Ritidian Gate Cave. 6) smoothly dissolved stalagmite from Ritidian Beach Cave. 7) a stalagmite dissected by phreatic dissolution, in Ritidian Beach Cave. 8) Collapsed portion of Ritidian Pictograph Cave.

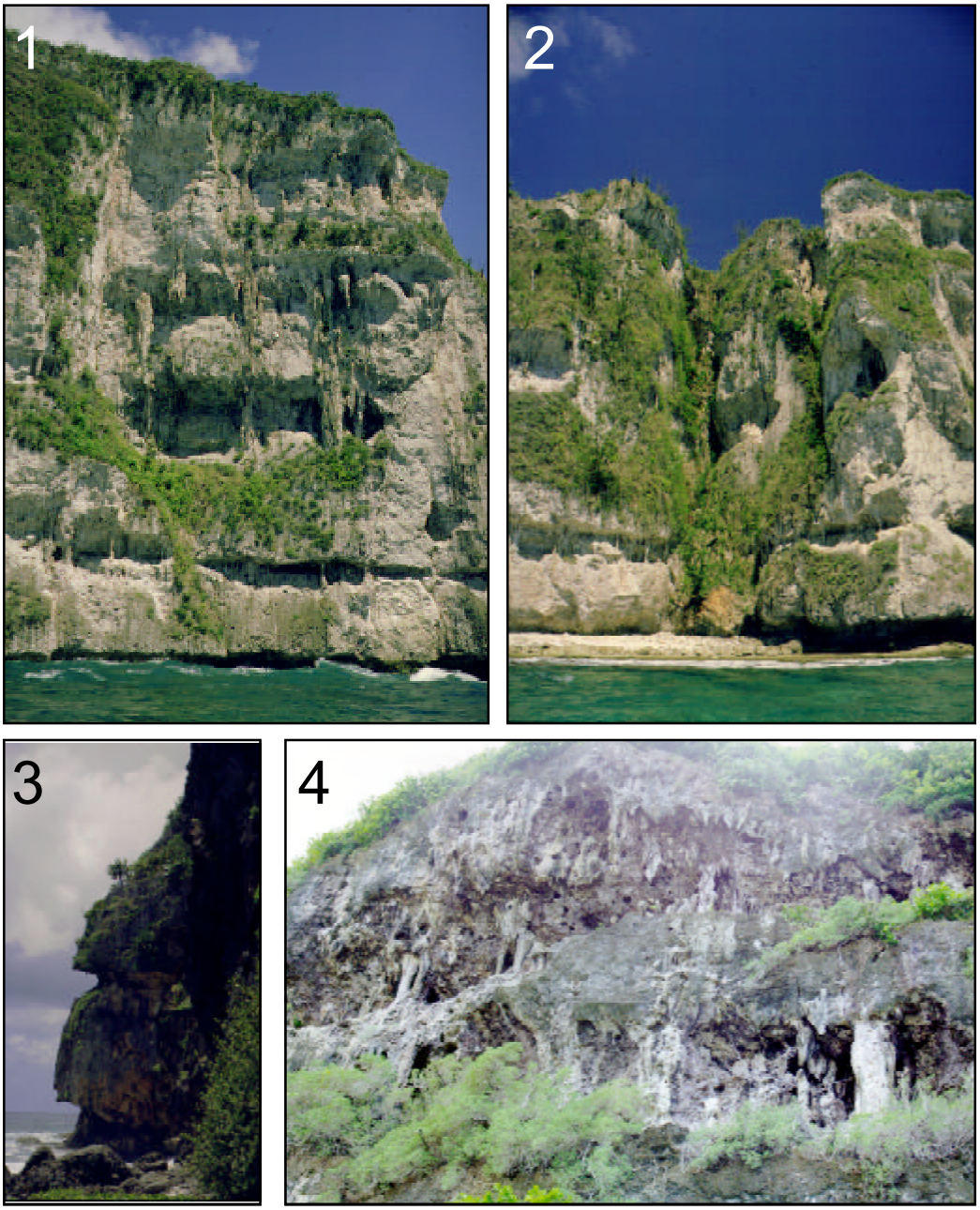

Plate 21: **Flank margin caves and cave-like features in northern Guam:** 1) Paleo-sea-level notches in Amantes Point cliff. 2) Pit caves breach-ing horizontal dissolution features, at Amantes Pt. 3) bioerosional notches at Iates Point. 4) notch in the cliff at Mergagan Pt., with extensive speleothem deposits.

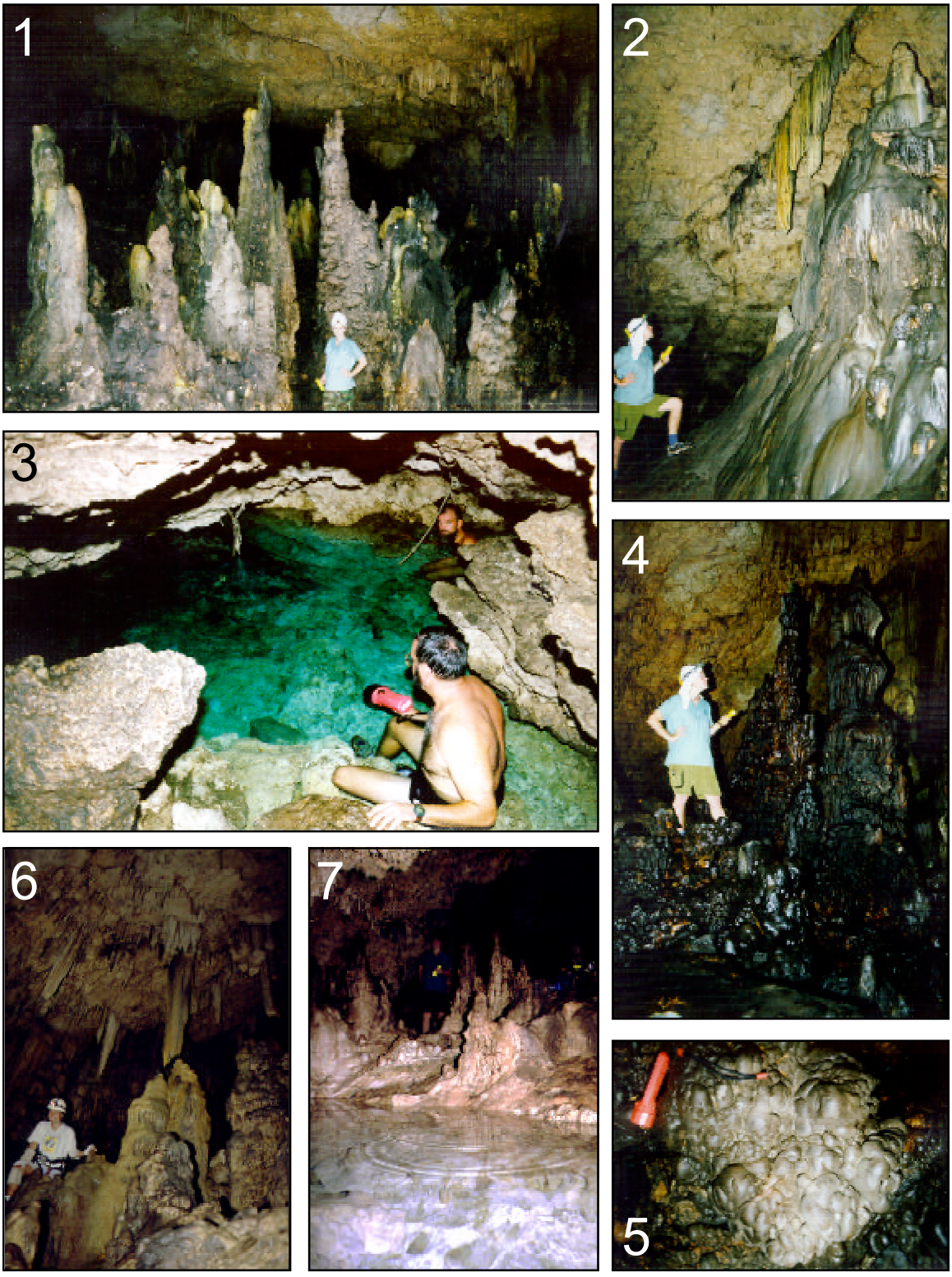

Plate 22: **Ritidian Cave:** 1) Massive stalagmites in the main room. 2) stalactites growing along a ceiling fracture. 3) freshwater pool, leading to submerged passages. 4) Massive speleothems. 5) Close-up of a speleothem (note cover by black layer). **Castro's Cave:** 6) Speleothems in the bottom of Castro's Cave. 7) Freshwater pool.

Plate 23: **Collapse Caves with freshwater:** 1) Submerged room in Marbo Cave (note vadose features). 2) Extremely jagged mixing zone dissolution features in Marbo Cave at a depth of 7 m. 3) Room in Fadian Fish Hatchery Cave, developed along a fracture. 4) Joe Quitigua's Water Cave. 5) Hawaiian Rock Quarry Cave. 6) Freshwater pool in Fafai Cave. 7) extremely jagged dissolution features in collapse blocks in Fafai Cave, at sea level.

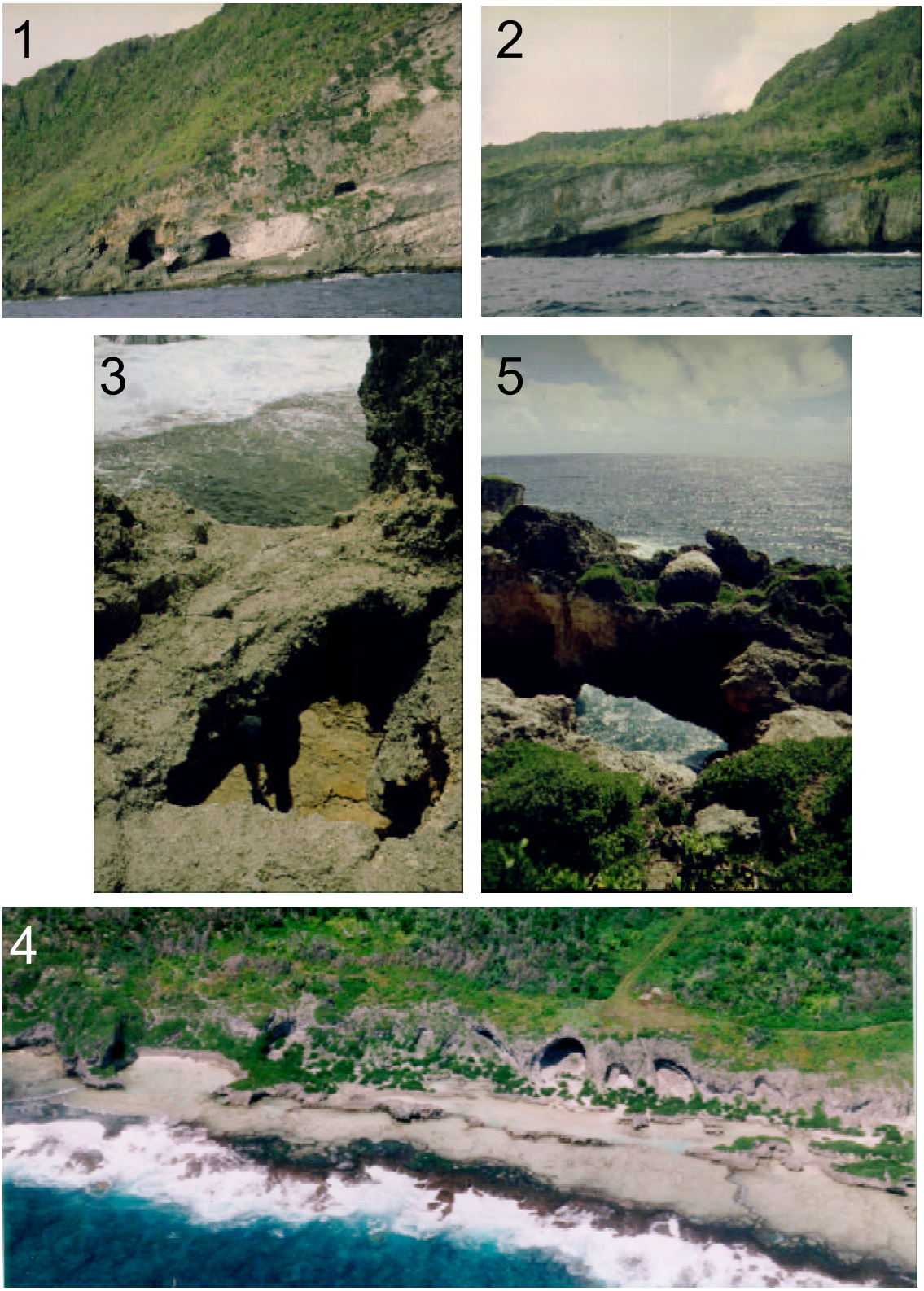

Plate 24: **Caves and related features from northern Guam's east coast:** 1) Coastal caves preferentially developed along bedding planes in limestone, at Anao Point. 2) Coastal caves preferentially developed along bedding planes in limestone north of Pagat Point. 3) One of several small caves at the contact of Janum Formation and Mariana Limestone, near Catalina Point. 4) Pagat Arch. 5) North Catalina Beach Caves.

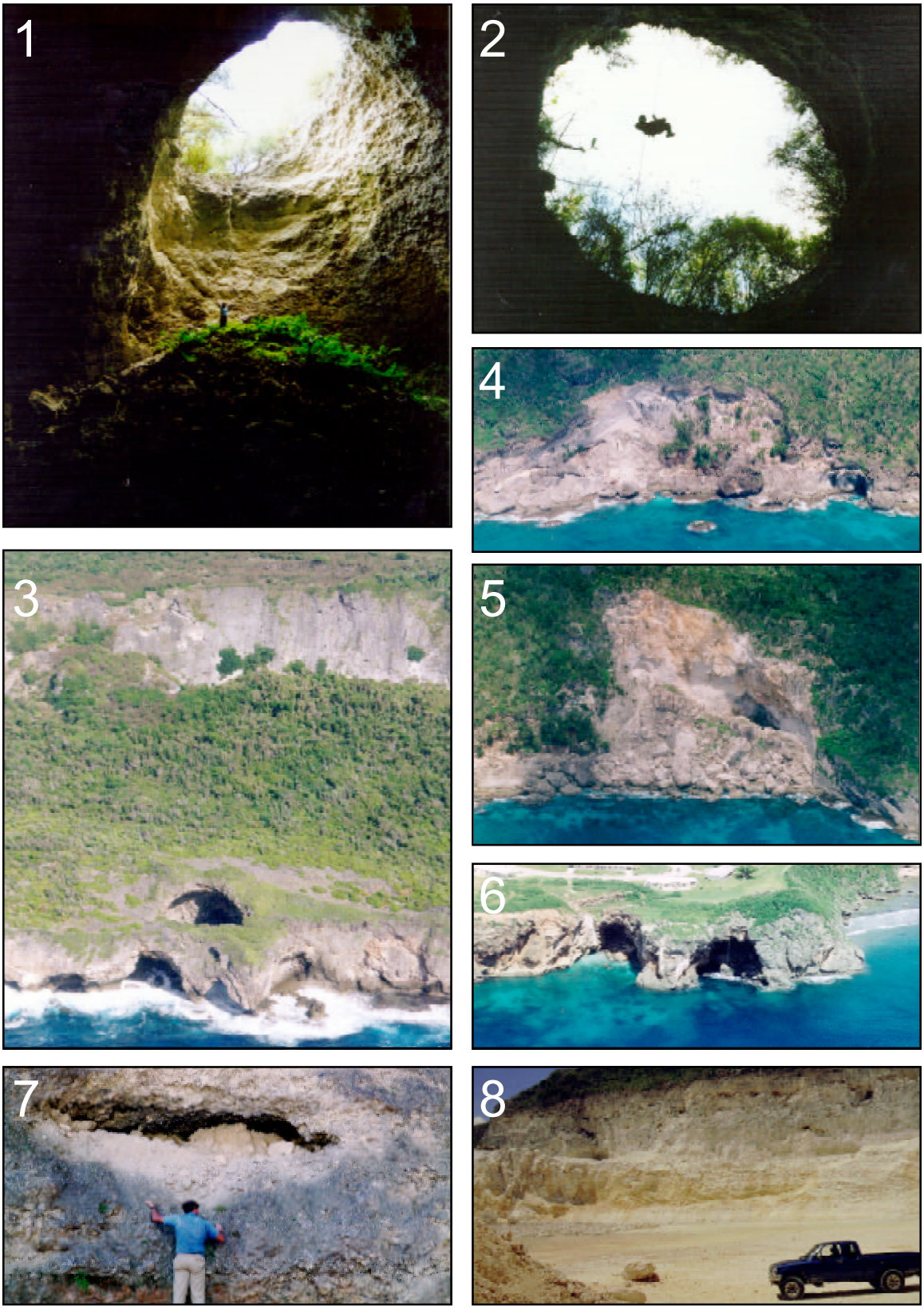

Plate 25: **Phreatic voids and collapse features from northern Guam:** 1) and 2) Devil's Punchbowl. 3) Lafac Grotto. 4) and 5) Large collapse scars in the cliffs between Lujuna Point and Pagat Point. 6) Orote Grottos. 7) an isolated void in the walls of Perez Brothers quarry. 8) a series of voids arranged along a horizon, in the walls of Hawaiian Rock quarry.

photo by Ed Crisostomo

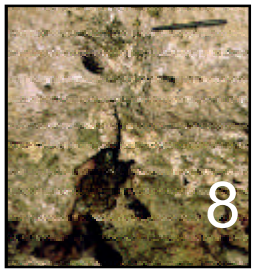

Plate 26: **Coastal springs in northern Guam.** 1) Beach springs in at Park Hotel in Tumon Bay. 2) Prolific growth of green algae in a beach spring at Hilton Hotel in Tumon Bay. 3) a submerged beach spring bubbling at high tide. 4) coastal vrulja in Tumon Bay. 5) a collapsed "sinkhole" at a Tumon Beach spring. 6) coastal spring in Ritidian emerging underneath beach rock deposits. 7) and 8) small fracture fed springs in Double Reef area.

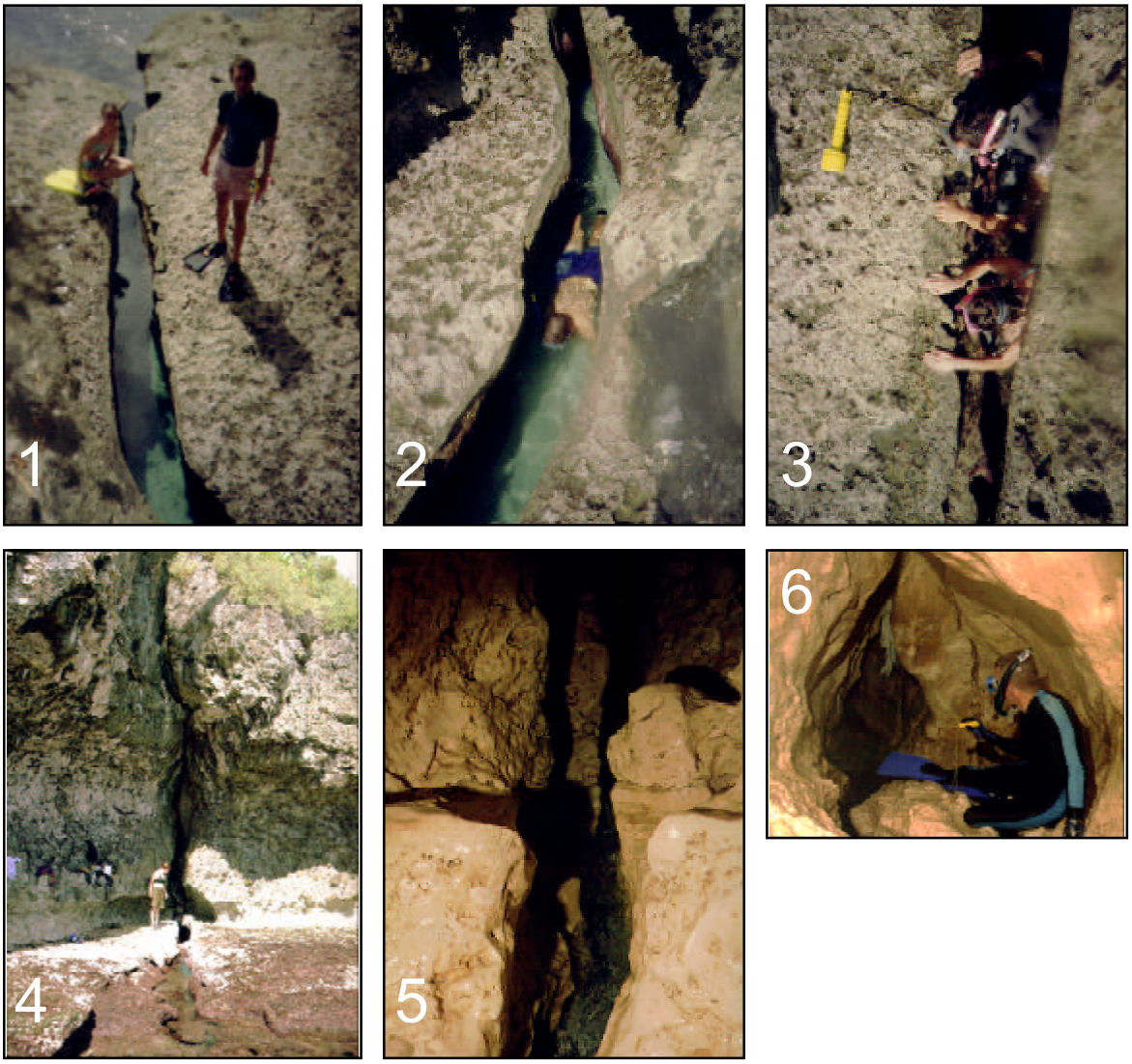

Plate 27: **Discharging fractures in northern Guam.** 1), 2) and 3) views of Scott's Fracture in Double Reef area. 4) mouth of the No Can Fracture. 5) No Can Fracture-- note fracture smooth fracture walls and a freshwater stream. 6) a teardrop shaped chamber in No Can Fracture, possibly a result of dissolution at a higher sea level still-stand. 7) a view from inside Menpachi Fracture. 8) Menpachi Fracture-- note phreatic dissolution features in fracture wall.

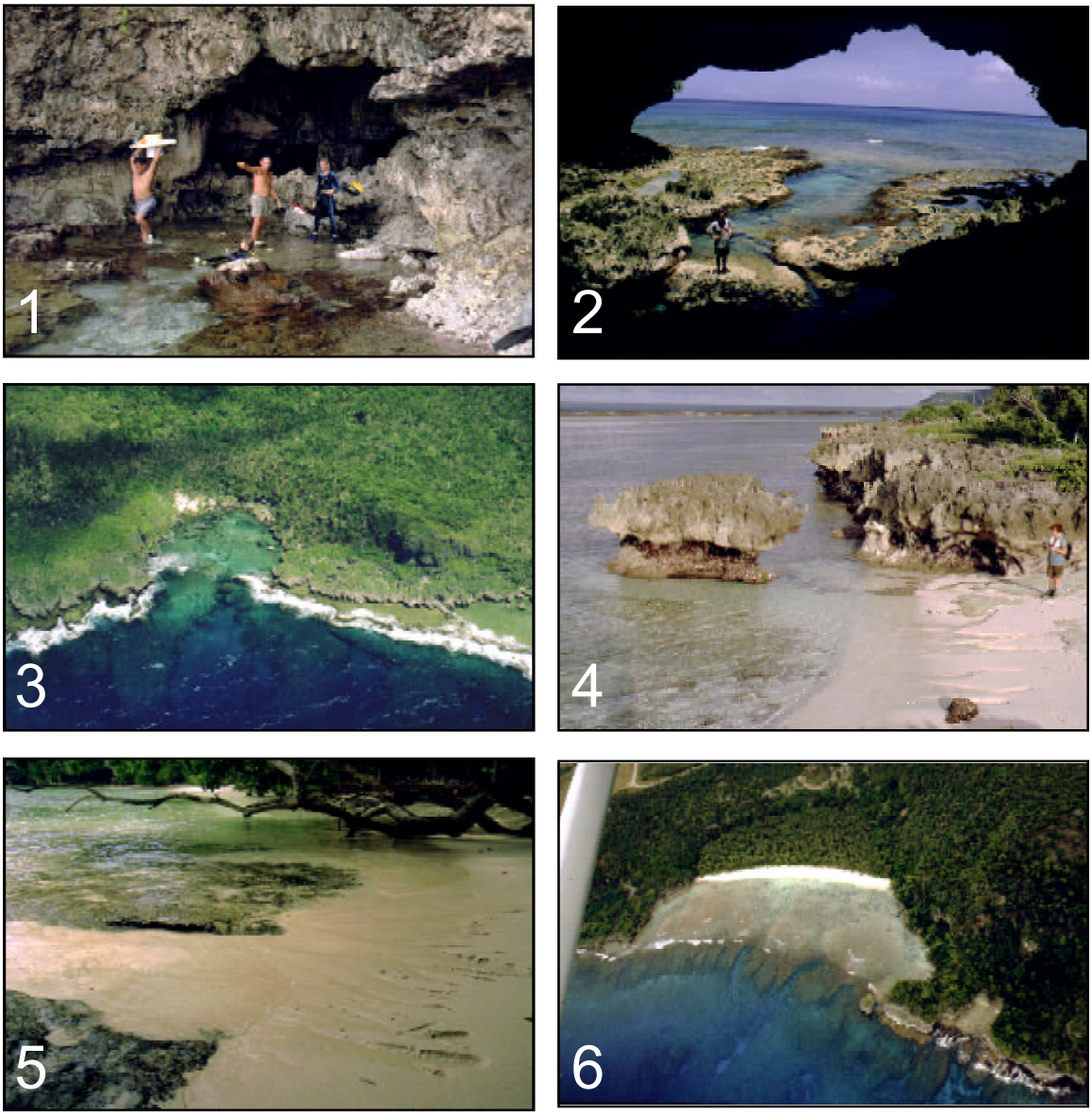

Plate 28: **Discharging caves and coastal geomorphology potentially associated with freshwater discharge.** 1) Coconut Crab Cave. 2) Arch Spring. 3) Fadian Cove. 4) one of several small coves between Ritidian and Tarague. 5) Double Reef Beach. 6) Haputo Beach.

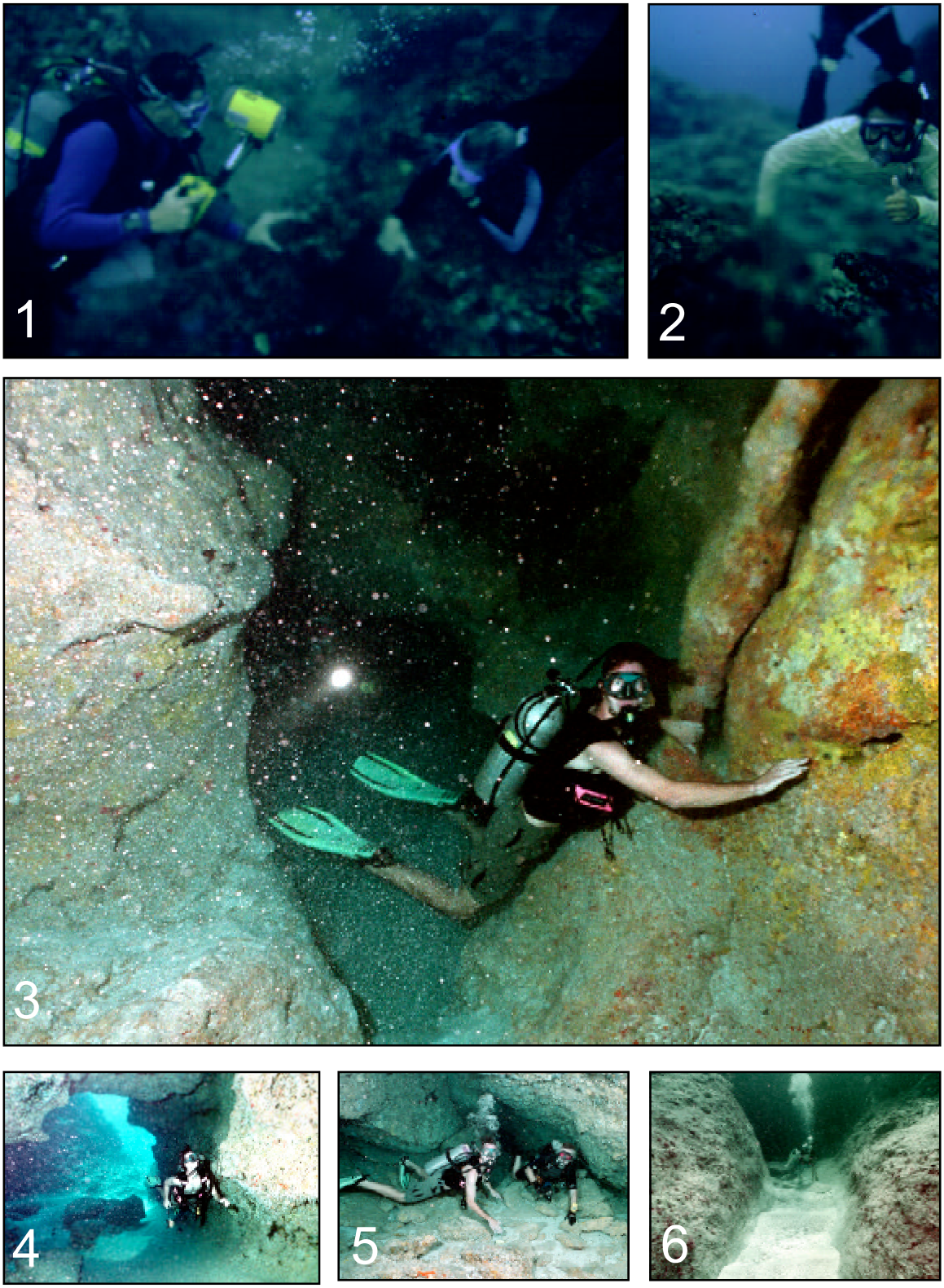

Plate 29: **Submarine freshwater discharge features.** 1) and 2) submarine vents north of Haputo Beach at a depth of 4 meters. 3) Freshwater discharge from fractures in Matt's Freshwater Cave. 4) and 5) Matt's Freshwater Cave. 6) outside portion of a submerged No-Can-like discharging fracture.

Plate 30: **Intertidal and submarine karst features.** 1) pools on a fringing reef platform in Inarajan. 2) Blue Hole, a submerged pit cave at Orote Peninsula. 3) Matt's Cave at a depth of 50 m at Palace Wall, Tamuning. 4) Piti Bomb Holes, probable submerged sinkholes. 5) Shark's Hole in Hilaan. 6) Inarajan Pools, probable submerged sinkholes.

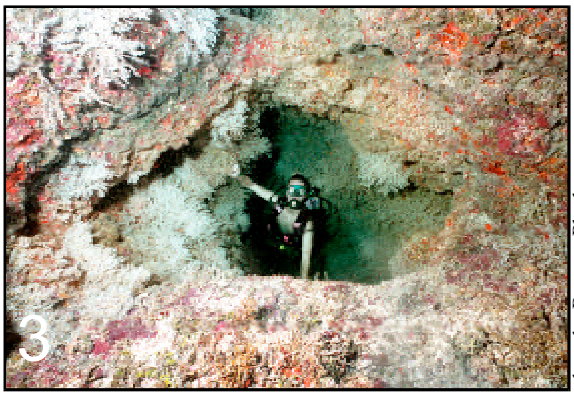

photo by Braxton Plunkett

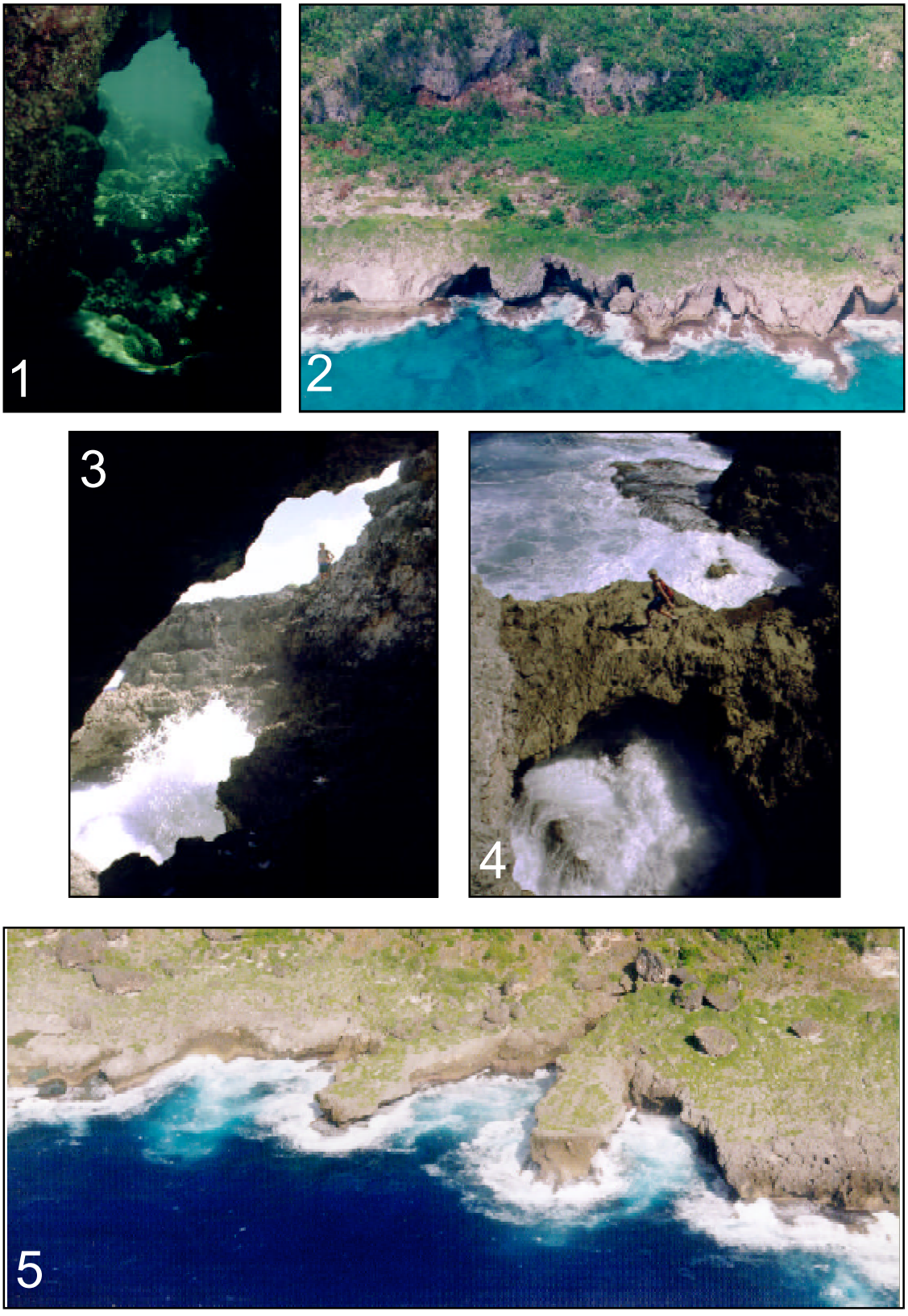

Plate 31: **Pseudokarst features.** 1) primary "cave" made by reef growth. 2) sea caves at XXX. 3) sea cave near Anao Point. 4) a partially collapsed sea cave near Anao Point. 5) coastal terrace south of Pati Point cut by waves along structural weaknesses.

Appendix 1: Inventory of permitted storm water disposal wells on Guam

Well #	Owner
DW- B 1	PACDIV CSO
DW- B 2	PACDIV CSO
DW- B 3	PACDIV CSO
DW- C 1	PACDIV CSO
DW- C 2	PACDIV CSO
DW- C 6	PACDIV CSO
DW- C 7	PACDIV CSO
DW- C 8	PACDIV CSO
DW- C 11	PACDIV CSO
DW- C 13	PACDIV CSO
DW- C 14	PACDIV CSO
DW- C 15	PACDIV CSO
DW- C 16	PACDIV CSO
DW- C 17	PACDIV CSO
DW- C 18	PACDIV CSO
DW- C 19	PACDIV CSO
DW- C 20	PACDIV CSO
DW- C 21	PACDIV CSO
DW- D 2	PACDIV CSO
DW- D 5	PACDIV CSO
DW- D 6	PACDIV CSO
DW- F 1	PACDIV CSO
DW- F 2	PACDIV CSO
DW- H 1	PACDIV CSO
DW- H 2	PACDIV CSO
DW- H 3	PACDIV CSO
DW- H 4	PACDIV CSO
DW- T 15*	GPA
DW- T 21*	GPA
DW- PIC1	PIC
DW- IE1	Island Equipment
DW- A 1	GIAA
DW- A 2	GIAA
DW- E 1	GIAA
DW- E 2	GIAA
DW- E 3	GIAA
DW- E 4	GIAA
DW- G 1	GIAA
DW- G 2	GIAA
DW- G 3	GIAA
DW- DPW1	DPW
DW- DPW2	DPW
DW- DPW3	DPW
DW- DPW4	DPW
DW- DPW5	DPW
DW- DPW6	DPW
DW- DPW7	DPW
DW- DPW8	DPW
DW- DPW9	DPW
DW- DPW10	DPW
DW- DPW11	DPW
DW- DPW12	DPW
DW- DPW13	DPW
DW- DPW14	DPW
DW- DPW15	DPW
DW- DPW16	DPW
DW- DPW18	DPW

Well #	Owner
DW- DPW20	DPW
DW- DPW21	DPW
DW- DPW22	DPW
DW- DPW23	DPW
DW- DPW24	DPW
DW- DPW25	DPW
DW- DPW26	DPW
DW- DPW27	DPW
DW- DPW28	DPW
DW- DPW29	DPW
DW- DPW30	DPW
DW- AF 1	USAF
DW- AF 2	USAF
DW- AF 3	USAF
DW- AF 4	USAF
DW- AF 5	USAF
DW- AF 6	USAF
DW- AF 7	USAF
DW- AF 8	USAF
DW- AF 9	USAF
DW- AF 10	USAF
DW- AF 11	USAF
DW- AF 12	USAF
DW- AF 13	USAF
DW- AF 14	USAF
DW- AF 15	USAF
DW- AF 16	USAF
DW- AF 17	USAF
DW- AF 18	USAF
DW- AF 19	USAF
DW- AF 20	USAF
DW- AF 21	USAF
DW- AF 22	USAF
DW- AF 23	USAF
DW- AF 24	USAF
DW- AF 25	USAF
DW- AF 26	USAF
DW- AF 28	USAF
DW- AF 29	USAF
DW- AF 30	USAF
DW- AF 31	USAF
DW- AF 32	USAF
DW- AF 33	USAF
DW- AF 34	USAF
DW- AF 35	USAF
DW- AF 36	USAF
DW- AF 37	USAF
DW- AF 38	USAF
DW- AF 40	USAF
DW- AF 41	USAF
DW- AF 42	USAF
DW- AF 43	USAF
DW- AF 44	USAF
DW- AF 45	USAF
DW- AF 46	USAF
DW- AF 47	USAF
DW- AF 48	USAF

Well #	Owner
DW- AF 49	USAF
DW- AF 50	USAF
DW- AF 51	USAF
DW- AF 52	USAF
DW- AF 53	USAF
DW- AF 54	USAF
DW- AF 55	USAF
DW- AF 56	USAF
DW- AF 56A	USAF
DW- AF 57	USAF
DW- AF 58	USAF
DW- AF 59	USAF
DW- AF 60	USAF
DW- AF 61	USAF
DW- AF 62	USAF
DW- AF 63	USAF
DW- AF 64	USAF
DW- AF 65	USAF
DW- AF 66	USAF
DW- AF 67	USAF
DW- AF 68	USAF
DW- AF 69	USAF
DW- AF 70	USAF
DW- AF 71	USAF
DW- AF 72	USAF
DW- AF 73	USAF
DW- AF 74	USAF
DW- AF 74A	USAF
DW- AF 75	USAF
DW- AF 76	USAF
DW- AF 77	USAF
DW- AF 78	USAF
DW- AF 79	USAF
DW- AF 80	USAF
DW- AF 80A	USAF
DW- AF 81	USAF
DW- AF 82	USAF
DW- AF 83	USAF
DW- AF 84	USAF
DW- AF 85	USAF
DW- AF 86	USAF
DW- AF 87	USAF
DW- AF 88	USAF
DW- AF 89	USAF
DW- AF 90	USAF
DW- AF 91	USAF
DW- AF 92	USAF
DW- AF 93	USAF
DW- AF 94	USAF
DW- AF 95	USAF
DW- AF 96	USAF
DW- AF 97	USAF
DW- AF 98	USAF
DW- AF 99	USAF
DW- AF 100	USAF
DW- AF 101	USAF
DW- AF 102	USAF

*- GPA operated wells are closed system wells and do not extend to the surface

Appendix 2: Inventory of surface flow related features in northern Guam

Landform identifiers			Landform	Setting		
ID#		Name	Type	Flow	Fm.	Source
SW	001	Santa Rosa runoff	sinking streams	ephemeral	Ta/	allogenic
SW	002	Mataguac Hill runoff	sinking streams	ephemaral	Ta/	allogenic
SW	003	Pago River	losing stream	permanent	Qal/Qtma	allogenic
SW	004	Fonte River	losing stream	permanent	Qal/Qtma	allogenic
SW	005	Machaute valley	dry valley	ephemeral	Qtma	autogenic
SW	006	Conga north valley	dry valley	ephemeral	Qtma	autogenic
SW	007	Penitentiary valley	dry valley	ephemeral	Qtma	autogenic
SW	008	Maimai valley	dry valley	never	Qtma	autogenic
SW	009	Tai north valley	dry valley	ephemeral	Qtma	autogenic
SW	010	Tai south valley	dry valley	ephemeral	Qtma	autogenic
SW	011	Pago Bay valley	dry valley	ephemeral	Qtma	autogenic
SW	012	Pago tributary 1	dry valley	ephemeral	Qtma	autogenic
SW	013	Pago tributary 2	dry valley	ephemeral	Qtma	autogenic
SW	014	Guacluluyao sinks	dry valley	never	Qtma	autogenic
SW	015	Cln Pago valley sinks	dry valley	never	Qtma	autogenic
SW	016	Chaot tributary	dry valley	ephemeral	Qtma	autogenic
SW	017	Conga south valley	dry valley	ephemeral	Qtma	autogenic
SW	018	Agana Swamp	flooded valleys	permanent	Qal	autogenic
SW	019	Agana River	autogenic stream	permanent	Qal	autogenic
SW	020	Chaot River	autogenic stream	permanent	Qtma	autogenic
SW	021	Harmon Sink blind valley	sinking stream	ephemeral	Qtmd	autogenic

Appendix 3: Inventory of surface flow related features in southern Guam

Landform identifiers			Landform	Setting		
ID#		Name	Type	Flow	Fm.	Source
SWs	001	Yllig River	through valley	permanent	Qtma	allogenic
SWs	002	Togcha River	through valley	permanent	Qtma	allogenic
SWs	003	Talofofo River	through valley	permanent	Qtma	allogenic
SWs	004	Asalonso River	through valley	permanent	Qtma	allogenic
SWs	005	Pauliluc River	through valley	permanent	Qtma	allogenic
SWs	006	Upper Togcha River	gorge	permanent	Tb	allogenic
SWs	007	Togcha River	sinking stream	semi-perm.	Tb	allogenic
SWs	008	Nomna Bay valley	abandoned valley	never	Qtma	n/a
SWs	009	Talae Yu'us River	underground flow	permanent	Tb	allogenic
SWs	010	Bonya River	underground flow	permanent	Tub/Tb	allogenic
SWs	011	Maemong River	underground flow	permanent	Tt/Tal/Tb	autogenic
SWs	012	Maemong Bridge north	natural bridge	permanent	Tb	n/a
SWs	013	Maemong Bridge south	natural bridge	permanent	Tb	n/a
SWs	014	Bonya River Arch	natural bridge	never	Tb	n/a
SWs	015	Fena area north pond	sinkhole lake	semi-perm.	Tal	autogenic
SWs	016	Fena area south pond	sinkhole lake	semi-perm.	Tb	autogenic

Appendix 4: Inventory of high level springs in northern Guam

HIGH-LEVEL SPRINGS		Spr.	Location			Estimated flow [lpd]		Geologic	W. Quality
KARST ID#	Name	Type	Elv [ft]	N [ft]	E [ft]	min	max	Formation	(Cl- [ppm])
HSP 001	Chunge Spring		830	N 13-31-58.92	E 144-54-14.39	few 100	46,200	Tbl / Ta	excellent
HSP 002	Santa Rosa Spring			N 13-31-49.05	E 144-54-40.41	3,800	25,000	Qtmd / Ta	
HSP 003	Janum Spring	B	2	N 13-30-50.46	E 144-54-37.60	3,800,000	15,000,000	Qtmd	excellent
HSP 004	Agana Springs (2)		5	N 13-27-36.93	E 144-45-18.05	3,028,000	9,462,500	Qtma	20-35 ppm
HSP 005	Pedonlisong Spring	D		N 13-27-16.93	E 144-45-55.13			Qtma	
HSP 006	Mataguac Spring	A	460	N 13-32-30.88	E 144-52-46.83	0	51,840	Qtmd / Ta	
HSP 007	Maina Spring	C	264	N 13-27-46.69	E 144-43-47.55	25,000	218,000	Tal / Ta	

Spring types: A- Free Draining, Contact Springs, with Allogenic water, B- Free Draining, Hanging Springs, with Allogenic water, C- Dammed spring, impounded by a faulted contact with another lithology, D- Stream Emergence Spring. Data on estimated flow from Ward and Brookhart (1962) and Rogers and Legge (1992).

Appendix 5: Inventory of high level springs in southern Guam

HIGH-LEVEL SPRINGS		Spr.	Location			Estimated flow [lpd]		Geol.	W. Quality
ID#	Name	Type	Elv [ft]	Latitude	Longitude	min	max	Form.	(Cl- [ppm])
HSPs 001	Siligin Spring	B	300	N 13-16-26.90	E 144-40-43.95	136,300	294,400	Tum/ Tuf	
HSPs 002	Asan Spring	A	140	N 13-28-04.88	E 144-42-51.04	370,000	3,790,000	Tal / Ta	16-35
HSPs 003	Bona Spring	C	~295	N 13-22-37.72	E 144-40-39.91	7,600	3,785,000	Tal/ Tt	<50 ppm
HSPs 004	Faata Springs- (2 n.)	A	~450	N 13-22-31.65	E 144-39-40.83	624,000	3,785,000	Tal/ Ta	
HSPs 005	Faata Springs- (1 s.)	A	~450	N 13-22-25.12	E 144-39-38.24			Tal/ Ta	
HSPs 006	Auau Spring (Anan)	A		N 13-22-08.94	E 144-39-30.09	76	378,500	Tal/ Ta	
HSPs 007	Mao Spring	A	550	N 13-21-50.28	E 144-39-34.92		479,700	Tal / Ta	
HSPs 008	Dobo Spring	A	700	N 13-20-43.86	E 144-40-39.34			Tal / Ta	
HSPs 009	Chepak Spring	A	700	N 13-20-43.01	E 144-40-18.26	3,407,000	18,244,000	Tal / Ta	11 ppm
HSPs 010	Almagosa Spring	A	700	N 13-20-40.91	E 144-40-19.44			Tal / Ta	
HSPs 011	Santa Rita Spring	A	284	N 13-22-57.63	E 144-40-11.15	379,000		Tal/ Tuf	
HSPs 012	Alatgue Spring	B	330	N 13-18-31.18	E 144-40-08.72	163,500		Tum / Tuf	
HSPs 013	Piga Spring	B	~330	N 13-18-06.20	E 144-40-34.20	3100	338,000	Tum / Tuf	good
HSPs 014	Malojloj Spring	A		N 13-18-10.60	E 144-44-48.59	38	57	Qtma / Tub	good
HSPs 015	Asalonso Spring	D		N 13-19-38.08	E 144-45-21.33			Qtma / Qal	

Spring types: A- Free Draining, Contact Springs, with Autogenic water, B- Free Draining, Contact Springs, with Allogenic water, C- Dammed spring, impounded by a comfortable contact with another lithology, D- Spring draining into a karst stream. Data on estimated flow from Ward and Brookhart (1962) and Rogers and Legge (1992).

Appendix 6: Inventory of closed contour depressions in northern Guam

Feature identifiers		Type or origin	Geometry of individual features					Nearest neighbor		Setting			Location	
KARST ID#	Name	of depression (if known)	length [m]	width [m]	long axis azimuth	depth [ft]	area [m2]	distance [m]	azimuth to n.n.	Geol. Fm.	general location	current/ past use	deepest point or center latitude	longitude
CCD 1	Ritidian cliff depression 1	unknown	355	62	294	20	9998	336	317	Qtmr	plateau edge	none	N 13-38-49.	E 144-51-55.
CCD 2	Ritidian cliff depression 2	unknown	320	108	282	20	22517	435	272	Qtmr	plateau edge	none	N 13-38-50.	E 144-51-39.
CCD 3	Ritidian cliff depression 3	unknown	230	36	308	20	9093	336	317	Qtmr	plateau edge	none	N 13-38-44.	E 144-51-59.
CCD 4	Machanao borrow pit	unknown	90	65	n/a	20	4681	1336	38	Qtmr	plateau edge	borrow pit	N 13-38-16.	E 144-51-12.
CCD 5	NW field borrow pit 1	unknown	230	63	60	20	16773	313	62	Qtmm	plateau	borrow pit	N 13-37-13.	E 144-51-13.
CCD 6	NW field borrow pit 2	unknown	267	70	62	20	15419	316	62	Qtmd	plateau	borrow pit	N 13-37-16.	E 144-51-21.
CCD 7	NW field depression 5	unknown	252	124	59	20	20368	878	318	Qtmr	plateau	borrow pit	N 13-37-43.	E 144-51-48.
CCD 8	NW field borrow pit 3	unknown	370	159	282	30	52716	760	292	Qtmm	plateau	borrow pit	N 13-36-38.	E 144-51-04.
CCD 9	NW field depression	unknown	443	147	10	20	43489	916	43	Qtmd	plateau	none	N 13-36-15.	E 144-50-43.
CCD 10	NW field depression 2	unknown	605	233	305	20	107041	724	31	Qtmd	plateau	none	N 13-36-25.	E 144-51-28.
CCD 11	NW field borrow pit 4	unknown	161	102	319	20	9991	724	31	Qtmd	plateau	borrow pit	N 13-36-02.	E 144-51-16.
CCD 12	NW field depression 3	unknown	519	268	317	20	148718	771	310	Qtmd	plateau	none	N 13-36-08.	E 144-51-51.
CCD 13	Brecciated zone depression 1	fault-related	349	143	9	10	34120	344	329	Qtmd	plateau	none	N 13-37-21.	E 144-52-06.
CCD 14	Brecciated zone depression 2	fault-related	283	115	283	25	31477	254	294	Qtmd	plateau	none	N 13-37-15.	E 144-52-09.
CCD 15	Brecciated zone depression 3	fault-related	274	143	355	35	26099	202	339	Qtmm	plateau	borrow pit	N 13-37-08.	E 144-52-17.
CCD 16	Brecciated zone depression 4	fault-related	100	86	n/a	10	5003	202	339	Qtmm	plateau	none	N 13-37-02.	E 144-52-22.
CCD 17	Brecciated zone depression 5	fault-related	330	259	n/a	35	57447	238	19	Qtmd	plateau	borrow pit	N 13-36-52.	E 144-52-17.
CCD 18	Brecciated zone depression 6	fault-related	1240	417	342	30	361406	820	329	Qtmd	plateau	military	N 13-36-23.	E 144-52-28.
CCD 19	Brecciated zone depression 7	fault-related	180	82	54	30	7790	240	293	Qtmd	plateau	none	N 13-36-01.	E 144-52-39.
CCD 20	Brecciated zone depression 8	fault-related	130	81	330	30	8291	111	26	Qtmd	plateau	none	N 13-35-58.	E 144-52-47.
CCD 21	Brecciated zone depression 9	fault-related	154	87	316	10	5241	111	26	Qtmd	plateau	none	N 13-35-54.	E 144-52-45.
CCD 22	Brecciated zone depression 10	fault-related	1353	188	345	60	547643	1044	332	Qtmd	plateau	none	N 13-35-30.	E 144-52-59.
CCD 23	Brecciated zone depression 11	fault-related	100	78	n/a	10	6393	368	26	Qtmd	plateau	none	N 13-35-27.	E 144-53-21.
CCD 24	Brecciated zone depression 12	fault-related	110	80	n/a	10	7641	368	26	Tbl	plateau	none	N 13-35-16.	E 144-53-16.
CCD 25	Brecciated zone depression 13	fault-related	515	132	319	10	61250	528	3	Tbl	plateau	none	N 13-35-01.	E 144-53-14.
CCD 26	Brecciated zone depression 14	fault-related	139	91	313	25	8922	503	307	Tbl	plateau	landfill	N 13-34-45.	E 144-53-36.
CCD 27	Mergagan cliff depression	unknown	113	37	304	20	2265	764	329	Qtmr	plateau edge	none	N 13-37-34.	E 144-53-03.
CCD 28	AAB 6th St Pit	unknown	73	31	352	25	1432	113	68	Qtmd	plateau	borrow pit	N 13-37-10.	E 144-52-44.
CCD 29	AAFB 5th St Pit	unknown	40	30	n/a	25	1166	113	68	Qtmd	plateau	borrow pit	N 13-37-11.	E 144-52-46.
CCD 30	AAFB 1st St Depression	drawdown?	70	86	n/a	55	4082	323	60	Qtmd	plateau edge	none	N 13-37-08.	E 144-53-07.
CCD 31	AAFB NE of 1st St depression	drawdown?	40	41	n/a	35	1010	323	60	Qtmd	plateau edge	none	N 13-37-13.	E 144-53-16.
CCD 32	Tarague cliff depression 1	unknown	104	37	356	20	2665	749	330	Qtmr	plateau edge	none	N 13-36-45.	E 144-53-19.
CCD 33	Tarague cliff depression 2	unknown	493	141	329	20	37614	827	63	Qtmr	plateau	none	N 13-36-13.	E 144-53-28.
CCD 34	Tarague embayment borrow pit	unknown	48	20	18	20	834	827	63	Qtmd	coastal	borrow pit	N 13-36-28.	E 144-53-51.
CCD 35	Tarague beach road depression	unknown	304	150	324	20	28737	482	62	Qtmr	plateau edge	none	N 13-35-59.	E 144-53-53.
CCD 36	Tarague Well #1	cenote	*17*	*15*		*5*				Qtmd	coastal	none	N 13-36-06.	E 144-54-06.
CCD 37	Tarague Well #2	cenote	*15*	*10*		*20*				Qtmd	coastal	none	N 13-36-03.	E 144-54-08.
CCD 38	Tarague Well #3	cenote	*25*	*20*		*15*				Qtmd	coastal	none	N 13-36-04.	E 144-54-12.
CCD 39	Tarague Well #4	cenote	*15*	*14*		*30*				Qtmd	coastal	none	N 13-36-01.	E 144-54-15.
CCD 40	Tarague Well #6	cenote								Qtmd	coastal	none	N 13-35-58.	E 144-54-16.
CCD 41	Tarague Well #7	cenote								Qtmd	coastal	none	N 13-35-55.	E 144-54-55.
CCD 42	Tarague Well #8	cenote								Qtmd	coastal	none	N 13-35-55.	E 144-55-02.

(continued on the next page)

Feature identifiers		Type or origin	Geometry of individual features					Nearest neighbor		Setting			Location	
KARST ID#	Name	of depression (if known)	length [m]	width [m]	long axis azimuth	depth [ft]	area [m2]	distance [m]	azimuth to n.n.	Geol. Fm.	general location	current/ past use	deepest point or center latitude	longitude
CCD 43	Tagua cliff depression	unknown	560	67	80	20	23201	611	313	Qtmd	plateau edge	none	N 13-35-40.	E 144-55-10.
CCD 44	AAFB NW Perimeter Rd depression	unknown	262	144	70	25	25037	1023	39	Tbl	plateau	borrow pit	N 13-35-18.	E 144-54-19.
CCD 45	AAFB 33rd St borrow pit	unknown	200	194	n/a	35	31146	649	322	Qtmm	plateau edge	borrow pit	N 13-35-24.	E 144-55-29.
CCD 46	Brecciated zone depression 15	fault-related	142	86	345	35	9848	475	28	Tbl	plateau	borrow pit	N 13-34-36.	E 144-53-49.
CCD 47	NW field depression 4	unknown	577	373	327	25	128394	475	28	Tbl	plateau	none	N 13-34-48.	E 144-53-56.
CCD 48	AAFB Pipeline borrow pit	unknown	330	300	n/a	(55)	71245	994	315	Tbl	plateau	borrow pit	N 13-34-14.	E 144-54-14.
CCD 49	AAFB Perimeter road depression	unknown	500	206	61	20	98934	1724	339	Qtmd	plateau	AF operations	N 13-34-13.	E 144-55-13.
CCD 50	Lafac cliff depression 1	unknown	296	70	59	20	12126	303	288	Qtmr	plateau edge	none	N 13-34-16.	E 144-56-09.
CCD 51	Lafac cliff depression 2	unknown	167	107	344	20	9563	303	288	Qtmd	plateau edge	borrow pit	N 13-34-16.	E 144-56-21.
CCD 52	Lafac cliff depression 3	unknown	663	284	50	(50)	84637	617	21	Qtmr	plateau edge	borrow pit	N 13-34-29.	E 144-56-28.
CCD 53	AAFB Injection wells depression	unknown	440	295	n/a	35	98423	660	353	Qtmd	plateau edge	injection wells	N 13-33-18.	E 144-55-24.
CCD 54	Agafo Gumas (north of) depression	unknown	591	569	46	45	308968	765	64	Tbl	plateau	military	N 13-35-25.	E 144-52-25.
CCD 55	Guam Observatory depression	unknown	191	61	338	20	7102	765	64	Tbl	plateau	none	N 13-35-15.	E 144-52-04.
CCD 56	Potts Junction depression	unknown	331	319	90	20	42778	816	50	Tbl	plateau	rural residential	N 13-35-00.	E 144-51-16.
CCD 57	Dededo golf course ponding basin 1	unknown	114	48	16	20	2847	309	21	Tbl	plateau	ponding basin	N 13-34-54.	E 144-51-46.
CCD 58	Potts Junction ponding basin 4	unknown	83	40	271	20	2452	288	304	Tbl	plateau	ponding basin	N 13-34-58.	E 144-51-58.
CCD 59	Potts Junction ponding basins 2-3	unknown	131	62	89	20	6322	288	304	Tbl	plateau	ponding basin	N 13-35-04.	E 144-51-50.
CCD 60	Potts Junction ponding basin 1	unknown	92	70	334	30	4368	373	313	Tbl	plateau	ponding basin	N 13-35-09.	E 144-51-42.
CCD 61	Anao depression	unknown	188	71	0	20	9198	660	353	Qtmd	plateau edge	none	N 13-32-56.	E 144-55-28.
CCD 62	Mati point depression	unknown	260	90	27	30	9913	911	338	Qtmd	plateau edge	none	N 13-32-30.	E 144-55-40.
CCD 63	Pugua point depression	unknown	195	60	354	20	8647	762	350	Qtmd	coastal	none	N 13-35-17.	E 144-50-03.
CCD 64	Haputo radio towers sink	drawdown ?	88	50	337	45	3614	559	31	Qtmd	plateau egde	none	N 13-34-51.	E 144-50-08.
CCD 65	Haputo sink 6	drawdown ?	241	140	384	35	13000	248	345	Qtmd	plateau egde	borrow pit	N 13-34-32.	E 144-50-11.
CCD 66	Haputo sink 5	drawdown ?	160	167	n/a	95	16531	248	345	Qtmd	plateau egde	borrow pit	N 13-34-24.	E 144-50-12.
CCD 67	Haputo sink 4	drawdown ?	152	93	55	55	14520	288	71	Qtmd	plateau egde	none	N 13-34-21.	E 144-50-03.
CCD 68	Haputo sink 3	drawdown ?	106	80	290	25	4791	434	276	Qtmm	plateau egde	none	N 13-34-24.	E 144-49-50.
CCD 69	Haputo sink 1	drawdown ?	70	43	n/a	25	2441	170	319	Qtmd	plateau egde	none	N 13-34-36.	E 144-49-59.
CCD 70	Haputo sink 2	drawdown ?	80	65	n/a	35	3673	170	319	Qtmd	plateau egde	none	N 13-34-33.	E 144-50-01.
CCD 71	Finagayan small depression 2	unknown	204	173	309	25	10533	217	306	Qtmd	plateau egde	none	N 13-34-06.	E 144-50-18.
CCD 72	Finagayan small depression 3	unknown	252	127	315	30	3007	217	306	Qtmd	plateau egde	none	N 13-34-03.	E 144-50-23.
CCD 73	Gugagon ponding basin	unknown	224	57	314	25	8735	793	81	Tbl	plateau	ponding basin	N 13-34-06.	E 144-50-47.
CCD 74	Finagayan small depression 1	unknown	40	40	n/a	20	1538	816	50	Tbl	plateau	none	N 13-34-41.	E 144-50-53.
CCD 75	Dededo small depression 1	unknown	100	74	n/a	20	6170	784	274	Tbl	plateau	none	N 13-34-22.	E 144-51-18.
CCD 76	Dededo golf course ponding basin 2	unknown	271	76	32	20	13359	784	274	Tbl	plateau	ponding basin	N 13-34-20.	E 144-51-45.
CCD 77	Mataguac depression 1	unknown	216	178	359	20	23755	1069	9	Qtmd	plateau	agricultural	N 13-33-59.	E 144-52-36.
CCD 78	Dededo small depression 2	unknown	223	97	354	20	16711	1216	280	Qtmm	plateau	none	N 13-33-30.	E 144-51-51.
CCD 79	Mataguac depression 2	unknown	250	185	303	20	31500	802	283	Qtmm	plateau	none	N 13-33-03.	E 144-52-16.
CCD 80	Mataguac big depression 2	unknown	842	544	1	35	281655	817	31	Qtmm	plateau	agricultural	N 13-33-19.	E 144-52-29.
CCD 81	Mataguac Hill North sink	allogenic p.r.	693	653	359	25	170261	536	27	Qtmd	volc contact	agricultural	N 13-32-57.	E 144-52-40.
CCD 82	Mataguac Hill West sink	allogenic p.r.	284	142	283	20	23822	536	27	Qtmd	volc contact	houses	N 13-32-40.	E 144-52-33.
CCD 83	Mataguac depression 3	unknown	180	189	n/a	20	17283	703	343	Qtmd	plateau	houses	N 13-33-03.	E 144-53-08.
CCD 84	Mataguac spring sink	allogenic p.r.	101	76	339	40	6549	143	333	Qtmd	volc contact	none	N 13-32-33.	E 144-52-57.

(continued on the next page)

Feature identifiers		Type or origin	Geometry of individual features					Nearest neighbor		Setting			Location	
KARST ID#	Name	of depression (if known)	length [m]	width [m]	long axis azimuth	depth [ft]	area [m2]	distance [m]	azimuth to n.n.	Geol. Fm.	general location	current/ past use	deepest point or center latitude	longitude
CCD 85	Mataguac Hill East sink	allogenic p.r.	167	97	354	40	11477	143	333	Qtmd	volc contact	none	N 13-32-38.	E 144-52-54.
CCD 86	Mataguac big depression 1	unknown	861	698	271	35	341562	703	343	Qtmd	plateau	agricultural	N 13-33-24.	E 144-53-02.
CCD 87	Ysengsong depression 4	unknown	207	91	68	20	15983	881	292	Qtmd	plateau	agricultural	N 13-32-26.	E 144-51-31.
CCD 88	Lupog depression	unknown	304	104	300	20	33059	1047	282	Qtmd	plateau	none	N 13-32-51.	E 144-53-51.
CCD 89	Ysengson depression 6	unknown	234	126	297	20	16912	82	358	Qtmd	plateau	none	N 13-32-16.	E 144-51-54.
CCD 90	Ysengson depression 7	collapse	30	24	n/a	20	647	220	86	Qtmd	plateau	none	N 13-32-16.	E 144-52-01.
CCD 91	Ysengsong long depression	unknown	455	93	272	20	31682	286	297	Qtmd	plateau	none	N 13-32-11.	E 144-52-12.
CCD 92	Yigo depression 1	unknown	240	131	354	20	23338	227	65	Tbl	plateau	none	N 13-32-02.	E 144-52-30.
CCD 93	Mataguac Hill South sink	allogenic p.r.	319	101	290	35	20666	391	7	Qtmd	plateau	none	N 13-32-19.	E 144-52-38.
CCD 94	Yigo ponding basin 1	unknown	97	33	333	20	3154	145	322	Tbl	plateau	ponding basin	N 13-32-07.	E 144-52-37.
CCD 95	Yigo ponding basin 2	unknown	130	74	n/a	20	6272	299	334	Tbl	plateau	ponding basin	N 13-31-54.	E 144-52-43.
CCD 96	Yigo depression 2	unknown	317	164	311	20	29433	355	73	Tbl	plateau	urbanized	N 13-31-58.	E 144-52-55.
CCD 97	Yigo Sink	allogenic p.r.	948	274	66	45	269412	528	325	Tbl	plateau	agricultural	N 13-31-44.	E 144-53-13.
CCD 98	Yigo ponding basin 3	allogenic p.r.	160	142	n/a	25	18185	579	340	Tbl	plateau	ponding basin	N 13-31-52.	E 144-53-41.
CCD 99	Yigo School quarry	unknown	150	93	n/a	(75)	12188	579	340	Tbl	plateau	quarry	N 13-32-09.	E 144-53-35.
CCD 100	Lupog depression	unknown	413	237	304	20	49335	318	342	Qtmd	volc contact	none	N 13-32-44.	E 144-54-26.
CCD 101	Mt Santa Rosa quarry 1	unknown	60	47	n/a	35	2390	103	330	Qtmd	volc contact	quarry	N 13-32-35.	E 144-54-30.
CCD 102	Mt. Santa Rosa ponding basin	allogenic p.r.	61	39	36	20	1075	103	330	Qtmd	volc contact	none	N 13-32-32.	E 144-54-31.
CCD 103	Mt Santa Rosa quarry 2	unknown	135	64	359	20	7851	475	45	Tal	plateau	quarry	N 13-32-24.	E 144-55-01.
CCD 104	Mt. Santa Rosa spring sink	allogenic p.r.	209	156	322	35	19516	475	45	Ta	volcanics	none	N 13-32-14.	E 144-54-50.
CCD 105	Gayinero sink a	border polje	630	400	48	40	152441	392	348	Qtmd	volc contact	agricultural	N 13-31-56.	E 144-54-24.
CCD 106	Gayinero sink b	allogenic p.r.	550	270	52	30	106659	392	348	Qtmd	volc contact	agricultural	N 13-31-41.	E 144-54-27.
CCD 107	Awesome sink	allogenic p.r.	110	90	n/a	30	8735	93	54	Qtmd	volc contact	none	N 13-31-47.	E 144-54-49.
CCD 108	Interesting sink	allogenic p.r.	60	50	n/a	20	1508	93	54	Qtmd	volc contact	none	N 13-31-48.	E 144-54-52.
CCD 109	Mt. Santa Rosa eastern sink	allogenic p.r.	156	158	320	30	23365	465	311	Tal	volc contact	none	N 13-32-04.	E 144-55-02.
CCD 110	Catalina point depression	unknown	99	37	57	20	2455	855	291	Qtmd	plateau edge	none	N 13-31-53.	E 144-55-29.
CCD 111	Guam Rock Products quarry	unknown	334	145	71	(55)	34660	1247	54	Tal	plateau edge	quarry	N 13-31-15.	E 144-53-47.
CCD 112	Lujuna point sink	collapse?	587	112	52	30	55866	1052	330	Qtmd	plateau edge	none	N 13-31-10.	E 144-54-39.
CCD 113	Hilaan Pool (The Lost Pond)	cenote	*30*	*25*		*8*				Qtmd	coastal	none	N 13-33-22.	E 144-48-53.
CCD 114	Finagayan borrow pit 1	unknown	74	30	301	20	8726	79	291	Qtmd	plateau edge	borrow pit	N 13-32-44.	E 144-49-04.
CCD 115	Finagayan borrow pit 2	unknown	146	41	299	20	1897	79	291	Qtmd	plateau edge	borrow pit	N 13-32-44.	E 144-49-07.
CCD 116	Finagayan banana hole	banana hole?	*10*	*10*		*7*				Qtmd	plateau	none	N 13-32-48.	E 144-49-27.
CCD 117	Finagayan borrow pit 3	unknown	101	59	85	35	2731	943	0	Qtmd	plateau edge	borrow pit	N 13-33-18.	E 144-49-29.
CCD 118	US Weather Bureau depression 1	unknown	380	240	327	25	77847	646	81	Qtmm	plateau	rural residential	N 13-33-25.	E 144-50-06.
CCD 119	US Weather Bureau depression 2	unknown	258	148	339	20	19949	411	14	Qtmd	plateau	rural residential	N 13-33-17.	E 144-50-19.
CCD 120	Gugagon ponding basin 2	unknown	50	35	331	20	1002	411	14	Tbl	plateau	ponding basin	N 13-33-29.	E 144-50-23.
CCD 121	Callon Tramojo ponding basin 2	unknown	69	35	61	20	1223	543	332	Tbl	plateau	ponding basin	N 13-33-01.	E 144-50-27.
CCD 122	Callon Tramojo ponding basin 1	unknown	132	42	274	20	4473	688	68	Tbl	plateau	ponding basin	N 13-33-08.	E 144-50-49.
CCD 123	Harmon annex depression 1	unknown	464	224	274	20	77713	681	39	Tbl	plateau edge	none	N 13-32-00.	E 144-48-50.
CCD 124	Harmon radio facility depression	unknown	90	51	n/a	20	4175	681	39	Qtmm	plateau edge	none	N 13-31-46.	E 144-48-39.
CCD 125	Harmon annex depression 2	unknown	901	382	321	20	247232	753	73	Qtmm	plateau	none	N 13-31-40.	E 144-49-02.
CCD 126	Ukudu depression	unknown	260	114	n/a	20	11875	753	73	Qtmd	plateau	none	N 13-31-42.	E 144-49-28.

(continued on the next page)

Feature identifiers		Type or origin	Geometry of individual features					Nearest neighbor		Setting			Location	
KARST ID#	Name	of depression (if known)	length [m]	width [m]	long axis azimuth	depth [ft]	area [m2]	distance [m]	azimuth to n.n.	Geol. Fm.	general location	current/ past use	deepest point or center latitude	longitude
CCD 127	Wettengel Junction depression	unknown	228	52	351	20	7082	1066	341	Qtmd	plateau	ponding basin	N 13-31-07.	E 144-49-39.
CCD 128	Ysengsong depression 1	unknown	88	48	352	20	2841	169	90	Tbl	plateau	none	N 13-31-52.	E 144-50-39.
CCD 129	Ysengsong depression 2	unknown	413	109	317	20	29767	169	90	Tbl	plateau	none	N 13-31-51.	E 144-50-45.
CCD 130	Public works quarry	unknown	310	210	n/a	65	60294	299	30	Tbl	plateau	quarry	N 13-31-43.	E 144-50-41.
CCD 131	Dededo Jr. High School depression	unknown	237	165	278	20	24534	859	280	Tbl	plateau	borrow pit	N 13-31-19.	E 144-50-24.
CCD 132	G. municipal golf course depr. 1	unknown	123	34	14	20	2857	859	280	Tbl	plateau	golf course	N 13-31-13.	E 144-50-52.
CCD 133	War dog cemetary sink	unknown	166	100	69	30	15901	967	59	Tbl	plateau	none	N 13-30-51.	E 144-51-13.
CCD 134	G. municipal golf course depr. 2	unknown	197	98	283	20	15758	262	270	Tbl	plateau	golf course	N 13-31-42.	E 144-51-05.
CCD 135	Ysengsong depression 3	unknown	281	158	291	20	35108	262	270	Tbl	plateau	none	N 13-31-42.	E 144-51-13.
CCD 136	Ipapao depression 1	unknown	200	201	n/a	20	35486	543	313	Tbl	plateau	none	N 13-31-32.	E 144-51-25.
CCD 137	Ipapao depression 2	unknown	252	126	300	20	16594	515	300	Tbl	plateau	none	N 13-31-24.	E 144-51-38.
CCD 138	Ipapao ponding basin	unknown	40	39	n/a	20	782	544	358	Tbl	plateau	ponding basin	N 13-31-07.	E 144-51-40.
CCD 139	Marbo pumping station depression	unknown	280	264	n/a	20	43381	1655	280	Tbl?	plateau	none	N 13-30-26.	E 144-52-09.
CCD 140	Asdonlucas sink 2	unknown	755	250	37	20	102876	746	45	Qtmr	plateau edge	none	N 13-30-34.	E 144-53-21.
CCD 141	Asdonlucas sink 1	unknown	550	421	n/a	30	158749	746	45	Qtmr	plateau edge	none	N 13-30-19.	E 144-53-05.
CCD 142	Harmon flea market sink	collapse	94	72	307	30	3037	769	339	Tbl	plateau	none	N 13-30-06.	E 144-49-12.
CCD 143	Perez Brothers quarry (c)	unknown	180	181	n/a	(50)	19641	275	358	Tbl	plateau	quarry	N 13-29-43.	E 144-49-20.
CCD 144	Perez Brothers quarry (a-b)	unknown	330	167	n/a	(55)	44938	324	33	Tbl	plateau	quarry	N 13-29-34.	E 144-49-19.
CCD 145	Mt Barrigada borrow pit	unknown	230	77	n/a	40	14761	324	33	Tbl	plateau	borrow pit	N 13-29-23.	E 144-49-11.
CCD 146	Mecheche depression	unknown	200	163	n/a	20	23916	937	345	Tbl	plateau	none	N 13-29-59.	E 144-50-14.
CCD 147	Latte Heights ponding basin 1	unknown	30	35	n/a	20	708	278	309	Qtmd	plateau	ponding basin	N 13-29-30.	E 144-50-22.
CCD 148	Latte Heights ponding basin 2	unknown	120	69	n/a	30	6715	278	309	Qtmd	plateau	ponding basin	N 13-29-24.	E 144-50-29.
CCD 149	Latte Heights depression	unknown	438	237	51	20	71407	502	68	Qtmd	plateau	houses	N 13-29-04.	E 144-50-17.
CCD 150	Latte Heights ponding basin 3	unknown	70	53	56	20	1823	502	68	Qtmd	plateau	ponding basin	N 13-29-09.	E 144-50-29.
CCD 151	Sabanan Pagat sink	unknown	464	134	46	20	36373	1376	31	Qtmr	plateau edge	none	N 13-29-39.	E 144-52-39.
CCD 152	Oca borrow pit	unknown	290	137	n/a	75	16905	602	281	Qtmd	plateau edge	borrow pit	N 13-30-01.	E 144-46-34.
CCD 153	Tamuning school borrow pit	unknown	370	160	n/a	75	73982	602	281	Qtmd	plateau edge	borrow pit	N 13-29-58.	E 144-46-50.
CCD 154	Harmon sink (a)	autogenic p.r.	509	93	84	20	37249	294	72	Qtmd	valley	none	N 13-29-42.	E 144-47-51.
CCD 155	Harmon sink (c)	unknown	60	60	n/a	35	2606	294	72	Qtmd	valley	none	N 13-29-39.	E 144-47-30.
CCD 156	Harmon sink (b)	autogenic p.r.	647	195	283	30	114895	336	302	Qtmd	valley	none	N 13-29-48.	E 144-47-24.
CCD 157	Barrigada sink	collapse	72	41	60	40	2038	315	336	Qtma	plateau	none	N 13-28-15.	E 144-47-18.
CCD 158	Barrigada depression 1	unknown	344	96	341	20	20396	315	336	Qtma	plateau	borrow pit	N 13-28-24.	E 144-47-16.
CCD 159	Barrigada depression 2	unknown	428	134	337	30	31859	607	272	Qtma	plateau	none	N 13-28-21.	E 144-47-32.
CCD 160	Barrigada depression 3	unknown	330	149	338	20	39575	595	84	Qtmd	plateau	none	N 13-28-20.	E 144-47-49.
CCD 161	Barrigada depression 4	unknown	300	233	n/a	20	52114	595	84	Qtmd	plateau	none	N 13-28-21.	E 144-48-06.
CCD 162	Exxon sink	collapse	82	49	40	20	2902	630	24	Qtma	plateau	ponding basin	N 13-28-02.	E 144-47-57.
CCD 163	Barrigada depression 5	unknown	140	97	n/a	20	11200	911	272	Qtma	plateau	none	N 13-28-21.	E 144-48-37.
CCD 164	Aspengo depression 1	unknown	290	148	78	40	27949	362	315	Qtma	plateau	urbanized	N 13-27-36.	E 144-47-47.
CCD 165	Aspengo depression 2	unknown	220	194	n/a	20	35628	362	315	Qtma	plateau	urbanized	N 13-27-30.	E 144-47-54.
CCD 166	Aspengo depression 3	unknown	180	142	n/a	20	18360	634	41	Qtma	plateau	agricultural	N 13-27-50.	E 144-48-19.
CCD 167	Aspengo main depression	unknown	1303	539	314	50	474125	634	41	Qtma	plateau	urban residential	N 13-27-38.	E 144-48-04.
CCD 168	Navy golf course depression 2	unknown	424	193	66	20	32978	601	342	Qtma	plateau	none	N 13-27-51.	E 144-48-46.

(continued on the next page)

Feature identifiers		Type or origin	Geometry of individual features					Nearest neighbor		Setting			Location	
KARST ID#	Name	of depression (if known)	length [m]	width [m]	long axis azimuth	depth [ft]	area [m2]	distance [m]	azimuth to n.n.	Geol. Fm.	general location	current/ past use	deepest point or center latitude	longitude
CCD 169	Navy golf course depression 1	unknown	455	238	332	35	54333	360	68	Qtma	plateau	golf course	N 13-27-38.	E 144-48-51.
CCD 170	Navy golf course depression 3	unknown	368	130	359	20	49798	360	68	Qtma	plateau	none	N 13-27-34.	E 144-48-40.
CCD 171	Navy golf course depression 4	unknown	434	164	8	20	44716	395	345	Qtma	plateau	none	N 13-27-20.	E 144-48-43.
CCD 172	Hawaiian Rock quarry (b)	unknown	180	175	n/a	(20)	26101	375	77	Qtmd	coastal	quarry	N 13-27-16.	E 144-49-58.
CCD 173	Hawaiian Rock quarry (a)	unknown	300	234	n/a	(25)	52625	375	77	Qtmd	coastal	quarry	N 13-27-12.	E 144-49-46.
CCD 174	Hawaiian sink 1	drawdown?	60	55	n/a	45	3256	166	11	Qtmd	coastal	none	N 13-26-50.	E 144-49-34.
CCD 175	Hawaiian sink 2	cenote	90	96	n/a	55	4593	166	11	Qtmd	coastal	none	N 13-26-46.	E 144-49-32.
CCD 176	Fadian depression	unknown	157	95	276	20	9609	311	43	Qtmr	plateau edge	none	N 13-26-44.	E 144-49-16.
CCD 177	Fadian borrow pit 3	unknown	186	84	34	25	8659	311	43	Qtmr	plateau edge	borrow pit	N 13-26-37.	E 144-49-11.
CCD 178	Depression behind GCC	unknown	30	26	n/a	25	528	713	19	Qtmd	coastal	none	N 13-26-13.	E 144-48-33.
CCD 179	Fadian borrow pit 4	unknown	40	30	n/a	20	633	270	69	Qtmd	plateau edge	borrow pit	N 13-26-35.	E 144-48-42.
CCD 180	Fadian borrow pit 1	unknown	70	75	n/a	20	2728	270	69	Qtmd	plateau edge	borrow pit	N 13-26-38.	E 144-48-49.
CCD 181	Fadian borrow pit 2	unknown	85	51	313	30	2640	342	62	Qtmd	plateau edge	borrow pit	N 13-26-43.	E 144-48-59.
CCD 182	Pinate sink 1	drawdown?	100	100	n/a	45	6881	206	72	Qtmd	plateau edge	none	N 13-27-05.	E 144-48-59.
CCD 183	Pinate sink 2	drawdown?	100	100	n/a	55	5234	150	319	Qtmd	plateau edge	none	N 13-27-06.	E 144-49-05.
CCD 184	Pinate sink 3	drawdown?	100	100	n/a	60	4329	144	16	Qtmd	plateau edge	none	N 13-27-02.	E 144-49-08.
CCD 185	Pinate sink 4	drawdown?	100	50	358	20	3014	144	16	Qtmr	plateau edge	none	N 13-26-58.	E 144-49-07.
CCD 186	Pinate main depression	drawdown?	192	193	348	40	27682	260	2	Qtmr	plateau edge	none	N 13-26-51.	E 144-49-07.
CCD 187	Maina sink	faulted contact	121	52	24	30	5131	244	323	Qtma	faulted contact	none	N 13-28-00.	E 144-43-57.
CCD 188	Maina Spring sink	faulted (spring)	188	81	35	45	14659	244	323	Qtma	faulted contact	none	N 13-27-55.	E 144-44-02.
CCD 189	Sinajana sink 1	unknown	384	159	352	25	48102	623	340	Qtma	plateau	none	N 13-27-49.	E 144-44-45.
CCD 190	Sinajana sink 2	unknown	268	60	340	30	21357	463	59	Qtma	plateau	none	N 13-27-39.	E 144-44-48.
CCD 191	Sinajana sink 3	unknown	150	104	n/a	30	7785	463	59	Qtma	plateau	none	N 13-27-43.	E 144-45-03.
CCD 192	Ordot depression	unknown	470	240	n/a	30	97467	803	70	Qtma	plateau	none	N 13-26-27.	E 144-45-15.
CCD 193	Ordot small depression	unknown	90	50	n/a	20	2671	427	72	Qtma	valley	none	N 13-26-38.	E 144-45-41.
CCD 194	Apusento Gardens sink (a)	valley sink	110	36	277	40	3047	58	282	Qtma	valley	none	N 13-26-42.	E 144-45-55.
CCD 195	Apusento Gardens sink (b)	valley sink	65	51	n/a	30	2841	58	282	Qtma	valley	none	N 13-26-41.	E 144-45-58.
CCD 196	Pulatar dry valley sinks	valley sinks	282/235/390	96	78/64/312	30	41941	304	278	Qtma	valley	none	N 13-26-37.	E 144-46-11.
CCD 197	Pulatar sink	valley sink	155	20	60	20	6551	426	296	Qtma	valley	none	N 13-26-32.	E 144-46-23.
CCD 198	Chalan Pago uvala	uvala	560	315	n/a	90	427460	848	36	Qtma	plateau	none	N 13-26-13.	E 144-46-09.
CCD 199	Carino sinkhole	collapse sink								Qtma	plateau	none	N 13-25-58.	E 144-46-04.
CCD 200	Guacluluyao sink (north)	valley sink	350	70	303	20	16633	246	304	Qtma	valley	none	N 13-25-52.	E 144-46-01.
CCD 201	Guacluluyao sink (south)	valley sink	150+199	76	301/33	20	11686	247	305	Qtma	valley	fish pond	N 13-25-45.	E 144-46-08.
CCD 202	Maimai dry valley sink	valley sink	141/235/233	57	60/47/313	20		983	80	Qtma	valley	none	N 13-26-34.	E 144-46-59.
CCD 203	Pago River tributary sink	valley sink	96	20	338	20	1793	513	278	Qtma	valley	none	N 13-25-40.	E 144-46-46.
CCD 204	Pago Bay depression	unknown	336	154	329	35	41064	500	66	Qtma	plateau edge	none	N 13-25-40.	E 144-47-04.
CCD 205	Pago Bay dry valley sink	valley sink	340	50	317	30	16269	500	66	Qtma	valley	none	N 13-25-48.	E 144-47-16.
CCD 206	Uruno cliff burrow pit 1	unknown	123	64	11	35	7224	103	14	Qtmr	plateau edge	borrow pit	N 13-37-12.	E 144-50-26.
CCD 207	Uruno cliff burrow pit 2	unknown	161	46	54	20	7307	108	15	Qtmr	plateau edge	borrow pit	N 13-37-08.	E 144-50-26.
CCD 208	Ysengsong depression 5	collapse								Tbl	plateau	none	N 13-32-18.	E 144-51-54.

Appendix 7: Inventory of closed contour depressions in southern Guam

Feature identifiers		Type or origin	Geometry of individual features					Nearest neighbor		Setting		Location	
KARST ID#	Name	of depression (if known)	length [m]	width [m]	long axis azimuth	depth [ft]	area [m2]	distance [m]	azimuth to n.n.	Geol. Fm.	general location	deepest point or center latitude	longitude
sCCD 1	Nimitz Hill depression 1	unknown	270	120	80	20	20299	710	304	Tal	within limestone inlier	N 13-27-52.	E 144-43-29.
sCCD 2	Asan depression 1	unknown	62	63	n/a	20	2845	200	4	Qtma	adjacent to volcanics	N 13-27-59.	E 144-42-24.
sCCD 3	Asan depression 2	unknown	92	63	346	20	4153	200	4	Qtma	adjacent to volcanics	N 13-27-54.	E 144-42-24.
sCCD 4	Nimitz Hill depression 2	unknown	111	59	290	20	3359	710	304	Tal	within limestone inlier	N 13-27-38.	E 144-43-49.
sCCD 5	Orote depression 1	unknown	95	41	278	20	2988	594	324	Qtmr	limestone peninsula	N 13-26-20.	E 144-37-44.
sCCD 6	Orote depression 2	unknown	699	165	313	40	65834	623	322	Qtmr	limestone peninsula	N 13-26-00.	E 144-37-59.
sCCD 7	Orote depression 3	unknown	47	42	n/a	20	1260	194	342	Qtmr	limestone peninsula	N 13-25-48.	E 144-38-08.
sCCD 8	Orote depression 4	unknown	68	44	15	25	1369	999	327	Qtmr	limestone peninsula	N 13-25-20.	E 144-38-27.
sCCD 9	Manengon sink	allogenic rechar	55	28	37	20	1198	3149	271	Qtma	adjacent to volcanics	N 13-24-10.	E 144-44-19.
sCCD 10	Yona depression 1	unknown	331	153	33	20	37020	850	271	Qtma	within limestone belt	N 13-24-08.	E 144-46-02.
sCCD 11	Yona depression 2	unknown	220	192	n/a	20	29637	850	271	Qtma	border b/w limestones	N 13-24-07.	E 144-46-32.
sCCD 12	Togcha depression	unknown	126	25	286	20	3295	1224	79	Tb	limestone inlier	N 13-22-08.	E 144-44-55.
sCCD 13	Ito and Minagawa sink	collapse sink	36	29	n/a	30	721	377	284	Tb	limestone inlier	N 13-22-15.	E 144-45-36.
sCCD 14	County Club depression	unknown	87	72	n/a	25	4410	377	284	Qtmf	border b/w limestones	N 13-22-13.	E 144-45-48.
sCCD 15	Talofofo depression 1	unknown	362	147	n/a	60	35055	651	25	Qtmr	border b/w limestones	N 13-21-35.	E 144-45-33.
sCCD 16	Talofofo depression 3	unknown	403	121	8	20	32035	533	60	Qtma	border b/w limestones	N 13-21-12.	E 144-45-43.
sCCD 17	Talofofo depression 4	unknown	83	67	n/a	35	3641	112	345	Qtmr	border b/w limestones	N 13-20-58.	E 144-45-28.
sCCD 18	Talofofo depression 5	unknown	104	68	27	20	4581	112	345	Qtmr	border b/w limestones	N 13-21-01.	E 144-45-27.
sCCD 19	Talofofo depression 2	unknown	111	62	49	25	5583	392	342	Qtma	limestone inlier	N 13-21-13.	E 144-45-22.
sCCD 20	Talofofo depression 6	unknown	245	113	82	30	20511	267	36	Qtma	border b/w limestones	N 13-20-52.	E 144-45-22.
sCCD 21	Talofofo depression 7	unknown	332	106	297	20	21945	290	336	Qtma	border b/w limestones	N 13-20-43.	E 144-45-24.
sCCD 22	Asanite sink	collapse sink	94	44	310	20	3385	961	277	Qtma	within limestone belt	N 13-20-37.	E 144-45-58.
sCCD 23	Talofofo golf course sink 1	unknown	51	44	n/a	20	1405	318	279	Tam	limestone inlier	N 13-21-53.	E 144-43-37.
sCCD 24	Talofofo golf course sink 2	unknown	288	123	4	30	23820	318	279	Tam	limestone inlier	N 13-21-53.	E 144-43-47.
sCCD 25	Malojloj depression 1	unknown	316	149	352	20	31312	356	336	Qtma	border b/w limestones	N 13-19-02.	E 144-45-49.
sCCD 26	Malojloj depression 2	unknown	72	48	n/a	20	2922	246	61	Qtmf	border b/w limestones	N 13-18-49.	E 144-45-53.
sCCD 27	Malojloj landfill	unknown/ modif	227	167	n/a	40	14433	246	61	Qtmf	border b/w limestones	N 13-18-46.	E 144-45-46.
sCCD 28	Malojloj depression 4	unknown	127	140	n/a	20	12584	343	13	Qtmf	border b/w limestones	N 13-18-26.	E 144-45-45.
sCCD 29	Malojloj depression 5	unknown	326	97	16	30	23916	343	13	Qtmf	border b/w limestones	N 13-18-34.	E 144-45-47.
sCCD 30	Malojloj depression 6	unknown	381	91	36	20	16253	752	7	Qtmf	border b/w limestones	N 13-17-56.	E 144-45-43.
sCCD 31	Malojloj depression 7	unknown	206	74	58	20	9793	752	7	Qtmf	border b/w limestones	N 13-17-32.	E 144-45-39.
sCCD 32	Alifan ridge sink 1	collapsed condu	200	135	342	45	15308	286	288	Tal	limestone capping mountains	N 13-21-08.	E 144-39-59.
sCCD 33	Alifan ridge sink 2	collapsed condu	179	86	313	20	7512	286	288	Tal	limestone capping mountains	N 13-21-05.	E 144-40-07.
sCCD 34	Alifan ridge sink 3	collapsed condu	491	241	346	45	83879	403	317	Tal	limestone capping mountains	N 13-20-51.	E 144-40-17.
sCCD 35	Alifan ridge sink 4	collapsed condu	573	198	16	50	79256	919	349	Tal	limestone capping mountains	N 13-20-24.	E 144-40-22.
sCCD 36	Alifan ridge sink 5	collapsed condu	134	70	25	45	6262	1514	293	Tal	limestone capping mountains	N 13-22-15.	E 144-40-16.
sCCD 37	Bonya river sink 1	valley doline	532	204	79	40	78276	639	285	Tt	transitional facies	N 13-21-55.	E 144-40-58.
sCCD 38	Fena cockpit sink 30	cockpit karst do	106	111	n/a	25	7064	219	313	Tb	limestone inlier	N 13-21-51.	E 144-41-23.
sCCD 39	Fena cockpit sink 31	cockpit karst do	176	84	30	30	9295	219	313	Tb	limestone inlier	N 13-21-46.	E 144-41-27.
sCCD 40	Bonya river sink 2	incised valley d	618	132	89	20	34605	293	298	Tb	non-limestone	N 13-22-05.	E 144-41-37.
sCCD 41	Fena cockpit sink 32	cockpit karst do	121	79	n/a	20	7176	293	298	Tb	limestone inlier	N 13-22-01.	E 144-41-46.
sCCD 42	Bonya river sink 3	incised valley d	284	23	283	20	4862	165	0	Tt	transitional facies	N 13-22-09.	E 144-42-02.

(continued on the next page)

Feature identifiers		Type or origin	Geometry of individual features					Nearest neighbor			Setting	Location	
KARST ID#	Name	of depression (if known)	length [m]	width [m]	long axis azimuth	depth [ft]	area [m2]	distance [m]	azimuth to n.n.	Geol. Fm.	general location	deepest point or center latitude	longitude
sCCD 43	Fena cockpit sink 28	valley doline	262	38	359	20	8194	176	85	Tal	limestone inlier	N 13-22-42.	E 144-42-13.
sCCD 44	Fena cockpit sink 29	cockpit karst do	98	47	3	20	2989	176	85	Tal	limestone inlier	N 13-22-42.	E 144-42-19.
sCCD 45	Fena cockpit sink 18	cockpit karst do	101	79	n/a	20	4902	133	319	Tal	limestone inlier	N 13-22-22.	E 144-42-32.
sCCD 46	Fena cockpit sink 19	cockpit karst do	141	84	326	30	8947	135	320	Tal	limestone inlier	N 13-22-18.	E 144-42-35.
sCCD 47	Fena cockpit sink 20	cockpit karst do	184	76	333	20	9085	137	83	Tb	limestone inlier	N 13-22-20.	E 144-42-40.
sCCD 48	Fena cockpit sink 21	cockpit karst do	247	53	338	20	5854	170	277	Tb	limestone inlier	N 13-22-12.	E 144-42-23.
sCCD 49	Fena cockpit sink 22	cockpit karst do	148	87	341	20	9369	64	324	Tb	limestone inlier	N 13-22-14.	E 144-42-30.
sCCD 50	Fena cockpit sink 23	cockpit karst do	46	31	n/a	20	1003	61	8	Tb	limestone inlier	N 13-22-11.	E 144-42-30.
sCCD 51	Fena cockpit sink 24	cockpit karst do	106	59	297	20	4634	61	8	Tb	limestone inlier	N 13-22-09.	E 144-42-30.
sCCD 52	Fena cockpit sink 25	cockpit karst do	111	70	n/a	20	5785	169	31	Tb	limestone inlier	N 13-22-04.	E 144-42-27.
sCCD 53	Fena cockpit sink 26	cockpit karst do	71	40	25	20	1634	321	88	Tal	limestone inlier	N 13-22-20.	E 144-42-51.
sCCD 54	Fena cockpit sink 27	cockpit karst do	134	73	15	40	8037	363	327	Tal	limestone inlier	N 13-22-10.	E 144-42-57.
sCCD 55	Fena cockpit sink 1	cockpit karst do	83	36	56	20	2421	116	323	Tb	limestone inlier	N 13-21-48.	E 144-42-17.
sCCD 56	Fena narrow sink	valley doline	158	13	325	10	1266	141	9	Tb	limestone inlier	N 13-21-51.	E 144-42-24.
sCCD 57	Fena cockpit sink 2	cockpit karst do	246	173	73	30	2261	116	323	Tb	limestone inlier	N 13-21-45.	E 144-42-21.
sCCD 58	Bonya-Tolae Yu'us river	incised valley	1588-total	90	multiple	40	60445	n/a	n/a	Tb	limestone inlier	N 13-21-50.	E 144-42-44.
sCCD 59	Fena cockpit sink 4	cockpit karst do	142	67	49	20	6708	147	18	Tb	limestone inlier	N 13-21-53.	E 144-42-50.
sCCD 60	Fena cockpit sink 5	cockpit karst do	164	86	23	30	9909	130	280	Tb	limestone inlier	N 13-21-33.	E 144-42-41.
sCCD 61	Fena cockpit sink 6	cockpit karst do	110	52	313	40	4120	142	280	Tb	limestone inlier	N 13-21-35.	E 144-42-37.
sCCD 62	Fena cockpit sink 7	cockpit karst do	78	58	54	40	3089	96	353	Tb	limestone inlier	N 13-21-35.	E 144-42-32.
sCCD 63	Fena cockpit sink 8	cockpit karst do	53	30	321	20	945	92	73	Tb	limestone inlier	N 13-21-38.	E 144-42-32.
sCCD 64	Fena cockpit sink 9	cockpit karst do	72	46	312	30	1881	92	73	Tb	limestone inlier	N 13-21-37.	E 144-42-29.
sCCD 65	Fena cockpit sink 10	cockpit karst do	176	156	37	60	15089	107	316	Tb	limestone inlier	N 13-21-39.	E 144-42-27.
sCCD 66	Fena cockpit sink 11	cockpit karst do	134	93	63	60	9162	114	9	Tb	limestone inlier	N 13-21-45.	E 144-42-30.
sCCD 67	Fena cockpit sink 12	cockpit karst do	104	54	297	50	3612	103	64	Tb	limestone inlier	N 13-21-41.	E 144-42-32.
sCCD 68	Fena cockpit sink 13	cockpit karst do	148	102	35	60	10484	101	342	Tb	limestone inlier	N 13-21-40.	E 144-42-36.
sCCD 69	Fena cockpit sink 14	cockpit karst do	59	55	n/a	20	1577	103	64	Tb	limestone inlier	N 13-21-43.	E 144-42-35.
sCCD 70	Fena cockpit sink 15	cockpit karst do	96	44	307	20	3223	126	44	Tb	limestone inlier	N 13-21-45.	E 144-42-38.
sCCD 71	Fena cockpit sink 16	cockpit karst do	169	93	309	40	10242	114	9	Tb	limestone inlier	N 13-21-49.	E 144-42-30.
sCCD 72	Fena cockpit sink 17	cockpit karst do	245	142	22	40	28355	219	360	Tb	limestone inlier	N 13-21-51.	E 144-42-37.

Appendix 8: Inventory of caves in northern Guam

Feature identifiers		Cave	Entrance			Room/pass. dimen.			Setting			Location	
KARST ID#	Cave Name	Type	setting	width [m]	height [m]	max length	max width	max height	Cave Floor*	Fresh water?	Geol. Fm.	Cave entrance Latitude	Longitude
CAVE 001	Two Lovers' Pit Cave	pit cave	cliff top				50 m deep pit		br	no	Qtmd	Two Lovers tourist area	
CAVE 002	Tarague Cliff Pit	pit cave	cliff side						br	no	Qtmr	Tarague embayment cliff	
CAVE 003	Harmon Sink Shafts	shafts	sinking stream		D~.5m		4 m max depth		soil	no	Qtmd	Harmon Sink blind valley	
CAVE 004	Mati Cliff Pit Complex	pit caves	a complex of 30+ pit caves, <2m diam., 2-8 m depth; area inland from cliff rampart at Mati point.										
CAVE 005	Ritidian Beach Cave	fm	cliff base	3.0		30.0	15.0	10.0	soil	no	Qtmr	E 144-51-33	N 13-39-04.40
CAVE 006	Ritidian Cave	fm	roof coll.	1.3 m diam.		60.0	30.0	11.0	br/ fs	lens	Qtmr	E 144-51-33	N 13-38-56.69
CAVE 007	Uruno Point Cave	fm	cliff face	18.0	3.7	45.0	18.0	5.0	soil	no	Qtmr	E 144-50-17	N 13-37-32.00
CAVE 008	Tarague Cave	fm	cliff face	4.5	4.8	6.0	6.0	6.0	soil	no	Qtmd	E 144-52-52	N 13-37-34.31
CAVE 009	Mergagan Point Cave	fm	cliff face	1.0	3.0	7.0	6.0	6.0	br	no	Qtmd	E 144-53-07	N 13-37-21.75
CAVE 010	Tagua Cave	fm	cliff face	4.6	4.8	3.0	4.6	6.0	soil	no	Qtmd	E 144-55-24	N 13-35-46.92
CAVE 011	Tweed's Cave	cutter	cliff face			16.0	3.0	2.5	soil	no	Qtmr	E 144-49-56	N 13-35-14.53
CAVE 012	Pugua Point Cave	fm		2.0	1.8		3 small rms ~4x2		soil	no	Qtmr	E 144-49-51	N 13-35-05.07
CAVE 013	Haputo Cave	fm		18.0	6.0	18.0	46.0	9.0		no	Qtmd	E 144-50-05	N 13-34-04.65
CAVE 014	Haputo Collapsed Cave	fm	coastal cliff				single collps. roc		rubble	no	Qtmd	north end of Haputo Beach	
CAVE 015	Anao Point Cave	fm	cliff base			4.0	3.0	1.8	rubble	no	Qtmd	E 144-56-03	N 13-33-01.32
CAVE 016	Mataguac Spring Cave	stream	volc bas.	3.0	1.2	~30	2.0	1.5	volc	eph.str.	Qtmd/Ta	E 144-52-46	N 13-32-30.88
CAVE 017	Mt.Santa Rosa Cave	stream	3 entrances, pits						soil	eph.str.	volc?	E 144-54-35	N 13-32-02.51
CAVE 018	Amantes Point Cave	fm	cliff-46m	3.0	15.0	18.0	6.0	12.0	soil/rb	no	Qtmd	E 144-48-26	N 13-31-57.23
CAVE 019	Fafai Cave	fm	cliff face	7.0	2.0			12.0	soil/rb	lens	Qtmd	E 144-46-50	N 13-31-34.59
CAVE 020	Janum Cave	fm	surf (6x4.5) +	1 skylight		15.0	12.0	9.0	rubble	saltwater	Qtmd	E 144-55-13	N 13-31-14.35
CAVE 021	Janum Beach Cave	fm	beach	2.0	3.0	6.0	6.0		sand	no	Qtmd	E 144-55-20	N 13-31-00.25
CAVE 022	Janum Spring Cave	spring	0.6 amsl	9.0	6.0	21.0	6.0		br	stream	Qtmd	E 144-54-37	N 13-30-50.46
CAVE 023	Lujuna Point Cave	fm	cliff face	7.0	9.0	15.0	9.0	12.0	br	no	Qtmd	E 144-54-17	N 13-30-47.04
CAVE 024	Asdonlucas Cave	fm	cliff base	1.0	1.5	10.4	8.2	4.5	br	yes?	Qtmr	E 144-53-21	N 13-30-46.57
CAVE 025	Ypao Stalactite Cave	fm	2.6 amsl	50.0	8.0				rubble	no	Qtmd	E 144-46-52	N 13-29-42.04
CAVE 026	Ypao Cave	fm	2.6 amsl	10.0	6.0				rubble	no	Qtmd	E 144-46-53	N 13-29-41.73
CAVE 027	Devil's punchbowl	collapse		20 m diameter		60 m across		30.0	rubble	lens	Qtm?	E 144-46-28	N 13-29-56.47
CAVE 028	Pagat Cave	fm	collapse sink			see section 9. 2. 5.			br	lens	Qtmd	E 144-52-24	N 13-29-16.29
CAVE 029	Haya Pagat Cave	fm	collapse sink			see section 9. 2. 5.			br/rubble	lens	Qtmd	E 144-52-24	N 13-29-16.23
CAVE 030	Mt. Barrigada Pit	abnd. conduit	pit, 1.8 diam., 15m deep			160+ m passage			rubb/ soil	pooling		E 144-50-01	N 13-29-04.99
CAVE 031	Marbo Cave	fm?	cliff base	5	9	see fig. 9.7			rubble	lens	Qtmd	E 144-51-50	N 13-29-03.64
CAVE 032	Fadian Point Cave	described as large, multichambered, complex and with a small stream (!?)									Qtmr	~E 144-47-0	~N 13-26-36
CAVE 033	Fadian Stream Cave	described as oval chamber (3x5.5x3.7), soil floor, with a flowing stream (!?)									Qtmr	~E 144-47-0	~N 13-26-30
CAVE 034	Chalan Pago Cave	fm?	cliff face	3.7	2.5	2 rooms (11x5.5; 4x9x1)				no	Qtma	E 144-47-01	N 13-25-46.59
CAVE 035	Carino Sink Cave	ex-conduit	sinkhole	20m deep		3 pass., total ~100m			soil	no	Qtma	contact John Jenson	

(continued on the next page)

Feature identifiers		Cave	Entrance			Room/pass. dimen.			Setting			Location	
KARST ID#	Cave Name	Type	setting	width [m]	height [m]	max length	max width	max height	Cave Floor*	Fresh water?	Geol. Fm.	Cave entrance Latitude	Longitude
CAVE 036	Appealing Sink Cave	ex-conduit	sinkhole	~10m deep		3 pass., total ~100m			soil	no		contact Curt Wexel	
CAVE 037	Ritidian Pictograph Cave	fm				see figure 9.5			br/fs	no	Qtmr	contact NWR Ritidian	
CAVE 038	Ritidian Gate Cave	fm	very large cave breached by cli			see figure 9.6				no	Qtmr	N of road, GWR gate	
CAVE 039	Ritidian View Cave	fm		cliff retreat					br/fs	no	Qtmr	cliff N of access road	
CAVE 040	Mataguac Mud Cave	stream		swallet		see figure 8.3			mud	eph.str.	Qtmd/Ta	SW Mataguac Hill, contact	
CAVE 041	North Mataguac Cave	stream		swallet					mud	eph.str.	Qtmd/Ta	N Mataguac, contact	
CAVE 042	Awesome Cave	stream		roof collapse		see figure 8.5			br/fs/rb	eph.str.	Qtmd/Ta	Mt. Santa Rosa, contact	
CAVE 043	Interesting Cave	stream		roof collapse					br/fs/rb	eph.str.	Qtmd/Ta	Mt. Santa Rosa, contact	
CAVE 044	Piggy Cave	stream		roof collapse		see figure 8.4			br/rb	eph.str.	Tal/Ta	Mt. Santa Rosa, contact	
CAVE 045	Elvis' Pelvis Cave	stream								eph.str.	Qtmd/Ta	Mt. Santa Rosa, contact	
CAVE 046	Virgin Cave	stream								eph.str.	Qtmd/Ta	Mt. Santa Rosa, contact	
CAVE 047	Fadian Fish Hatchery Cave	fm?		roof collapse		see figure 9.8			rubble	lens	Qtmr	Fadian Fish Hatchery	
CAVE 048	Joe Quitigua's Water Cave	fm?		roof collapse					rubble	lens	Qtmr	Hawaiian Rock Quarry	
CAVE 049	Frankie's Cave	fm?		roof collapse		see figure 9.9			rubble	lens	Qtmr	Tweed's Cave Trail	
CAVE 050	Tarague Well #5	fm?		roof collapse					rubble	lens	Qtmd		
CAVE 051	Hawaiian Rock Quarry Cav.	ex-conduit?		cliff retreat					br	no	Qtmr	Hawaiian Rock Quarry	
CAVE 052	Earl's Bottomless Pit	fracture								no			
CAVE 053	Amantes Cliff Caves	fm/ notch		cliff retreat					br	no	Qtmd		
CAVE 054	Falcona High Cliff Cave	fm?		cliff retreat						no	Qtmr		
CAVE 055	Uruno Point small cave1	fm?		cliff retreat						no	Qtmr		
CAVE 056	Uruno Point small cave2	fm?		cliff retreat						no	Qtmr		
CAVE 057	Ritidian Cliff Caves	fm/ notch	three openings in the cliff south of Ritidian Pt.							no	Qtmr		
CAVE 058	Margagan Point notches	fm/ notch		cliff retreat					br	no	Qtmr		
CAVE 059	Tarague East Cliff Cave	fm?		cliff retreat					br	no	Qtmr		
CAVE 060	Tarague West Cliff Cave	fm		cliff retreat					br	no	Qtmr		
CAVE 061	Tarague Beach View Cave			cliff retreat		see figure 9.3			fs/br	no	Qtmr		
CAVE 062	Tarague Copra Cave			cliff retreat		see figure 9.2			soil	no	Qtmr		
CAVE 063	Small Cave south of Pati	fm?		cliff retreat						no	Qtmd		
CAVE 064	Small Cave south of Latte	fm?		cliff retreat						no	Qtmd		
CAVE 065	Lafac Grotto	collapse		roof collapse					rubble	ocean	Qtmd		
CAVE 066	Lafac Point Cliff Caves	fm?		cliff retreat						no	Qtmr		
CAVE 067	Mati Point High Cliff Cave	fm?		cliff retreat						no	Qtmr		
CAVE 068	Janum Contact Small Caves								br	no	Tj/Qtm		
CAVE 069	North Catalina Beach Caves	fm?		cliff retreat		3 beach caves			sand	no	Qtmd		
CAVE 070	South Catalina Beach Caves	fm?		cliff retreat		4 beach caves			sand	no	Qtmd		

* cave floor: br-bedrock, rb-rubble, fs-flowstone

(continued on the next page)

Feature identifiers		Cave	Entrance			Room/pass. dimen.			Setting			Location	
KARST	Cave	Type	setting	width	height	max	max	max	Cave	Fresh	Geol.	Cave entrance	
ID#	Name			[m]	[m]	length	width	height	Floor*	water?	Fm.	Latitude	Longitude
CAVE 071	Pagat Point Shelter Cave	fm?	cliff collapse						rubble	ocean	Qtmd		
CAVE 072	Mang. Golf. Course fracture cave	fracture								ocean	Qtmd		
CAVE 073	Hawaiian Rock north sink caves	fracture	fractures						br	no	Qtmd		
CAVE 074	Hawaiian Rock south sink caves	fracture	fractures						br	lens	Qtmd		
CAVE 075	Iates Point Cliff Cave	fm?	cliff retreat						br	no	Qtmr		
CAVE 076	Marine Lab Beach Caves	fm?	cliff retreat						br/rb	no	Qtmr		
CAVE 077	Joan's Cave	fm	roof collapse						br/fs	lens	Qtmr		
CAVE 078	Hilaan Water Fracture		roof collapse						br/rb	lens	Qtmr		
CAVE 079	Lost Pond Shelter Caves	fm	cliff retreat						br/soil	no	Qtmr		

* cave floor: br-bedrock, rb-rubble, fs-flowstone

Appendix 9: Inventory of caves in southern Guam

Feature identifiers		Cave	Entrance			Room/pass. dimen.			Setting			Location	
KARST ID#	Cave Name	Type (if known)	setting	width [m]	height [m]	max length	max width	max height	Cave Floor*	Fresh water?	Geol. Fm.	Cave entrance Latitude	Longitude
sCAVE 001	Taga'chang Beach Pit	pit cave	cliff side	de-walled			20 m deep pit		br	no	Qtmr	~20m N of Taga'chang Bea	
sCAVE 002	Pit near Lost River Rise	pit cave	hill slope	~2m diam.			single small roor		soil	no	Tb	E 144.71173	N 13.36020
sCAVE 003	Adelup Cave	fm	cliff base	1.5 diam.		7.5	4.8	1.5	rubble	no	Qtmr	E 144-42-42	N 13-28-31.48
sCAVE 004	Palasao Cave	volc. contact?	collapse	~2m diam.		3 rms, 25+ m each			br	pool?	Tal	E 144-43-05	N 13-28-01.11
sCAVE 005	Hoyo Matugan	pit cave	shaft, 1m diam, 5m deep			18.5	6.0	3.0		no		E 144-43-24	N 13-27-46.48
sCAVE 006	Nimitz Hill Cave		exact location unknown, may be same as Palasao C. (Rogers & L., 1992)									~E 144-43-1	~N 13-27-39
sCAVE 007	Fonte Cave	abnd. conduit?		1.5 m diam.		23.0	3.0	3.0		no		E 144-43-34	N 13-27-31.93
sCAVE 008	Orote Sagan Basula Cave		listed by Rogers & L., 1992; no information provided, located near Orote dump									~E 144-38-1	~N 13-25-19
sCAVE 009	Tipalao Cave	fm?	near s.l.	2 (.8x3.4; 5x4.6)		2 rooms, passages			br	no	Qtmr	E 144-38-40	N 13-24-46.08
sCAVE 010	Ylig Bay Cave									no	Qtma	E 144-46-05	N 13-23-24.41
sCAVE 011	Ylig Point Caves	primary construction, reef spur & groove "cave"								no		E 144-46-26	N 13-22-55.64
sCAVE 012	Mt. Alutom Cave	ls pocket	small (3 sq.m., 1.2m high) cave in limestone lens within Alutom volcanics									E 144-43-07	N 13-22-36.79
sCAVE 013	Bay Rum Cave	stream?	large, complex cave, 172m total length, small stream (Rogers, 1992)								Tal	E 144-42-28	N 13-22-25.70
sCAVE 014	Gumayas Guma'Yu'us Cave	abnd. str.	valley	4.0	3.0	12.0	21.0	15.0	soil	no	Tb	E 144-45-13	N 13-22-11.40
sCAVE 015	Gumayas Chiget Cave	abnd. str.	valley			12.0	3.0	2.0	soil	no	Tb	46 m downstream from pre	
sCAVE 016	Hoyu Sabana Lamlam	pit cave	pit	(1x2), 4.5 deep		tubular passage				no	Tal/Tt	E 144-40-01	N 13-21-56.05
sCAVE 017	Maemong River Cave	swallet	swallet of entire Maemong River, underground course 100+ m								Tb	E 144-42-37	N 13-21-54.88
sCAVE 018	Maemong Rise	resurgence	resurgence of Maemong River, at a base of a cliff							river	Tb	E 144-42-35	N 13-21-51.93
sCAVE 019	Ibaba Cave		hill foot	6.0	4.6	9.0	6.0	4.6	mud/soil		Tb	E 144-42-18	N 13-21-50.47
sCAVE 020	Liyang Namu Kanutu	abnd. str.	sink bottom	tube passages, ~1m in diamater, 22m length, blows air							Tb	E 144-42-23	N 13-21-44.17
sCAVE 021	Lost River Cave	stream	collapse	pit 1.5x3.0		2 lrg rms, passage 85m t			soil	river	Tb	E 144-42-38	N 13-21-40.90
sCAVE 022	Tolae Yu'us Cave	swallet	swallet of Tolaeyuus River, underground course 420+ m								Tb	E 144-42-34	N 13-21-34.62
sCAVE 023	Hoyu Fena	pit cave	pit	2.4	4.6		6 m deep		soil	no	Tb	E 144-42-21	N 13-21-29.03
sCAVE 024	Tolae Yu'us Kinahulo'guan	resurgence	resurgence of Tolaeyuus River, at a base of a cliff							river	Tb	E 144-42-24	N 13-21-27.99
sCAVE 025	Liyang Almagosa Gelagu	abnd. str.		1.5	3.7	1 passage, ~20m long			soil	no	Tal	E 144-40-18	N 13-20-42.85
sCAVE 026	Mt. Almagosa Caves		cliff face			~3x1.2x1.8			soil	no	Tal	E 144-40-32	N 13-20-28.18
sCAVE 027	Pinnacle Cave			1.5	1.5	4.6	6.0	1.8	soil	no	Qtma	E 144-39-55	N 13-20-27.51
sCAVE 028	Mata Cave		cliff base	1.5	1.2	3.0	3.4	2.4	soil	no	Qtma	E 144-45-11	N 13-20-27.44
sCAVE 029	Asanite Cave		cliff base	pit, 12m diam		~8 m deep to water			rubble	lens	Qtma	E 144-45-54	N 13-20-25.87
sCAVE 030	Talofofo Cave 1	paleo-stream?	see Fig. 8. 9						br/fs	no	Qtmr	E 144-45-42	N 13-20-22.19
sCAVE 031	Talofofo Cave 2	paleo-stream?	see Fig. 8. 10						br/fs	no	Qtmr	same area as sCAVE030	
sCAVE 032	Talofofo Cave 3	paleo-stream?	see Fig. 8. 9						br/fs	no	Qtmr	same area as sCAVE030	
sCAVE 033	Talofofo Cave 4	paleo-stream?	see Fig. 8. 9						br/fs	no	Qtmr	same area as sCAVE030	
sCAVE 034	Talofofo Cave 5	paleo-stream?	see Fig. 8. 9						br/fs	no	Qtmr	same area as sCAVE030	

* cave floor: br-bedrock, rb-rubble, fs-flowstone

(continued on the next page)

Feature identifiers		Cave	Entrance			Room/pass. dimen.			Setting			Location	
KARST ID#	Cave Name	Type (if known)	setting	width [m]	height [m]	max length	max width	max height	Cave Floor*	Fresh water?	Geol. Fm.	Cave entrance Latitude	Longitude
sCAVE 035	Talofofo Cave 6	paleo-stream?	see Fig. 8. 9						br/fs	no	Qtmr	same area as sCAVE030	
sCAVE 036	Talofofo Pit Cave	pit cave (roofed)							br/fs	no	Qtmr	same area as sCAVE030	
sCAVE 037	Adjoulan Point Cave	fm	cliff, @6m	2 (~1.5x2)		~6	~6		br/ rubble	no	Qtmr	E 144-45-48.	N 13-20-21.26
sCAVE 038	Asquiroga Cave	fm	cliff							no		E 144-45-38.	N 13-20-18.25
sCAVE 039	Tres Botsas	fm	cliff face, @~30 m			three small caves, (two ~			soil	no	Qtma	E 144-45-18.	N 13-20-17.42
sCAVE 040	Matala Caves	fm	cliff face	4 (~1.2x1.5)		four small caves, (~1.8x1			soil	no	Qtmr	E 144-45-45.	N 13-19-35.69
sCAVE 041	Gumoje Cave	small cave reported in western headwaters of Liyog River, must be small							limestone	no	Tub	~E 144-41-5	~N 13-15-10
sCAVE 042	Suma Cave	small cave reported in eastern headwaters of Suma River, must be small							limestone	no	Tub	~E 144-41-5	~N 13-15-05
sCAVE 043	Asiga Water Cave	fm	collapse							lens	Qtmr	contact Dept of Parks & Re	
sCAVE 044	Asalonso Cave		cliff face	2.4	3.0	4.6	3.0	2.4		no	Qtma	E 144-45-12.	N 13-19-22.38
sCAVE 045	Assupian Cave									no	Tub	E 144-49-58.	N 13-18-23.06
sCAVE 046	Asiga Cave	fm	cliff top							no	Qtmr	E 144-45-37.	N 13-18-11.03
sCAVE 047	Gadao's Cave	fm	sea level	3 (1.8x2.4, 1.5x1		9.8	2.0	1.9	rubble	no	Qtma	E 144-44-53.	N 13-16-25.73
sCAVE 048	Lost River Rise Cliff Cave	ex-resurg.								no	Tb	just above the Lost River R	
sCAVE 049	Fena Sinkhole Cave	eph. str.								no	Tb	one of the SW Fena sinkho	
sCAVE 050	Orote Channel Cave	fm								lens	Qtmr	opposite Orote Island	
sCAVE 051	Anae Island Cave	fm							br	lens		west side of Anae Island	
sCAVE 052	Almagosa Cave	spring							br	stream	Tal	Naval Magazine	
sCAVE 053	Asanite Road Caves	fm							br	no	Qtma	right hand side of the road	
sCAVE 054	Talofofo Bay Overhang	fm								no	Qtma	Talofofo Bay	
sCAVE 055	Notre Dame School caves	fm							br/fs	no	Qtma	Behind Notre Dame schl.	
sCAVE 056	Virgin Mary Shelter Cave	fm							br	no	Tal	trail to Jumullong Manglo	
sCAVE 057	Orotte Grottos (n)	collapse							rubble	ocean	Qtmr	south side of Orote	
sCAVE 058	Orote Grottos (s)	collapse							rubble	ocean	Qtmr	south side of Orote	
sCAVE 059	Orote Cliff Cave	fm							br	no	Qtmr	south side of Orote	
sCAVE 060	Cool Cave	fm							br/fs	no	Qtmr	Asiga area	

* cave floor: br-bedrock, rb-rubble, fs-flowstone

Appendix 10: Inventory of natural arches, bridges and prominent collapse features

Feature identifiers		Type	Additional Information
KARST ID#	Feature Name		
COL 001	Pagat Sea Arch	arch made by collapse of a flank margin cave or a sea cave	Qtmr Ls.
COL 002	Ritidian Double Arch	double arch made by roof collapse of a flank margin cave	Qtmr Ls.
COL 003	Window Rock	natural arch (or former natural bridge) made by chamber roof collapse	span 21m; height 11m; E 144-45-42.85, N 13-20-22.19
COL 004	Tipoco Island Arch	collapse of a small flank margin cave or primary void in reef limestone	Qtma Ls.
COL 005	Orote Window	partial collapse of a roof of a flank margin cave at the top of the cliff	Qtmr Ls.
COL 006	Maemong Bridge north	natural bridge on Maemong River	Bonya Ls. E 144-42-13.09 N 13-22-57.12
COL 007	Maemong Bridge south	natural bridge on Maemong River	Bonya Ls. (~location same as the previous bridge)
COL 008	Bonya River Arch	natural bridge on Bonya River	Bonya Ls. E 144-42-23.09 N 13-21-44.34
COL 009	Collapse south of Pati Pt.	collapse scar on the cliff south of Pati Point	
COL 010	Collapse, Lafac/Anao 1	collapse scar on the cliff S of Lafac, N of Anao Pt. (northernmost)	35 m tall, 65 m wide
COL 011	Collapse, Lafac/Anao 2	collapse scar on the cliff S of Lafac, N of Anao Pt. (middle)	75 m tall, 230 m wide
COL 012	Collapse, Lafac/Anao 3	collapse scar on the cliff S of Lafac, N of Anao Pt. (southernmost)	150 m tall, 300 m wide; caves at the north end
COL 013	Anao Point Collapse	collapse scar on the cliff at Anao Point	90 m tall, 107 m wide
COL 014	Lujuna Collapse 1	collapse scar on the cliff at Lujuna Point (northern)	95 m tall, 125 m wide; cave remnants
COL 015	Lujuna Collapse 2	collapse scar on the cliff at Lujuna Point (southern)	60 m tall, 230 m wide
COL 016	Pagat Collapse	collapse scar on the cliff north of Pagat Point	
COL 017	Golf Course Collapse	collapse scar on the cliff at the Mangilao Golf Course	

Appendix 11: Inventory of voids intercepted by drilling

WELL ID #	Well Log Entry	well log data (ft) void/ lost. circ. starts	ends	well information well elev. (ft a. s. l.)	total depth* ft	depth (ft) to volcanics**
A-2	lost circulation	155	164	119.41	171.41	
A-6	cavern	163	167	153.33	307.33	
A-3	clay	31	39	103.85	366.4	-255.988
A-3	clay	47	51	103.85	366.4	-255.988
A-3	clay	109	112	103.85	366.4	-255.988
A-3	scattered clay layers	125	200	103.85	366.4	-255.988
A-3	clay	337	338	103.85	366.4	-255.988
A-3	clay	345	346	103.85	366.4	-255.988
A-5	clay	130	134	146.7	323.14	-185.991
A-7	clay	12	26	136.86	186.86	
A-7	clay	97	100	136.86	186.86	
A-7	clay	110	115	136.86	186.86	
A-8	lost circulation	125		124	305.17	
A-9	clay	38	49	187.15	235.78	
A-9	scattered clay layers	49	65	187.15	235.78	
A-9	clay with coral	65	83	187.15	235.78	
A-9	streaks of clay in ls.	83	109	187.15	235.78	
A-9	lost circulation	109		187.15	235.78	
A-10	lost circulation	70		191.01	215.25	
A-11	clay	12	17	173.63	340.63	-180.991
A-11	clay	18	33	173.63	340.63	-180.991
A-11	clay	47	60	173.63	340.63	-180.991
A-11	lost circulation	50		173.63	340.63	-180.991
A-11	clay	60	82	173.63	340.63	-180.991
A-11	clay with coral	84	121	173.63	340.63	-180.991
A-11	clay	124	138	173.63	340.63	-180.991
A-11	coral w scattered clay layers	159	175	173.63	340.63	-180.991
A-11	clay	244	273	173.63	340.63	-180.991
A-11	clay with wood	320	321	173.63	340.63	-180.991
A-11	clay with wood	323	324	173.63	340.63	-180.991
A-11	clay	339	343	173.63	340.63	-180.991
A-11	clay	352	356	173.63	340.63	-180.991
A-11	clay	356	375	173.63	340.63	-180.991
A-12	clay	35	38	138.45	338.45	-197.989
A-12	coral w clay	51	58	138.45	338.45	-197.989
A-12	clay	58	60	138.45	338.45	-197.989
A-12	lost circulation	135		138.45	338.45	-197.989
A-12	void	203	204	138.45	338.45	-197.989
A-12	possible clay	241	251	138.45	338.45	-197.989
A-12	clay	251	263	138.45	338.45	-197.989
A-12	possible clay	275	285	138.45	338.45	-197.989
A-12	possible clay	305	310	138.45	338.45	-197.989
A-12	possible clay	333	335	138.45	338.45	-197.989
A-12	possible clay	338	343	138.45	338.45	-197.989
A-12	possible clay	349	354	138.45	338.45	-197.989
A-12	clay	376	390	138.45	338.45	-197.989
A-13	clay	35	46	130.38	324.38	
A-13	clay with coral	46	165	130.38	324.38	
A-13	clay	185	194	130.38	324.38	
A-19	lost circulation	100	115	144	160	
A-19	lost circulation	120		144	160	
A-21	dropped fast (voids)	43	44	194	244	
A-21	dropped fast (voids)	57.5	60	194	244	
A-21	dropped fast (voids)	194	200	194	244	

* from Quenga (in prep.); ** from Vann (in prep.)

(continued on the next page)

WELL ID #	Well Log Entry	well log data (ft) void/ lost. circ. starts	ends	well information well elev. (ft a. s. l.)	total depth* ft	depth (ft) to volcanics**
AG3	cavity	30				
A-31	clay	150	155	194.7	245	
A-31	slightly clayish	100	105	194.7	245	
AG-2	lost circulation	132	138	503	582.97	-72.995
AG-2	clay	576	582	505.97	582.97	-72.995
AG-2	clay	590	597	505.97	582.97	-72.995
AG-2	clay	639	668	505.97	582.97	-72.995
AG-2	clay	668	680	505.97	582.97	-72.995
AG-6	lost circulation	455				
AG-8	very loose (drills fast)	467	470			-13.999
AG-9	lost circulation	360				25
D-1	lost circulation	217		381	417	
D-2	lost circulation	117		381	417	
D-5	lost circulation	220		381	410	
D-8	lost circulation	370		415	450	
D-17	lost circulation	125		305	350	
D-17	small cavities	135	140	305	350	
D-17X	lost circulation	199				
D-18	drop - lost circulation	335	337	310	360	
D-23	possible small cavities	220	225			6.001
D-23A	possible small cavities	220	225			
ETD-8	lost circulation	137	143			
ETD-8	lost circulation	163	175			
ETD-8	lost circulation	186	192			
ETD-8	lost circulation	195	225			
ETD-8	lost circulation	305				
Y-2	lost circulation	280		417		
F-1	lost circulation	350		423	460	
F-1	open	418		423	460	
F-2	lost circulation	162		446.7	490	
F-3	lost circulation	80		454.76	491.76	
F-4	lost circulation	240		460	495	
F-7	lost circulation	180		363	388	
F-7	lost circulation	300		363	388	
F-7	lost circulation	360		363	388	
F-9	lost circulation	165		398	445	
F-9	lost circulation	250		395	445	
F-15	lost circulation	340		465.5	540	a.k.a. F-13
CT-2	lost circulation	335				a.k.a. F-15
CT-5	lost circulation	80				
CT-5	lost circulation	460				
G-1	lost circulation	110				
G-1	small cavities	320				
M-1	cavity	620	630	396	450	
M-1	cavity	647	655			
KGC-1	lost circulation	90				
KGC-2	lost circulation	97				
KGC-3	lost circulation	105				
M-2	open	155	156	401	451	
M-2	open	159	160	401	451	
M-2	lost circulation	140		401	451	
M-2	open	271	273	401	451	
M-3	open	289	293	423	473	
M-3	open	327	329	423	473	

* from Quenga (in prep.); ** from Vann (in prep.)

(continued on the next page)

WELL ID #	Well Log Entry	well log data (ft) void/ lost. circ. starts	ends	well information well elev. (ft a. s. l.)	total depth* ft	depth (ft) to volcanics**
M-3	open	383	387	423	473	
M-3	open	449	451	423	473	
M-3	lost circulation	22		423	473	
M-4	lost circulation	158		421	472	
M-4	lost mud in hole	320		421	472	
M-5	lost circulation	324		273	405	
M-6	lost circulation	275	276	236	406	
M-7	open	84	86	289	340	
M-8	lost circulation	68		443	495	
M-8	lost circulation	240		443	495	
M-8	clay	52	68	443	495	
M-9	lost circulation	223		440	480	-6.001
M-17A	lost circulation	260		430.5	475.51	
M-17B	possible cavity	50		479.6	520.92	
M-17B	lost circulation	140		479.6	520.92	
M-17B	lost circulation	195		479.6	520.92	
M-23	lost circulation	100		401	475	
Y-5A	lost circulation	105				
Y-5A	lost circulation	140				
Y-5	lost circulation	75		430	480	
Y-21A	lost circulation	355				
NCS02	cavity	92	95			
NCS02	cavity	188	194			
3A	cavity	120	125		naval hospital well	
3A	cavity	175	180		naval hospital well	
Y-1	lost circulation	150		413.8	460	
Y-1	lost mud in hole	277	279	413.8	460	
Y-2	lost circulation	247		417	467	-209.99
Y-2	open	374	377	417	467	-209.99
Y-2	open	391	393	417	467	-209.99
Y-2	open	452	454	417	467	-209.99
Y-2	open	466	467	417	467	-209.99
Y-4A	lost circulation	300		398.5		
UOG-1	drop	20.5	21.1			
UOG-1	lost circulation/ void from 20.5 to 38 feet	20.5	72			
Y-5	lost circulation	135	140	434	480	
Y-5	drop (cavity)	174	176	434	480	
Y-5	cavern	262	263	434	480	
Y-7	lost circulation	35	40	411.75	475.27	-165.991
Y-7	lost circulation	240	243	411.75	475.27	-165.991
Y-7	lost circulation	293	334	411.75	475.27	-165.991
Y-7	lost circulation	400		411.75	475.27	-165.991
Y-7	caving	126	130	411.75	475.27	-165.991
Y-7	caving	420	475	411.75	475.27	-165.991
Y-10	lost circulation	140	150	390.01	445	-106.995
Y-10	lost circulation	312	318		445	-106.995
Y-10	lost circulation	335	340		445	-106.995
Y-11	lost circulation	266				
Y-11	drills fast- cavities	285	289			
Y-12	lost circulation	171	175	390.01		-164.993
Y-12	lost circulation	332				-164.993
Y-12	lost circulation	363				-164.993
Y-13	lost circulation	166	210			296.985
Y-14	lost circulation	387				
Y-16	drop	343.5	345			

* from Quenga (in prep.); ** from Vann (in prep.)

(continued on the next page)

WELL ID #	Well Log Entry	well log data (ft) void/ lost. circ. starts	ends	well information well elev. (ft a. s. l.)	total depth* ft	depth (ft) to volcanics**
Y-16	drop	362.5	363			
Y-19	possible clayey pockets	430	450			
Y-20A	lost circulation	198	209			222.989
Y-21	lost circulation	232	238			
Y-21	lost circulation	341	351			
Y-21	lost circulation	385	387			
Y-21	lost circulation	396	398			
Y-22	lost circulation	112	115			337.982
Y-22	lost circulation	145	150			
Y-24	lost circulation	361	380			162.993
Y-32	sandy silt pocket	120	123			275.988
AAFB1	cavity	268	270		AAFB monitoring well #1	
AAFB1	cavity	271	276		AAFB monitoring well #1	
AAFB1	lost circulation	300			AAFB monitoring well #1	
IRP-1	numerous voids	45	60			
IRP-1	large clay filled cavern	87				
IRP-2	poor circulation	175	180			
IRP-2	lost circulation	275	320			
IRP-2	lost circulation	350	365			
IRP-2	lost circulation	400	405			
IRP-3	very carvernous	60	65			
IRP-4	lost circulation	385	571			
IRP-5	encountering caverns	30				17.999
IRP-5	large cavern/ lost circ	40	42			
IRP-5	numerous cavities	60	65			
IRP-5	lost circulation	270	330			
IRP-5	lost circulation	355				
IRP-5	ocassional caverns	350	370			
IRP-6	cavity	370				81.995
IRP-7	ocassional small vug	105	145			
IRP-7	cavernous limestone	285	305			
IRP-9	large cavern / drop 3ft	100				
IRP-9	3 ft cavern	232				
IRP-11	3.5 ft void	126				
IRP-12	cavity, 3 ft drop	235	238			
IRP-13	lost circulation	355	365			
IRP-13	fracture zone or small voids	370	390			
IRP-13	lost circulation	395	470			
IRP-13	lost circulation	480	525			
IRP-14	clay zone	240				
IRP-14	lost circulation	242				
IRP-14	cavern	333	336			
IRP-15	cavern	235	238			
IRP-16	clay zone	212				
IRP-17	lost circulation	245	357			25
IRP-17	lost circulation	365	407			
IRP-17	lost circulation	411	475			
IRP-20	poor circulation	195				
IRP-20	lost circulation	280	298			
IRP-20	lost circulation	310	313			
IRP-20	lost circulation	320	343			
IRP-20	lost circulation	459	463			
IRP-20	lost circulation	470	484.5			
IRP-20	lost circulation	488				
IRP-22	void	60	68			

* from Quenga (in prep.); ** from Vann (in prep.)

(continued on the next page)

WELL ID #	Well Log Entry	well log data (ft) void/ lost. circ. starts	ends	well information well elev. (ft a. s. l.)	total depth* ft	depth (ft) to volcanics**
IRP-22	void	78	80			
IRP-22	void	165	170			
IRP-22	void	235	238			
IRP-22	void	282	284			
IRP-29	no circulation	340	359			
IRP-29	void	382	398			
IRP-30	lost circulation	465	475			
IRP-31	no circulation	300	305			
IRP-31	no circulation	422	428			
IRP-31	no circulation	445	448			
IRP-32	no circulation	250	259			
IRP-32	possible void	288				
IRP-32	lost circulation	330				
IRP32A	lost circulation	254				
IRP32A	possible void	288				
IRP32B	no circulation	170	182			
IRP32B	possible void	221	225			
IRP32B	possible void	285				
IRP32B	possible cavernous zone	414				
IRP-34	poor circulation	230	239			
IRP-34	no circulation	245	260			
IRP-34	no circulation	265	275			
IRP-34	very poor circulation	305				
IRP-34	very poor circulation	380				
IRP-34	no circulation	400	425			
IRP-34	no circulation	490	498			
IRP-35	void likely/ no circulation	65	75			
IRP-35	lost circulation for 30 sec	148				
IRP-36	no circulation	242				
IRP-37	lost circulation	280	282			
IRP-37	lost circulation	325				
IRP-39	lost circulation	116	128			
IRP-50	no circulation	170	280			
IRP-50	lost circulation	435	460			
IRP-50	very poor circulation	500				
IRP-50	no circulation	560				
IRP-51	lost circulation	67	71			
IRP-59	lost circulation	126	145			
IRP-59	lost circulation	156	184			
IRP-59	sporadic circulation	184	210			
IRP-59	lost circulation	210	246			
IRP-59	cavity	291	293			
IRP-59	lost circulation	293	321			
IRP-59	caving	314	316			
IRP-59	caving	355	356			168.993
TH-A	lost circulation	210				
TH-D	lost circulation, large opening at 350 ft	350	550		568	514ft amsl
TH-E	large openings	160	190		565	449 amsl
TH-E	large openings	250	300			
TH-E	large openings	450	500			
LF-1-1	cavity, 2ft	265	267			
LF-1-1	cavity, 4ft	271	275			
LF-1-1	no circulation	300	510			
LF-1-2	lost circulation	150				
OU-3	lost circulation	115	155	~200		a.k.a. MW-1

* from Quenga (in prep.); ** from Vann (in prep.)

Appendix 12: Inventory of coastal discharge features in Guam

Feature identifiers		Type	Discharge estimates (mgd) (Jocson, 1998)
KARST ID#	Feature Name		
CDF 001	Hilton Spring & Seeps	Beach springs and seeps	2.0
CDF 002	PIC Seeps	Beach seeps	0.6
CDF 003	Pacific Star Spring	Beach spring	5.0
CDF 004	Tropicana Seeps	Beach seeps	0.1
CDF 005	Parc Hotel Spring	Beach spring	0.7
CDF 006	Fujita Spring & Seeps	Beach springs and seeps	1.5
CDF 007	Hyatt Spring & Seeps	Beach springs and seeps	1.5
CDF 008	Wet Willies Spring	Beach spring	1.5
CDF 009	Reef Hotel Seeps	Beach seeps	1.5
CDF 010	Westin Spring & Seeps	Beach springs and seeps	2.0
CDF 011	Okura Springs	Beach spring	4.0
CDF 012	Gun Beach Springs	Beach spring	1.5
CDF 013	Fafai Seeps	Beach seeps	0.1
CDF 014	Amantes Springs	Small cavernous opening	0.7
CDF 015	NCS Beach Seeps	Beach seeps	0.2
CDF 016	Tanguisson Springs	Beach spring	0.2
CDF 017	Tanguisson Springs 2	Beach spring	0.3
CDF 018	Tanguisson Springs 3	Beach spring	1.0
CDF 019	Hilaan Springs	Beach spring	6.0
CDF 020	Ocean View Spring	Small cavernous opening	0.8
CDF 021	Ague Spring 1	Small cavernous opening	2.0
CDF 022	Ague Spring 2	Small cavernous opening	3.0
CDF 023	Ague Cove Spring	Calita-type cove	5.0
CDF 024	Ulua Cave	Discharging cave	0.4
CDF 025	Grotto Spring	Small cavernous opening	1.0
CDF 026	Turkey Rock Spring	Small cavernous opening	0.5
CDF 027	Fountain	Small cavernous opening	2.0
CDF 028	South Haputo Springs	Small cavernous opening	1.5
CDF 029	North Haputo Spring	Beach Spring	2.0
CDF 030	Submarine vents (Haputo)	Submarine vents	0.4
CDF 031	Evian Spring	Cavernous opening	0.6
CDF 032	Sw imming Hole	Cavernous opening	2.0
CDF 033	Lunch Fracture	Diss. enlarged fracture	0.1
CDF 034	Coconut Crab Cave	Discharging cave	5.0
CDF 035	Frankie's Cave	Cavernous opening	2.0
CDF 036	Patinian Spring	Cavernous opening	2.0
CDF 037	Menpachi Fracture	Diss. enlarged fracture	0.9
CDF 038	Scott's Fracture	Diss. enlarged fracture	0.3
CDF 039	Arch Spring	Discharging cave (arch)	2.0
CDF 040	Kiw i Spring	Cavernous opening	2.0
CDF 041	No Can Fracture	Diss. enlarged fracture	0.4
CDF 042	Randall Spring	Cavernous opening	1.0
CDF 043	Nicole's Spring	Cavernous opening	
CDF 044	7 Little Springs	Fractures	
CDF 045	Beach Rock Spring	Beach spring/ beachrock cap	
CDF 046	Ritidian Spring	Cavernous opening	
CDF 047	Castro's Beachrock Spring	Beach spring/ beachrock cap	
CDF 048	Scout's Beach Seeps	Beach seeps	
CDF 049	Taragues Seeps	Beach seeps	
CDF 050	Tagua Point Seeps	Beach seeps	
CDF 051	Fadian Cove Spring	Cavernous opening	
CDF 052	Haw aiian Rock Quarry	Beach seeps	
CDF 053	Janum Spring	Basement conduit system	

Appendix 13: Inventory of submerged karst features and significant sea caves

Feature identifiers		Description	Location
KARST ID#	Feature Name		
SBM 001	Blue Hole	submerged pit cave, starts at 20 m, bottom at 95 m, wall opens at 40 m	E 144-37-77 N 13-26-11
SBM 002	Anae Caverns	submerged small caves, at Anae Island, depth ~10 m	E 144-38-08 N 13-21-09
SBM 003	Ague Cove Cave	north of Ague Cove, depth 12 m	north of Ague Cove
SBM 004	MDA Cave (near Haputo)	south of Haputo Beach, entrance at 12m, continues to inland f-w cave	contact MDA
SBM 005	Matt's Cave	entrance 2 m diam., at 50 m depth on Palace Wall; extends 200+ m	contact Matt Howes
SBM 006	Piti Bomb Holes	submerged sinkholes on a reef in Piti, the deepest is 11 m	E 144-42-10 N 13-28-23
SBM 007	Shark's Hole	depression on a reef in Hilaan, ~3 m deep	reef at Hilaan
SBM 008	Inarajan Pools	two submerged sinkholes in Inarajan, 80 m diam., 10 m deep	Inarajan-- roadside park
SBM 009	Orote Pond	depression on the tip of Orote Peninsula, brackish water/marine lake	opposite Orote Island
SEA 001	Pugua Point Sea Caves	~5 small caves in the surf zone at the base of a cliff at Tweed's Cave	E 144-49-56.94 N 13-35-14.37
SEA 002	Anao Tunnel	12 m long, 1.8 m diam. Tunnel; wave cut (maybe part solutional)	E 144-55-54.30 N 13-32-39.45
SEA 003	Haputo Skylight Sea Cave	sea cave south of Haputo Beach, collapsed roof forms a low arch	just south of Haputo Beach
SEA 004	Pati Point 3 Sea Caves	a group of 3 sea caves south of Pati Point	south of Pati Point
SEA 005	Pati Point 3 fissures	a group of 3 fissures cut by waves along structural weaknesses	could be de-roofed sea caves
SEA 006	Lafac Point Sea Caves	probable sea caves	Lafac Point
SEA 007	Mati Point Sea Caves	probable sea caves	Mati Point
SEA 008	Janum Area Sea Caves	probable sea caves	
SEA 009	Lujuna-Pagat notch cave	probable sea caves	between Lujuna and Pagat Points
SEA 010	Pagat Point Sea Cave	probable sea caves	Pagat Point
SEA 011	Ague Sea Cave	wave cut small cave at the sea level north of Ague Cove	just north of Ague Cove